DDX3 in cancer
Identifying motives, targets and partners in crime
© Marise Rosa Heerma van Voss, 2017

ISBN/EAN 9789462336087

Cover by Suze Swarte
Lay-out by wenz iD | www.wenzid.nl
Printed by Gildeprint Drukkerijen, Enschede

The work described in this thesis was financially supported by the Dutch Cancer Society (UU2013-5851), the UMC Utrecht Alexandre Suerman Stipend, the Saal van Zwanenberg Stichting and the Jo Kolk Studiefonds.

Financial support for printing this thesis was kindly provided by ChipSoft.

DDX3 in cancer

Identifying motives, targets and partners in crime

De rol van DDX3 in kanker

Motieven, doelwitten en handlangers

met een samenvatting in het Nederlands

Proefschrift

ter verkrijging van de graad van doctor aan de Universiteit Utrecht op gezag van de rector magnificus, prof. dr. G.J. van der Zwaan, ingevolge het besluit van het college voor promoties in het openbaar te verdedigen op woensdag 3 mei 2017 des middags te 2.30 uur.

door

Marise Rosa Heerma van Voss

geboren op 12 juni 1988 te Amsterdam

Promotoren: Prof. dr. P.J. van Diest
Prof. dr. E. van der Wall

Copromotor: Dr. V. Raman

Voor mijn ouders

TABLE OF CONTENT

CHAPTER 1 General Introduction 9

MOTIVES

CHAPTER 2 Targeting mitochondrial translation by inhibiting DDX3: a novel radiosensitization strategy for cancer treatment 19

CHAPTER 3 Global effects of DDX3 inhibition on cell cycle regulation identified by a combined phosphoproteomics and single cell tracking approach 53

TARGETS

CHAPTER 4 Identification of the DEAD box RNA helicase DDX3 as a therapeutic target in colorectal cancer 75

CHAPTER 5 Nuclear DDX3 Expression Predicts Poor Outcome in Colorectal and Breast Cancer 101

CHAPTER 6 The prognostic effect of DDX3 upregulation in distant breast cancer metastases 121

CHAPTER 7 DDX3 has divergent roles in head and neck squamous cell carcinomas in smoking versus non-smoking patient 137

PARTNERS IN CRIME

CHAPTER 8 Combination treatment using DDX3 and PARP inhibitors induces synthetic lethality in BRCA1-proficient breast cancer 145

CHAPTER 9 Targeting RNA helicases in cancer: the translation trap 161

CHAPTER 10 Summarizing discussion 189

APPENDIX

Nederlandse samenvatting 200
Acknowledgements 208
List of publications 212
Contributing authors 214
Curriculum Vitae 218

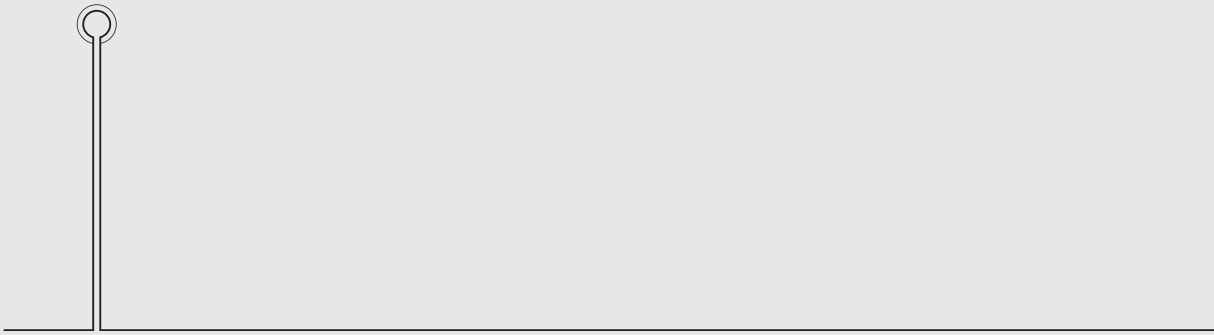

CHAPTER 1

General Introduction

The basis of anti-cancer drug development lies in identification of factors that are essential for survival of cancer cells, but are compensated, redundant or absent in normal healthy tissues. A common approach is to begin with identifying mutations that drive oncogenesis in cancer cells. Subsequently, one would try to develop inhibitors to these oncogenes, which cause cancer specific cell death. Albeit logical and specific, this approach has at least two major hurdles that need to be overcome. The first issue is that few driver mutations are actually targetable. In addition, recent large-scale sequencing studies have shown that there are only a few common driver mutations shared among many cancers[1]. Instead cancers are mostly driven by their own unique set of low-frequency genetic alterations, limiting the use of potential oncogene inhibitors to a small group of patients. An alternative approach to therapeutic target identification is not to look for those factors that initially drive oncogenesis, but for the vulnerabilities that arise as a result of the high demands the oncogenic phenotype asserts on cells. Cancer cells become addicted to certain cellular pathways for execution of oncogenic functions and simultaneous maintenance of sufficient cellular homeostasis for survival[2]. Since these so-called "non-oncogene addiction" pathways are often shared among different tumors, they could provide interesting and more widely applicable targets for development of therapeutics[3].

Dead box RNA helicases

Recent studies found that protein expression is predominantly controlled at the mRNA translation level[4-6] and RNA chaperones, like DEAD box RNA helicases, therefore have a large influence on the protein expression profiles observed in different cells. These so-called DDX proteins belong to superfamily 2, the largest group of eukaryotic RNA helicases. They are characterized by 12 conserved motifs involved in RNA and ATP binding[7], with one of them containing the DEAD amino acid sequence (Asp-Glu-Ala-Asp)[8], from which they derive their name (Figure 1). This enzymatic core domain facilitates ATPase dependent helicase activity, allowing DDX proteins to unwind and restructure RNA molecules with a complex secondary structure and to dissociate RNA from bound proteins[9].

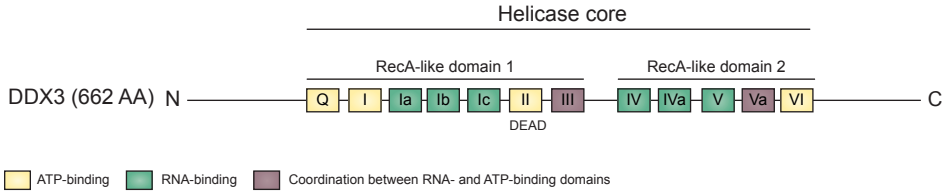

Figure 1. Schematic representation of the conserved structural domains of human DDX3.
Boxes represent the conserved ATP-binding, RNA-binding and linking domains that together form the enzymatic helicase core, which is flanked by variable N- and C-terminal domains that are responsible for interactions with other proteins[7].

The flanking N- and C-terminal domains are specific to each DDX protein and determine interactions with other protein or RNA molecules and subcellular localization[10]. Through their RNA helicase activity, they play a role in virtually all steps of both endogenous and viral RNA metabolism, such as transcription, ribosome biogenesis, nuclear export of mRNA, splicing, translation initiation and RNA decay via regulation of small non-coding RNAs[11, 12]. DEAD box RNA helicases are conserved from human to yeast and have essential cellular functions, as knockout of these helicases is often embryonically lethal[12].

DDX3, a tumor promoting DEAD box protein

DDX3, also known as DDX3X, is one of the most studied DEAD box RNA helicase family members. The *DDX3X* gene lies on the X-chromosome in a pseudo-autosomal region and is one of the rare genes that is not hypermethylated on the inactivated X-chromosome in females[13]. A *DDX3X* homologue is present on the Y-chromosome (*DDX3Y*), but its expression is tightly regulated and restricted to the testis[14]. Although, DDX3Y expression is different from DDX3X[15], there may be overlap in functionality, as partial rescue of a DDX3X mutation is possible by DDX3Y[16]. In the remainder of this thesis, we will refer only to DDX3X with DDX3. The majority of DDX3 in the cell is expressed in the cytoplasm, but nuclear expression is occasionally observed as well. Like its RNA helicase family members, DDX3 is a multifunctional and evolutionary conserved protein: deletion of Ded1 (the DDX3 homologue in the yeast *Saccharomyces cerevisiae*) can be rescued with human DDX3[17]. Some of DDX3s functionality is clearly related to its RNA processing capacity, like its role in nuclear mRNA export[18, 19], splicing[20, 21], RNA interference[22, 23], ribosomal assembly and translation initiation of mRNAs with a complex 5'UTR[19, 24, 25].

DDX3 was first identified by our group as one of the proteins that was upregulated in breast cancer cells after exposure to benzo(a)pyrene diolepoxide (BPDE), a carcinogen found in cigarette smoke[26]. Recent functional studies have demonstrated that DDX3 plays an oncogenic role in the development of breast[26] and several other types of cancer[27-29]. DDX3 was found to have anti-apoptotic properties [30-32] and to facilitate migration[26, 33] and invasion of cancer cells[34, 35]. Several studies have linked DDX3 to cell cycle progression[36, 37] and DDX3 inhibition has been reported to result in a G1-arrest[27]. In addition, DDX3 was found to be a multilevel activator of the Wnt-signaling pathway[27, 35, 38]. Interestingly, the mechanism by which DDX3 regulates these processes is not limited to mRNA translational control. DDX3, like other DEAD box RNA helicases, was found to function in a plethora of cellular pathways[39] and for instance directly regulates the kinase activity of CK1ε[38]. The tumor-promoting role of DDX3 was corroborated by studies on DDX3 expression in lung cancer patient samples[27]. DDX3 is also an important factor in cellular innate immunity and viral mRNA processing. However, these topics are beyond the scope of this thesis, which will focus on the role of DDX3 in cancer biology.

Development of the DDX3 inhibitor RK-33

To target DDX3 for cancer treatment, a small molecule inhibitor, RK-33, was designed using the X-ray crystallographic structure of the core domains of DDX3[40]. RK-33 is the lead compound of a series of tricyclic 5:7:5-fused diimidazo[4,5-d:4',5'-f][1, 3]diazepine analogues that fit the ATP-binding cleft of DDX3 and thereby inactivate it[41-43]. DDX3 has a unique insert of 10 amino-acids in its helicase core that distinguishes it from all other RNA helicase family members[40]. With biotin pull-down experiments, we showed that RK-33 selectively binds DDX3 and not its close relatives DDX5 and DDX17[27]. In addition RK-33 potently inhibits the RNA helicase activity of the DDX3 yeast homologue Ded1[27]. Efficacy of RK-33 has been shown in several pre-clinical models of human cancer. RK-33 showed potent radiosensitizing properties in mouse models of lung[27] and prostate cancer[29]. Furthermore, RK-33 was found to have single-agent activity against Ewing sarcoma human xenografts with high DDX3 expression[28]. Toxicity studies in mice did not show toxic effects on normal tissues[27]. While RK-33 treatment was shown to inhibit DNA repair after radiation[27, 29], exactly how its effect on DDX3 inhibition is linked to DNA repair remained unknown. As such, better understanding of the working mechanism behind DDX3 inhibitors in cancer was required.

Thesis outline: identifying motives, targets and partners in crime of DDX3 in cancer

In this thesis, we evaluate DDX3 as a target in cancer by, as the title implies, a three-step approach. The first part of this thesis focuses on the **motives** that cancer cells have to upregulate DDX3 and why inhibiting DDX3 is a feasible anti-cancer strategy. In chapter 2, we evaluate the effect of DDX3 inhibition with RK-33 on the metabolic profile of breast cancer cells. Chapter 3 shows the effect of DDX3 inhibition on cell cycle progression, by using both a single cell tracking and phosphoproteomics approach. The second part of this thesis focuses on the selection of cancers that can be **targeted** by DDX3 inhibitors. In chapter 4, we show that DDX3 inhibition reduces constitutively activated Wnt-signaling in colorectal cancers. In chapter 5, we observe that while most DDX3 expression is cytoplasmic, some cancers express DDX3 in the nucleus, and we evaluate the significance of this expression pattern. In chapter 6 we look at DDX3 expression in distant breast cancer metastasis. Chapter 7 evaluates the different roles of DDX3 in smoking and non-smoking patients with head and neck squamous cell carcinomas. The third and last part of this thesis is named **partners in crime**. In chapter 8 we look at the effect of combination therapy with poly ADP-ribose polymerase (PARP) and DDX3 inhibitors in both BRCA1 pro- and deficient breast cancers. In chapter 9 we put DDX3 inhibition with RK-33 in a broader perspective by reviewing the role of different DEAD box RNA helicases in oncogenic mRNA translation.

REFERENCES

1 Kandoth C, McLellan MD, Vandin F, Ye K, Niu B, Lu C *et al*. Mutational landscape and significance across 12 major cancer types. Nature 2013; **502**: 333-339.

2 Dobbelstein M, Moll U. Targeting tumour-supportive cellular machineries in anticancer drug development. Nature reviews Drug discovery 2014; **13**: 179-196.

3 Luo J, Solimini NL, Elledge SJ. Principles of cancer therapy: oncogene and non-oncogene addiction. Cell 2009; **136**: 823-837.

4 Ghazalpour A, Bennett B, Petyuk VA, Orozco L, Hagopian R, Mungrue IN *et al*. Comparative analysis of proteome and transcriptome variation in mouse. PLoS genetics 2011; **7**: e1001393.

5 Vogel C, Marcotte EM. Insights into the regulation of protein abundance from proteomic and transcriptomic analyses. Nature reviews Genetics 2012; **13**: 227-232.

6 Schwanhausser B, Busse D, Li N, Dittmar G, Schuchhardt J, Wolf J *et al*. Global quantification of mammalian gene expression control. Nature 2011; **473**: 337-342.

7 Soto-Rifo R, Ohlmann T. The role of the DEAD-box RNA helicase DDX3 in mRNA metabolism. Wiley interdisciplinary reviews RNA 2013; **4**: 369-385.

8 Linder P, Lasko PF, Ashburner M, Leroy P, Nielsen PJ, Nishi K *et al*. Birth of the D-E-A-D box. Nature 1989; **337**: 121-122.

9 Leitao AL, Costa MC, Enguita FJ. Unzippers, resolvers and sensors: a structural and functional biochemistry tale of RNA helicases. International journal of molecular sciences 2015; **16**: 2269-2293.

10 Kwong AD, Rao BG, Jeang KT. Viral and cellular RNA helicases as antiviral targets. Nature reviews Drug discovery 2005; **4**: 845-853.

11 Tanner NK, Linder P. DExD/H box RNA helicases: from generic motors to specific dissociation functions. Molecular cell 2001; **8**: 251-262.

12 Linder P, Fuller-Pace FV. Looking back on the birth of DEAD-box RNA helicases. Biochimica et biophysica acta 2013; **1829**: 750-755.

13 Lahn BT, Page DC. Functional coherence of the human Y chromosome. Science 1997; **278**: 675-680.

14 Ditton HJ, Zimmer J, Kamp C, Rajpert-De Meyts E, Vogt PH. The AZFa gene DBY (DDX3Y) is widely transcribed but the protein is limited to the male germ cells by translation control. Human molecular genetics 2004; **13**: 2333-2341.

15 Foresta C, Ferlin A, Moro E. Deletion and expression analysis of AZFa genes on the human Y chromosome revealed a major role for DBY in male infertility. Human molecular genetics 2000; **9**: 1161-1169.

16 Sekiguchi T, Iida H, Fukumura J, Nishimoto T. Human DDX3Y, the Y-encoded isoform of RNA helicase DDX3, rescues a hamster temperature-sensitive ET24 mutant cell line with a DDX3X mutation. Experimental cell research 2004; **300**: 213-222.

17 Mamiya N, Worman HJ. Hepatitis C virus core protein binds to a DEAD box RNA helicase. The Journal of biological chemistry 1999; **274**: 15751-15756.

18 Yedavalli VS, Neuveut C, Chi YH, Kleiman L, Jeang KT. Requirement of DDX3 DEAD box RNA helicase for HIV-1 Rev-RRE export function. Cell 2004; **119**: 381-392.

19 Lai MC, Lee YH, Tarn WY. The DEAD-box RNA helicase DDX3 associates with export messenger ribonucleoproteins as well as tip-associated protein and participates in translational control. Molecular biology of the cell 2008; **19**: 3847-3858.

20 Deckert J, Hartmuth K, Boehringer D, Behzadnia N, Will CL, Kastner B *et al*. Protein composition and electron microscopy structure of affinity-purified human spliceosomal B complexes isolated under physiological conditions. Molecular and cellular biology 2006; **26**: 5528-5543.

21 Merz C, Urlaub H, Will CL, Luhrmann R. Protein composition of human mRNPs spliced in vitro and differential requirements for mRNP protein recruitment. RNA 2007; **13**: 116-128.

22 Pek JW, Kai T. DEAD-box RNA helicase Belle/DDX3 and the RNA interference pathway promote mitotic chromosome segregation. Proceedings of the National Academy of Sciences of the United States of America 2011; **108**: 12007-12012.

23 Kasim V, Wu S, Taira K, Miyagishi M. Determination of the role of DDX3 a factor involved in mammalian RNAi pathway using an shRNA-expression library. PloS one 2013; **8**: e59445.

24 Lee CS, Dias AP, Jedrychowski M, Patel AH, Hsu JL, Reed R. Human DDX3 functions in translation and interacts with the translation initiation factor eIF3. Nucleic acids research 2008; **36**: 4708-4718.

25 Geissler R, Golbik RP, Behrens SE. The DEAD-box helicase DDX3 supports the assembly of functional 80S ribosomes. Nucleic acids research 2012; **40**: 4998-5011.

26 Botlagunta M, Vesuna F, Mironchik Y, Raman A, Lisok A, Winnard P, Jr. *et al*. Oncogenic role of DDX3 in breast cancer biogenesis. Oncogene 2008; **27**: 3912-3922.

27 Bol GM, Vesuna F, Xie M, Zeng J, Aziz K, Gandhi N *et al*. Targeting DDX3 with a small molecule inhibitor for lung cancer therapy. EMBO molecular medicine 2015; **7**: 648-669.

28 Wilky BA, Kim C, McCarty G, Montgomery EA, Kammers K, DeVine LR *et al*. RNA helicase DDX3: a novel therapeutic target in Ewing sarcoma. Oncogene 2016; **35**: 2574-2583.

29 Xie M, Vesuna F, Tantravedi S, Bol GM, Heerma van Voss MR, Nugent K *et al*. RK-33 radiosensitizes prostate cancer cells by blocking the RNA helicase DDX3. Cancer research 2016: doi:10.1158/0008-5472.CAN-1116-0440.

30 Li Y, Wang H, Wang Z, Makhija S, Buchsbaum D, LoBuglio A *et al*. Inducible resistance of tumor cells to tumor necrosis factor-related apoptosis-inducing ligand receptor 2-mediated apoptosis by generation of a blockade at the death domain function. Cancer research 2006; **66**: 8520-8528.

31 Sun M, Song L, Li Y, Zhou T, Jope RS. Identification of an antiapoptotic protein complex at death receptors. Cell death and differentiation 2008; **15**: 1887-1900.

32 Shih JW, Wang WT, Tsai TY, Kuo CY, Li HK, Wu Lee YH. Critical roles of RNA helicase DDX3 and its interactions with eIF4E/PABP1 in stress granule assembly and stress response. The Biochemical journal 2012; **441**: 119-129.

33 Sun M, Song L, Zhou T, Gillespie GY, Jope RS. The role of DDX3 in regulating Snail. Biochimica et biophysica acta 2011; **1813**: 438-447.
34 Hagerstrand D, Tong A, Schumacher SE, Ilic N, Shen RR, Cheung HW *et al*. Systematic interrogation of 3q26 identifies TLOC1 and SKIL as cancer drivers. Cancer discovery 2013; **3**: 1044-1057.
35 Chen HH, Yu HI, Cho WC, Tarn WY. DDX3 modulates cell adhesion and motility and cancer cell metastasis via Rac1-mediated signaling pathway. Oncogene 2015; **34**: 2790-2800.
36 Lai MC, Chang WC, Shieh SY, Tarn WY. DDX3 regulates cell growth through translational control of cyclin E1. Molecular and cellular biology 2010; **30**: 5444-5453.
37 Rosner A, Rinkevich B. The DDX3 subfamily of the DEAD box helicases: divergent roles as unveiled by studying different organisms and in vitro assays. Current medicinal chemistry 2007; **14**: 2517-2525.
38 Cruciat CM, Dolde C, de Groot RE, Ohkawara B, Reinhard C, Korswagen HC *et al*. RNA helicase DDX3 is a regulatory subunit of casein kinase 1 in Wnt-beta-catenin signaling. Science 2013; **339**: 1436-1441.
39 Fuller-Pace FV. DEAD box RNA helicase functions in cancer. RNA biology 2013; **10**: 121-132.
40 Hogbom M, Collins R, van den Berg S, Jenvert RM, Karlberg T, Kotenyova T *et al*. Crystal structure of conserved domains 1 and 2 of the human DEAD-box helicase DDX3X in complex with the mononucleotide AMP. Journal of molecular biology 2007; **372**: 150-159.
41 Kondaskar A, Kondaskar S, Kumar R, Fishbein JC, Muvarak N, Lapidus RG *et al*. Novel, Broad Spectrum Anti-Cancer Agents Containing the Tricyclic 5:7:5-Fused Diimidazodiazepine Ring System. ACS medicinal chemistry letters 2010; **2**: 252-256.
42 Kumar R, Ujjinamatada RK, Hosmane RS. The first synthesis of a novel 5:7:5-fused diimidazodiazepine ring system and some of its chemical properties. Organic letters 2008; **10**: 4681-4684.
43 Kondaskar A, Kondaskar S, Fishbein JC, Carter-Cooper BA, Lapidus RG, Sadowska M *et al*. Structure-based drug design and potent anti-cancer activity of tricyclic 5:7:5-fused diimidazo[4,5-d:4',5'-f][1,3]diazepines. Bioorganic & medicinal chemistry 2013; **21**: 618-631.

MOTIVES

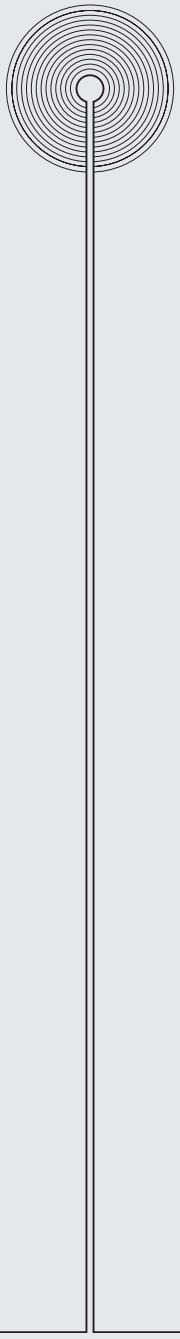

CHAPTER 2

Targeting mitochondrial translation by inhibiting DDX3: a novel radiosensitization strategy for cancer treatment

Marise R. Heerma van Voss, Farhad Vesuna, Guus M. Bol, Junaid Afzal, Yehudit Bergman, Kai Kammers, Mohamed Lehar, Reem Malek, Matthew Ballew, Natalie ter Hoeve, Diane Abou, Daniel Thorek, Cynthia Berlinicke, Meysam Yazdankhah, Debasish Sinha, Anne Le, Roselle Abrahams, Phuoc T. Tran, Paul J. van Diest, Venu Raman

ABSTRACT

DDX3 is a DEAD box RNA helicase with oncogenic properties. RK-33 is developed as a small molecule inhibitor of DDX3 and showed potent radiosensitizing activity in preclinical tumor models. This study aimed to assess DDX3 as a target in breast cancer and to elucidate how RK-33 exerts its anti-neoplastic effects. High DDX3 expression was present in 35% of breast cancer patient samples and correlated with markers of aggressiveness and shorter survival. With a quantitative proteomics approach, we identified proteins involved in the mitochondrial translation and respiratory electron transport pathways to be significantly downregulated after RK-33 or DDX3 knockdown. DDX3 localized to the mitochondria and DDX3 inhibition with RK-33 reduced mitochondrial translation. As a consequence, oxygen consumption rates and intracellular ATP concentrations decreased and reactive oxygen species (ROS) increased. RK-33 antagonized the increase in oxygen consumption and ATP production observed after exposure to ionizing radiation and reduced DNA repair. Overall, we conclude that DDX3 inhibition with RK-33 causes radiosensitization in breast cancer through inhibition of mitochondrial translation, which results in reduced oxidative phosphorylation capacity and increased ROS levels, culminating in a bioenergetic catastrophe.

INTRODUCTION

DEAD box RNA helicases are a family of proteins with ATPase-dependent helicase activity, which allows for the restructuring of complex RNA structures and unwinding of double-stranded RNA[1]. DDX3, also known as DDX3X, is an RNA helicase that has been associated with several cytosolic steps of mRNA processing[2]. Recent functional studies have demonstrated that DDX3 plays an oncogenic role in the development of breast[3] and several other types of cancer[4-7]. DDX3 was found to have anti-apoptotic properties[8, 9] and to play a role in cell cycle progression[4, 5], migration[3, 10] and invasion[11, 12]. However, the oncogenic role of DDX3 in breast cancer remains to be validated in patient samples.

To target DDX3 for cancer treatment, a small molecule inhibitor, RK-33, was recently developed[13]. RK-33 is designed to fit into the ATP-binding pocket of DDX3 and thereby inactivate it. It was shown to selectively bind DDX3 over other DEAD box RNA helicases and to potently inhibit RNA helicase activity[4]. Furthermore, RK-33 was found to have selective anti-cancer activity in mouse models, both as a monotherapy[6] and as a radiosensitizer[4, 7]. However, the exact working mechanisms behind the action of RK-33 in cancer remain to be elucidated.

Using a quantitative proteomics approach, we here identified mitochondrial translation as a potential target of RK-33. Mitochondria have their own ribosomal machinery, responsible for translating the thirteen genes that are located on the mitochondrial genome, which all play a role in facilitating oxidative phosphorylation (OXPHOS). Increasing evidence indicates that cancer cells are dependent on upregulation of OXPHOS when encountering cellular stressors, like chemotherapy[14, 15], or during metastasis[16]. Irradiated cells also increase oxygen consumption and mitochondrial ATP production[17] allowing for more efficient repair of radiation induced DNA damage[18]. Since we have previously shown that RK-33 has radiosensitizing abilities, we hypothesized that this might be due to RK-33 inhibiting mitochondrial translation and thereby limiting the cellular capacity to upregulate OXPHOS. In this work, we evaluate DDX3 as a target in breast cancer and investigated the effect of DDX3 inhibition on the bioenergetic profile of breast cancer cells. We show that RK-33 radiosensitizes breast cancer cells through inhibition of mitochondrial translation, resulting in reduced OXPHOS and increased production of reactive oxygen species (ROS).

MATERIAL AND METHODS

Patient samples

Tissue microarrays (TMAs) with 540 breast cancers archived in the UMC Utrecht between 1993 and 2009 were used[19]. The patient group consisted out of 422 consecutive breast cancer patients, supplemented with a collection of 95 invasive lobular carcinomas and 23

distant metastases. Cases were subclassified in molecular subtypes as was described before[20,21]. We used anonymous archival leftover pathology material. Therefore, no ethical approval or informed consent is required according to Dutch legislation[22] as use of letover material is part of the standard agreement with patients in our hospital. The UMC Utrecht Medical Research Ethics Committee confirmed that official approval of this study is not required by law (reference number WAG/mb/16/021628).

Immunohistochemistry

Immunohistochemical staining for DDX3 has been described in detail previously[23]. Briefly, sections were labeled for 1 hour with anti-DDX3 (1:1000, pAb r647)[24]. Cases with absent to moderate DDX3 expression were classified as having low DDX3 expression and evaluated against cases with high expression, as before[5].

Statistics

Discrete variables were compared by $\chi 2$ or Fisher's exact test. Student's t-test and Mann Whitney U-tests were calculated for normal and non-normal distributed variables respectively. Survival was compared by Kaplan-Meier curves and Breslow tests. Multivariate analysis was performed by Cox regression. Effect modifiers were identified by including multiplicative interaction terms into the model. Statistical analyses were performed with SPSS 20.0 (IBM Inc, Armonk, NY, USA) or R version 3.2.0 regarding p-values smaller than 0.05 as significant.

Cell culture

MCF10A, MCF7, MDA-MB-231 and MDA-MB-435 cells were originally purchased from the American Type Culture Collection (ATCC, Manassas, VA, USA) and regularly STR-profiled and mycoplasma tested. DDX3 knockdown in MDA-MB-435 cells was achieved by lentiviral transduction with an shDDX3 construct or empty vector control, as before[3].

Cell viability assays

For cell viability assays 1 x 103 - 3 x 103 cells were plated per well in a 96-well plate and allowed to attach overnight. The number of viable cells was estimated after 72 hours of drug exposure with an MTS assay (CellTiter 96 Aqueous One Solution, Promega, Madison, WI, USA). RK-33 cytotoxicity was assessed in the presence of: 5.5 mM glucose or sodium pyruvate, 15-20 mM n-acetyl-L-cysteine (Sigma-Aldrich, St Louis, MO, USA), 25 μM chloroquine (Sigma-Aldrich).

A non-mitochondrial based cell viability assay was performed by exposing cells for 48 hours to RK-33 and subsequently labeling the cells with 1.875 μg/mL Calcein AM, and 5 μM Ethidium homodimer. Fluorescence was measured using a Cellomics Arrayscan VTI HCS Reader (Thermo Fisher Scientific, MA, USA). Calcein AM positive Ethidium homodimer negative cells were considered viable.

Immunoblotting

Whole cellular protein extracts were lysed in SDS-extraction buffer. Mitochondrial and cytoplasmic extracts were prepared using a mitochondria isolation kit (ThermoFisher Scientific, Waltham, MA, USA) and Dounce homogenizer. The following primary antibodies were used: DDX3 (1:1000, mAb AO196[24]), β-actin (1:10000, A5441, Sigma-Aldrich), OXPHOS complexes (1:1000, ab110411, Abcam, Cambridge UK), COX IV (1:5000, #4850, Cell Signaling Technology, Danvers, MA, USA), PARP (1:1000, #9542, Cell Signaling Technology), Caspase 3 (1:500, #9665, Cell Signaling Technology), and LC3 (1:1000, #1775S, Cell Signaling Technology).

Proteomics

MDA-MB-435 cells were exposed for 24 hours to 4.5 μM RK-33 or were harvested 72 hours after shDDX3 transduction in extraction buffer. Proteins were harvested in extraction buffer containing 1% SDS, 1 mM EDTA, 1 mM sodium orthovanadate, 1 mM sodium pyrophosphate, 1 mM β-glycerophosphate, 1 mM sodium fluoride and proteinase inhibitor cocktail. 50 μg of protein was digested with trypsin. Peptides were labeled with TMT10plex isobaric mass tags (ThermoFisher Scientific), fractionated with basic reverse phase chromatography and analyzed on a Thermo Scientific Q Exactive Plus mass spectrometer interfaced with an Easy-nLC 1000 (Thermo Fisher Scientific).

Bioinformatics

Peptides were identified form isotopically resolved masses in precursor (MS) and fragmentation (MS/MS) spectra extracted using 3 nodes (without deconvolution and with deconvolution by Xtract or MS2 Processor) in Proteome Discoverer (PD) software (v1.4, Thermo-Fisher Scientific, San Jose, CA. USA) and searched with Mascot 5.2.1 (Matrix Sciences, Boston, MA, USA) against the RefSeq2015 database. Search criteria included sample's species; trypsin as the enzyme, allowing one missed cleavage; cysteine carbamidomethylation and TMT 10-plex labeling of N-termini as fixed modifications; methionine oxidation, asparagine and glutamine deamidation, and TMT 10-plex labeling of lysine and tyrosine as variable modifications. Only spectra with a false discovery rate smaller than 1% and mass isolation interference smaller than 30%, in which all reporter ions were detected, were included for downstream analyses. Individual protein relative abundances were calculated by (1) log2-transformation of the reporter ion intensities, (2) subtracting the spectrum medians of the log2 transformed reporter ion intensities (median-polishing), and (3) summarizing all reporter ion intensities that belong to the same protein by their median value. In a final step (4), the channel medians across all proteins were subtracted to correct for potential loading differences, as described previously (1). Only proteins quantified by reporter ion spectra from more than one peptide were included for statistical downstream analyses. Protein abundances were compared between three RK-33

treated vs DMSO treated samples, and between two shDDX3 and control samples. Moderated t-test statistics and multiple comparison corrected q-values were calculated[25,26]. Proteins with a $q < 0.05$ and a fold change larger than 1.15 were considered significantly altered. Overlap between the set of proteins changed after RK-33 and shDDX3 was assessed by calculating a representation factor and p-value based on an exact hypergeometric distribution (http://nemates.org/). Gene set expression analysis was performed by searching the Reactome database using the Enrichr web tool (http://amp.pharm.mssm.edu/Enrichr/)[27]. Protein interactions within the group of significantly altered proteins were surveyed by searching the STRING database (http://string-db.org/)[28] version 9.1, using a confidence level of 0.9.

Immunofluorescence

For mitochondrial colocalization experiments, cells were labeled with 100 nM Mitotracker red (CMXRos #9082, Cell Signaling Technology) and fixed in methanol. For DNA damage experiments, cells were treated with RK-33 two hours before exposure to 2 Gy ionizing radiation (CIDX, XStrahl, Camberley, United Kingdom), followed by fixation in formalin and permeabilization with 0.2% Triton-X. The following primary antibodies were used: DDX3 (1:50; AO196[24]), γH2AX (1:1600, DAM1782241, EMD Millipore, Billirica, MA, USA). Anti-mouse Alexa488 (1:200; 1 hour, Life Technologies, Carlsbad, CA, USA) was used as a secondary antibody. Photographs were taken with Nikon Eclipse 80i fluorescence microscope for the DNA damage experiments and with an Olympus FV10MP-LACDS/BX61W1 multiphoton microscope for colocalization analysis (Olympus, Center Valley, PA, USA).

Mitochondrial translation assay

Pulse labeling was performed as described by Leary, *et al.*[29]. Briefly, 4×10^5 cells were plated in 60 mm dishes and allowed to attach overnight. After 2 hour exposure to RK-33, cells were pulse labeled for 60 minutes with [S^{35}]-methionine (150 μCi/ml, Easytag, PerkinElmer, Waltham, MA, USA) and 100 μg/ml Emetine. Cells were chased for 10 minutes and subsequently harvested. 50 μg whole cellular protein extract was run over a 15-20% gradient SDS-PAGE gel. After fixation and Coomassie blue staining the gel was dried and imaged by autoradiography.

Measurements of oxygen consumption

Real time oxygen consumption (OCR) and extracellular acidification (ECAR) rates were measured using a Seahorse XF96 Extracellular Flux Analyzer (Agilent Technologies, Santa Clara, CA, USA). If applicable, cells were irradiated three hours after the onset of RK-33 treatment (CIDX, XStrahl). Complex inhibitors were used in the following final concentrations in Seahorse media: oligomycin (1 μM), FCCP (0.35 μM), antimycin (4 μM)

and rotenone (4 μM). Respiratory measurements were normalized by cell numbers as estimated by a DNA assay. For this the wells were lysed in TE lysis buffer containing 0.2% Triton-X and proteinase K for 10 minutes on ice and stained with PicoGreen (ThermoFisher scientific; 1:200). Fluorescent intensity was measured using a Victor^{3}V plate reader (PerkinElmer). The range of fold changes and highest p-value as calculated by student's t-test is reported in the text.
Alternatively, oxygen consumption rates were measured in 10*106 MCF7 cells by a Clark electrode (Oxygraph, Hansatech Instruments, Norfolk, UK) after 12 hours exposure to RK-33. Cells were trypsinized and counted. Directly prior to measurements the cells were centrifuged at 500 g for 5 minutes at room temperature and resuspended in 1 ml growth media.

ATP quantification
7.5-17.5 x 10^4 cells were plated in a 12 well plate and allowed to attach overnight. Cells were treated with RK-33 and three hours later with ionizing radiation (CIDX, XStrahl) if applicable. Intracellular ATP concentrations of 2 x 10^4 cells were measured 12 hours after RK-33 addition by CellTiter-Glo (Promega) luminometry.

Mitotracker flow cytometry
For detection of mitochondrial mass and membrane potential cells were treated with RK-33 and subsequently labeled with 100 nM Mitotracker green FM (#9074 Cell Signaling Technology) and 100 nM Mitotracker red (CMXRos #9082, Cell signaling Technology) respectively, after which cells were harvested by trypsinization. Fluorescent intensity of cells was detected by flow cytometry on a FACSCalibur instrument (BD Biosciences, San Jose, CA, USA). Data were analyzed using FlowJo software (Tree Star Inc., Ashland, OR, USA).

Measurement of reactive oxygen species
1.4-6 x 10^5 cells were plated on collagen coated 35 mm dishes and after 12 hour of RK-33 treatment labeled with 5 μM DCFDA and 2.5 μM MitoSox for 30 minutes. After a recovery time of 30 minutes cells were imaged with Olympus FV10MP-LACDS/BX61W1 multiphoton microscope. Fluorescent intensity per cell was measured with ImageJ[30].

Electron microscopy
Fixation took place in 2% paraformaldehyde, 2.5% glutaraldehyde, 0.1 M cacodylate buffer. Cells were post-fixed in 0.1 M cacodylate buffer containing 1% osmium tetroxide and 0.8% ferrocyanide, subsequently stained with 2% aqueous uranyl acetate and dehydrated in increasing ethanol concentrations, followed by overnight infiltration with equal parts EPON 8/2 and ethanol. After five hours in 100% EPON 1.5% DMP-30, catalyst was added and the

resin was allowed to polymerize overnight at 60 ^{0}C and cure for three days at 37 ^{0}C. Blocks were sectioned at a 65 nm thickness with a diamond knife and imaged with a Hitachi H7600 transmission electron microscope at 25.000 x magnification.

Colony forming assay
200 MCF7 cells were plated per well in a 6-well plate and allowed to attach overnight. Cells were exposed to RK-33 three hours before irradiation (CIDX, XStrahl). 24 hours after radiation treatment the media was refreshed. After 7 days, colonies were stained with 0.5% crystal violet in methanol and counted.

Flow cytometric analysis of apoptotic cells
Cells were exposed for 12 hours to RK-33, harvested by trypsinization and stained with Annexin and Propidium Iodide (ThermoFisher Scientific) for detection of early and late apoptotic cells respectively. Fluorescent intensity of cells was detected by flow cytometry on a FACSCalibur instrument (BD Biosciences, San Jose, CA, USA). Data were analyzed using FlowJo software (Tree Star Inc., Ashland, OR, USA).

RESULTS

DDX3 in human breast cancer samples
To evaluate DDX3 as a target in breast cancer, we assessed DDX3 expression by immunohistochemistry in 366 breast cancer patient samples (Figure 1A). As shown in Table 1 high cytoplasmic DDX3 expression was present in 127 cases (35%) and correlated with slightly higher age at diagnosis ($p = 0.042$), higher mitotic index (MAI; $p = 0.002$), ductal histological type ($p = 0.003$), higher grade ($p = 0.002$) and negative estrogen ($p = 0.005$), progesterone ($p = 0.007$) and HER2 receptor ($p = 0.001$). In addition, tumors with high DDX3 expression more frequently had a basal like ($p = 0.032$) or HER2 driven ($p = 0.002$) molecular subtype. High DDX3 expression was also associated with worse outcome in breast cancer patients. The five-year survival rate was 78.9% in patients with high DDX3 expressing tumors, as compared to 87.4% in those with low DDX3 expression (HR 2.01, $p = 0.042$; Figure 1B). In a Cox regression model including tumor size, lymph node status, grade, MAI and DDX3 expression, only lymph node status was an independent prognostic factor (Supplementary Table 1). Analysis of multiplicative interaction terms indicated that both MAI and lymph node status acted as effect modifiers and the relation between DDX3 and survival was most strong in tumors with low MAI and positive lymph node status (Supplementary Figure 1A & B). Together, these findings indicate that DDX3 associates with markers of aggressive disease in breast cancer patient samples, making it a suitable target for further evaluation.

Table 1. Clinicopathological correlations of cytoplasmic DDX3 expression in invasive breast cancer

	Cytoplasmic DDX3		
	Low	**High**	**p-value**
N	239	127	
Mean age (range)	59.7 (28-88)	62.4 (34-87)	0.042[a]
Mean tumor size (range)	2.4 (0.6-8.0)	2.6 (0.2-10.0)	0.233[a]
Mitotic index (mitosis / 2mm²)	15.0 (0-151)	22.6 (0-131)	0.002[a]
Histological type			
ductal	78.2% (187)	89.7% (113)	0.003[c]
lobular	12.1% (29)	2.4% (3)	
other	9.6% (23)	7.9% (10)	
Grade			
1	23.5% (55)	10.2% (13)	0.002[b]
2	37.6% (88)	34.6% (44)	
3	38.9% (91)	55.1% (70)	
Estrogen receptor			
Positive	82.4% (197)	69.3% (88)	0.005[b]
Negative	17.6% (42)	30.7% (39)	
Progesterone receptor			
Positive	64.3% (153)	49.6% (63)	0.007[b]
Negative	35.7% (85)	50.4% (64)	
HER2			
Positive	7.1% (17)	18.9% (24)	0.001[b]
Negative	92.9% (222)	81.1% (103)	
Lymph node status			
Positive	51.8% (118)	49.2% (60)	0.646[b]
Negative	48.2% (110)	50.8% (62)	
Molecular subtype			
Luminal	84.5% (202)	70.1% (80)	
Basal like	13.0% (31)	20.5% (26)	0.032[d]
HER2 driven	2.5% (6)	9.4% (12)	0.002[d]

a = t-test. b = chi-square test. c = fisher's exact test. d = chi-square test as compared to luminal

The efficacy of the DDX3 inhibitor RK-33 in breast cancer cell lines

The efficacy of the DDX3 inhibitor RK-33 was evaluated in several cancer cell lines and the normal breast cell line MCF10A by an MTS assay (Figure 1C-D). The sensitivity to RK-33 was higher in cancer cell lines (IC50 2.8-4.5 μM) when compared to MCF10A (IC50 7.4 μM), with the latter also expressing lower amounts of DDX3 (Figure 1E). To ensure that this difference in potency reflected viable cell numbers and not just alterations in metabolism, we confirmed this finding in a calcein green based cytotoxicity assay (Supplementary Figure 1C).

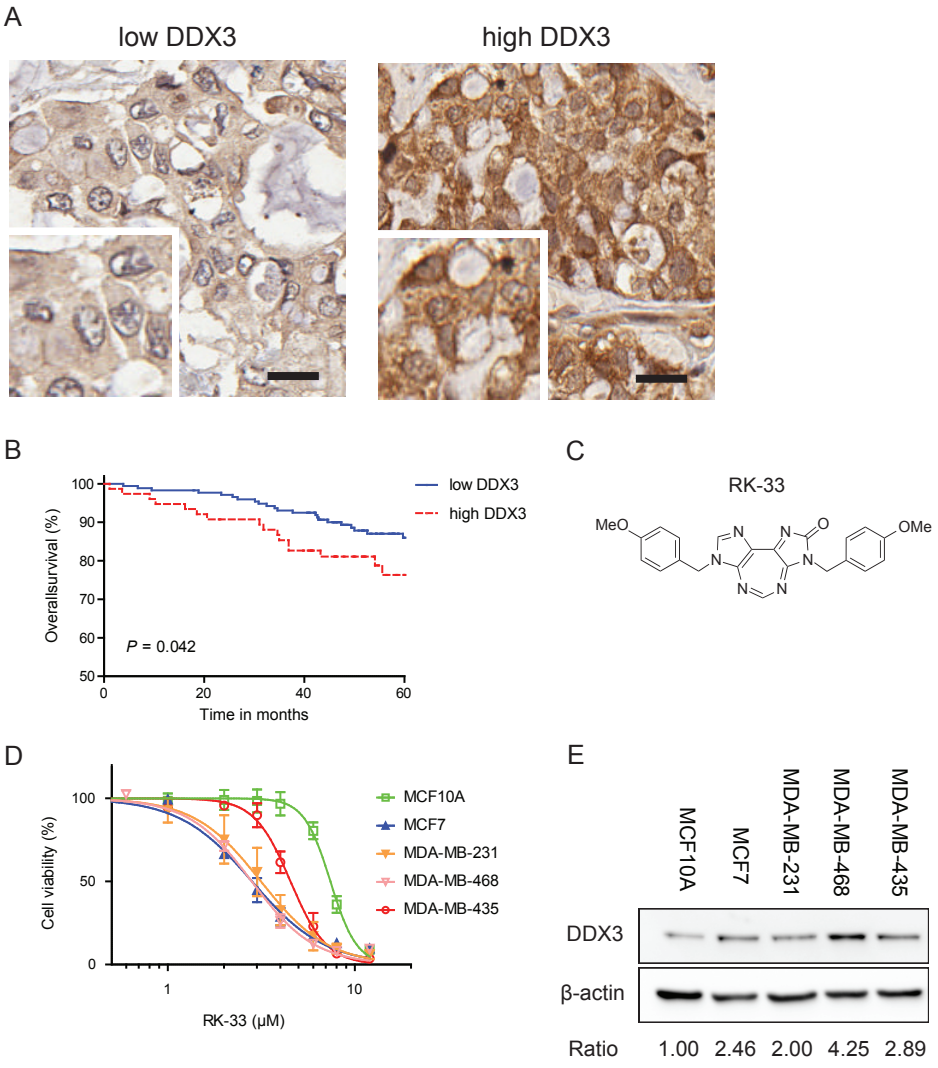

Figure 1A-E. DDX3 is a therapeutic target in breast cancer
A. Example of low and high cytoplasmic DDX3 expression assessed by immunohistochemistry in breast cancer patient samples. Scale bar indicates 20 μm. B. Kaplan-Meier curve plot showing worse overall survival for breast cancer patients with high DDX3 expression. N = 250. P-value calculated by Breslow test. C. Molecular structure of the small molecule inhibitor of DDX3, RK-33 D. MTS assay showing RK-33 cytotoxicity in a normal breast cell line (MCF10A) and four cancer cell lines (MCF7, MDA-MB-231, MDA-MB-468 & MDA-MB-435). Graphs represent mean ± SD of 3 biological replicates. E. Immunoblot showing the relative DDX3 expression in cell lines.

DDX3 inhibition causes reduced expression of proteins involved in mitochondrial translation and OXPHOS

To further evaluate the effect of DDX3 inhibition, changes in protein expression levels were assessed after RK-33 or shDDX3 treatment (Figure 2A) in the metastatic cancer cell line MDA-MB-435 with quantitative proteomics. 666 identified proteins were significantly altered after RK-33 and 770 after shDDX3 (Supplementary Figure 2A). 186 proteins had altered protein expression after both treatments, which was 1.7 times more than could be expected based on chance ($p < 0.001$; Supplementary Figure 1B). Gene set enrichment analysis in the Reactome database [31] identified the "mitochondrial translation" ($p < 0.001$) and "respiratory electron transport" ($p < 0.001$) pathways among the most enriched after RK-33 treatment. The proteins significantly altered by shDDX3 were also enriched for these pathways (Figure 2B). In addition, network analysis using the STRING database [28] revealed tight networks of mitochondrial ribosome proteins and proteins that were part of the electron transport chain (ETC) complexes to be downregulated after both RK-33 and shDDX3 (Figure 2C). We identified two out of the thirteen proteins that the mitochondrial genome encodes for. Of which the complex IV protein MT-COII was among the significantly altered proteins (downregulated by -1.285 times, $q = 0.001$) and MT-NDI had a borderline significant fold change (-1.149, $q = 0.009$). Interestingly, the remainder of the ETC complex proteins was encoded on the nuclear genome, but belonged to OXPHOS complex I and IV, which are the ETC complexes that contain most mitochondrially encoded proteins.

DDX3 localizes to the mitochondria

The potential involvement of DDX3 in mitochondrial translation made us evaluate whether DDX3 localizes to the mitochondria. DDX3 was identified in a mitochondrial extract, and also to a lesser extent in the free cytosolic fraction of MCF7 (Figure 2D). A similar distribution was observed in MDA-MB-231 (Supplementary Figure 2C). In addition, we found DDX3 to colocalize with mitotracker-red labeled mitochondria by immunofluorescence (Figure 2E).

RK-33 causes mitochondrial translation inhibition

To assess whether treatment with RK-33 resulted in inhibition of mitochondrial translation, we performed an S35-methionine pulse-labeling experiment in the presence of the cytoplasmic translation inhibitor emetine. As shown in Figure 3A, two hours of RK-33 treatment resulted in potent inhibition of S35-methionine incorporation, indicating a block of mitochondrial translation. A reduction of nascent (newly synthesized) mitochondrial proteins was observed to a lesser extent, in the more resistant MCF10A normal breast cell line. Equal loading of protein was insured by Coomassie blue staining of the gel (Supplementary Figure 3A). In addition, immunoblotting showed that low mitochondrial translation rates also significantly reduced total expression levels of the OXPHOS complexes in breast cancer cell lines (Figure 3B-C). Specifically, a decrease in COX II expression, which

A

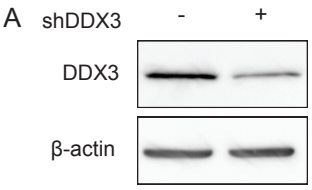

B

	RK-33		shDDX3	
Pathway	Genes (altered/total)	p-value	Genes (altered/total)	p-value
Mitochondrial translation	58/90	1.12E-36	19/90	1.78E-04
Respiratory electron transport	16/88	1.01E-03	12/88	4.03E-02

C

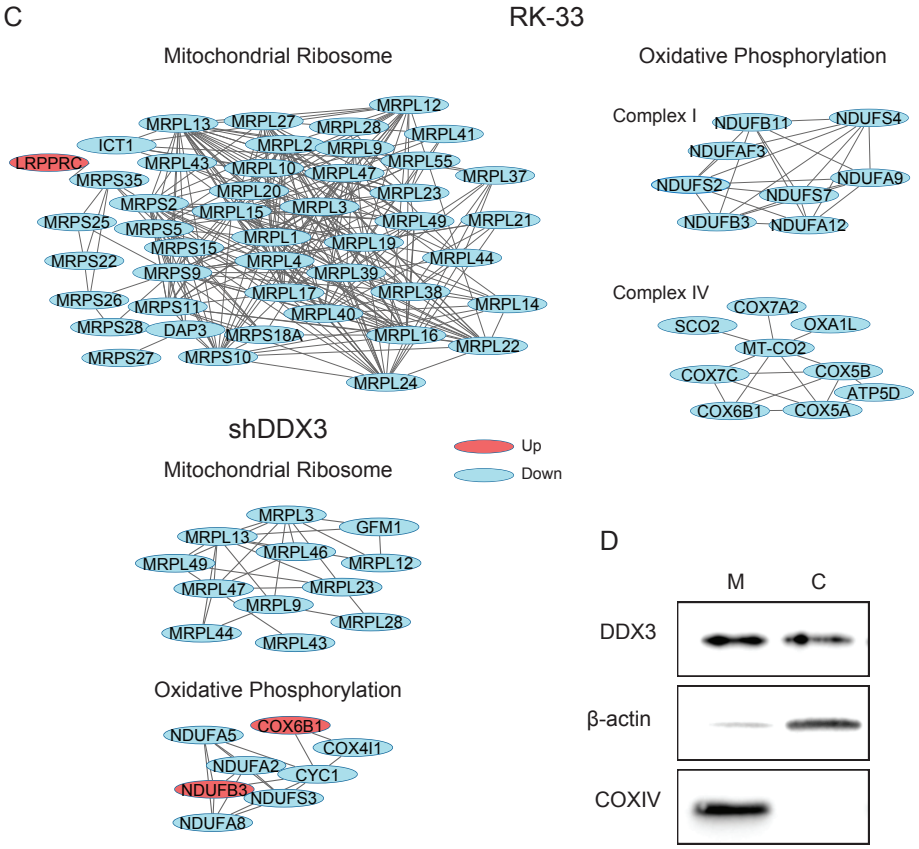

D

E

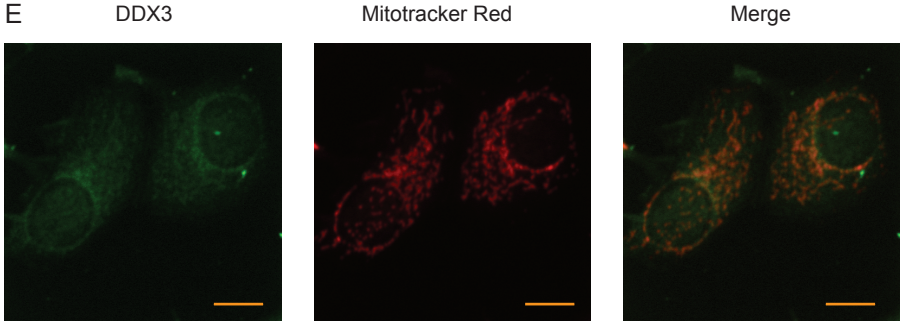

is mitochondrially encoded and translated, was observed in MCF7 (fold change 0.67; p = 0.017) and MDA-MB-231 (fold change 0.52; p = 0.012). It is not surprising that multiple OXPHOS complexes are downregulated as a result of reduced translation of mitochondrially encoded components, since the stability of these complexes is highly dependent on single components and mutations in one gene affects expression of the whole complex it belongs to and even other OXPHOS complexes[32].

RK-33 causes a bioenergetic shortage by reducing oxidative phosphorylation

Next we queried if the reduced expression of OXPHOS complexes resulted in decreased OCR. As shown in Figure 3D, basal respiration (fold change range 0.50-0.70; p <0.001) and maximum respiration rates (fold change range 0.32-0.44; p <0.001) were markedly reduced in MCF7 after 12 hours of RK-33 exposure. This result was confirmed by measuring OCR with a Clark's electrode in both MCF-7 (fold change 0.61; p = 0.077, Supplementary Figure 3B) and MDA-MB-435 (fold change 0.78; p = 0.008). In MDA-MB-231 no reduction in basal OCR was observed, but incomplete decline of OCR after oligomycin indicated an increased proton leak (fold change range 2.28-3.26; p = 0.002) and reduced ATP production (fold change range 0.90-0.64; p = 0.001). In addition, maximum respiration rates after FCCP were also reduced (fold change range 0.79-0.48; p < 0.001). No changes in OCR were observed after RK-33 treatment in MCF10A cells. At this time point less than ten percent of cells were found to be apoptotic by Annexin-PI flow cytometry (Supplementary Figure 3C). The effect of RK-33 on OCR did not occur immediately after addition (Supplementary Figure 3D). As seen in Figure 2E, a compensatory increase in ECAR, indicative of increased glycolysis, could be observed in MCF7 (fold change 2.55, p <0.001) and MDA-MB-231 12 hours after RK-33 treatment (fold change range 1.25-2.04; p = 0.031). In MCF10A, ECAR levels were unaffected. A significant drop in intracellular ATP levels was observed after exposure to RK-33 in MCF7 (fold change range 0.74-0.81; p = 0.015; Figure 3F).

Increased glycolysis adequately compensated ATP levels in MDA-MB-231 and no change was observed in MCF10A. MCF7 were more sensitive to DDX3 inhibition by RK-33, when cells were pushed to derive more of their energy from oxidative phosphorylation, by substitution of glucose with pyruvate (IC50 1.9 μM vs 3.2 μM; Supplementary Figure 3E). No difference in sensitivity was observed in MDA-MB-231.

◀ **Figure 2A-E.** DDX3 inhibition results in reduced expression of proteins involved in mitochondrial translation
A. Immunoblot showing the DDX3 expression before and after transduction with shDDX3 in MDA-MB-435 cells. B. Table showing two overrepresented Reactome pathways identified by gene set enrichment analysis of significantly altered proteins in MDA-MB-435 cells after 24 hours exposure to 4.5 μM RK-33 or after shDDX3 transduction. C. Protein networks identified by string network analysis in the group of significantly altered proteins explained under B. D. Immuno blot showing the DDX3 expression in mitochondrial (M) and cytoplasmic (C) fractions of MCF7. E. 2-foton microscopy image of MCF7 immunofluorescently stained for DDX3 and labeled with mitotracker red. Scale bar indicates 5 μm. All experiments have been replicated a minimum of two independent times.

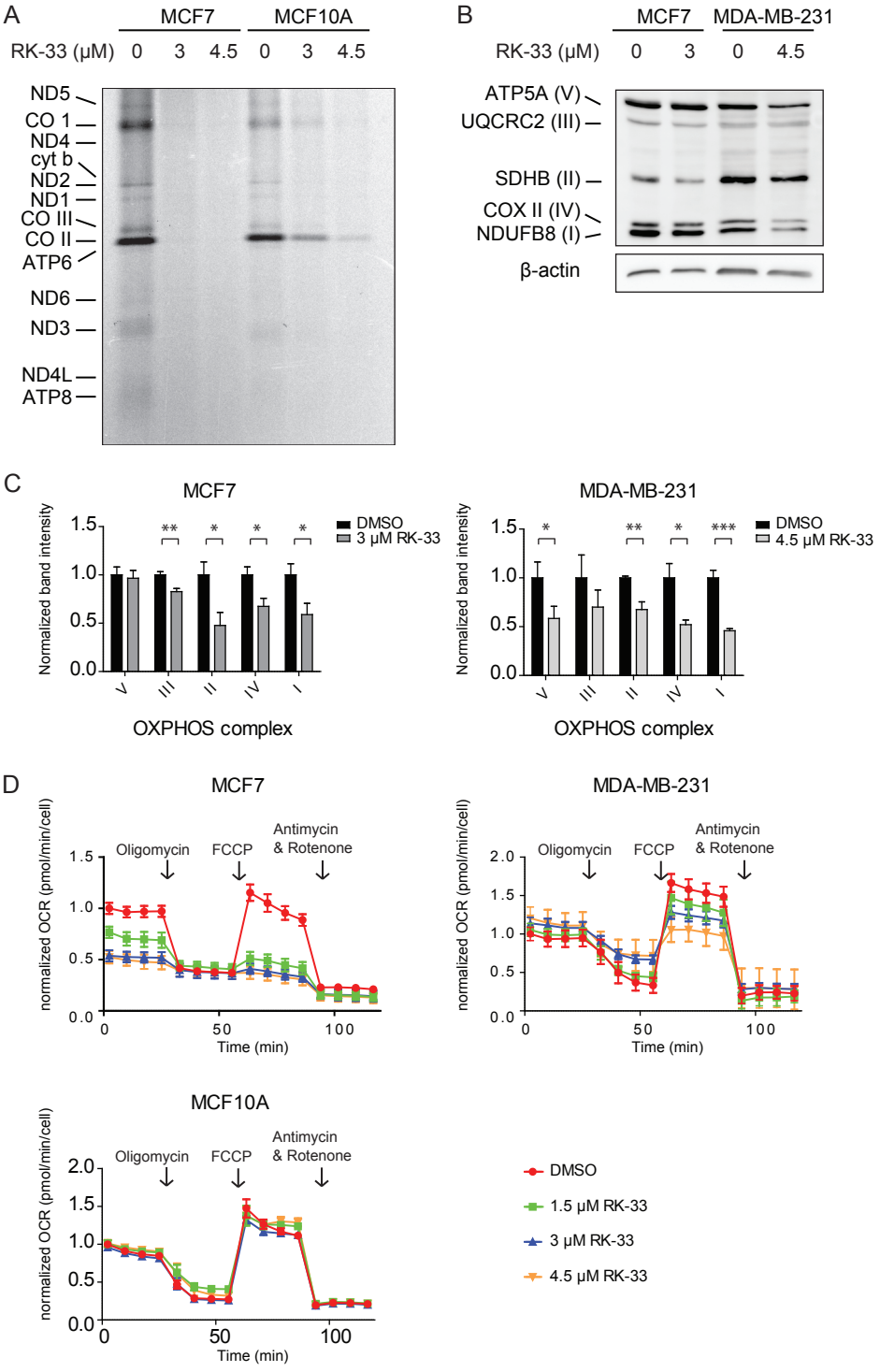
A
MCF7
MCF10A
RK-33 (μM) 0 3 4.5 0 3 4.5
ND5
CO 1
ND4
cyt b
ND2
ND1
CO III
CO II
ATP6
ND6
ND3
ND4L
ATP8
B
MCF7
MDA-MB-231
RK-33 (μM) 0 3 0 4.5
ATP5A (V)
UQCRC2 (III)
SDHB (II)
COX II (IV)
NDUFB8 (I)
β-actin
C
MCF7
Normalized band intensity
DMSO
3 μM RK-33
OXPHOS complex
MDA-MB-231
4.5 μM RK-33
D
MCF7
MDA-MB-231
MCF10A
normalized OCR (pmol/min/cell)
Oligomycin
FCCP
Antimycin & Rotenone
Time (min)
DMSO
1.5 μM RK-33
3 μM RK-33
4.5 μM RK-33

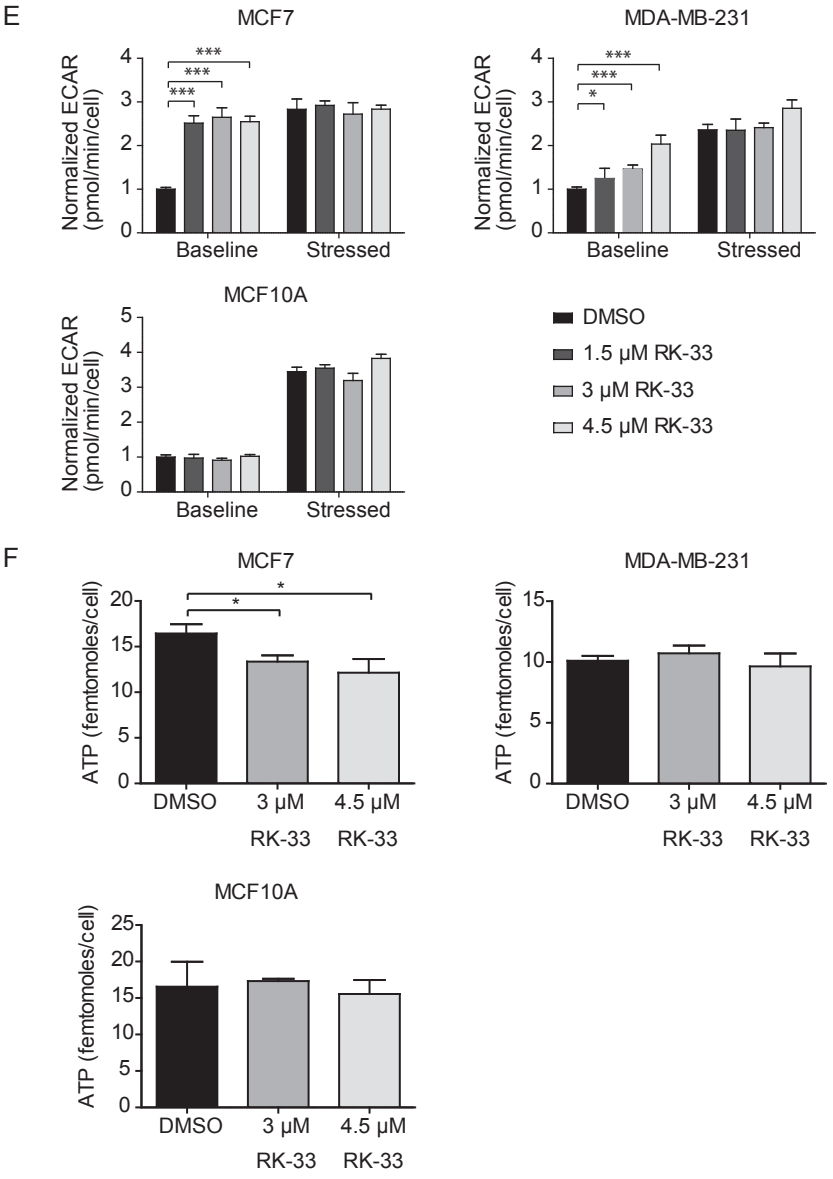

◀ **Figure 3A-F.** RK-33 reduces oxidative phosphorylation by blocking mitochondrial translation
A. Autoradiograph showing the effect of two hours RK-33 exposure on mitochondrial translation, measured by a S35-methionine pulse labeling experiment. B. Immunoblot showing the expression of OXPHOS complexes after twelve hours of RK-33 exposure. C. Bar graphs showing the OXPHOS complex band intensities normalized for β-actin after twelve hours exposure to RK-33. Graphs represent mean ± SD of 3 biological replicates. D. Normalized oxygen consumption rates (OCR) per cell measured by a Seahorse assay after twelve hours exposure to RK-33. Graphs represent mean ± SD of 6 biological replicates. E. Extracellular acidification rates (ECAR) as measured by a Seahorse assay after twelve hours exposure to RK-33 at baseline and stressed (after oligomycin and FCCP) conditions. Graphs represent mean ± SD of 6 biological replicates. F. Intracellular ATP concentrations after twelve hours exposure to RK-33. Graphs represent mean ± SD of 2 biological replicates. *$p < 0.05$, ** $p < 0.01$, *** $p < 0.001$. P-values were calculated by a Student's t-test. All experiments have been replicated a minimum of two independent times.

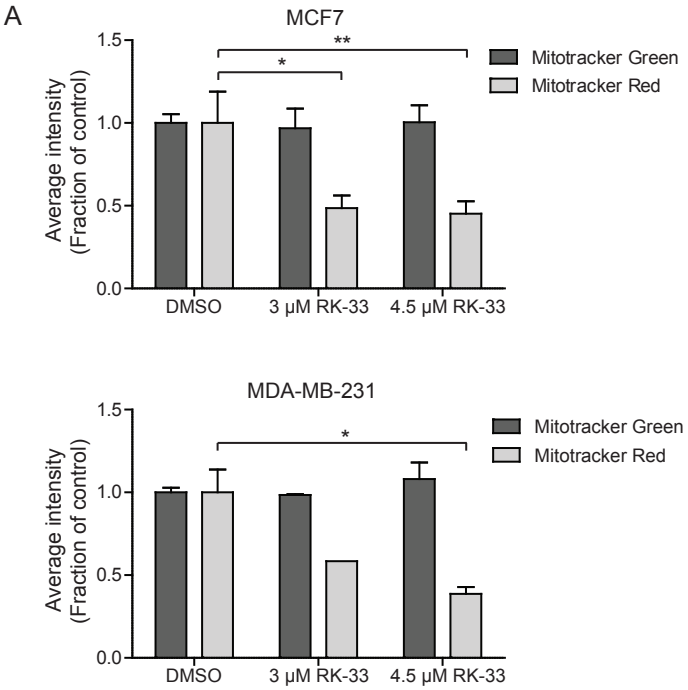
A
MCF7
Average intensity (Fraction of control)
1.5
1.0
0.5
0.0
*
**
Mitotracker Green
Mitotracker Red
DMSO
3 μM RK-33
4.5 μM RK-33
MDA-MB-231
Average intensity (Fraction of control)
1.5
1.0
0.5
0.0
*
Mitotracker Green
Mitotracker Red
DMSO
3 μM RK-33
4.5 μM RK-33

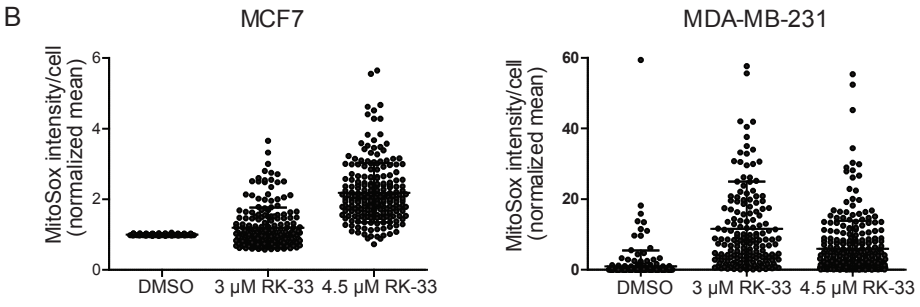
B
MCF7
MitoSox intensity/cell (normalized mean)
6
4
2
0
DMSO
3 μM RK-33
4.5 μM RK-33
MDA-MB-231
MitoSox intensity/cell (normalized mean)
60
40
20
0
DMSO
3 μM RK-33
4.5 μM RK-33

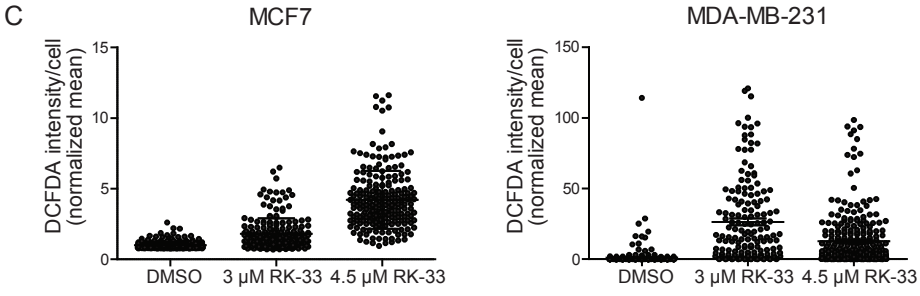
C
MCF7
DCFDA intensity/cell (normalized mean)
15
10
5
0
DMSO
3 μM RK-33
4.5 μM RK-33
MDA-MB-231
DCFDA intensity/cell (normalized mean)
150
100
50
0
DMSO
3 μM RK-33
4.5 μM RK-33

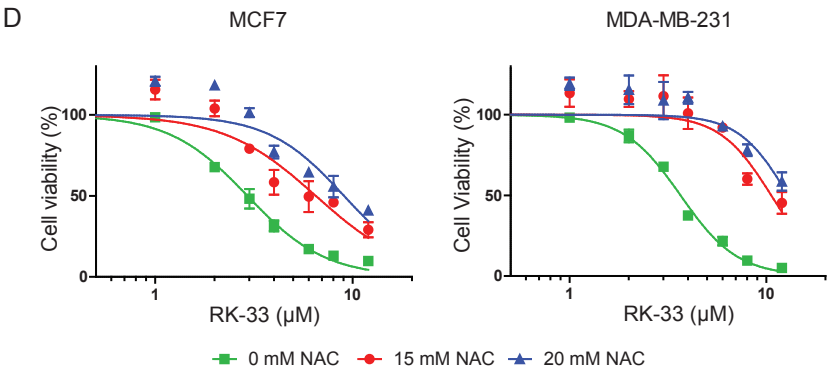

◀ **Figure 4A-D.** RK-33 treatment causes reduced mitochondrial potential and increased production of reactive oxygen species
A. Bar graphs showing the mean mitochondrial mass (mitotracker green) and membrane potential (mitotracker red) per cell after twelve hours exposure to RK-33 as measured by flow cytometry. Graphs represent mean ± SD of two biological controls. B. Dot plots showing the amount of mitochondrial superoxide production after twelve hours exposure to RK-33 as measured by the MitoSox intensity per cell. Graphs represent mean ± SD. C. Dot plots showing the amount of ROS production per cell as measured by the DCFDA intensity per cell. Graphs represent mean ± SD. D. MTS assays showing the cytotoxicity of RK-33 in the absence and presence of 15-20 mM n-acetylcysteine (NAC). Graphs represent mean ± SD of two biological replicates. *$p < 0.05$, **$p < 0.01$. P-values were calculated by a Student's t-test. All experiments have been replicated a minimum of two independent times.

RK-33 causes a collapse in mitochondrial membrane potential

A reduction in mitochondrial translation can both reduce mitochondrial biogenesis and cause defective ETC complexes resulting in a reduced H^+ membrane potential. Mitotracker labeled MCF7 and MDA-MB-231 cells, following RK-33 treatment, were analyzed with flow cytometry (Figure 4A, Supplementary Figure 4A). DDX3 inhibition with RK-33 did not affect the total amount of mitochondria as measured by mitotracker green, but a significant reduction in mitotracker red staining was observed in MCF7 (fold change range 0.39-0.45, $p = 0.012$) and MDA-MB-231 (fold change range 0.39-0.58, $p = 0.051$), indicative of a collapsed membrane potential.

RK-33 acts through generation of reactive oxygen species

Malfunctioning of the ETC complexes can elevate the extent to which electrons leak out of the chain prematurely and are being accepted by oxygen, resulting in elevated superoxide formation. RK-33 treatment resulted in increased mitochondrial superoxide and cytosolic reactive oxygen species (ROS) levels in MCF7 and MDA-MB-231 (Figure 4B & C; Supplementary Figure 4B). No change in ROS levels was observed in MCF10A (Supplementary Figure 4C). To evaluate whether ROS formation played a causative role in RK-33 induced cytotoxicity, cells were treated with the antioxidant n-acetylcysteine (NAC) and RK-33 simultaneously. Addition of 20 mM NAC significantly reduced the sensitivity to RK-33 in both MCF7 (IC50 9.05 μM vs. 2.93 μM) and MDA-MB-231 (IC50 12.91 μM vs. 3.66 μM; Figure 4D).

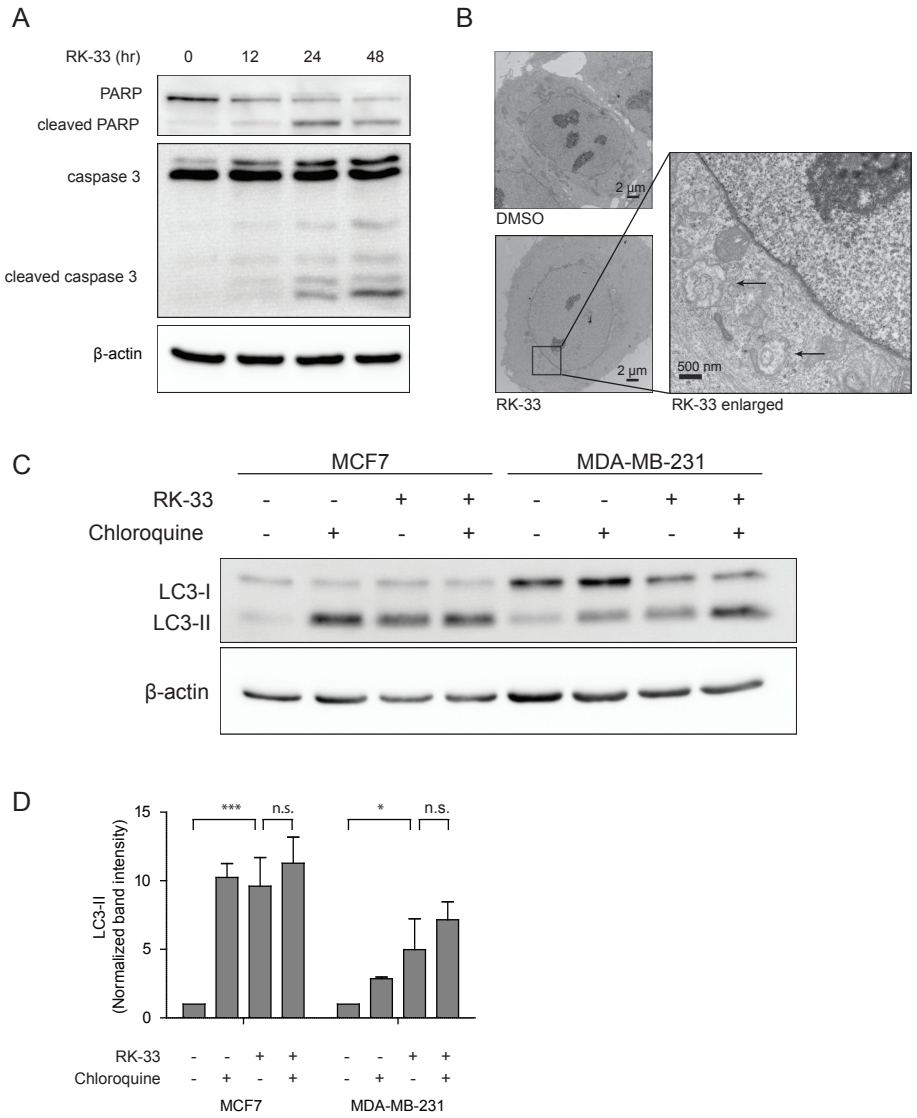

Figure 5 A-D. RK-33 induces autophagosome formation
A. Immunoblot showing PARP and caspase 3 cleavage in RK-33 treated MDA-MB-231, indicating induction of apoptosis after 24 hours of exposure. B. Transmission electron microscopy images showing the presence of autophagosomes in MCF7 cells, as indicated by arrows, after 12 hours treatment with 3 µM RK-33. C. Immunoblot showing accumulation of autophagosome specific LC3-II after twelve hours exposure to 3 µM RK-33 or one hour exposure to 50 µM Chloroquine (CQ). D. Bar graph showing the LC3-II band intensities after twelve hours RK-33 exposure normalized for β-actin. Graphs represent mean ± SD of 2 (MDA-MB-231) or 3 (MCF7) biological replicates. *p < 0.05, **p < 0.01, ***P < 0.001. P-values were calculated by a Student's t-test. All experiments have been replicated a minimum of two independent times.

RK-33 induces apoptosis and autophagosome formation

Damaged mitochondria can ultimately trigger apoptosis and cause cell death. Immunoblotting for cleaved PARP and caspase 3 as shown in Figure 5A indicated apoptosis occurred 24-48 hours after RK-33 exposure. Consistent with Annexin-PI flow cytometry (Supplementary Figure 3C), no apoptosis was observed at 12 hours at which time the changes in mitochondrial respiratory function were observed. Interestingly, acidic vesicular organelles were observed from 12 hours onward (Supplementary Figure 5), indicating that the damaged mitochondria may trigger an autophagy response. Transmission electron microscopy was used to confirm that the vesicles were indeed autophagosomes (Figure 5B). Immunoblotting for LC3-II revealed an induction after RK-33 treatment of 9.4 fold ($p < 0.001$) and 4.6 fold ($p = 0.023$) in MCF7 and MDA-MB-231 respectively, confirming an increase in the number of autophagosomes. However, inhibition of the breakdown of autophagosomes by the lysosomal inhibitor chloroquine, resulted only in limited further elevation of LC3-II levels in MCF7 (to 11.4 fold; $p = 0.371$) and MDA-MB-231 (to 7.0 fold; $p = 0.101$). Addition of 25 μM chloroquine did not affect the RK-33 sensitivity in MCF7 or MDA-MB-231 (Supplementary Figure 5B).

Combination of RK-33 and radiation therapy results in a bioenergetic catastrophe

As RK-33 was previously demonstrated to have radiosensitizing abilities[4], we explored whether these were attributable to reduced mitochondrial functions. In MCF7 basal respiration levels increased after radiation (fold change 1.21, $p = 0.002$; Figure 6A). Interestingly, RK-33 antagonized the radiation-induced increase in OCR (fold change 0.40; $p < 0.001$). In MDA-MB-231 a small reduction was observed after radiation (fold change 0.89, $p = 0.022$). Addition of RK-33 resulted in further reduction of respiration rates (fold change 0.58, $p <0.001$). Intracellular ATP levels increased after exposure to radiation in MCF7 (fold change 1.28, $p = 0.036$) and MDA-MB-231 radiation (fold change 1.37, $p = 0.016$), and this increase was blocked by RK-33 addition in both cell lines (Figure 6B). Evaluation of γH2AX foci showed that RK-33 significantly slows down DNA double strand break repair at 6 (fold change range 1.7-2.9; $p = 0.003$) and 24 hours (fold change range 3.2-5.1; $p < 0.001$) after radiation (Figure 6C-D). Furthermore, we showed that treatment with 3 μM ($p = 0.009$) and 4.5 μM RK-33 ($p = 0.006$) synergized with radiation therapy in these cells and this effect can be reversed by addition of the antioxidant NAC (Figure 6E).

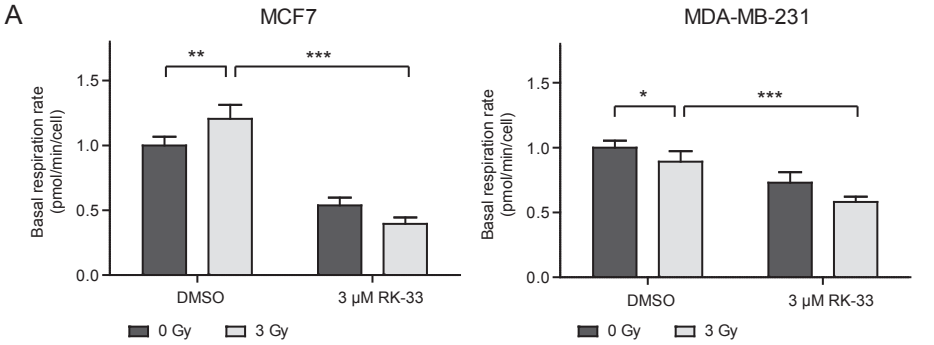
A
MCF7
MDA-MB-231
Basal respiration rate (pmol/min/cell)
1.5
1.0
0.5
0.0
**
***
*
***
DMSO
3 μM RK-33
0 Gy
3 Gy

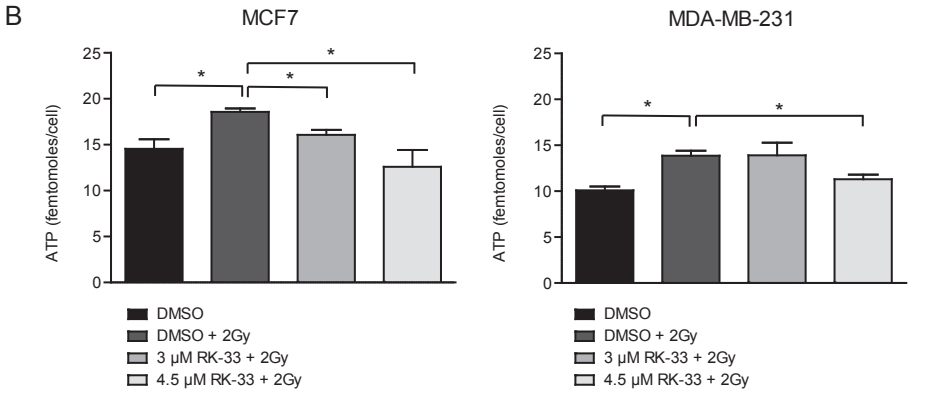
B
MCF7
MDA-MB-231
ATP (femtomoles/cell)
25
20
15
10
5
0
*
*
*
*
DMSO
DMSO + 2Gy
3 μM RK-33 + 2Gy
4.5 μM RK-33 + 2Gy

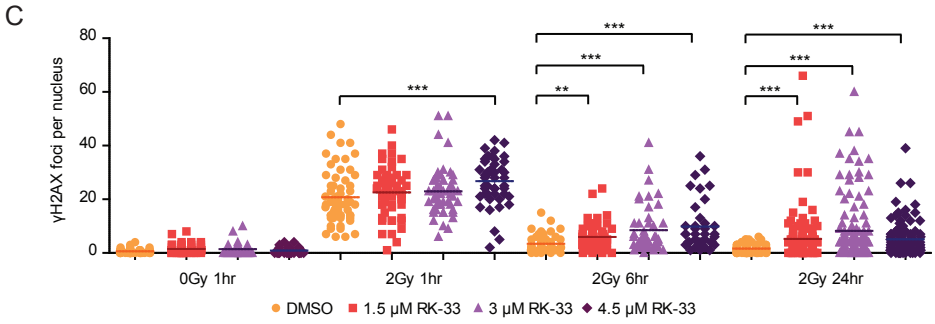
C
γH2AX foci per nucleus
80
60
40
20
0
***
**
***
***
***
***
***
0Gy 1hr
2Gy 1hr
2Gy 6hr
2Gy 24hr
DMSO
1.5 μM RK-33
3 μM RK-33
4.5 μM RK-33

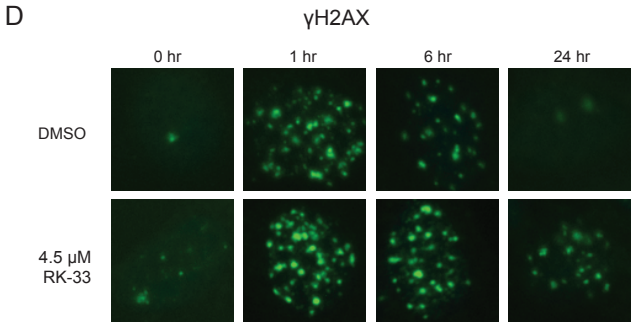
D
γH2AX
0 hr
1 hr
6 hr
24 hr
DMSO
4.5 μM RK-33

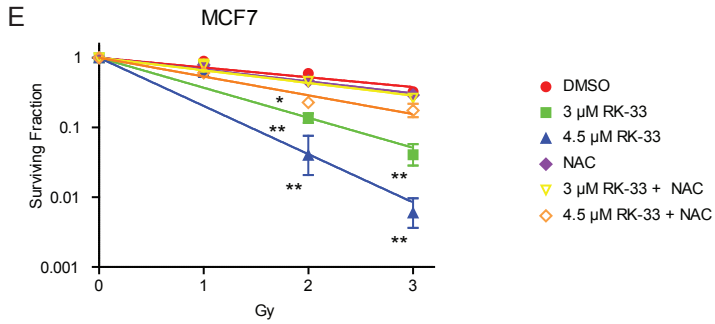

◀ **Figure 6A-E.** RK-33 radiosensitizes through reduced OXPHOS and increased ROS production
A. Bar graphs showing basal respiration rates (OCR) as measured by the Seahorse XF96 Extracellular Flux Analyzer 15 hours after exposure to 3 μM RK-33 and twelve hours after exposure to 3 Gy ionizing radiation. Graphs represent mean ± SD of 6 biological replicates. P-values were calculated by a student's t-test. B. Intracellular ATP levels 15 hours after exposure to RK-33 and twelve hours after 3 Gy ionizing radiation. Graphs represent mean ± SD of 2 biological replicates. P-values were calculated by a student's t-test. C. Dot plot showing the number of γH2AX foci after exposure to 2 Gy radiation, preceded by three hours exposure to RK-33. P-values calculated by a Mann-Whitney U test. D. Immunofluores cent image of γH2AX foci (green) as a measure of DNA double strand breaks at different timepoints after exposure to 2 Gy ionizing radiation preceded by three hours exposure to RK-33. Nuclei are labeled with DAPI. E. Colony forming assay showing the surviving fraction after ionizing radiation preceded by three hours exposure to RK-33. Values are normalized to the response to RK-33 alone. Graphs represent mean ± SD of 2 biological replicates. P-values calculated with a Student's t-test. *$p < 0.05$; ** $p < 0.01$ *** $p < 0.001$. All experiments have been replicated a minimum of two independent times.

DISCUSSION

This study aimed to elucidate the working mechanism of the DDX3 inhibitor RK-33 by studying its effect on the metabolic profile of breast cancer cells. High DDX3 expression is present in 35% of breast cancers and is associated with an aggressive phenotype and worse overall survival, making it an attractive target in breast cancer patients. We showed that RK-33 functions as a potent inhibitor of mitochondrial translation and thereby reduced the mitochondrial OXPHOS capacity and increased ROS production in cancers cells. Our results explain the selective anti-cancer activity observed after RK-33 treatment, especially in combination with radiation (Figure 7). Since normal cells have a relatively low baseline ATP demand as compared to cancer cells, the effect of RK-33 on non-transformed cells is limited. However, in cancer cells, energy use is higher and a larger OXPHOS reserve capacity is required to deal with sudden increases in ATP demand as a result of exposure to cellular stressors like ionizing radiation[14-17], especially in tumor areas that are glucose deprived[33]. The cytotoxic effect of RK-33 in these cells is therefore much larger. In addition, both ionizing radiation and RK-33 increase the intracellular ROS levels. Together these treatments result in metabolic catastrophe.
We found that the effect of RK-33 treatment on mitochondrial respiration was greater in MCF7, when compared to MDA-MB-231. However, ROS levels were increased to a similar

extent in both cell lines. Addition of the antioxidant NAC was especially protective in MDA-MB-231, indicating that the effect of RK-33 might be more ROS-mediated in this cell line. This finding is also in line with MCF7 being relatively more reliant on OXPHOS for ATP production[34]. Promotion of mitochondrial ROS production has been recognized as an effective strategy to induce cancer cell death and increase chemosensitivity[35].
Mitochondrial damage often induces the formation of autophagosomes ("mitophagy")[36]. We indeed observed an accumulation of autophagosomes after RK-33. Only a minor further increase was observed after addition of the autophagy inhibitor chloroquine, implying that the increased number of autophagosomes after RK-33 is the result of both increased production and decreased breakdown of autophagosomes. Although, autophagy has also been reported to have a chemoprotective role[37], we did not find that inhibiting autophagy with chloroquine altered the response to RK-33. This indicates that accumulation of autophagosomes following RK-33 exposure may not be a major determinant of RK-33 mediated cell death.
Although concurrent chemoradiation strategies are not mainstay treatments in breast cancer, certain breast cancer subtypes, like triple negative breast cancer, are relatively radioresistant and have higher local recurrence rates corresponding with worse overall survival[38]. The development of radiosensitizers in breast cancer could benefit this group of

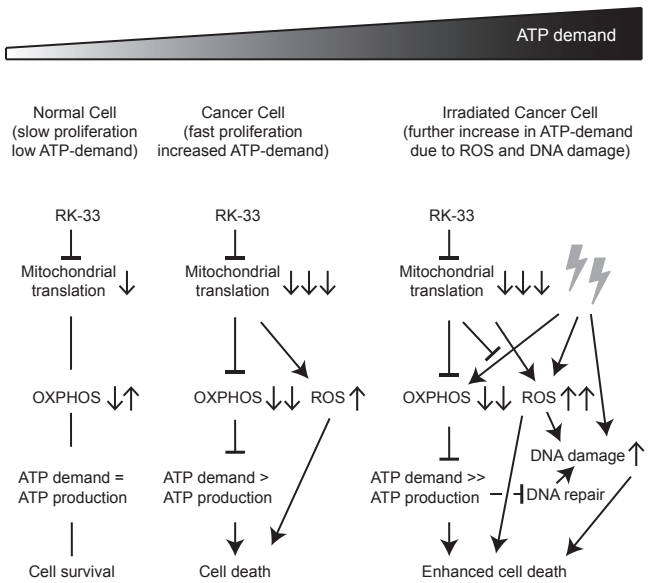

Figure 7. DDX3 inhibition with RK-33 causes metabolic synthetic lethality
Schematic overview of the mechanism behind RK-33 cytotoxicity in breast cancer cells. ATP = adenosine triphosphate, OXPHOS = oxidative phosphorylation, ROS = reactive oxygen species.

patients that we found to have particularly high DDX3 expression levels. In addition, radiosensitizers could allow for reduced radiation dose and consequently reduce normal tissue toxicity, commonly occurring after axillary and internal mammary nodal radiation for breast cancer treatment. We previously showed that the DDX3 inhibitor RK-33 is a potent radiosensitizer in cancer types where local control is particularly challenging, like lung[4] and prostate cancer[7]. Although our study focuses on breast cancer cells, it is likely that inhibition of mitochondrial translation is also part of the working mechanism of RK-33 radiosensitization in these cancers. One study in Ewing sarcoma showed RK-33 can be used as a monotherapy as well[6]. More research focusing on the use of DDX3 inhibitors as a single agent or in combination with chemotherapeutics is warranted.

Importantly, normal cell toxicity can be a concern with treatments targeting mitochondrial function. However, no toxicity was observed after RK-33 treatment in extensive toxicology studies performed in mice[4]. This is in line with the fact that normal cells have lower energy demands in general, encounter less stressors causing sudden increases in ATP demand (eg. DNA damage), have lower ROS levels and express lower amounts of DDX3.

This is the first study suggesting that DDX3 is involved in mitochondrial translation and could therefore be of paramount importance for maintenance of the bioenergetics machinery of oxidative phosphorylation. The fact that we and others[39] found DDX3 to localize to the mitochondria supports a role for DDX3 in mitochondrial translation. In addition, another DEAD/H box RNA helicase family members, DDX28 and DHX30, were recently found to be responsible for the assembly of mitochondrial ribosomes[40, 41]. Interestingly, DDX3 was identified by mass spectrometry analysis of the mitochondrial DDX28 and DHX30 interactome[41], implying that DDX3 might also be involved in mitochondrial ribosome assembly. This potentially explains why we observed a reduction in mitoribosomal proteins that are encoded on the nuclear genome as well, since disassembly of the mitoribosome could reduce its stability and therefore protein expression levels. Geissler, *et al.* previously showed that DDX3 has a role in the assembly of functional 80S ribosomes[2]. The role of DDX3 in cap-dependent cytosolic translation is disputed in literature[2, 42, 43], with most studies concluding that DDX3 inhibition does not result in major changes in general protein synthesis[44-47], but could play a role in translation of mRNAs with complex features in their 5'UTR[47, 4845]. It is possible that DDX3 functions in both cytoplasmic and mitochondrial translation. However, the timeline of events with a profound decrease in mitochondrial translation as early as two hours after treatment onset and apoptosis occurring only after 24 hours, does suggest that the effect of RK-33 on mitochondrial translation is direct.

Decades after Otto Warburg's initial observation that tumor cells upregulate glycolysis in the presence of oxygen, so-called aerobic glycolysis, cancer metabolism is an area of renewed attention[15, 49]. Increased aerobic glycolysis is often erroneously interpreted as a sign of reduced and damaged oxidative phosphorylation in cancer cells. In fact, accumulating evidence now

indicates that cancer cells are reliant on the mitochondria for their bioenergetic machinery and macromolecule synthesis function[15, 50]. Consequently, mitochondrial respiration is increasingly recognized as a viable target for anti-cancer therapy[50] and (triple negative) breast cancer treatment in particular[51, 52]. OXPHOS was found to be upregulated in cancer stem cells[53] and during metastases[16]. In addition, chemo- and radioresistant cells exhibit increased respiration rates[17, 54]. A recent study showed that irradiated cells increase OXPHOS to favor DNA repair and cell survival[18] and inhibitors of electron transport complexes can enhance radiosensitivity[55, 56]. In addition, mitochondrial translation has previously been identified as a therapeutic target in the treatment of acute myeloid leukemia[57].

We conclude that DDX3 is involved in mitochondrial translation and could therefore be of paramount importance for maintenance of the bioenergetics machinery of oxidative phosphorylation. The DDX3 inhibitor RK-33 causes radiosensitization in breast cancer cells through direct inhibition of mitochondrial translation, which results in reduced OXPHOS capacity and increased intracellular ROS levels, culminating in a bioenergetic catastrophe and eventual apoptosis.

Acknowledgements

We would like to thank Bob Cole, Tatiana Boronina and Bob O' Meally of the Johns Hopkins Mass Spectrometry and Proteomics core facility for their help with the proteomics experiments, Tri Nguyen for his help with interpretation of the electron microscopy images, the Dawson laboratory at the Johns Hopkins School of Medicine for their help with the mitochondrial translation assay and Beth Rodgers, who kindly provided us with S^{35}-methionine.

REFERENCES

1 Tanner NK, Linder P. DExD/H box RNA helicases: from generic motors to specific dissociation functions. Molecular cell 2001; **8**: 251-262.

2 Geissler R, Golbik RP, Behrens SE. The DEAD-box helicase DDX3 supports the assembly of functional 80S ribosomes. Nucleic acids research 2012; **40**: 4998-5011.

3 Botlagunta M, Vesuna F, Mironchik Y, Raman A, Lisok A, Winnard P, Jr. *et al.* Oncogenic role of DDX3 in breast cancer biogenesis. Oncogene 2008; **27**: 3912-3922.

4 Bol GM, Vesuna F, Xie M, Zeng J, Aziz K, Gandhi N *et al.* Targeting DDX3 with a small molecule inhibitor for lung cancer therapy. EMBO molecular medicine 2015; **7**: 648-669.

5 Heerma van Voss MR, Vesuna F, Trumpi K, Brilliant J, Berlinicke C, de Leng W *et al.* Identification of the DEAD box RNA helicase DDX3 as a therapeutic target in colorectal cancer. Oncotarget 2015; **6**: 28312-28326.

6 Wilky BA, Kim C, McCarty G, Montgomery EA, Kammers K, DeVine LR *et al.* RNA helicase DDX3: a novel therapeutic target in Ewing sarcoma. Oncogene 2016; **35**: 2574-2583.

7 Xie M, Vesuna F, Tantravedi S, Bol GM, Heerma van Voss MR, Nugent K *et al.* RK-33 radiosensitizes prostate cancer cells by blocking the RNA helicase DDX3. Cancer research 2016: doi:10.1158/0008-5472.CAN-1116-0440.

8 Li Y, Wang H, Wang Z, Makhija S, Buchsbaum D, LoBuglio A *et al.* Inducible resistance of tumor cells to tumor necrosis factor-related apoptosis-inducing ligand receptor 2-mediated apoptosis by generation of a blockade at the death domain function. Cancer research 2006; **66**: 8520-8528.

9 Shih JW, Wang WT, Tsai TY, Kuo CY, Li HK, Wu Lee YH. Critical roles of RNA helicase DDX3 and its interactions with eIF4E/PABP1 in stress granule assembly and stress response. The Biochemical journal 2012; **441**: 119-129.

10 Sun M, Song L, Zhou T, Gillespie GY, Jope RS. The role of DDX3 in regulating Snail. Biochimica et biophysica acta 2011; **1813**: 438-447.

11 Hagerstrand D, Tong A, Schumacher SE, Ilic N, Shen RR, Cheung HW *et al.* Systematic interrogation of 3q26 identifies TLOC1 and SKIL as cancer drivers. Cancer discovery 2013; **3**: 1044-1057.

12 Chen HH, Yu HI, Cho WC, Tarn WY. DDX3 modulates cell adhesion and motility and cancer cell metastasis via Rac1-mediated signaling pathway. Oncogene 2015; **34**: 2790-2800.

13 Kondaskar A, Kondaskar S, Kumar R, Fishbein JC, Muvarak N, Lapidus RG *et al.* Novel, Broad Spectrum Anti-Cancer Agents Containing the Tricyclic 5:7:5-Fused Diimidazodiazepine Ring System. ACS medicinal chemistry letters 2010; **2**: 252-256.

14 Vellinga TT, Borovski T, de Boer VC, Fatrai S, van Schelven S, Trumpi K *et al.* SIRT1/PGC1alpha-Dependent Increase in Oxidative Phosphorylation Supports Chemotherapy Resistance of Colon Cancer. Clinical cancer research : an official journal of the American Association for Cancer Research 2015; **21**: 2870-2879.

15 Viale A, Corti D, Draetta GF. Tumors and mitochondrial respiration: a neglected connection. Cancer research 2015; **75**: 3685-3686.

16 LeBleu VS, O'Connell JT, Gonzalez Herrera KN, Wikman H, Pantel K, Haigis MC *et al.* PGC-1alpha mediates mitochondrial biogenesis and oxidative phosphorylation in cancer cells to promote metastasis. Nature cell biology 2014; **16**: 992-1003, 1001-1015.

17 Lu CL, Qin L, Liu HC, Candas D, Fan M, Li JJ. Tumor cells switch to mitochondrial oxidative phosphorylation under radiation via mTOR-mediated hexokinase II inhibition--a Warburg-reversing effect. PloS one 2015; **10**: e0121046.

18 Qin B, Minter-Dykhouse K, Yu J, Zhang J, Liu T, Zhang H *et al.* DBC1 functions as a tumor suppressor by regulating p53 stability. Cell reports 2015; **10**: 1324-1334.

19 Moelans CB, de Weger RA, van Blokland MT, Ezendam C, Elshof S, Tilanus MG *et al.* HER-2/neu amplification testing in breast cancer by multiplex ligation-dependent probe amplification in comparison with immunohistochemistry and in situ hybridization. Cellular oncology : the official journal of the International Society for Cellular Oncology 2009; **31**: 1-10.

20 Carey LA, Perou CM, Livasy CA, Dressler LG, Cowan D, Conway K *et al.* Race, breast cancer subtypes, and survival in the Carolina Breast Cancer Study. JAMA : the journal of the American Medical Association 2006; **295**: 2492-2502.

21 Vermeulen JF, van de Ven RA, Ercan C, van der Groep P, van der Wall E, Bult P *et al.* Nuclear Kaiso expression is associated with high grade and triple-negative invasive breast cancer. PloS one 2012; **7**: e37864.

22 The Medical Research Involving Human Subjects Act [In Dutch: Wet medisch-wetenschappelijk onderzoek met mensen, WMO]. *Burgerlijk Wetboek*, 1998.

23 Bol GM, Raman V, van der Groep P, Vermeulen JF, Patel AH, van der Wall E *et al.* Expression of the RNA helicase DDX3 and the hypoxia response in breast cancer. PloS one 2013; **8**: e63548.

24 Angus AG, Dalrymple D, Boulant S, McGivern DR, Clayton RF, Scott MJ *et al.* Requirement of cellular DDX3 for hepatitis C virus replication is unrelated to its interaction with the viral core protein. The Journal of general virology 2010; **91**: 122-132.

25 Kammers K, Cole RN, Tiengwe C, Ruczinski I. Detecting Significant Changes in Protein Abundance. EuPA open proteomics 2015; **7**: 11-19.

26 Smyth GK. Linear models and empirical bayes methods for assessing differential expression in microarray experiments. Statistical applications in genetics and molecular biology 2004; **3**: Article3.

27 Chen EY, Tan CM, Kou Y, Duan Q, Wang Z, Meirelles GV *et al.* Enrichr: interactive and collaborative HTML5 gene list enrichment analysis tool. BMC bioinformatics 2013; **14**: 128.

28 Franceschini A, Szklarczyk D, Frankild S, Kuhn M, Simonovic M, Roth A *et al.* STRING v9.1: protein-protein interaction networks, with increased coverage and integration. Nucleic acids research 2013; **41**: D808-815.

29 Leary SC, Sasarman F. Oxidative phosphorylation: synthesis of mitochondrially encoded proteins and

assembly of individual structural subunits into functional holoenzyme complexes. Methods Mol Biol 2009; **554**: 143-162.
30 Rasband WS. ImageJ, vol. 2015. U. S. National Institutes of Health, Bethesda, Maryland, USA.
31 Croft D, Mundo AF, Haw R, Milacic M, Weiser J, Wu G *et al*. The Reactome pathway knowledgebase. Nucleic acids research 2014; **42**: D472-477.
32 Acin-Perez R, Bayona-Bafaluy MP, Fernandez-Silva P, Moreno-Loshuertos R, Perez-Martos A, Bruno C *et al*. Respiratory complex III is required to maintain complex I in mammalian mitochondria. Molecular cell 2004; **13**: 805-815.
33 Zhang X, Fryknas M, Hernlund E, Fayad W, De Milito A, Olofsson MH *et al*. Induction of mitochondrial dysfunction as a strategy for targeting tumour cells in metabolically compromised microenvironments. Nature communications 2014; **5**: 3295.
34 Pelicano H, Zhang W, Liu J, Hammoudi N, Dai J, Xu RH *et al*. Mitochondrial dysfunction in some triple-negative breast cancer cell lines: role of mTOR pathway and therapeutic potential. Breast cancer research : BCR 2014; **16**: 434.
35 Chen Y, McMillan-Ward E, Kong J, Israels SJ, Gibson SB. Oxidative stress induces autophagic cell death independent of apoptosis in transformed and cancer cells. Cell death and differentiation 2008; **15**: 171-182.
36 Youle RJ, Narendra DP. Mechanisms of mitophagy. Nature reviews Molecular cell biology 2011; **12**: 9-14.
37 Huang Z, Zhou L, Chen Z, Nice EC, Huang C. Stress management by autophagy: Implications for chemoresistance. International journal of cancer Journal international du cancer 2016; **139**: 23-32.
38 Eiermann W, Vallis KA. Locoregional treatments for triple-negative breast cancer. Annals of oncology : official journal of the European Society for Medical Oncology / ESMO 2012; **23 Suppl 6**: vi30-34.
39 Oshiumi H, Sakai K, Matsumoto M, Seya T. DEAD/H BOX 3 (DDX3) helicase binds the RIG-I adaptor IPS-1 to up-regulate IFN-beta-inducing potential. European journal of immunology 2010; **40**: 940-948.
40 Antonicka H, Shoubridge EA. Mitochondrial RNA Granules Are Centers for Posttranscriptional RNA Processing and Ribosome Biogenesis. Cell reports 2015.
41 Tu YT, Barrientos A. The Human Mitochondrial DEAD-Box Protein DDX28 Resides in RNA Granules and Functions in Mitoribosome Assembly. Cell reports 2015.
42 Shih JW, Tsai TY, Chao CH, Wu Lee YH. Candidate tumor suppressor DDX3 RNA helicase specifically represses cap-dependent translation by acting as an eIF4E inhibitory protein. Oncogene 2008; **27**: 700-714.
43 Lee CS, Dias AP, Jedrychowski M, Patel AH, Hsu JL, Reed R. Human DDX3 functions in translation and interacts with the translation initiation factor eIF3. Nucleic acids research 2008; **36**: 4708-4718.
44 Abaeva IS, Marintchev A, Pisareva VP, Hellen CU, Pestova TV. Bypassing of stems versus linear base-by-base inspection of mammalian mRNAs during ribosomal scanning. The EMBO journal 2011; **30**: 115-129.
45 Soto-Rifo R, Rubilar PS, Limousin T, de Breyne S, Decimo D, Ohlmann T. DEAD-box protein DDX3 associates with eIF4F to promote translation of selected mRNAs. The EMBO journal 2012; **31**: 3745-3756.
46 Fukumura J, Noguchi E, Sekiguchi T, Nishimoto T. A temperature-sensitive mutant of the mammalian RNA helicase, DEAD-BOX X isoform, DBX, defective in the transition from G1 to S phase. Journal of biochemistry 2003; **134**: 71-82.
47 Lai MC, Lee YH, Tarn WY. The DEAD-box RNA helicase DDX3 associates with export messenger ribonucleoproteins as well as tip-associated protein and participates in translational control. Molecular biology of the cell 2008; **19**: 3847-3858.
48 Lai MC, Chang WC, Shieh SY, Tarn WY. DDX3 regulates cell growth through translational control of cyclin E1. Molecular and cellular biology 2010; **30**: 5444-5453.
49 Koppenol WH, Bounds PL, Dang CV. Otto Warburg's contributions to current concepts of cancer metabolism. Nature reviews Cancer 2011; **11**: 325-337.
50 Weinberg SE, Chandel NS. Targeting mitochondria metabolism for cancer therapy. Nature chemical biology 2015; **11**: 9-15.
51 Sansone P, Ceccarelli C, Berishaj M, Chang Q, Rajasekhar VK, Perna F *et al*. Self-renewal of CD133(hi) cells by IL6/Notch3 signalling regulates endocrine resistance in metastatic breast cancer. Nature communications 2016; **7**: 10442.
52 Jones RA, Robinson TJ, Liu JC, Shrestha M, Voisin V, Ju Y *et al*. RB1 deficiency in triple-negative breast cancer induces mitochondrial protein translation. The Journal of clinical investigation 2016.
53 Farnie G, Sotgia F, Lisanti MP. High mitochondrial mass identifies a sub-population of stem-like cancer cells that are chemo-resistant. Oncotarget 2015; **6**: 30472-30486.
54 Matassa DS, Amoroso MR, Lu H, Avolio R, Arzeni D, Procaccini C *et al*. Oxidative metabolism drives inflammation-induced platinum resistance in human ovarian cancer. Cell death and differentiation 2016.
55 Wardman P, Anderson RF, Hodgkiss RJ, Parrick J, Smithen CE, Wallace RG *et al*. Radiosensitization by non-nitro compounds. International journal of radiation oncology, biology, physics 1982; **8**: 399-401.
56 Zhang X, Zhou X, Chen R, Zhang H. Radiosensitization by inhibiting complex I activity in human hepatoma HepG2 cells to X-ray radiation. Journal of radiation research 2012; **53**: 257-263.
57 Skrtic M, Sriskanthadevan S, Jhas B, Gebbia M, Wang X, Wang Z *et al*. Inhibition of mitochondrial translation as a therapeutic strategy for human acute myeloid leukemia. Cancer cell 2011; **20**: 674-688.

SUPPLEMENTARY

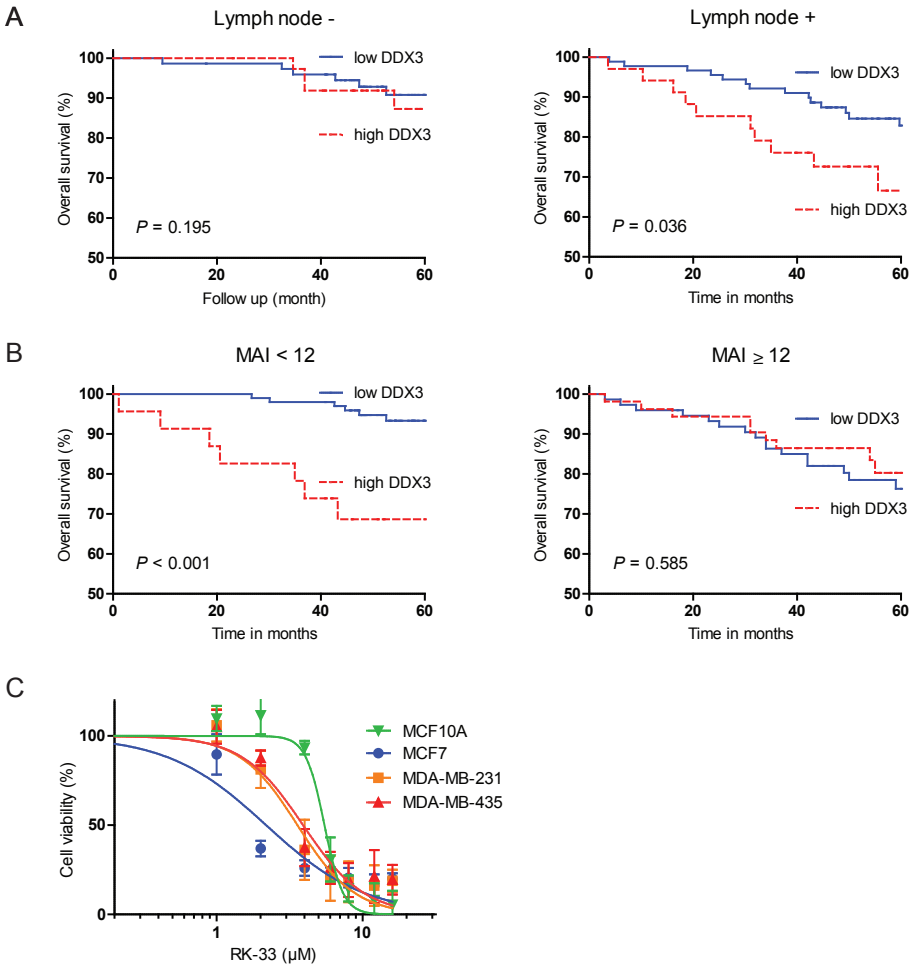

Supplementary Figure 1. DDX3 is a therapeutic target in breast cancer
A. Kaplan-Meier plot showing overall survival in low vs. high DDX3 expression in 112 lymph node negative and 123 lymph node positive breast cancer patients. P-values calculated by Breslow test. B. Kaplan-Meier plot showing overall survival in low vs. high DDX3 expression in 123 patients with low proliferating breast cancer (MAI < 12) and in 127 patients with high proliferating breast cancer (MAI ≥ 12). P-values calculated by Breslow test. C. Sensitivity of cell lines to RK-33 as measured by a calcein green based cell viability assay. Graphs represent mean ± SD of 3 biological replicates.

Supplementary table 1. Multivariate survival analysis (Cox regression)

Feature	Hazard ratio	P-value
Tumor size	1.096	0.486
Lymph node status	2.245	0.039
Grade	1.134	0.857
Mitotic index (mitosis / 2mm²)	1.865	0.161
DDX3	1.697	0.154

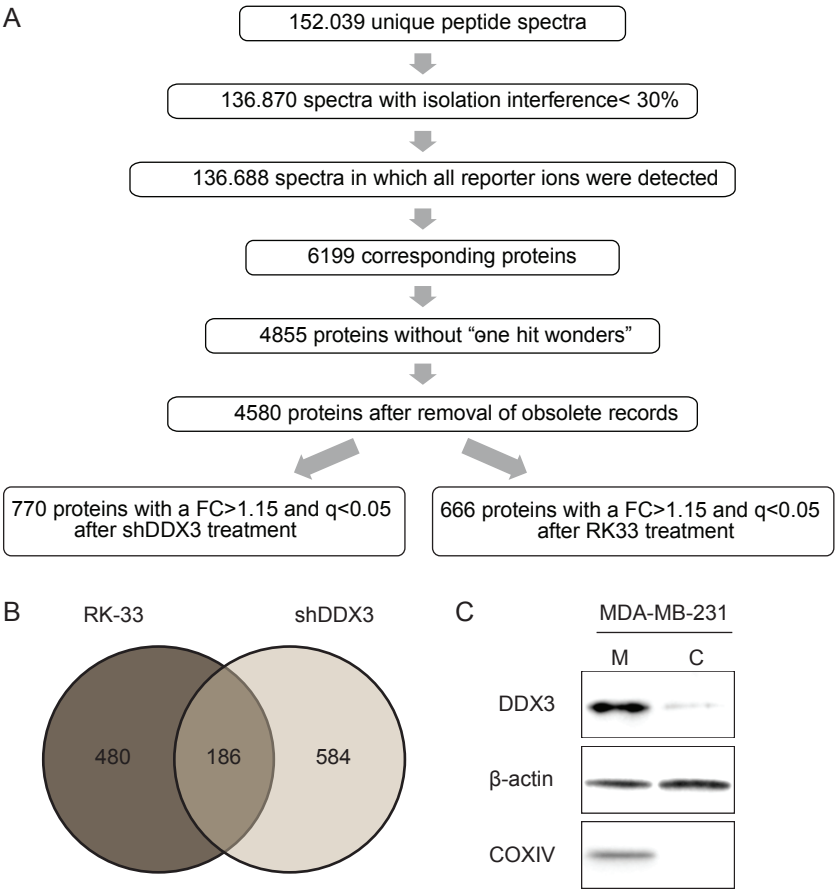

Supplementary Figure 2. Proteomic analysis of RK-33 and shDDX3 treated cells
A. Flow chart showing bioinformatic processing of the proteomics results. B. Venn diagram showing the overlap of proteins significantly altered after RK-33 treatment and knockdown of DDX3 with shDDX3. C. Immunoblot showing DDX3 expression in cytoplasmic and mitochondrial protein extraction of MDA-MB-231 cells. All experiments have been replicated a minimum of two independent times.

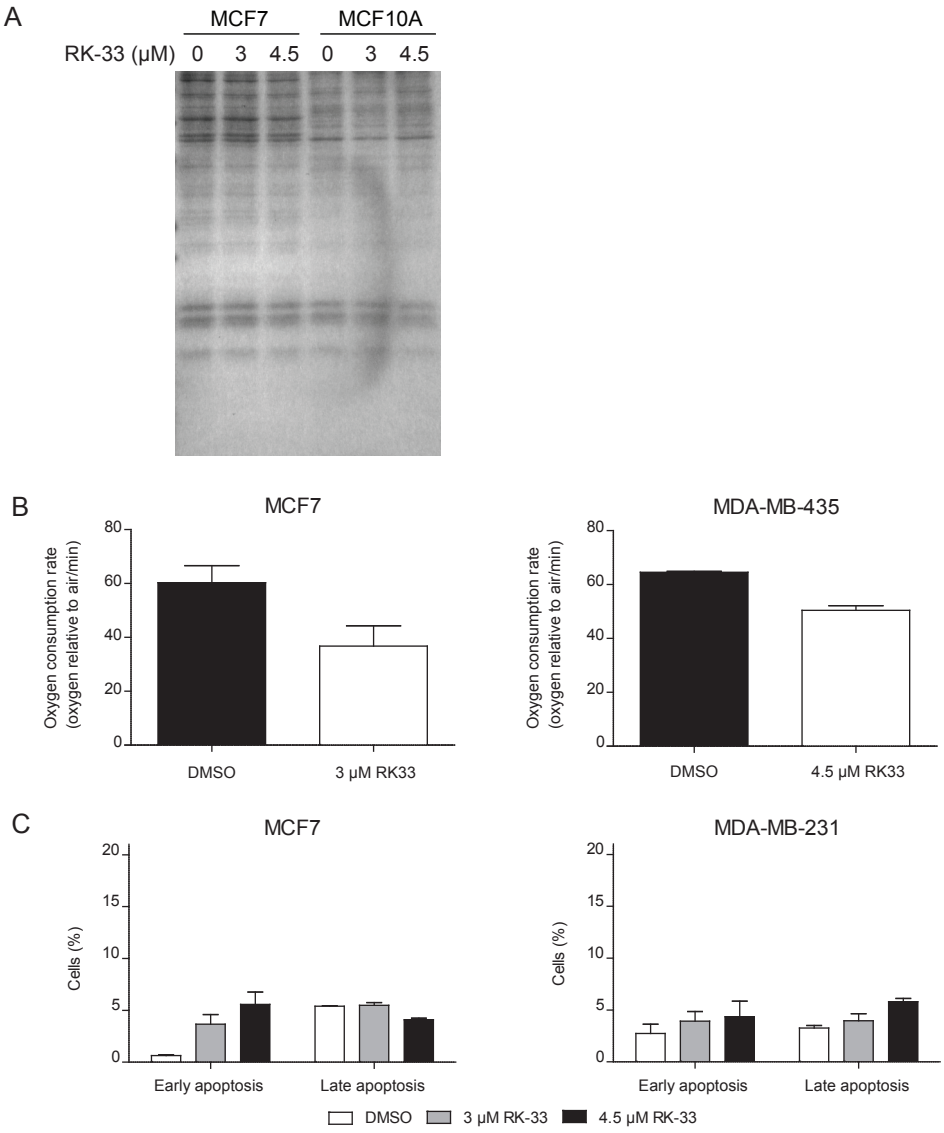

Supplementary Figure 3. RK-33 inhibits mitochondrial translation and OXPHOS in breast cancer cells
A. Coomassie staining of SDS-PAGE gel loaded with protein extracts of the mitochondrial translation S35-methionine pulse labeling experiment, showing equal amounts of protein loaded for all samples. B. Bar graph representing OCR as measured by a Clark's electrode in MCF7 and MDA-MB-435 after 12 hours RK-33 exposure. Graphs represent mean ± SD of 2 biological replicates. C. Bar graphs representing percentage of early and late apoptotic cells as measured by annexin and PI flow cytometry respectively. Graphs represent mean ± SD of 2 biological replicates.
See next page for D and E ▶

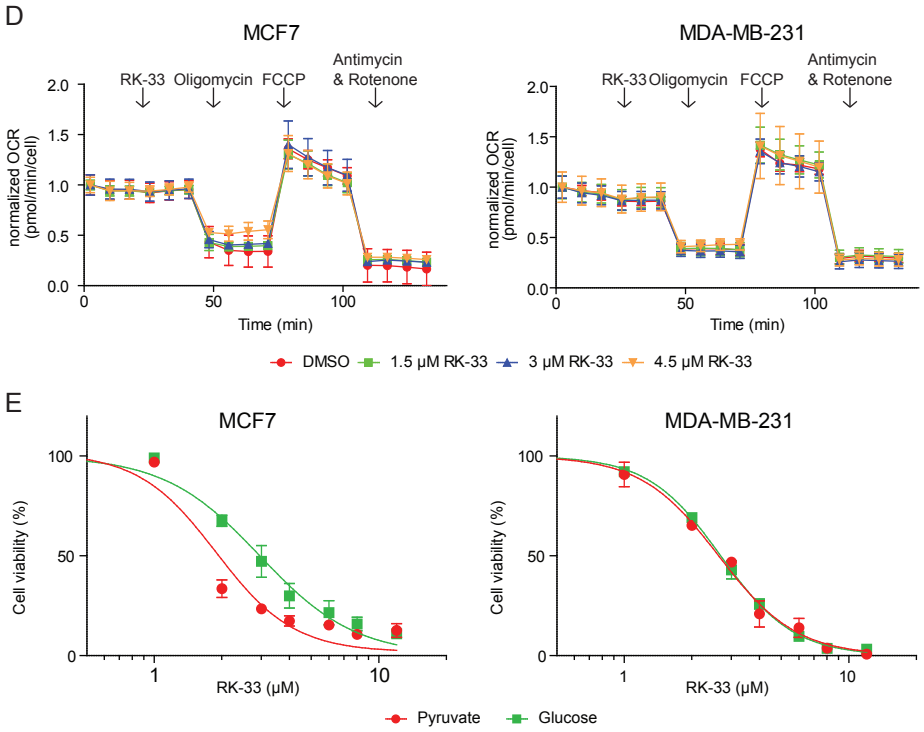

◀ **Supplementary Figure 3.** RK-33 inhibits mitochondrial translation and OXPHOS in breast cancer cells
D. Oxygen consumption rates do not change directly after RK-33 injection as measured by a Seahorse XF96 extracellular flux analyzer. Graphs represent mean ± SD of 6 biological replicates. E. MTS assays showing the cytotoxicity of RK-33 in the presence of glucose or pyruvate. Graphs represent mean ± SD of 2 biological replicates.

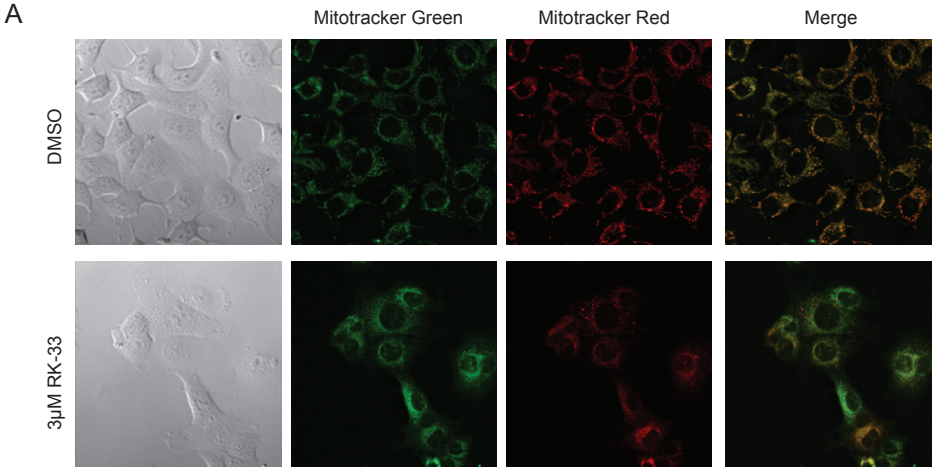

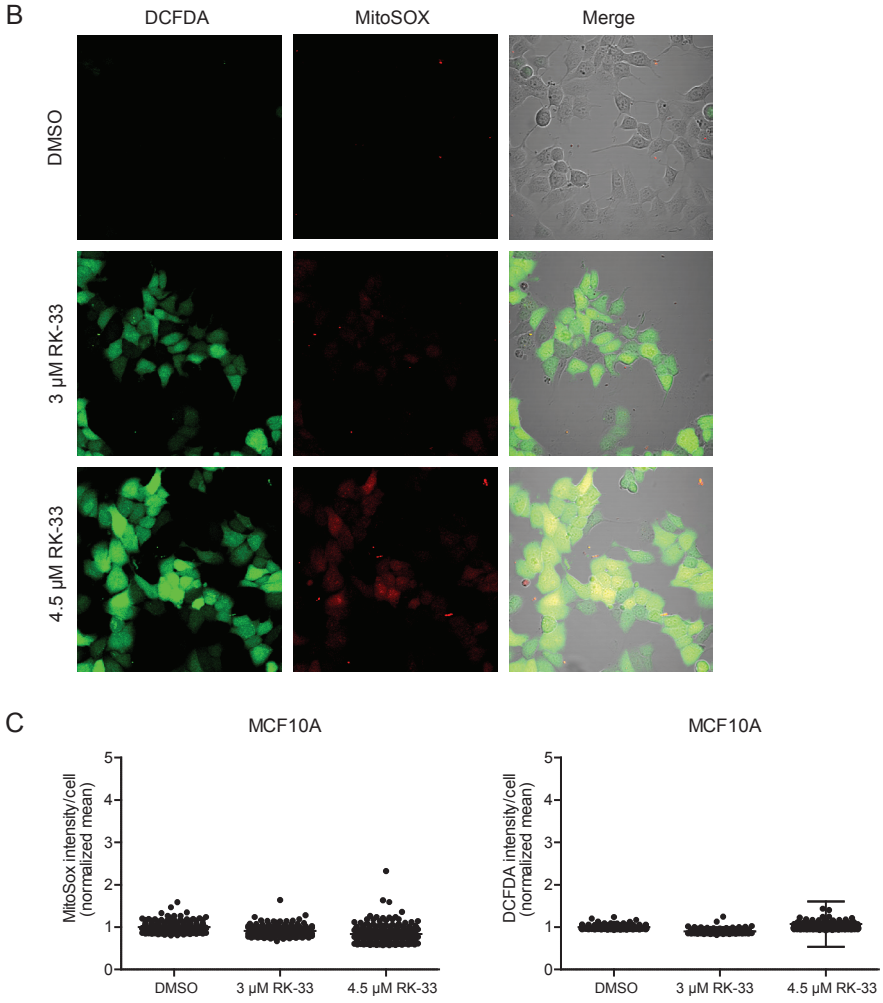

◀ **Supplementary Figure 4.** DDX3 inhibition with RK-33 results in a collapses mitochondrial membrane potential A. Fluorescent images showing MCF7 cells after 12 hours exposure to RK-33, labeled with mitotracker red to detect membrane potential and mitotracker green as a measure of mitochondrial mass. B. Examples of fluorescent images showing DCFDA and MitoSox labeling in MCF7 treated for twelve hours with RK-33. C. Dot plots showing the amount of mitochondrial superoxide production as measured by MitoSox intensity per cell and the amount of ROS production per cell as measured by the DCFDA intensity per cell in MCF10A cells. Graphs represent mean ± SD.

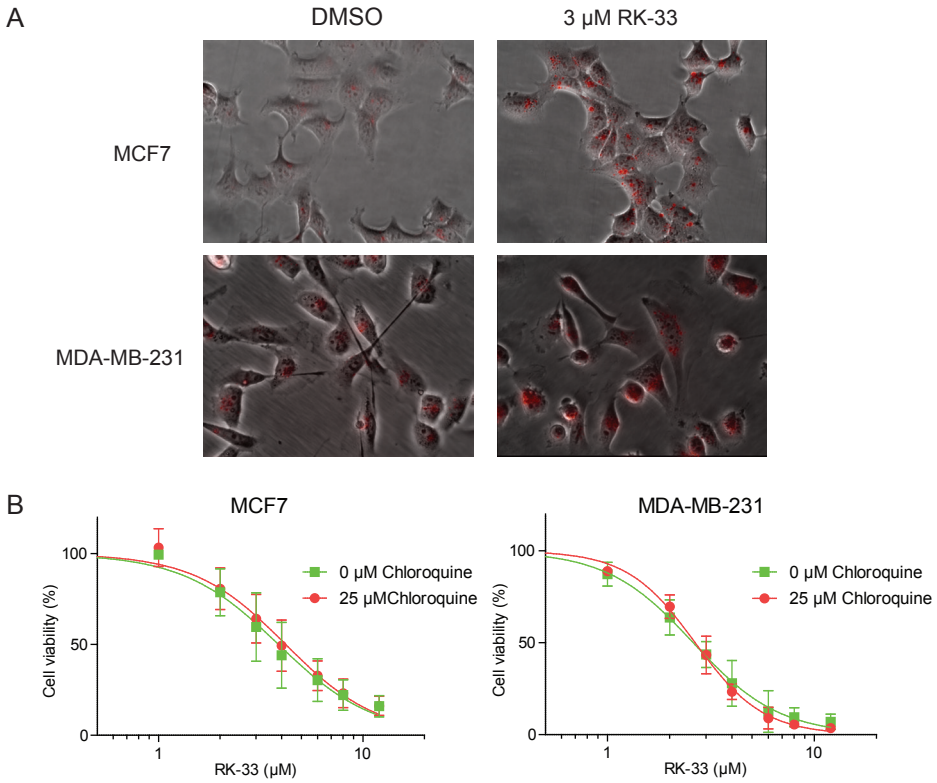

Supplementary Figure 5. RK-33 causes accumulation of acidic vesicular organelles in breast cancer cells
A. Fluorescent images showing MCF7 after 12 hours exposure to RK-33 labeled with acridine orange to detect acidic vesicular organelles as an indication of the presence of autophagosomes. B. MTS assays showing the cytotoxicity of RK-33 in the absence or presence of 25 µM chloroquine. Graphs represent mean ± SD of biological replicates.

CHAPTER 3

Global effects of DDX3 inhibition on cell cycle regulation identified by a combined phosphoproteomics and single cell tracking approach

Marise R Heerma van Voss, Kai Kammers, Farhad Vesuna, Justin Brilliant, Yehudit Bergman, Saritha Tantravedi, Xinyan Wu, Robert N. Cole, Andrew Holland, Paul J van Diest, Venu Raman

ABSTRACT

DDX3 is an RNA helicase with oncogenic properties. The small molecule inhibitor RK-33 is designed to fit into the ATP binding cleft of DDX3 and hereby block its activity. RK-33 has shown potent activity in preclinical cancer models. However, the mechanism behind the antineoplastic activity of RK-33 remains largely unknown. In this study we used a dual phosphoproteomic and single cell tracking approach to evaluate the effect of RK-33 on cancer cells.

MDA-MB-435 cells were treated for 24 hours with RK-33 or vehicle control. Changes in tandem mass tag labeled (phospho)peptide abundance were analyzed with quantitative mass spectrometry. At the proteome level we mainly observed changes in mitochondrial translation, cell division pathways and proteins related to cell cycle progression. Analysis of the phosphoproteome indicated decreased CDK1 activity after RK-33 treatment. To further evaluate the effect of DDX3 inhibition on cell cycle progression over time we performed timelapse microscopy of Fluorescent Ubiquitin Cell Cycle Indicators labeled cells after RK-33 or siDDX3 exposure. DDX3 inhibition resulted in a global delay in cell cycle progression in all interphases and mitosis. In addition, we observed an increase in endoreduplication.

Overall we conclude that DDX3 inhibition affects cells in all phases and causes a global cell cycle progression delay. Both single cell tracking and (phospho)proteomic data indicated a central role for CDK1.

INTRODUCTION

DEAD box RNA helicases form a large protein family with ATPase dependent helicase activity and are characterized by the presence of a highly conserved D-E-A-D motif. Due to their ability to unwind complex RNA structures, they have been linked to virtually all steps of RNA processing: from transcription and translation to the regulation of small non-coding RNA's[1]. DDX3, also known as DDX3X, is a family member which has an oncogenic role in the development of breast[2] and several other types of cancer[3-5]. DDX3 was demonstrated to have anti-apoptotic properties[6-8] and to play a role in migration[2, 9] and invasion[10-12]. In addition, several studies have linked DDX3 to cell cycle progression[13, 14] and DDX3 inhibition has been reported to result in a G1-arrest[3, 4]. Interestingly, the mechanism by which DDX3 regulates these processes is not limited to mRNA translational control. DDX3, like other DEAD box RNA helicases, was found to be multifunctional[15] and for instance directly regulates the kinase activity of CK1ε[16].

A small molecule inhibitor, RK-33, was recently developed to target DDX3 for cancer treatment[17]. RK-33 is designed to inactivate DDX3 by binding to its ATP pocket and was found to block the *in vitro* helicase activity of the yeast homologue of DDX3, Ded1p. Pull down experiments showed that RK-33 selectively binds DDX3 over other DEAD box RNA helicase family members[4]. Several preclinical models demonstrated RK-33 to have potent anti-cancer activity, both as a monotherapy[18] and as a radiosensitizer[4, 5]. However, better understanding of the mechanism through which RK-33 exerts its effect is needed.

This study aims to further elucidate the working mechanism of DDX3 inhibition with RK-33 by using a dual approach. Given the known role of DDX3 in translation and regulation of kinase activity we performed a phosphoproteomics experiment, to monitor the changes after RK-33 treatment on the protein expression level, as well as the protein phosphorylation status. In addition, since DDX3 has been linked to cell cycle progression, and cell cycle status has a strong influence on the phosphoproteomic landscape of the cell, we tracked the cell cycle status of single cells after RK-33 exposure, to shed further light on the influence of DDX3 inhibition on cell cycle progression over time.

METHODS

Cell culture

MCF7 and MDA-MB-435 cells were originally purchased from the American Type Culture Collection (ATCC, Manassas, VA, USA). Cell lines were STR-profiled (Geneprint 10, Promega, Madison, WI, USA, last in November 2015) and mycoplasma tested (Universal Mycoplasma Detection Kit, ATCC, last in January 2016) on a regular basis. For proteomics experiments MDA-MB-435 cells were plated in 100 mm dishes and allowed to attach

overnight. Three replicates were exposed to 4.5 μM RK-33 or DMSO for 24 hours and harvested in extraction buffer, containing 1% SDS, 1 mM EDTA, 1 mM sodium orthovanadate, 1 mM sodium pyrophosphate, 1 mM β-glycerophosphate, 1 mM sodium fluoride and proteinase inhibitor cocktail. 500 μg of protein was digested with trypsin.

Proteomics

Peptides were labeled with 10plex isobaric tandem mass tags (TMT) (ThermoFisher Scientific) and mixed. 500 μg of peptides was fractionated with basic reverse phase chromatography into 24 fractions. 10% of each fraction, or approximately 50 μg of 24 fractions, was used directly for overall protein abundance analysis. The remaining 450 μg of peptides in 24 fraction was enriched with TiO_2 for analysis of the phosphorylation at Serine and Threonine residues. Not enriched and phosphor-enriched peptides were analyzed on a Thermo Scientific Q Exactive Plus mass spectrometer interfaced with an Easy-nLC 1000 (Thermo Fisher Scientific). Peptides were identified from isotopically resolved masses in precursor (MS) and fragmentation (MS/MS) spectra extracted using 3 nodes (without deconvolution and with deconvolution by Xtract or MS2 Processor) in Proteome Discoverer (PD) software (v1.4, Thermo-Fisher Scientific, San Jose, CA. USA) and searched with Mascot 5.2.1 (Matrix Sciences, Boston, MA, USA) against the RefSeq2015 database. Search criteria included sample species; trypsin as the enzyme, allowing one missed cleavage; cysteine carbamidomethylation and TMT 10-plex labeling of N-termini as fixed modifications; methionine oxidation, asparagine and glutamine deamination, and TMT 10-plex labeling of lysine and phosphorylation of serine and threonine as variable modifications.

Bioinformatics and Statistics; Proteomics

Only spectra with a false discovery rate smaller than 1% and mass isolation interference smaller than 30%, in which all reporter ions were detected, were included for downstream analyses. Individual protein relative abundances were calculated by: (1) log2-transformation of the reporter ion intensities, (2) subtracting the spectrum medians of the log2 transformed reporter ion intensities (median-polishing), and (3) summarizing all reporter ion intensities that belong to the same protein by their median value. In a final step (4), the channel medians across all proteins were subtracted to correct for potential loading differences, as described previously[19]. Only proteins quantified by reporter ion spectra from more than one peptide were included for statistical downstream analyses. Protein abundances were compared between three RK-33 treated vs DMSO treated samples. Statistical inference between two groups of interest was assessed by moderated t-test statistics[20, 21]. For multiple comparison correction, q-values were calculated from the observed moderated p-values. Proteins with a $q < 0.05$ and a fold change larger than 1.15 were considered significantly altered.

Gene set expression analysis and network analysis

Gene set expression analysis was performed by searching Geneontology Biological Processes database using the Gorilla web tool, with all identified proteins (significantly altered and unaltered) as the background dataset[22]. FDR q-values were calculated using the Benjamini and Hochberg method from unadjusted p-values of hypergeometric enrichment tests. GOterms with a q-value < 0.05 were considered significant. Only the most specific GOterm in a family is shown, ignoring less-specific parent terms. Interactions within the group of significantly altered proteins were surveyed by searching the STRING database[23, 24] version 9.1, using a confidence level of 0.9.

Bioinformatics and Statistics; Phosphoproteomics

Phosphopeptide abundances were normalized to the abundance of the corresponding protein in the unenriched analysis and were than compared between three RK-33 treated vs DMSO treated samples. Only unique phosphopeptides with an isolation interference < 30% and a PhosphoRS score >70%, that corresponded to a single protein and for which all reporter ions could be detected, were included in the final analysis.

Motif analysis

The surrounding sequence (7 amino acids up- and downstream) of all identified phosphorylation sites was downloaded from the RefSeq database. This was not possible for phosphosites in close proximity of the C- or N-terminus, which were therefore excluded from the motif analysis. The motif-x algorithm was used to identify motifs that were enriched among the significantly up- or downregulated phosphopeptides[25]. Only motifs with a $p < 0.01$ and a minimum occurrence of 9 times were selected. Enrichment of motifs was calculated against a background dataset with all identified phosphosites. Kinases known to phosphorylate the phosphopeptides of the identified motifs were looked up in the Networkin database[26].

Kinase enrichment analysis

Kinase enrichment analysis (KEA) was performed with the KEA2 webtool[27], using both significantly altered individual phosphopeptide sites and phosphorylated proteins as input. Only kinases with a Benjamini-Hochberg corrected p-value smaller than 0.05 were considered statistically significant.

FUCCI timelapse microscopy

MDA-MB-435 and MCF7 cells were lentivirally transduced with constructs encoding the Fluorescent Ubiquitin Cell Cycle Indicators (FUCCI) sensors mCherry-hCdt1 (Genbank accession nr: AB512478) and mVenus-hGeminin (Genbank accession nr: AB512479) in the pCSII-EF vector[28]. Double positive cells were selected by fluorescence activated cell

sorting. For DDX3 knockdown in MCF7 FUCCI cells, cells were transfected with jetPrime transfection reagent (Polyplus, New York, NY, USA) and 80 nM sicontrol (non-targeting pool) or siDDX3 sequences (ON-*TARGETplus,* Dharmacon, Lafayette, CO, USA). For tracking of single cells after DDX3 inhibition, FUCCI transduced cells were grown on collagen-coated, four chamber, glass bottom, 35 mm dishes (Greiner) and allowed to attach overnight. Timelapse imaging was started directly after RK-33 addition or 48 hours after siDDX3 transfection. Seven by three μm z-sections were acquired with five minute intervals during 24 hours in the FITC and TRITC channel and by differential interference contrast, using a Deltavision Elite system (GE Healthcare) controlling a Scientific CMOS camera (pco.edge 5.5.) and an Olympus 20× 0.75 NA air objective. After projection, the movies were assembled and analyzed in FIJI[29]. The duration of each cell cycle of single cells was monitored and compared between treatment conditions. Cell cycle analysis was halted when a cell underwent extensive vacuolization, apoptosis or necrosis. Cells were declared arrested when no progression to the next cell cycle phase occurred within 24 hours. Mitotic duration was calculated as the time taken from nuclear envelope breakdown until cytokinesis was completed. Median time in mitosis was compared by a Mann-Whitney U test. Time to vacuolization or death was compared per cell cycle phase at onset of RK-33 treatment by plotting Kaplan-Meijer curves and performing log-rank tests.

Immunoblotting

All cells were harvested at 50-70 % confluency. Cells were lysed in SDS-extraction buffer and sonicated on ice. 30 μg protein was loaded on SDS-PAGE gels for gel-electrophoresis. The blots were probed overnight with primary antibodies against DDX3 (1:1000, mAb AO196)[30], β-actin (1:10000, A5441, Sigma-Aldrich), CDK1 (1:1000, #9116, Cell Signaling Technology) and p-CDK1 (Tyr15, #9111, Cell Signaling Technology) followed by appropriate secondary antibodies, development with ECL (Bio-Rad, Hercules, CA, USA) and imaging with a G:BOX Chemi XR5 (Syngene, Frederick, MD, USA).

RESULTS

Proteomic analysis after treatment with the DDX3 inhibitor, RK-33

In order to evaluate changes in the protein landscape after RK-33 treatment we performed quantitative proteomics in the metastatic cancer cell line MDA-MB-435 treated with either DMSO as a vehicle control or 4.5 μM RK-33 for 24 hours. 152.039 unique peptide spectra were identified, corresponding to 4580 proteins that could be used for downstream analysis. Of these, 666 were significantly altered with a fold change of larger than 15% and a moderated q-value smaller than 0.05 after exposure to RK-33 (Figure 1A). Gene set enrichment analysis was performed in the Gene Ontology Biological Processes database

using the full dataset with 4580 proteins as a background.As shown in Figure 1B, the strongest enrichment was observed for the mitochondrial translation termination (6.2 fold enriched, q = 6.27 x 10^{-38}) and elongation GOterms (6.1 fold enriched, q = 2.25 x 10^{-37}). In addition, proteins involved in mitotic nuclear division (fold enrichment 2.24, q = 5.64 x 10^{-4}) and cell division (fold enrichment 1.96, q = 1.39 x 10^{-3}) were commonly altered.

Network analysis of significantly altered proteins

Network analysis using the STRING database[23] revealed several tight networks among the significantly altered proteins (Figure 1C). A clear cluster of downregulated mitochondrial ribosomal proteins was observed. Correspondingly, clusters of respiratory electron transport proteins, which are translated in part by the mitochondrial ribosome, were downregulated as well. We more elaborately investigated the effect of DDX3 inhibition on mitochondrial translation and reported about our findings in a dedicated paper (chapter 2).

In addition to a clear effect on mitochondrial translation, several other more closely interrelated protein clusters were identified. With regard to nuclear and cell division a large cluster of proteins involved in chromosome segregation and the mitotic cell cycle was observed (Figure 1C).

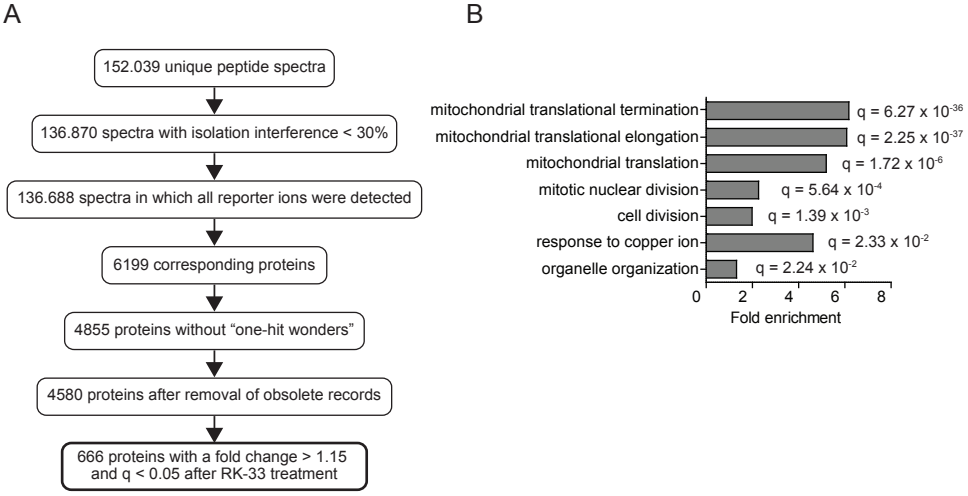

Figure 1. The proteomic landscape after DDX3 inhibition with RK-33

A. Flowchart showing bioinformatical processing and analysis of peptide spectra identified by quantitative proteomics after 24 hours DMSO or 4.5 μM RK-33 exposure in MDA-MB-435 cells. B. Bar graph showing significantly enriched GOterms identified by gene-set enrichment analysis among proteins significantly altered after DDX3 inhibition with RK-33 treatment. Q-values are calculated are Benjamini and adjusted p-values generated by hypergeometric enrichment test. C. STRING network analysis showing clusters of is interrelated proteins among the significantly altered proteins after RK-33 treatment. Each circle corresponds to a protein and is labeled with the gene symbol. The color fills indicate groups of proteins with a particular function (see labels). Direction of the fold change is indicated by the border color for each protein: green indicates downregulation, red indicates upregulation. (See next page for Figure 1C ▶)

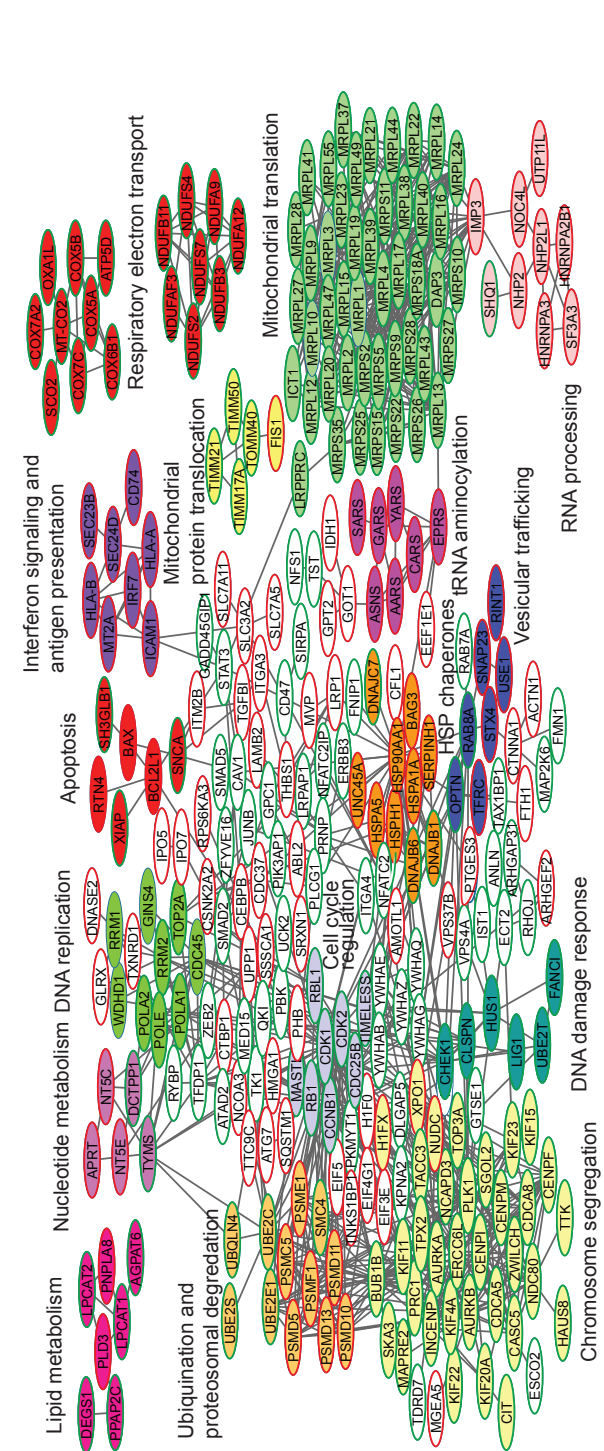

Figure 1C. STRING network analysis showing clusters of is interrelated proteins among the significantly altered proteins after RK-33 treatment. Each circle corresponds to a protein and is labeled with the gene symbol. The color fills indicate groups of proteins with a particular function (see labels). Direction of the fold change is indicated by the border color for each protein: green indicates downregulation, red indicates upregulation.

The expression level of most of these proteins was also decreased after RK-33 exposure. In close relation to this cluster, a cluster of several ubiquitin-conjugating enzymes went down, whereas regulatory subunits of the proteasome mainly increased. With regard to cell cycle progression, proteins involved in DNA damage response and DNA replication both went down. Very central among all these clusters was a cluster with downregulated cell cycle regulation proteins, including CDK1 (fold change 0.81, q = 0.0009) and CDK2 (fold change 0.73, q = 0.0004). Several proteins that play a role in apoptosis clustered together as well, with an increase in pro-apoptotic and a decrease in anti-apoptotic proteins. Given the known role of DDX3 in lipogenesis[30] and RNA processing translation[31], it was also interesting to see clusters that contained proteins involved in lipid metabolism and tRNA aminocylation.

Phosphoproteomic changes indicate decreased CDK1 activity after RK-33 treatment

After TiO_2 enrichment 5274 phosphopeptides could be reliably identified. Of 1501 phosphopeptides the corresponding protein was also identified in the unenriched analysis, allowing the abundance of the phosphopeptide to be normalized for the abundance of the whole protein (Figure 2A). This normalization ensured that changes in the phosphopeptide abundance reflected changes in phosphorylation status and not changes in relative abundance of the whole protein. 122 phosphopeptides with 134 unique phosphosites were significantly altered after RK-33 treatment.

As shown in Figure 2B, motif analysis of the surrounding amino acids of the downregulated phosphosites found enrichment for the S……t (3.72 fold), s..K (2.98 Fold) and the S…..s motif (1.83 Fold). Phosphopeptides with these motifs are known to be phosphorylated by kinases from the CDK1/2/3/5 and CK1 kinases, among others (Figure 2B). Upregulated phosphosites were enriched for the s….E motif (2.81 fold), commonly phosphorylated by ATM/ATR kinases and again for the S……s motif (2.5 fold). KEA at the phosphosite level also indicated enrichment for sites phosphorylated by CDK1 ($p = 5.5 \times 10^{-5}$). Total CDK1 and abundance of phosphorylated CDK1 (pCDK1) was also found to be decreased by immunoblotting in MDA-MB-435 cells 12 hours after RK-33 exposure (Figure 2D). Since not all identified phosphosites were associated with known kinases and the same kinases often phosphorylate proteins at more than one position, we performed KEA at the phosphorylated protein level as well. This analysis indicated that proteins that are known to be phosphorylated by CDC2 (p = 0.023) or CDK2 (p = 0.025) were overrepresented among the proteins with an altered phosphorylation status.

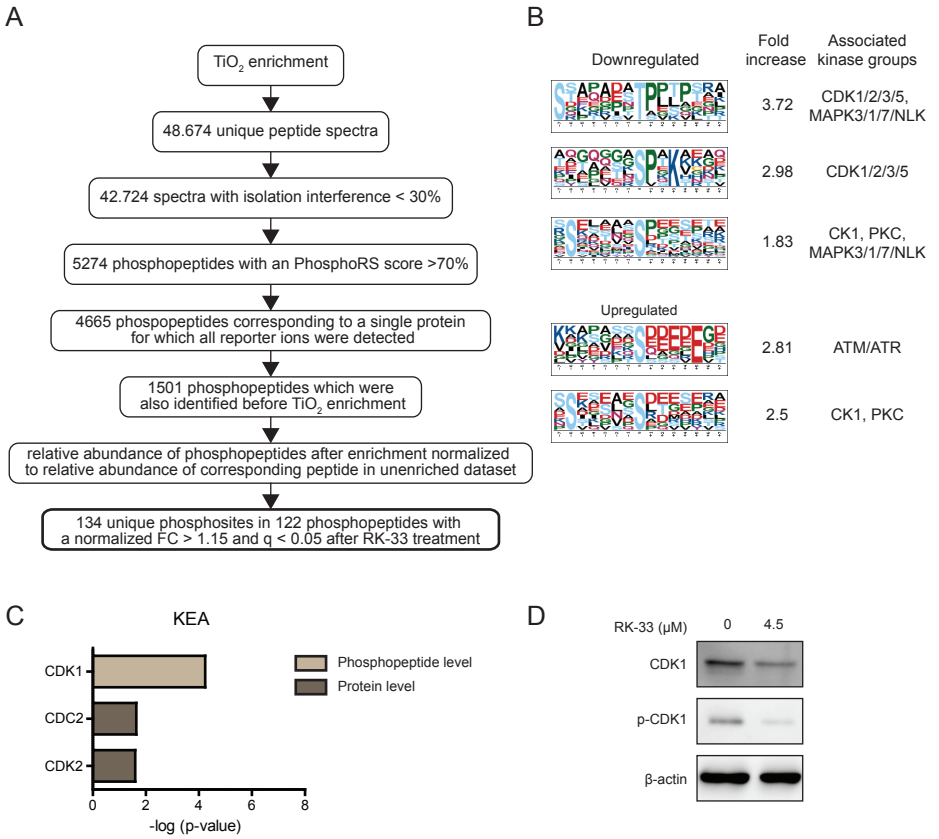

Figure 2. Changes in the phosphoproteome after RK-33 treatment indicate altered CDK1 activity
A. Flowchart showing bioinformatical processing and analysis of phospopeptide spectra identified by quantitative phospoproteomics after 24 hours DMSO or 4.5 μM RK-33 exposure in MDA-MB-435 cells. B. Motif-x analysis showing enriched motifs among the significantly up- or downregulated phosphopeptides and their associated kinase groups in the Networkin database. C. Bar graphs showing kinase enrichment analysis (KEA) among kinases known to phosphorylate the phosphopeptides and phosphoproteins significantly altered after RK-33 treatment. Benjamini and Hochberg corrected p-values of hypergeometric enrichment tests. D. Immunoblot showing a decrease in CDK1 and pCDK1 expression after 12 hours 4.5 μM RK-33 exposure in MDA-MB-435 cells.

RK-33 causes a delay in all cell cycle phases

Both the proteomic and phosphoproteomic changes after 24 hours of RK-33 treatment indicated global changes in proteins directly or indirectly involved in cell cycle progression and cell division, with a central role for CDK1. However, since it is hard to separate cause from effect when analyzing at a static 24 hour time point, we decided to monitor the changes in cell cycle progression and cell division in single cells over time using the FUCCI system and timelapse microscopy (Figure 3A). Interestingly, a delay in all cell cycle phases was seen in both MDA-MB-435 and MCF7 cells (Figure 3B and 3C). The median time spent

in mitosis could be properly estimated, since the relatively short duration of this cell cycle phase allowed for observation of both the beginning and end of this phase. As shown in Figure 3D, mitosis was significantly longer after 1.5 μM (0.96 hr, p = 0.048), 3 μM (2.0 hr, p = 0.003) and 4.5 μM RK-33 (1.17 hr, p = 0.002) in MDA-MB-435 cells, when compared to DMSO treated cells (0.83 hr). A similar delay was observed in MCF7 cells, but this was only significantly different after 3 μM RK-33 (1.41 hr vs. 0.83 hr, p <0.001). A delay was also observed for all interphases, but was hard to quantify, since it was uncommon to observe both the beginning and end of these phases.

Vacuolization and endoreduplication are frequent after RK-33 treatment

Morphological changes were also more commonly observed after RK-33 treatment. Especially in MCF7 extensive vacuolization was frequent (Figure 3E). In MDA-MB-435 vacuolization was less common, but apoptosis (nuclear membrane blebbing) and necrosis (disintegration of the cells) were observed here as well. Since it was hard to determine whether and at what exact point cells died after vacuolization, we lumped vacuolization and cell death when scoring cellular fate. As shown in Figure 3F, both the amount of arrested cells and of cells undergoing vacuolization and/or cell death increased after RK-33 exposure in a dose-dependent manner. The time to vacuolization or cell death in MCF7 was slightly shorter for cells first exposed to 3 μM RK-33 in S-phase, when compared to those first exposed in the G1- or G2 phase (Figure 3G), but this difference was not statistically significant (log rank test p = 0.229). Another aberrancy that was more frequent in both cell lines after RK-33 treatment was endoreduplication. Endoreduplication is a phenomenon where the cell does not undergo mitosis after replicating its DNA content, but returns to the biochemical state of the G1 phase[32] (Figure 3E & 3F). In MCF7 6.3-12.8% of cells underwent endoreduplication after 1.5-4.5 μM RK-33, as compared to 1% in of control cells. In MDA-MB-435 the phenotype was less clear, but endoreduplication was also more common after 3-4.5 μM RK-33 (4.0-4.5%), when compared to DMSO treated cells (2.1%).

DDX3 knockdown slows down cell cycle progression and induces endoreduplication

To evaluate whether a similar effect on the cell cycle could be observed after knockdown of DDX3, we treated MCF7-FUCCI cells with siDDX3 and compared them to sicontrol treated cells with timelapse microscopy (Figure 4A). As shown in Figure 4B, a similar global delay or arrest in all was observed after DDX3 knockdown. This was again best quantifiable for the median duration of mitosis, which was longer after siDDX3 (1.38 hr), when compared to sicontrol (0.92 hr), but this difference was not statistically significant (p = 0.080; Figure 4C). A clear increase in arrested cells (35.2% vs 6.7%) and cells undergoing endoreduplication (11.1% vs 2.9%) was observed after siDDX3, as well. The amount of cells undergoing vacuolization and/or cell death in this timeframe was comparable after sicontrol or siDDX3 treatment (Figure 4D).

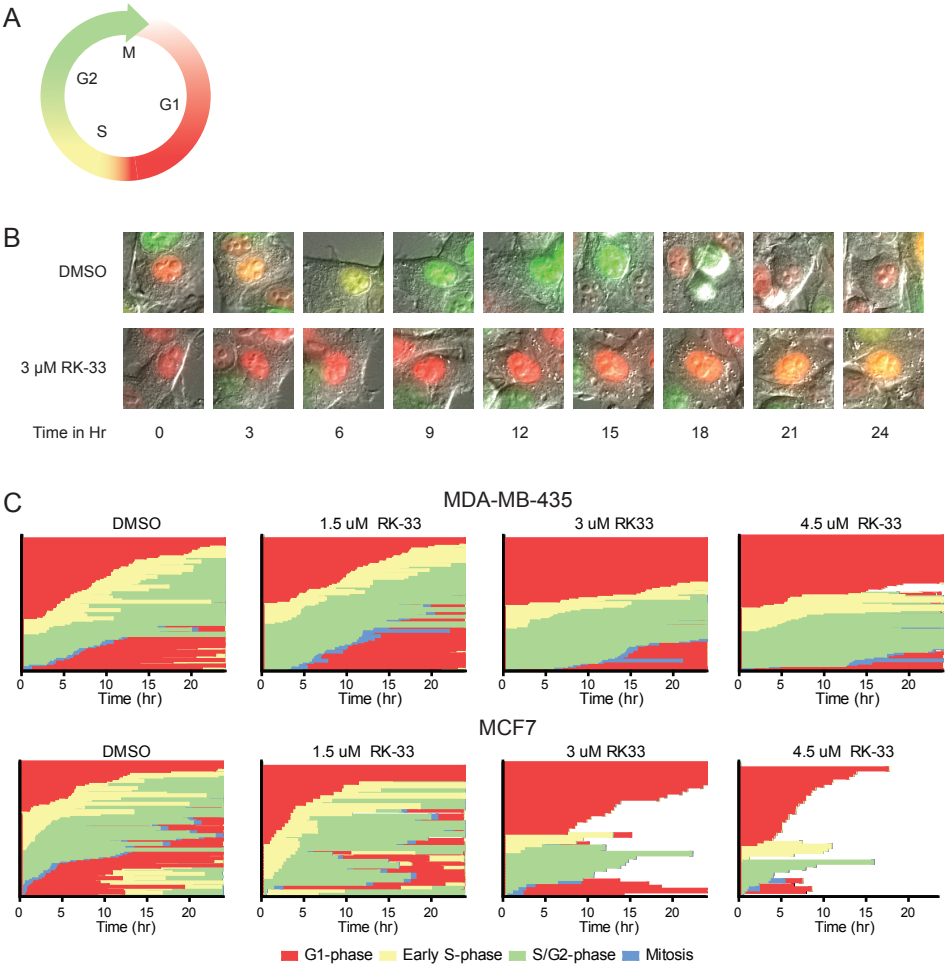
A
M
G2
G1
S
B
DMSO
3 μM RK-33
Time in Hr
0
3
6
9
12
15
18
21
24
C
MDA-MB-435
DMSO
1.5 uM RK-33
3 uM RK33
4.5 uM RK-33
MCF7
Time (hr)
G1-phase
Early S-phase
S/G2-phase
Mitosis
D
MDA-MB-435
MCF7
Duration of mitosis (hr)
RK-33 (μM)
DMSO
1.5
3
4.5

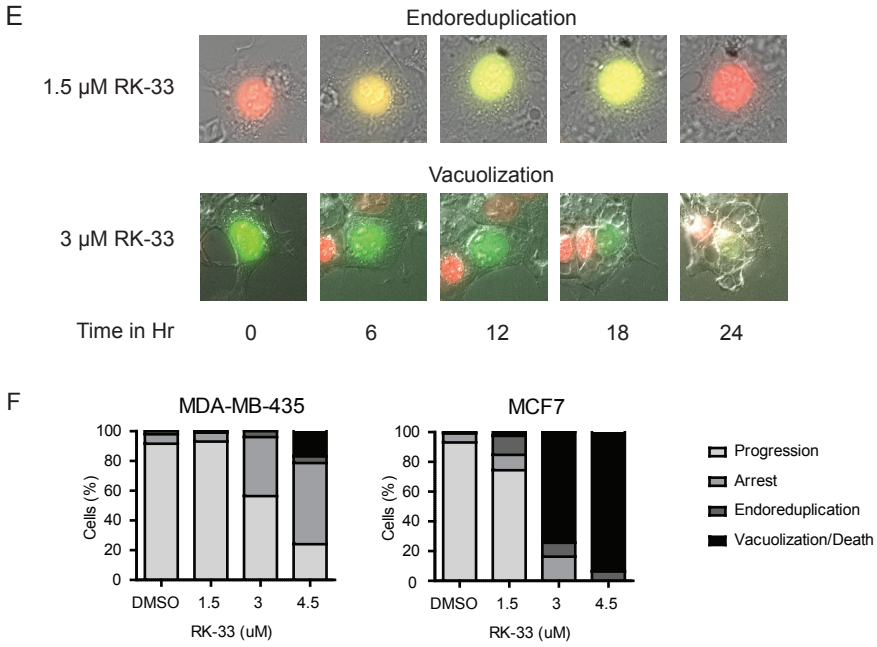

◀ **Figure 3.** Single cell tracking shows RK-33 causes a delay in all cell cycle phases
A. Schematic overview of cell cycle progression with fluorescent changes of the FUCCI constructs mCherry-hCdt1 and mVenus-hGeminin. B. Example merged DIC and fluorescent images showing the color change in a single DMSO and RK-33 treated MDA-MB-435-FUCCI cell over 24 hours. C. Graphs showing delayed cell cycle progression in single FUCCI labeled MDA-MB-435 and MCF7 cells after RK-33 treatment over 24 hours. Each line on the y-axis represents a single cell. D. Dot plot showing the median duration of mitosis after RK-33 treatment in FUCCI labeled MDA-MB-435 and MCF7 cells. Graphs represent median with interquartile range. P-values were calculated by a Mann-Whitney U Test. * $p < 0.05$, ** $p < 0.01$, *** $p < 0.001$. E. Example of endoreduplication and vacuolization occurring after RK-33 treatment in FUCCI-labeled MCF7 cells. F. Bar graphs showing the cell fate of RK-33 treated, FUCCI-labeled MCF7 and MDA-MB-435 cells. G. Kaplan Meijer plots showing the time to vacuolization or cell death for each phase during which the cell was first exposed to RK-33.

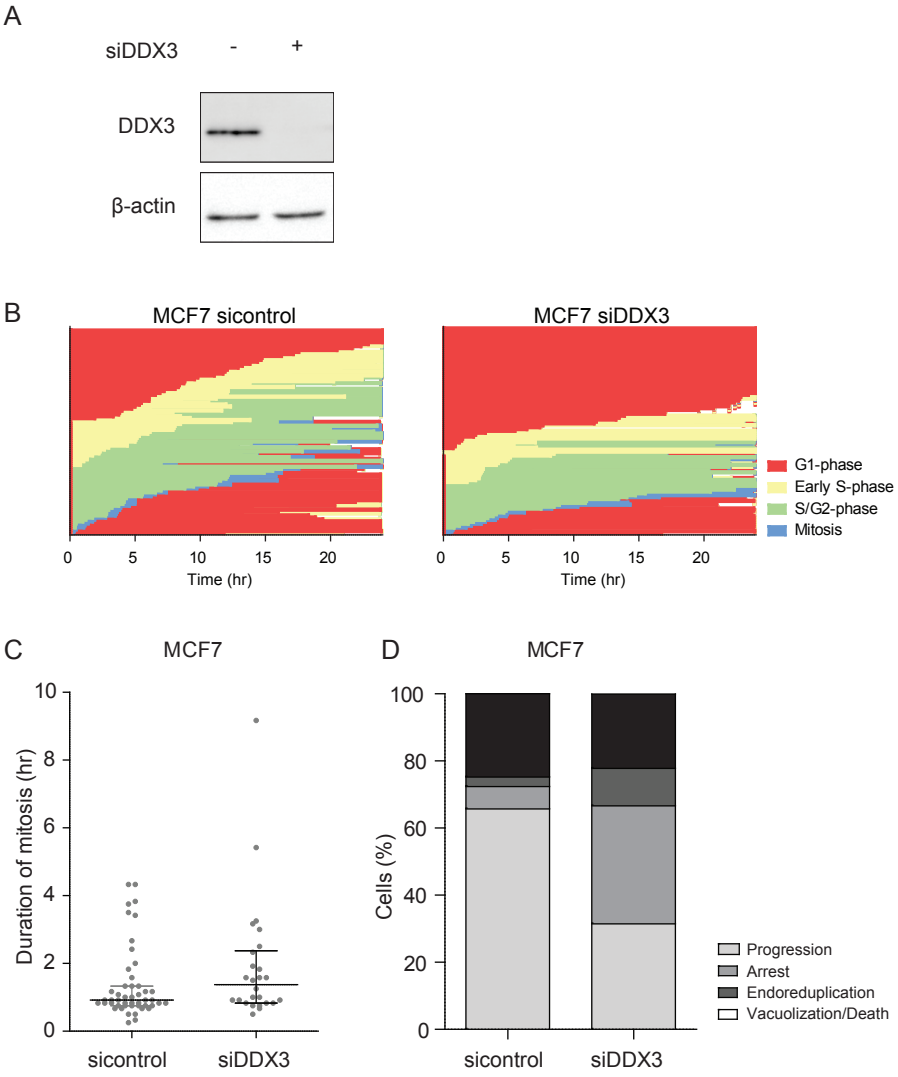

Figure 4. DDX3 knockdown results in a global cell cycle delay and endoreduplication
A. Immunoblot showing DDX3 expression 48 hours after sicontrol or siDDX3 transfection in MCF7 cells. B. Graphs showing delayed cell cycle progression in single MCF7-FUCCI cells 48 hours to 72 hours after sicontrol or siDDX3 transfection. Each line on the y-axis represents a single cell. C. Dot plot showing the median duration of mitosis after siDDX3 transfection in FUCCI labeled MCF7 cells. Graphs represent median with interquartile range. P-values were calculated by a Mann-Whitney U Test. D. Bar graphs showing the cell fate of MCF7-FUCCI cells 48 to 72 hours after siDDX3 transfection.

DISCUSSION

In this paper we evaluated the effect of DDX3 inhibition with RK-33. At the protein level RK-33 treatment mainly resulted in altered expression of proteins involved in mitochondrial translation, cell division and cell cycle progression. Reduced CDK1 and CDK2 expression seemed to have a central role in the network of affected cell cycle related proteins. We identified motifs among the phosphopeptides with changed expression levels after RK-33 treatment, of which several were associated with the CDK1 kinase family. KEA also indicated a significant enrichment for phosphopeptides that are phosphorylated by CDK1. Cell cycle evaluation by tracking single FUCCI labeled cells with timelapse microscopy showed a global delay in all cell cycle interphases and mitosis after both RK-33 treatment and DDX3 knockdown. In addition, endoreduplication was more frequently observed after DDX3 inhibition.

Downregulation of CDK1 has been linked to a global delay in cell cycle progression[33] and endoreduplication[34], by other studies as well. There are multiple pathways by which DDX3 inhibition with RK-33 could affect CDK1. Wang, *et al* showed that the DEAD box RNA helicase family member DDX6 mediates CDK1 expression through interaction with stem-loop structures in its 3'UTR[35]. Furthermore, a functional internal ribosome entry site (IRES) was identified in the CDK1 5'UTR[36]. DDX3 is known to be involved in translation of both mRNAs with a complex 5'UTR region[37], as well as cap-independent translation of proteins with an IRES[31]. We identified a reduction in CDK1 protein levels after RK-33 treatment with both proteomics and immunoblotting. It is therefore possible that DDX3 is involved in cap- dependent or independent translation of CDK1. Another possibility is that DDX3 directly affects the kinase activity of CDK1, as was observed previously for CK1 family members[16]. Further validation of the decrease in either abundance or activity of CDK1 and the mechanism behind this decrease after DDX3 inhibition is required.

Interestingly, DDX3 inhibition was previously associated with an increased proportion of cells in G1 as measured by flow cytometry, suggestive of a specific G1 arrest[3, 4, 38]. This can be explained cells dying faster in other cell phases than in G1 (Figure 3C & 3G) and by the possibility that cells are relatively more delayed in G1 than in other phases. It is hard to estimate the relative delay in each cell cycle phase, because the beginning and end of the interphases are frequently not observed in our 24 hour time window, especially not after RK-33 treatment. However, our data clearly indicate a delay in all phases and not one that is limited to the G1 cell cycle phase.

We identified changes after RK-33 treatment in several cellular pathways that were previously linked to functions of DDX3. Proteins involved in nuclear/cell division and chromosome segregation were prominent among the altered proteins. Pek, *et al.* previously identified DDX3 to be responsible for chromosomal localization of hCAP-H, a condensin 1 component, and found that inhibition of DDX3 resulted in lagging chromosomes[39].

This is in line with our observation that the duration of mitosis is increased after RK-33 treatment. In addition, a network of altered proteins involved in lipid metabolism was also identified after RK-33 treatment. DDX3 regulates an IKK-α mediated induction of lipogenesis after Hepatitis C infection[30]. Furthermore, we found lower expression of several DNA damage response proteins after DDX3 inhibition with RK-33. RK-33 was previously found to impede DNA repair[4, 30]. An interesting group of proteins that was upregulated after RK-33 treatment, was the group of tRNA ligases and other proteins involved in tRNA aminocylation. tRNA ligases function in maturation of tRNAs to facilitate protein translation [40]. DDX1, another DEAD box RNA helicase family member, was recently found regulate the tRNA ligase complex[40]. Further research on the involvement of DDX3 in this context is warranted.
DDX3 was previously shown to play a regulatory role both in the intrinsic[41] and extrinsic[6, 7] pathways of apoptosis. RK-33 treatment resulted in upregulation of pro-apoptotic proteins (e.g. BAX, BCL2L1) and downregulation of anti-apoptotic proteins (e.g. XIAP), confirming the previously described anti-apoptotic role of DDX3[7]. However, since we evaluated the proteomic landscape only at a static and late time point (24 hours), it is not possible to say whether the effects on apoptosis, and several other pathways, are a result of direct involvement of DDX3 or occurring as a downstream effect of other cellular perturbations. Vacuolization, ultimately resulting in cell death, was more frequent in MCF7 than MDA-MB-435 cells and is most likely part of an autophagy response we previously observed after DDX3 inhibition with RK-33 in this cell line (chapter 2).
The most prominent change in the proteome landscape after RK-33 treatment was mitochondrial translation. We dedicated a full paper to explore the effect of DDX3 inhibition on mitochondrial ribosomes, oxidative phosphorylation and the relation to radiosensitizing capacities of RK-33 (chapter 2). We confirmed that DDX3 inhibition with RK-33 indeed results in reduced mitochondrial translation, causing a decrease in oxidative phosphorylation capacity and an increase in reactive oxygen species production, culminating in a bioenergetics catastrophe. It is possible that the effect observed on cell cycle regulation described in the present paper, is partly a result of reduced bioenergetic capacity to fuel cell cycle progression. Further studies will need to confirm whether the effect of RK-33 on cell cycle progression through CDK1 regulation is a separate direct phenomenon, or secondary to the previously described metabolic changes.

CONCLUSION

Overall we conclude that DDX3 inhibition with RK-33 results in a global delay in cell cycle progression, at the proteome level characterized by altered expression of proteins involved in mitochondrial translation, cell division and cell cycle progression and at the phosphoproteomic level by changes indicative of reduced CDK1 activity.

REFERENCES

1 Linder P, Fuller-Pace FV. Looking back on the birth of DEAD-box RNA helicases. Biochimica et biophysica acta 2013; **1829**: 750-755.

2 Botlagunta M, Vesuna F, Mironchik Y, Raman A, Lisok A, Winnard P, Jr. *et al*. Oncogenic role of DDX3 in breast cancer biogenesis. Oncogene 2008; **27**: 3912-3922.

3 Heerma van Voss MR, Vesuna F, Trumpi K, Brilliant J, Berlinicke C, de Leng W *et al*. Identification of the DEAD box RNA helicase DDX3 as a therapeutic target in colorectal cancer. Oncotarget 2015; **6**: 28312-28326.

4 Bol GM, Vesuna F, Xie M, Zeng J, Aziz K, Gandhi N *et al*. Targeting DDX3 with a small molecule inhibitor for lung cancer therapy. EMBO molecular medicine 2015; **7**: 648-669.

5 Xie M, Vesuna F, Tantravedi S, Bol GM, Heerma van Voss MR, Nugent K *et al*. RK-33 radiosensitizes prostate cancer cells by blocking the RNA helicase DDX3. Cancer research 2016: doi:10.1158/0008-5472.CAN-1116-0440.

6 Li Y, Wang H, Wang Z, Makhija S, Buchsbaum D, LoBuglio A *et al*. Inducible resistance of tumor cells to tumor necrosis factor-related apoptosis-inducing ligand receptor 2-mediated apoptosis by generation of a blockade at the death domain function. Cancer research 2006; **66**: 8520-8528.

7 Sun M, Song L, Li Y, Zhou T, Jope RS. Identification of an antiapoptotic protein complex at death receptors. Cell death and differentiation 2008; **15**: 1887-1900.

8 Shih JW, Wang WT, Tsai TY, Kuo CY, Li HK, Wu Lee YH. Critical roles of RNA helicase DDX3 and its interactions with eIF4E/PABP1 in stress granule assembly and stress response. The Biochemical journal 2012; **441**: 119-129.

9 Sun M, Song L, Zhou T, Gillespie GY, Jope RS. The role of DDX3 in regulating Snail. Biochimica et biophysica acta 2011; **1813**: 438-447.

10 Hagerstrand D, Tong A, Schumacher SE, Ilic N, Shen RR, Cheung HW *et al*. Systematic interrogation of 3q26 identifies TLOC1 and SKIL as cancer drivers. Cancer discovery 2013; **3**: 1044-1057.

11 Chen HH, Yu HI, Cho WC, Tarn WY. DDX3 modulates cell adhesion and motility and cancer cell metastasis via Rac1-mediated signaling pathway. Oncogene 2015; **34**: 2790-2800.

12 Xie M, Vesuna F, Botlagunta M, Bol GM, Irving A, Bergman Y *et al*. NZ51, a ring-expanded nucleoside analog, inhibits motility and viability of breast cancer cells by targeting the RNA helicase DDX3. Oncotarget 2015; **6**: 29901-29913.

13 Lai MC, Chang WC, Shieh SY, Tarn WY. DDX3 regulates cell growth through translational control of cyclin E1. Molecular and cellular biology 2010; **30**: 5444-5453.

14 Rosner A, Rinkevich B. The DDX3 subfamily of the DEAD box helicases: divergent roles as unveiled by studying different organisms and in vitro assays. Current medicinal chemistry 2007; **14**: 2517-2525.

15 Fuller-Pace FV. DEAD box RNA helicase functions in cancer. RNA biology 2013; **10**: 121-132.

16 Cruciat CM, Dolde C, de Groot RE, Ohkawara B, Reinhard C, Korswagen HC *et al*. RNA helicase DDX3 is a regulatory subunit of casein kinase 1 in Wnt-beta-catenin signaling. Science 2013; **339**: 1436-1441.

17 Kondaskar A, Kondaskar S, Kumar R, Fishbein JC, Muvarak N, Lapidus RG *et al*. Novel, Broad Spectrum Anti-Cancer Agents Containing the Tricyclic 5:7:5-Fused Diimidazodiazepine Ring System. ACS medicinal chemistry letters 2010; **2**: 252-256.

18 Wilky BA, Kim C, McCarty G, Montgomery EA, Kammers K, DeVine LR *et al*. RNA helicase DDX3: a novel therapeutic target in Ewing sarcoma. Oncogene 2016; **35**: 2574-2583.

19 Herbrich SM, Cole RN, West KP, Jr., Schulze K, Yager JD, Groopman JD *et al*. Statistical inference from multiple iTRAQ experiments without using common reference standards. Journal of proteome research 2013; **12**: 594-604.

20 Kammers K, Cole RN, Tiengwe C, Ruczinski I. Detecting Significant Changes in Protein Abundance. EuPA open proteomics 2015; **7**: 11-19.

21 Smyth GK. Linear models and empirical bayes methods for assessing differential expression in microarray experiments. Statistical applications in genetics and molecular biology 2004; **3**: Article3.

22 Eden E, Navon R, Steinfeld I, Lipson D, Yakhini Z. GOrilla: a tool for discovery and visualization of enriched GO terms in ranked gene lists. BMC bioinformatics 2009; **10**: 48.

23 Franceschini A, Szklarczyk D, Frankild S, Kuhn M, Simonovic M, Roth A *et al*. STRING v9.1: protein-protein interaction networks, with increased coverage and integration. Nucleic acids research 2013; **41**: D808-815.

24 STRING database, vol. 2015.

25 Chou MF, Schwartz D. Biological sequence motif discovery using motif-x. Current protocols in bioinformatics 2011; **Chapter 13**: Unit 13 15-24.

26 Horn H, Schoof EM, Kim J, Robin X, Miller ML, Diella F *et al*. KinomeXplorer: an integrated platform for kinome biology studies. Nature methods 2014; **11**: 603-604.

27 Lachmann A, Ma'ayan A. KEA: kinase enrichment analysis. Bioinformatics 2009; **25**: 684-686.

28 Sakaue-Sawano A, Kurokawa H, Morimura T, Hanyu A, Hama H, Osawa H *et al*. Visualizing spatiotemporal dynamics of multicellular cell-cycle progression. Cell 2008; **132**: 487-498.

29 Schindelin J, Arganda-Carreras I, Frise E, Kaynig V, Longair M, Pietzsch T *et al*. Fiji: an open-source platform for biological-image analysis. Nature methods 2012; **9**: 676-682.

30 Li Q, Pene V, Krishnamurthy S, Cha H, Liang TJ. Hepatitis C virus infection activates an innate pathway involving IKK-alpha in lipogenesis and viral assembly. Nature medicine 2013; **19**: 722-729.

31 Geissler R, Golbik RP, Behrens SE. The DEAD-box helicase DDX3 supports the assembly of functional 80S ribosomes. Nucleic acids research 2012; **40**: 4998-5011.

32 Fox DT, Duronio RJ. Endoreplication and polyploidy: insights into development and disease. Development 2013; **140**: 3-12.

33 Kumper S, Mardakheh FK, McCarthy A, Yeo M, Stamp GW, Paul A *et al*. Rho-associated kinase (ROCK) function is essential for cell cycle progression, senescence and tumorigenesis. eLife 2016; **5**: e12994.
34 Ullah Z, Kohn MJ, Yagi R, Vassilev LT, DePamphilis ML. Differentiation of trophoblast stem cells into giant cells is triggered by p57/Kip2 inhibition of CDK1 activity. Genes & development 2008; **22**: 3024-3036.
35 Wang Y, Arribas-Layton M, Chen Y, Lykke-Andersen J, Sen GL. DDX6 Orchestrates Mammalian Progenitor Function through the mRNA Degradation and Translation Pathways. Molecular cell 2015; **60**: 118-130.
36 Marash L, Liberman N, Henis-Korenblit S, Sivan G, Reem E, Elroy-Stein O *et al*. DAP5 promotes cap-independent translation of Bcl-2 and CDK1 to facilitate cell survival during mitosis. Molecular cell 2008; **30**: 447-459.
37 Lai MC, Lee YH, Tarn WY. The DEAD-box RNA helicase DDX3 associates with export messenger ribonucleoproteins as well as tip-associated protein and participates in translational control. Molecular biology of the cell 2008; **19**: 3847-3858.
38 Fukumura J, Noguchi E, Sekiguchi T, Nishimoto T. A temperature-sensitive mutant of the mammalian RNA helicase, DEAD-BOX X isoform, DBX, defective in the transition from G1 to S phase. Journal of biochemistry 2003; **134**: 71-82.
39 Pek JW, Kai T. DEAD-box RNA helicase Belle/DDX3 and the RNA interference pathway promote mitotic chromosome segregation. Proceedings of the National Academy of Sciences of the United States of America 2011; **108**: 12007-12012.
40 Popow J, Jurkin J, Schleiffer A, Martinez J. Analysis of orthologous groups reveals archease and DDX1 as tRNA splicing factors. Nature 2014; **511**: 104-107.
41 Sun M, Zhou T, Jonasch E, Jope RS. DDX3 regulates DNA damage-induced apoptosis and p53 stabilization. Biochimica et biophysica acta 2013; **1833**: 1489-1497.

TARGETS

CHAPTER 4

Identification of the DEAD box RNA helicase DDX3 as a therapeutic target in colorectal cancer

Oncotarget. 2015 Sep 29;6(29):28312-26

Marise Heerma van Voss, Farhad Vesuna, Kari Trumpi, Justin Brilliant, Cynthia Berlinicke, Wendy de Leng, Onno Kranenburg, Johan Offerhaus, Horst Bürger, Elsken van der Wall, Paul van Diest, Venu Raman

ABSTRACT

Identifying druggable targets in the Wnt-signaling pathway can optimize colorectal cancer treatment. Recent studies have identified a member of the RNA helicase family DDX3 (*DDX3X*) as a multilevel activator of Wnt signaling in cells without activating mutations in the Wnt-signaling pathway. In this study, we evaluated whether DDX3 plays a role in the constitutively active Wnt pathway that drives colorectal cancer.

We determined DDX3 expression levels in 303 colorectal cancers by immunohistochemistry. 39% of tumors overexpressed DDX3. High cytoplasmic DDX3 expression correlated with nuclear β-catenin expression, a marker of activated Wnt signaling. Functionally, we validated this finding *in vitro* and found that inhibition of DDX3 with siRNA resulted in reduced TCF4-reporter activity and lowered the mRNA expression levels of downstream TCF4-regulated genes. In addition, DDX3 knockdown in colorectal cancer cell lines reduced proliferation and caused a G1 arrest, supporting a potential oncogenic role of DDX3 in colorectal cancer.

RK-33 is a small molecule inhibitor designed to bind to the ATP-binding site of DDX3. Treatment of colorectal cancer cell lines and patient-derived 3D cultures with RK-33 inhibited growth and promoted cell death with IC50 values ranging from 2.5 to 8 μM. The highest RK-33 sensitivity was observed in tumors with wild-type *APC*-status and a mutation in *CTNNB1*.

Based on these results, we conclude that DDX3 has an oncogenic role in colorectal cancer. Inhibition of DDX3 with the small molecule inhibitor RK-33 causes inhibition of Wnt signaling and may therefore be a promising future treatment strategy for a subset of colorectal cancers.

INTRODUCTION

Although significant advancements have been made in the prevention and treatment of colorectal cancer, this disease still ranks third on the list of causes of cancer related deaths in the United States, which underlines the need for development of new targeted therapies in this field.[1] On a genomic level colorectal cancer is frequently characterized by loss of the tumor suppressor gene p53 and activation of the RAS-RAF signaling pathway, alterations that are common in a multitude of solid tumors. In addition, activation of the Wnt/β-catenin signaling pathway is prevailing and more specific to the colorectal cancer setting, where genetic aberrations in this pathway are found in over 90 percent of cases. The most common alteration is inactivation of the *APC* gene (>70%). Activating mutations in *CTNNB1*, the gene encoding for β-catenin, are less prevalent (5-10%).[2] Thus, identifying druggable targets in this pathway would be beneficial for optimizing colorectal cancer treatment.

Within this context, we identified a member of the RNA helicase gene family, DDX3, which exhibits oncogenic properties in breast and lung carcinomas.[3, 4] In order to therapeutically exploit the benefits of abrogating DDX3 activity in these cancers, we developed a small molecule inhibitor, RK-33, designed to bind to the ATP-binding domain of DDX3 and inhibit its RNA-helicase activity.[4] Potent anti-cancer activity was observed in lung cancer mouse models after DDX3 inhibition by RK-33.

Recent studies indicate that DDX3 is a multilevel activator of the Wnt-signaling pathway. DDX3 was identified as an allosteric activator of CK1ε and hereby promotes phosphorylation of the scaffold protein dishevelled, which activates Wnt signaling during *Caenorhabditis elegans* and *Xenopus* development and in mammalian HEK293t cells. This function of DDX3 was independent of its RNA-helicase activity.[5] In addition, DDX3 was found to regulate the stability of β-catenin protein expression in a helicase-dependent manner through translational regulation of Rac1.[6] In addition, our group identified a direct interaction between DDX3 and β-catenin and its functional role in regulating TCF-4 mediated transcriptional activity in lung cancer cell lines.[4] Notably, DDX3 activity has also been linked to Wnt-signaling activity by the identification of coinciding *CTNNB1* and *DDX3X* activating mutations in Wnt-type medulloblastomas.[7-9]

These mechanistic studies all indicate an important role of DDX3 in Wnt signaling in both normal and transformed cells, but focus on a situation without activating mutations in the Wnt-signaling pathway. It remains to be determined whether colorectal cancer cells, which usually harbor activating mutations in the Wnt-signaling pathway, are dependent on DDX3 as well. In this study, we aimed to evaluate DDX3 as a potential player in the constitutionally activated Wnt signaling that drives colorectal cancer and to assess whether DDX3 inhibition by the small molecule RK-33 is a suitable therapeutic strategy in this cancer type.

METHODS

Cell lines

HCT116, HT29, Colo205, SW480 and DLD-1 were a kind gift of Professor Fred Bunz (Johns Hopkins University, Baltimore, MD, USA). The HCT116 p53[10] and β-catenin[11] knockout cell lines were kindly provided by Professor Bert Vogelstein (Johns Hopkins University). All adherent colorectal cancer cell lines were grown in McCoy's 5A supplemented with 10% fetal bovine serum. All cell lines were routinely tested for mycoplasma contamination by a PCR kit (30-1012K, ATCC, Manassas, VA, USA).

The colosphere cultures CR9, CRC29, CRC47 and L145 were a kind gift from Professor Onno Kranenburg (University Medical Center Utrecht, Utrecht, The Netherlands). These cell lines were established from tumor specimens of primary colorectal cancers (CR9, CRC29, CRC47) and colorectal cancer liver metastases (L145). A detailed description of how these colospheres were isolated and maintained has been provided previously.[12] These specimens were obtained in accordance with the ethical committee on human experimentation and informed consent was obtained from all patients.[12] Next generation sequencing was performed to assess the mutation status of 50 commonly mutated genes in these spheroids using the AmpliSeq Cancer Hotpot Panel v2 (LifeTechnologies, Carlsbad, CA, USA) on an Ion PGM platform. Publicly available mutation data of the adherent colorectal cancer cell lines were accessed through the canSAR platform.[13] Clinical information of these cell lines is summarized in Supplementary Table 2.

DDX3 knockdown cell lines were generated by transfecting cells with jetPrime transfection reagent (Polyplus, New York, NY, USA) and 50 nM sicontrol (non-targeting pool) or siDDX3 sequences (ON-*TARGETplus,* Dharmacon, Lafayette, CO, USA).

Immunoblotting

All cells were harvested at 50-70% confluency. For DDX3 knockdown experiments cells were harvested 72 hours after transfection. For RK-33 experiments cells were harvested after 24 hours exposure to the drug or vehicle control. For whole cellular protein extracts cells were lysed in SDS-extraction buffer (100nM Tris-HCl, 2% SDS, 12% glycerol, 10mM EDTA, pH6.7) and sonicated on ice. 30 μg protein was loaded on 10% SDS-PAGE gels. After gel-electrophoresis proteins were transferred onto PVDF membranes, blocked with 5% milk and probed overnight with primary antibodies against DDX3 (1:1000, mAb AO196)[14], Actin (1:10000, A5441, Sigma-Aldrich, St Louis, MO, USA), DDX5 (1:1000, pab204, EMD Millipore, Billarica, MA, USA), DDX17 (1:1000, Bethyl, Montgomery, TX, USA) and p53 (1:1000, DO-1, Santa-Cruz Biotechnology, Dallas, TX, USA) and followed by appropriate secondary antibodies. The blots were developed with clarity western ECL (Bio-Rad, Hercules, CA, USA) and imaged with G:BOX Chemi XR5 (Syngene, Frederick, MD, USA).

Proliferation assay and cytotoxicity assays

For the proliferation assays 4-10 x 10^4 cells were plated in a 24-well plate. The following day the cells were transfected with siDDX3 or sicontrol as described earlier. 48 hours after transfection 2-5 x 10^3 cells were plated per well in a 96-well plate. The amount of viable cells per well was estimated every 24 hours by an MTS-assay (CellTiter 96 Aqueous One Solution, Promega, Madison, WI, USA). For this, the cells were incubated with MTS reagent for 2 hours, after which absorbance was measured at 490 nm with a Victor^{3}V plate reader (PerkinElmer, Waltham, MA, USA).

For the cytotoxicity assays with adherent colorectal cancer cell lines 2-5 x 10^3 cells were plated per well in a 96-well plate. The following day RK-33 was added. DMSO was added as a vehicle control. Read out occurred after 72 hours of drug exposure with an MTS assay. The cytotoxicity assays on colosphere cultures have been described extensively elsewhere.[15] Briefly, 80-100 spheroids were plated per well in a 96-well plate with RK-33 or DMSO. After 72 hours of drug exposure the total cell population was labelled with DRAQ5™ (Abcam, Cambridge, UK) and live cells were labelled with Calcein Green AM (LifeTechnologies, Carlsbad, CA, USA). Fluorescence was measured using a Cellomics Arrayscan VTI HCS Reader (Thermo Fisher Scientific, MA, USA).The percentage of dead cells was calculated by normalizing the levels of intensity to and expressed as a relative percentage of the plate-averaged vehicle treated control.

Cell cycle analysis

Cell cycle analysis was performed as was described previously.[16] In short, for siDDX3 experiments 5-15 x 10^4 cells were plated per well in a 6-well plate. The following day cells were transfected with sicontrol or siDDX3 and incubated for 72 hours. For experiments with RK-33 4-7.5 x 10^5 cells were plated in a 6-well plate. The following day cells were incubated for 24 hours with RK-33. Subsequently, cells were harvested and fixed in 70% ethanol overnight at -20^{0}C. Fixed cells were incubated in DNA staining solution (5µg/ml propidium iodide, 0.5mg/ml RNAse A) for 1 hour. Cell cycle acquisition was performed on a FACScan I or FACSCalibur instrument (BD Biosciences, San Jose, CA, USA). Data was analyzed using FlowJo software (Tree Star Inc., Ashland, OR, USA). Statistical significance was assessed with a student's t-test.

TCF-reporter assays

Transcriptional activity of TCF4 was measured using the dual luciferase assay (Promega, Madison, WI, USA) according to the manufacturer's instructions. For this, cells were transfected with 500 ng TOP-FLASH or FOP-FLASH constructs[17] and 50 ng phRL Renilla constructs as transfection controls, using jetPrime transfection reagent (Polyplus, New York, NY, USA). Luminescence was measured using a luminometer (Berthold Sirius, Oak Ridge, TN, USA).

For the experiments with RK-33 3-4 x 10^4 HCT116 and HT29 cells were plated in a 24-well plate. After 24 hours the cells were transfected with the TOP/FOP constructs. 7 hours after transfection 2.5 μM RK-33 or DMSO was added for 12-24 hours after which the cells were lysed. For the DDX3 knockdown experiments 12.5-15 x 10^3 HCT116 and HT29 cells were plated in a 24-well plate. In the evening of the following day the cells were transfected with 50 nM siDDX3 as described earlier. The following morning the cells were transfected with the TOP/FOP constructs and incubated for another 48 hours after which the cells were lysed for the luciferase assay. Relative TCF4-promotor activity was calculated by normalizing TOP-FLASH and FOP-FLASH readings for Renilla luciferase readings and dividing normalized TOP-FLASH readings by normalized FOP-FLASH readings. Statistical significance was evaluated by a paired t-test.

Quantitative reverse transcriptase polymerase chain reaction

HCT116 and HT29 cells were harvested after 12-24 hour exposure to RK-33 or 72 hours after transfection with 50 nM siDDX3. RNA was extracted with an RNeasy kit (Qiagen, Valencia, CA, USA) and cDNA was manufactured using an iScript cDNA synthesis kit (Bio-Rad, Hercules, CA, USA), followed by qPCR using SYBR green (Bio-Rad, Hercules, CA, USA) on an CFX96 Real-Time PCR detection System (Bio-Rad, Hercules, CA, USA). Amplification of 36B4, a housekeeping gene, was used for normalizing gene expression values. Primer sequences:
DDX3 F 5'-GGAGGAAGTACAGCCAGCAAAG-3', *DDX3* R
5'-CTGCCAATGCCATCGTAATCACTC-3', *AXIN2* F
5'-TCAAGTGCAAACTTTCGCCAACC-3', *AXIN2* R
5'-TAGCCAGAACCTATGTGATAAGG-3', c-*MYC* F
5'-CGTCTCCACACATCAGCACAA-3', c-*MYC* R
5'-CACTGTCCAACTTGACCCTCTTG-3', *CCND1* F
5'-GGCGGAGGAGAACAAACAGA-3' *CCND1* R 5'-TGGCACAGAGGGCAACGA-3',
BIRC5A F 5'-CCACCGCATCTCTACATTCA-3', *BIRC5A* R
5'-TATGTTCCTCTATGGGGTCG-3'.
Fold changes in mRNA expression were calculated using the $2^{-\Delta\Delta CT}$ method. Statistical significance was calculated by performing a paired student's t-test on the ΔCT values.[18]

Patient samples

A tissue microarray (TMA's) with samples from 72 colorectal cancer patients from the Academic Medical Center, Amsterdam was kindly provided by professor Johan Offerhaus (University Medical Center Utrecht). This TMA also included one punch of surrounding normal mucosa per patient. The construction of this TMA has been reported in detail elsewhere.[19] An additional TMA with 292 colorectal cancer samples from Paderborn, Germany was provided by prof. Horst Bürger.

As we used archival leftover pathology material and our study does not affect the included patients, no ethical approval is required according to Dutch legislation.[20] Anonymous or coded use of redundant tissue for research purposes is part of the standard treatment agreement with patients in our hospitals.[21]

Immunohistochemistry

4μm sections were cut, mounted on SuperFrost slides (Menzel&Glaeser, Brunswick, Germany), deparaffinized in xylene and rehydrated in decreasing ethanol dilutions. For DDX3 staining, endogenous peroxidase activity was blocked with 1.5% hydrogen peroxide buffer for 15 minutes and was followed by antigen retrieval by boiling for 20 minutes in 10mM citrate buffer (pH 6.0). Slides were subsequently incubated in a humidified chamber for 1 hour with anti-DDX3 (1:1000, pAb r647).[14] After washing with PBS, slides were incubated with poly-HRP-anti-mouse/rabbit/rat IgG (Brightvision, Immunologic, Duiven, The Netherlands) as a secondary antibody for 30 minutes at room temperature. Peroxidase activity was developed with diaminobenzidine and hydrogen peroxide substrate solution for 10 minutes. The slides were lightly counterstained with haematoxylin and mounted. Positive controls (tonsil) were used throughout. Negative controls were obtained by omission of the primary antibodies from the staining procedure.

β-catenin staining was performed automatically with the Leica BOND RX (Leica Microsystems, Rijswijk, The Netherlands). Antigens were retrieved with Epitope Retrieval Solution 2. The primary antibody against β-catenin (clone 17C2, Novocastra, Eindhoven, The Netherlands) was used in a 1:20 concentration.

Scoring was performed by consensus of two observers (M.H.v.V., P.v.D.). Intensity of cytoplasmic DDX3 expression was scored semi-quantitatively as being absent, low, moderate or strong. The TMAs included multiple cores per patient; the highest score was used for further analysis. Cases with absent to moderate scores were classified as having low DDX3 expression and evaluated against cases with strong expression. Intratumoral DDX3 expression was compared to that of the surrounding normal tissue in case the latter was available for comparison.

β-catenin expression was scored separately for each subcellular compartment. Membrane expression was scored as complete, partial or lost. Cytoplasmic expression was scored as normal or overexpressed. The percentage of positive nuclei was scored. A cut-off of lower or higher than 10% was used for analysis.

Clinicopathological characteristics were compared between DDX3 low and high expressing tumors. Discrete variables were compared by $\chi 2$ or Fisher's exact test and odds ratios (OR) were calculated with 95% confidence intervals (95% CI). Statistical analyses were performed using SPSS version 20.0.

RESULTS

DDX3 inhibition results in growth inhibition in colorectal cancer cell lines

To assess DDX3 dependency, we used siRNA to knock down DDX3 expression in the colorectal cell lines HCT116 and HT29 (Figure 1A). DDX3 knockdown resulted in a reduction of cell proliferation in both cell lines (Figure 1B). To evaluate whether the reduction of viable cells was the result of reduced proliferation or increased cell death, we performed cell cycle analysis by flow cytometry on these cell lines after treatment with siDDX3. As seen in Figure 1C, cell cycle analysis indicated a clear G1 arrest in HCT116 cells with a 15.8% increase in G1-phase ($p = 0.02$) and a 17.0% decrease of cells in S-phase ($p = 0.01$). In addition, a slight decrease in S-phase was observed in HT29 (3.4%; $p = 0.05$). These results indicate that these colorectal cell lines are dependent on DDX3 for cell cycle progression.

DDX3 expression in colorectal cancer patient samples

To evaluate whether DDX3 is also expressed in colorectal cancers, we immunohistochemically stained 303 colorectal cancer specimens for DDX3 (Figure 2). High cytoplasmic DDX3 expression was present in 124 samples (40.9%). Corresponding normal mucosa was available for 59 cases. Intratumoral expression was higher in 23 patients (39.0%; Figure 2A-D), similar in 32 patients (54.2%; Figure 2E-F) and lower in 4 patients (6.8%; Figure 2G-H), when compared to the surrounding morphologically normal mucosa.

Next, we compared DDX3 expression to other known clinicopathological characteristics (Table 1). Within this cohort of samples, DDX3 expression did not correlate with any of the other clinicopathological variables.

High DDX3 expression correlates with nuclear β-catenin

Given the activating role of DDX3 in Wnt signaling in other settings,[4] we wanted to determine whether high DDX3 expression is associated with activated Wnt signaling in colorectal cancer patient samples as reflected by an increased cytoplasmic and nuclear β-catenin pool (Figure 3). We separately scored the membranous, cytoplasmic and nuclear localization of β-catenin in tumors with low and high DDX3 expression, which is shown in Table 2. Nuclear β-catenin expression was significantly more prevalent in the DDX3 high group (59.3%) when compared to the DDX3 low group (33.5%; RR = 1.77; 95% CI = 1.36-2.31; $p = 2.47 \times 10^{-5}$), indicating a connection between DDX3 levels and nuclear β-catenin accumulation. In addition, a trend was observed for more frequent overexpression of cytoplasmic β-catenin in DDX3 high tumors (73% vs 63%; RR = 1.16; 95% CI = 0.99-1.36; $p = 0.08$), which often coincides with nuclear β-catenin expression as shown in Figure 3D.

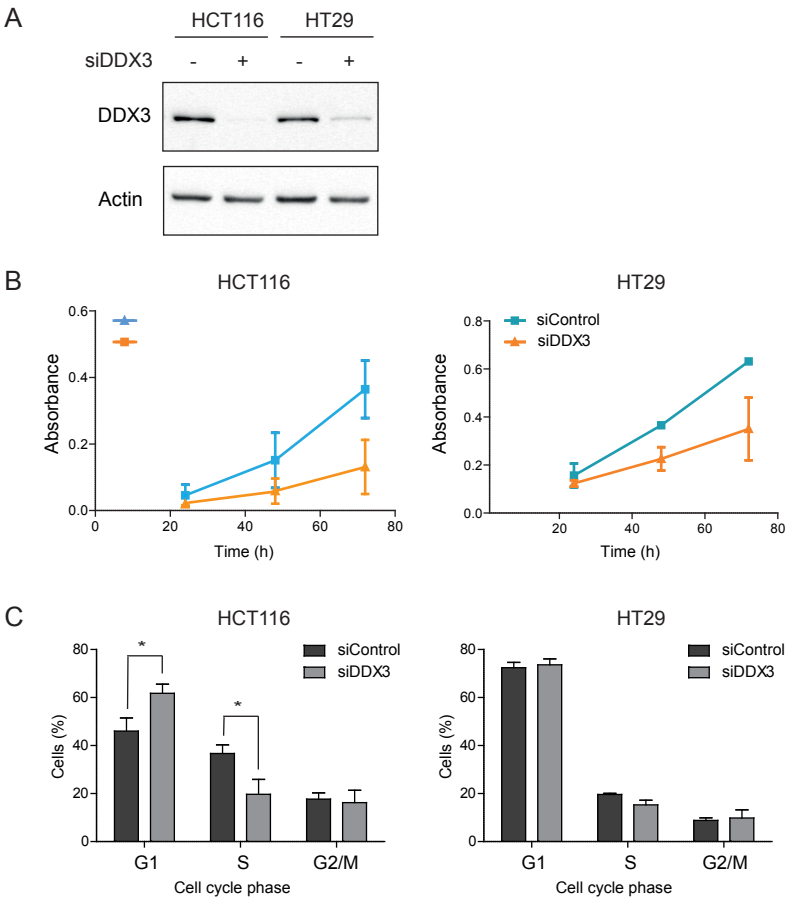

Figure 1. DDX3 dependency in colorectal cancer cell lines
A. Immunoblots of DDX3 expression in colorectal cancer cell lines HCT116 and HT29 before and after inhibition of DDX3 with 50 nM siDDX3. B. Proliferation of Colorectal cancer cell lines after knockdown of DDX3, measured by daily MTS assays. C. Cell cycle analysis after knockdown of DDX3. All experiments were performed three independent times, graphs represent mean ± SD, * $p < 0.05$

Sensitivity of colorectal cancers to RK-33, a small molecule inhibitor of DDX3

Considering the fact that DDX3 is overexpressed in colorectal cancers, we evaluated the *in vitro* sensitivity of colorectal cancer cells to DDX3 inhibition by RK-33, a small molecule inhibitor of DDX3. Five colorectal cancer cell lines (HCT116, HT29, DLD-1, SW480 and Colo205) were treated with RK-33 and cell viability was assessed by an MTS assay (Figure 4A-B). All cell lines had an IC50 value in the low micromolar range (3-7 μM). To assess whether RK-33 also showed cytotoxicity in 3D cultures, we expanded our panel with four patient-derived colorectal cancer spheroid cell lines. Spheroid viability after RK-33 exposure was evaluated with an arrayscan (Figure 4C-E). The spheroids displayed comparable

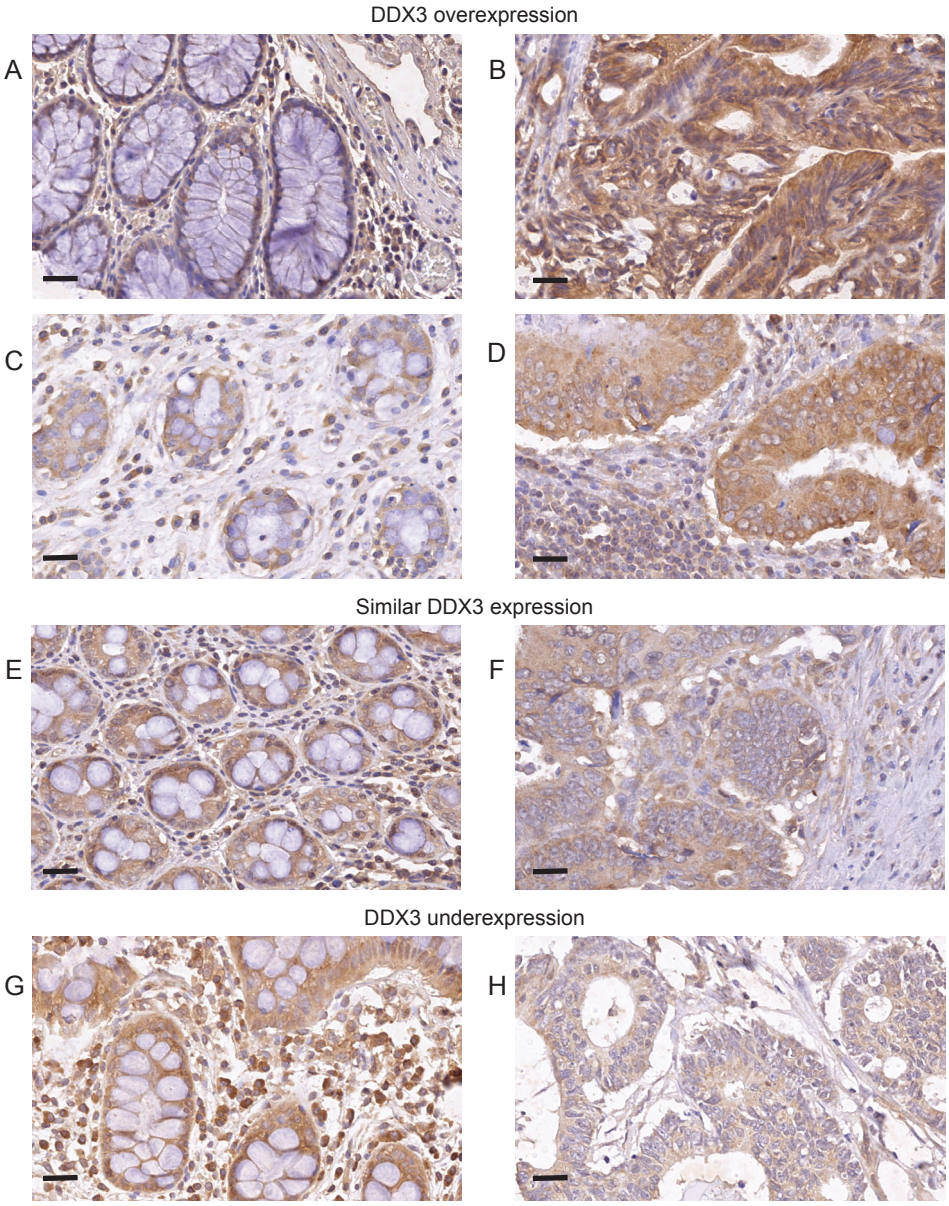

Figure 2. DDX3 is overexpressed in patients with colorectal cancer
DDX3 is overexpressed in 39% of patients. Low DDX3 expression in normal colon epithelium (A. & C.). High DDX3 expression in colorectal adenocarcinoma cells of the same patients (B. & D.) 54.2% of patients have similar levels of DDX3 expression in the normal mucosa (E.) and corresponding invasive cancer (F.). Only 6.8% of patients have decreased DDX3 in the invasive tumor (H.), when compared to adjacent normal mucosa (G.). 40 x magnification, scale bar indicates 25 µm

sensitivity to RK-33 as the adherent cell lines (IC50 value range 3-9 μM). Treatment with RK-33 resulted in a G1 arrest in a dose-dependent manner in both HCT116 and HT29 (Figure 4F). An increase in the percentage of apoptotic cells could also be observed in HCT116 after DDX3 inhibition, but not in HT29 (supplementary Figure 1). The differences in cell cycle distribution were more profound than the increase in apoptotic cells, indicating that the primary effect of DDX3 inhibition is a G1 arrest, which ultimately can result in apoptosis.

Table 1. Clinicopathological characteristics of DDX3 low and DDX3 high colorectal cancers

	Total		Low DDX3		High DDX3				
	n	%	n	%	n	%	P-value	RR	95% CI
Total	303	100.0	179	59.1%	124	40.9%			
Sex									
Male	169	55.8%	102	57.0%	67	54.0%	0.61	1.08	0.84-1.39
Female	134	44.2%	77	43.0%	57	46.0%			
TNM stage									
1	22	9.6%	13	9.7%	9	9.4%	0.73		
2	98	42.6%	54	40.3%	44	45.8%			
3	80	34.8%	47	35.1%	33	34.4%			
4	30	13.0%	20	14.9%	10	10.4%			
Differentiation grade									
well	16	5.3%	8	4.5%	8	6.5%	0.62		
moderate	228	75.7%	134	75.3%	94	76.4%			
poor	57	18.9%	36	20.2%	21	17.1%			
Site of origin									
Rectum	95	31.4%	56	31.3%	39	31.5%	0.98	1.00	0.85-1.16
Colon	208	68.6%	123	68.7%	85	68.5%			
Tumor size									
<40 mm	49	22.0%	24	19.0%	25	25.8%	0.44		
40-60 mm	120	53.8%	69	54.8%	51	52.6%			
>60 mm	54	24.2%	33	26.2%	21	21.6%			
Age at time of diagnosis									
< 65 years	82	27.1%	54	30.2%	28	22.6%	0.25		
65-80 years	167	55.1%	92	51.4%	75	60.5%			
>80 years	54	17.8%	33	18.4%	21	16.9%			
Surgical margins									
negative	230	99.1%	135	100.0%	95	97.9%	0.17		
positive	2	0.9%	0	0.0%	2	2.1%			

P-values are determined by a chi-square test unless otherwise indicated: * Fisher's exact test.

Table 2. β-catenin expression in DDX3 low and DDX3 high colorectal cancers

		Total		Low DDX3		High DDX3				
		n	%	n	%	n	%	P-value	RR	95% CI
Membranous β-catenin	complete expression	231	83.4%	136	83.4%	95	83.3%	0.82		
	partial expression	29	10.5%	16	9.8%	13	11.4%			
	loss of expression	17	6.1%	11	6.7%	6	5.3%			
Cytoplasmic β-catenin	normal expression	91	32.9%	60	37.0%	31	27.0%	0.08	1.16	0.99-1.36
	overexpression	186	67.1%	102	63.0%	84	73.0%			
Nuclear β-catenin	<10%	153	55.8%	107	66.5%	46	40.7%	2.47×10^{-5}	1.77	1.36-2.31
	>10%	121	44.2%	54	33.5%	67	59.3%			

P-values calculated by a chi-square test.

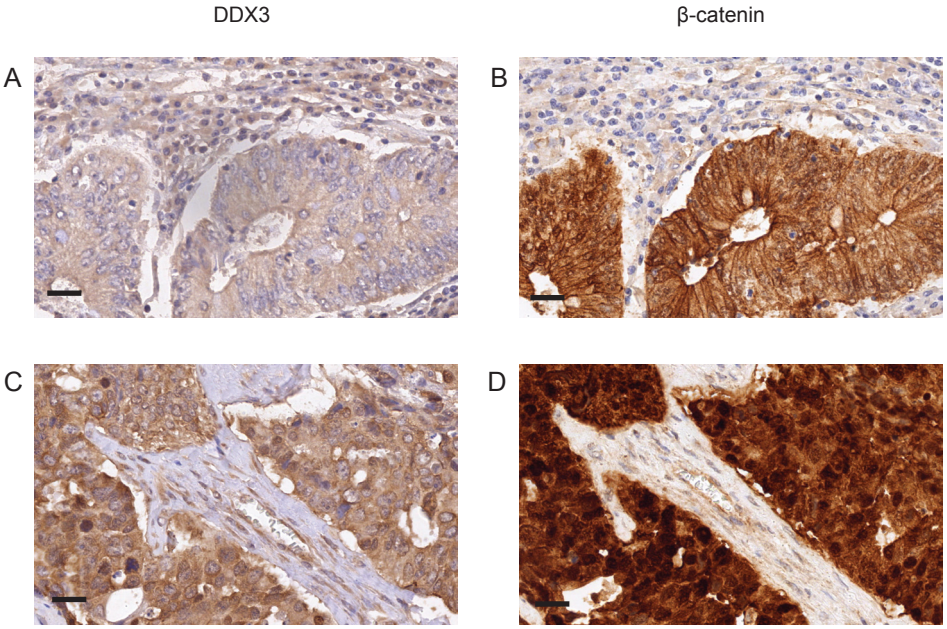

Figure 3. High DDX3 expression is associated with nuclear β-catenin in colorectal cancer samples
Low DDX3 expression (A.) is associated with strong expression of β-catenin on the membranes and absence of β-catenin in the nuclei (B.) High DDX3 expression (C.) is associated with increased β-catenin expression in the cytoplasm and the nucleus (D.). 40 x magnification, scale bar indicates 25 μm

Both adherent cell lines and spheroids could be separated into two groups; a sensitive group of cell lines with an IC50 value <3 μM (HCT116, CRC29, HT29) and a group with a 2-3 fold higher IC50 value ranging from 5-9 μM (CR9, DLD-1, CRC47, SW480, Colo205, L145). Next, we assessed the functional role of DDX3 in the cell lines that were less sensitive to RK-33, by knocking down DDX3 with siDDX3 (Figure 4G). Unlike the RK-33 sensitive cell lines HCT116 and HT29, proliferation in DLD-1 and SW480 was not affected by DDX3 knockdown (Figure 4H) and only a moderate drop in S-phase was observed in SW480 (3.7%; p = 0.02). No effect on cell cycle was seen in DLD-1 (Figure 4I).

Molecular predictors of DDX3 dependency

Centered on our finding of differential sensitivity to RK-33, we hypothesized that sensitivity to RK-33 in colorectal cancer cells may also be associated with other genomic drivers of cellular transformation. Almost all colorectal cell lines and spheroids expressed DDX3 protein (Figure 4A&C), but no direct correlation between RK-33 sensitivity and DDX3 expression levels was observed. Next, we assessed the most commonly occurring mutations in our cell line panel by next generation sequencing (Table 3). Interestingly, we found that two of the three RK-33 sensitive cell lines had wild-type *APC* and *TP53,* whereas the less sensitive group had mutations in these genes.

To further determine if *TP53* mutations in cell lines alters sensitivity to RK-33, we compared RK-33 sensitivity in isogenic cell lines with wild-type *TP53* (HCT116-p53$^{+/+}$) and without *TP53* (HCT116-p53$^{-/-}$; Figure 5A). Both cell lines were equally sensitive to DDX3 inhibition with RK-33 (IC50 2.52 *vs* 2.58 μM; Figure 5B). In addition, similar to the parental cell line that expresses p53 (Figure 1C), knockdown of DDX3 resulted in a G1 arrest (13.9% increase; p = 0.04) and a decrease of cells in S-phase (4.8%; p = 0.11; Figure 5C-D). This indicates that within our experimental setting the sensitivity of RK-33 is independent of p53 status.

Table 3. Correlation between RK-33 sensitivity and mutation status in colorectal cancer cell lines

	RK-33 Sensitivity		Mutations				
Cell line	**IC50 (uM)**	**95% CI**	***APC* Truncation**	***TP53***	***RAS/RAF***	***Others***	**MSI status**
HCT116*	2.71	2.64-2.80	-	-	*KRAS*	*PIK3CA, CTNNB1*	MSI
CRC29†	2.89	2.66-3.14	-	-	*KRAS, BRAF*	*SMAD4, STK11*	MSI
HT29*	2.96	2.84-3.08	E853X, T1556fsX3	R273H	*BRAF*	*PIK3CA, SMAD4*	MSS
CR9†	4.97	4.51-5.48	R1114X, S1503E	R213X, V157A	-	*SMAD4, FBXW7, ERBB2*	
DLD-1*	5.36	5.15-5.59	I1417X	S241F	*KRAS*		MSI
CRC47†	5.54	5.07-6.05	R1450X	P75LfsX48	-	*PIK3CA*	MSI
SW480*	6.32	5.60-7.15	Q1338X	R273H, P309S	*KRAS*	*SMAD4*	MSS
Colo205*	6.65	6.00-7.37	T1556fsX3	Y103fsX8	*BRAF*		MSS
L145†	8.77	7.63-10.08	S1436LfsX34	R110P	*KRAS*		MSS

Mutational status was derived from:*publicly available data in the CanSAR database †next-generation sequencing. - no mutation detected

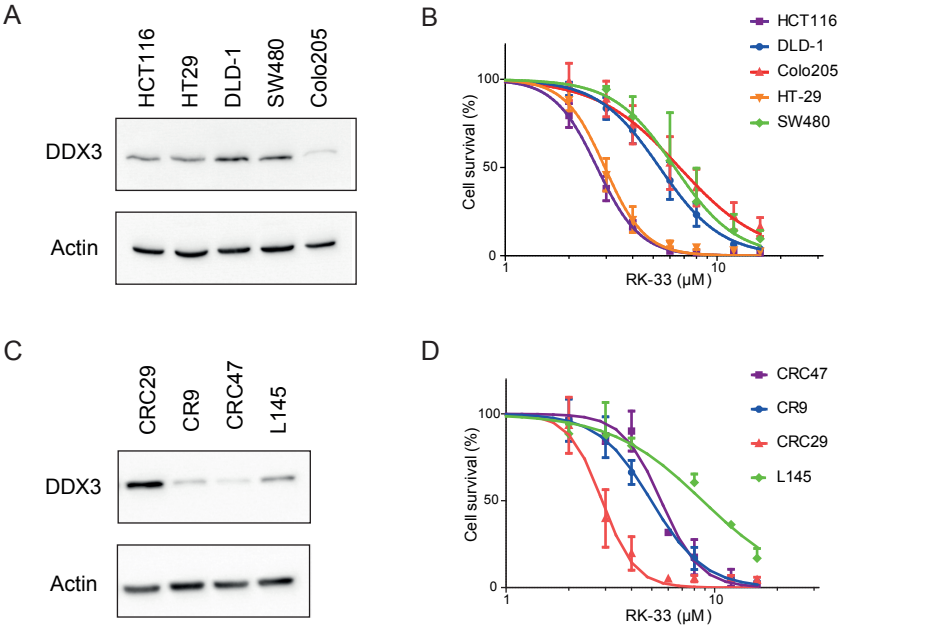
A
HCT116
HT29
DLD-1
SW480
Colo205
DDX3
Actin
B
HCT116
DLD-1
Colo205
HT-29
SW480
Cell survival (%)
RK-33 (μM)
C
CRC29
CR9
CRC47
L145
DDX3
Actin
D
CRC47
CR9
CRC29
L145
Cell survival (%)
RK-33 (μM)

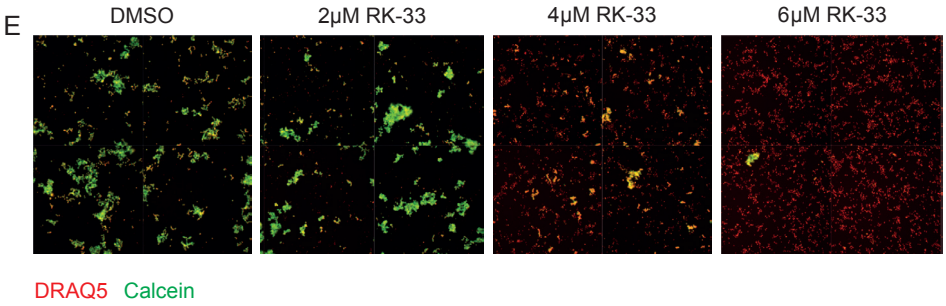
E
DMSO
2μM RK-33
4μM RK-33
6μM RK-33
DRAQ5 Calcein

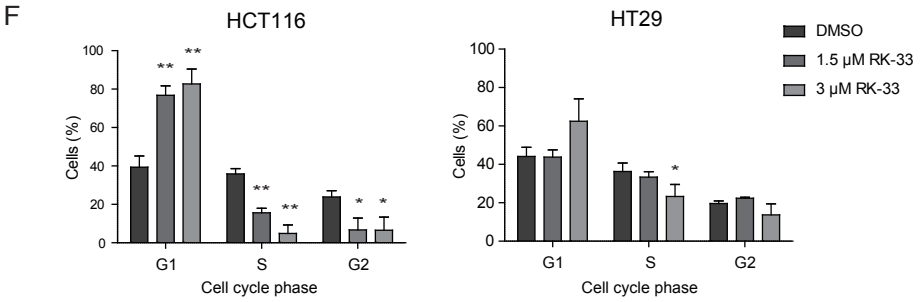
F
HCT116
HT29
DMSO
1.5 μM RK-33
3 μM RK-33
Cells (%)
G1
S
G2
Cell cycle phase

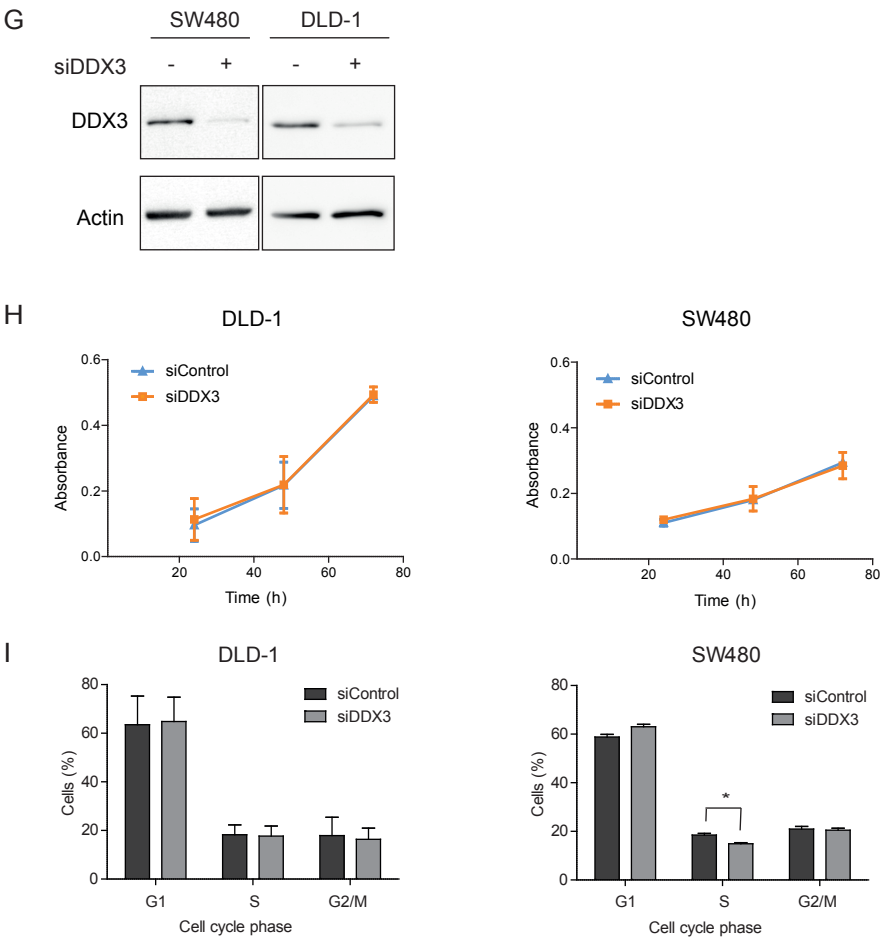

◀ **Figure 4.** RK-33 sensitivity in colorectal cancer cell lines
A. Immunoblot showing the relative DDX3 expression in adherent colorectal cancer cell lines. B. MTS assay showing cytoxicity of RK-33 in different colorectal cancer cell lines. C. Immunoblot showing the relative DDX3 expression in patient-derived 3D cultures. D. Cytotoxicity assay showing the sensitivity of patient-derived 3D cultures of colorectal cancer. E. Example of cytotoxicity assay with RK-33 in CRC29 3D cultures. The DRAQ5 positive (red) areas are used to determine the outline of the spheroids. The Calcein AM (green) intensity within this area is used as a measure for living cells. F. Cell cycle analysis after DDX3 inhibition with increasing concentrations RK-33 in HCT116 and HT29 G. Immunoblots of DDX3 expression in colorectal cancer cell lines SW480 and DLD-1 before and after inhibition of DDX3 with 50 nM siDDX3. H. Proliferation of Colorectal cancer cell lines SW480 and DLD-1 after knockdown of DDX3, measured by daily MTS assays. I. Cell cycle analysis after knockdown of DDX3 in SW480 and DLD-1. All experiments were performed three independent times, graphs represent mean ± SD, * $p < 0.05$, ** $p < 0.01$

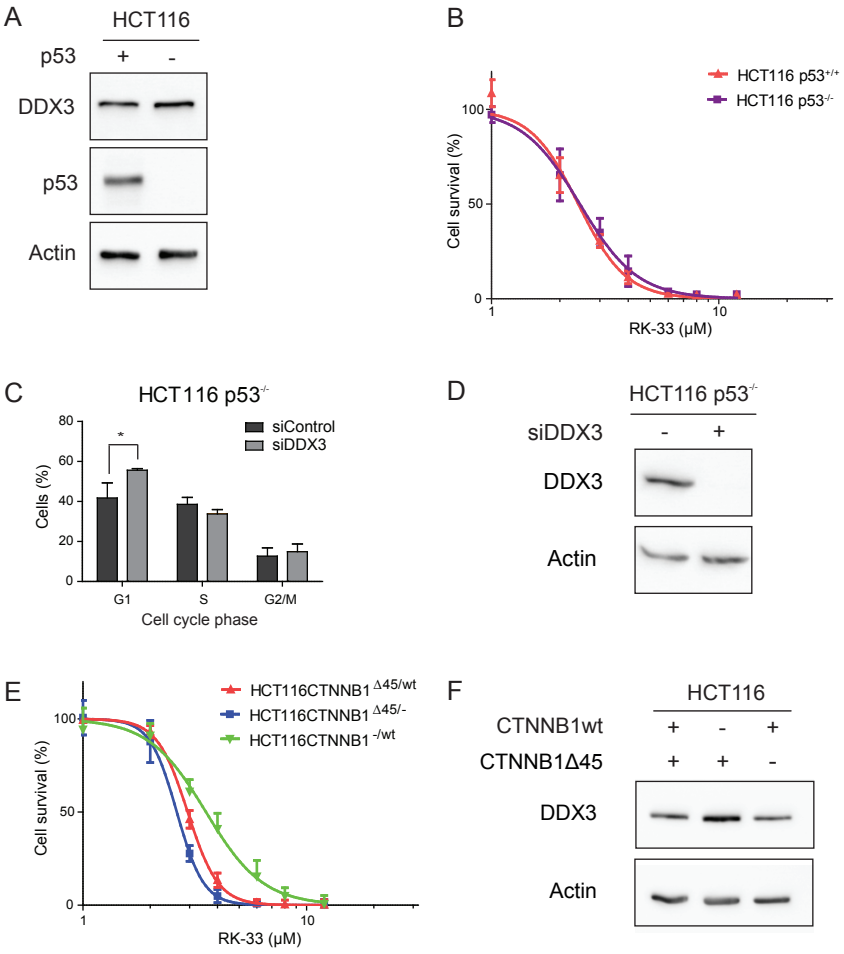

Figure 5. DDX3 dependency in different colorectal cancer genetic subtypes
A. Immunoblot showing p53 and DDX3 expression in HCT116 with and without p53. B. MTS assay showing the relative cytotoxicity after RK-33 treatment in HCT116 with and without p53. C. Cell Cycle analysis of HCT116-p53-/- cells after DDX3 knockdown with 50 nM siDDX3. D. Immunoblots of DDX3 expression in HCT116 p53-/- before and after inhibition of DDX3 with 50 nM siDDX3. E. Relative sensitivity to RK-33 in parental HCT116 (CTNNB1Δ45/wt) and HCT116 with either the mutant CTNNB1 allele (CTNNB1-/wt) or the wild-type allele deleted (CTNNB1Δ45/-). F. Immunoblot showing the DDX3 expression in HCT116 with different β-catenin variants. All experiments were performed three independent times, graphs represent mean ± SD, *p < 0.05

RK-33 sensitivity in relation to different mutations in the Wnt-signaling pathway

Although DDX3 is thought to play a role in Wnt signaling, cells that harbor an *APC* mutation were less sensitive to RK-33 than cells with wild-type *APC*. Since *CTNNB1* and *DDX3X* mutations co-occur in Wnt-type medulloblastomas[7-9], we hypothesized that DDX3 dependency may be higher in cells with other genetic aberrations in the Wnt-signaling pathway, like mutations in the gene encoding β-catenin. We used HCT116 cells with either the wild-type allele deleted (HCT116 *CTNNB1*$^{\Delta 45/-}$) or the mutant β-catenin allele deleted (HCT116 *CTNNB1*$^{-/wt}$) to study the contribution of each allele to RK-33 sensitivity. Interestingly, we found that cells with mutant β-catenin were slightly more sensitive (IC50 2.68 μM) than those with only a wild-type allele (IC50 3.71 μM) and that DDX3 expression is slightly higher in HCT116 β-catenin$^{\Delta 45/-}$ cells (Figure 5D-E). These results indicate that *APC* wild-type colorectal cancers harboring an activating *CTNNB1* mutation may be more sensitive to RK-33 treatment.

Inhibition of DDX3 results in reduced Wnt signaling

To evaluate whether the observed proliferation inhibition is the result of interference with oncogenic Wnt signaling, we tested whether DDX3 inhibition causes a reduction in TCF4-promoter activity with a reporter assay. Knockdown of DDX3 resulted in a significant decrease in Wnt signaling in HCT116 (42%, $p = 0.001$) and a small decrease in HT29 (17%, $p = 0.23$; Figure 6A). RK-33 treatment resulted in an even greater inhibition of TCF4-reporter activity of 74% in HCT116 ($p = 0.0008$) and of 44% in HT29 ($p = 0.03$; Figure 6B). To validate whether the reduced TCF4-reporter activity also resulted in reduced mRNA expression of TCF4-regulated genes, we quantified transcript expression for c-*MYC*, *AXIN2*, *CCND1* and *BIRC5A*. As seen in Figure 6C and Supplementary Table 1, DDX3 knockdown resulted in reduced expression of *AXIN2*, *CCND1* and *BIRC5A* in HCT116. Similarly, a decrease was observed in *CCND1*, c-*MYC* and *BIRC5A* expression in HT29. RK-33 treatment also significantly reduced the amount of transcripts of c-*MYC*, *AXIN2*, *CCND1* and *BIRC5A* in HCT116 (Figure 6D). Again this result was slightly less profound in HT29, where RK-33 caused a reduction in *AXIN2*, *CCND1* and *BIRC5A*. Overall, inhibition of DDX3 results in decreased Wnt signaling in HCT116 and to a lesser extent in HT29, which corresponds to their relative dependence on DDX3 for cell cycle progression.

RK-33 treatment reduces DDX5 protein levels

Since DDX5 and DDX17 are known mediators of Wnt signaling in colorectal cancer[22, 23] and DDX3 and DDX5 have been found to interact[24], we evaluated whether RK-33 treatment also influences DDX5 and DDX17 protein levels. Although we found earlier that RK-33 does not bind directly to DDX5[4], exposure to RK-33 resulted in decreased DDX5 protein levels, but did not affect DDX17 expression (Figure 7). This indicates that the observed reduction in Wnt signaling could be either as a direct result of decreased DDX3 levels, of the consequentially lowered DDX5 expression, or of a combination of both mechanisms.

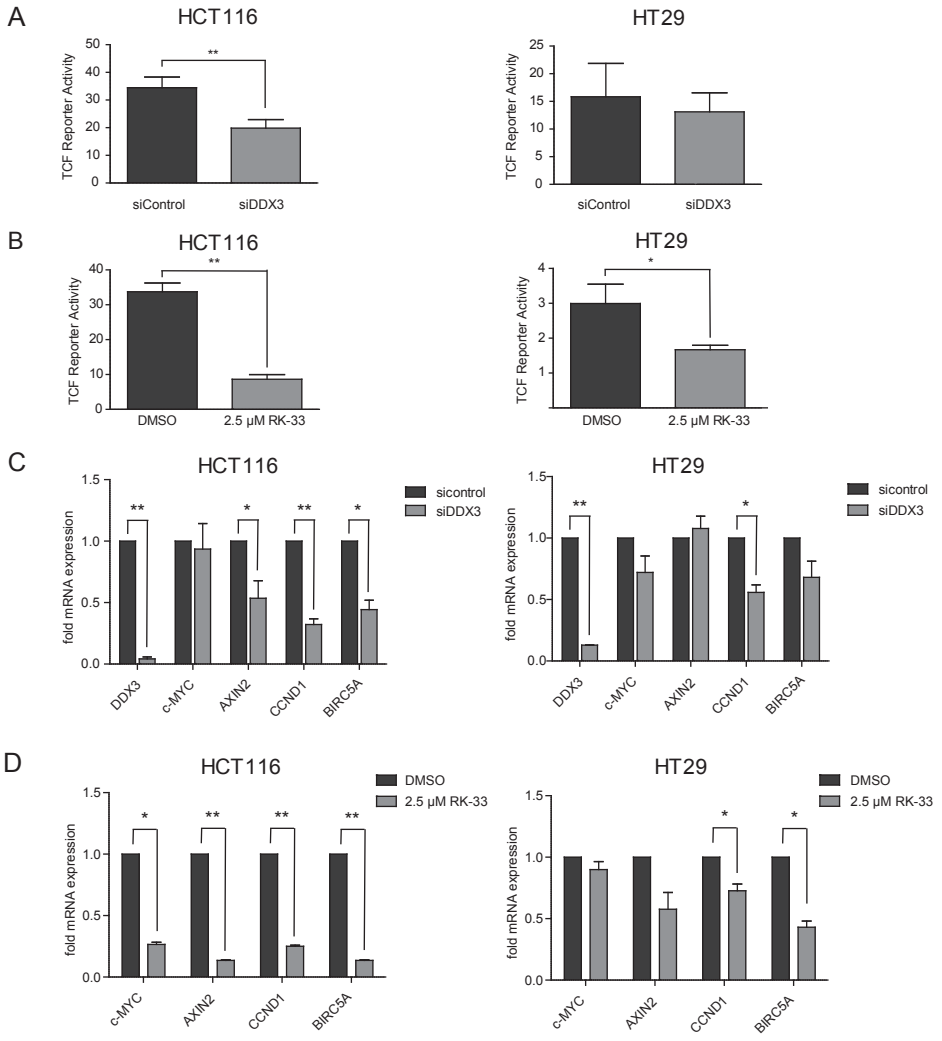

Figure 6. DDX3 inhibition results in reduced Wnt signaling activity
A. and B. TCF4-reporter assays after knockdown of DDX3 with 50 nM siDDX3 (A.) and inhibition of DDX3 with RK-33 (B.) in DDX3-dependent colorectal cancer cell lines HCT116 and HT29. C. and D. Relative mRNA expression of TCF4-target genes after knockdown of DDX3 with 50 nM siDDX3 (C.) or DDX3 inhibition with RK-33 (D.) All experiments were performed three independent times, graphs represent mean ± SD, * $p < 0.05$, ** $p < 0.01$.

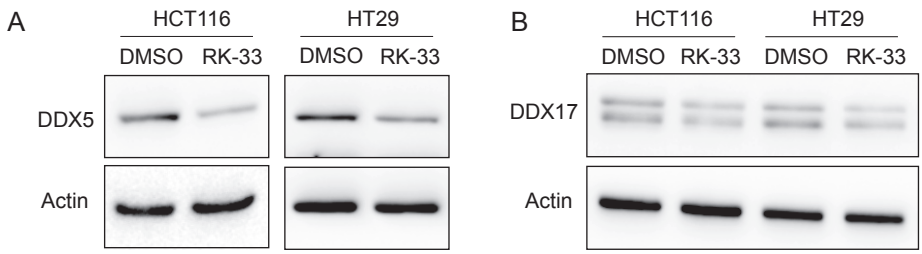

Figure 7. DDX5 and DDX17 expression after treatment with RK-33
A. DDX5 expression before and after DDX3 inhibition with RK-33. B. DDX17 expression before and after DDX3 inhibition with RK-33.

DISCUSSION

Previously, we demonstrated that DDX3 is overexpressed in breast and lung cancers and that targeting DDX3 by RK-33 promotes cell death.[3, 4] This requirement for DDX3 can in part be explained by its involvement in Wnt signaling, as was shown previously by our group and others.[4-6] As the majority of colorectal cancers is driven by mutations in the Wnt-signaling pathway, we explored the possible contribution of DDX3 to Wnt-associated colorectal cancer oncogenesis. In the present study, we showed that DDX3 is overexpressed in 39% of colorectal cancers and that inhibition of DDX3 results in reduced Wnt signaling and a G1 arrest, making DDX3 an attractive therapeutic target in these cancers.

The clinical relevance of the development of Wnt signaling inhibitors which work in a constitutively activated setting is tremendous, since mutations in the Wnt-signaling pathway are not only the first genetic alterations in the adenoma-carcinoma sequence, but advanced colorectal cancers with mutations in *APC* or *CTNNB1* remain dependent on upstream Wnt signaling activity.[25, 26] Especially colorectal cancer stem cells rely on Wnt signaling, and potent inhibition may therefore specifically inhibit the resistant tumor initiating cell population.[27] This potential is also reflected by the cytotoxic effect of RK-33 on 3D cultures of colorectal cancer stem cells in our study. Colorectal cancer drug development is currently limited by a lack of pathway specific targets, potential redundancy of pathway components and toxicity.[28] In this study we show that DDX3 is an integral component of Wnt signaling, and targeting DDX3 by RK-33 is a potential therapeutic option. Although previous mouse studies showed no RK-33-related toxicity[4], future studies will need to validate the anti-cancer activity of DDX3 inhibition in *in vivo* models of colorectal cancer.

Apart from several studies finding an oncogenic role of DDX3 in cancer[3, 4, 6, 29-34], others have suggested that DDX3 may also have a tumor suppressive role in certain cancers.[35-38] Although it is difficult to explain these discrepancies by the molecular backgrounds of different cancer types, it is possible that DDX3 levels can differ between different subsets

of patients within a particular cancer. For example, we found high DDX3 expression to be associated with worse prognosis in smoking patients with head and neck squamous cell carcinomas,[39] whereas the opposite was observed in non-smoking patients.[40] DDX3 inhibition resulted in a reduction of proliferation in several colorectal cell lines and all of the colorectal cancer cell lines used in this study were susceptible to RK-33, pleading for reliance of colorectal cancer cells on DDX3 for their survival and arguing against a tumor suppressive role in this particular setting. Interestingly, within our cohort of colorectal cancer cell lines, we observed differential sensitivity to RK-33, indicating that other genetic factors may contribute to oncogenic addiction to DDX3 in neoplastic cells.

Personalized cancer therapy, in which the treatment is adjusted to specific molecular characteristics of a tumor, is of great promise for future cancer treatment. The sensitivity to DDX3 inhibition with both RK-33 and siDDX3 was greatest in HCT116, closely followed by HT29. SW480 and DLD-1 were less sensitive to RK-33 and not affected by siDDX3 treatment. Within our experimental setting, DDX3 dependency was not necessarily reflected by absolute DDX3 protein expression levels. This could be due to the fact that the levels of DDX3 essential to maintain cellular homeostasis are variable in different colorectal cancer cells. Another possibility is that in conjunction with DDX3, there could be an association with other specific genetic alterations that promotes RK-33 sensitivity. DDX3 dependency seemed to be greater in the presence of wild-type APC-status and activating mutations in *CTNNB1*. This finding is in line with the co-occurrence of *DDX3X* and *CTNNB1* mutations in medulloblastomas[7-9] and provides a potential explanation for the fact that HT29, which harbors a mutation in *APC,* does not show a clear G1 arrest upon DDX3 knockdown. However, both our sample size and the differences in RK-33 sensitivity were too small to be able to make any definite claims with regard to predictors of DDX3 dependency.

Different levels of interference have been suggested for DDX3 in the Wnt-signaling pathway. In contrast with our findings, Cruciat, *et al.* found that DDX3 inhibition had no effect on Wnt signaling activity after induction with β-catenin overexpression and that the involvement of DDX3 in this pathway was independent of its helicase activity.[5] It is possible that other mechanisms by which DDX3 is involved in Wnt signaling, like stabilization of β-catenin indirectly through Rac1-signaling[6] or DDX5, or through a direct interaction with DDX3[4] are more prominent in colorectal cancers. Unfortunately, only a minority of colorectal cancers (23%) falls into the wild-type APC group. However, mutations in *CTNNB1* are highly prevalent in hepatocellular carcinoma (24%), sarcoma (44%) and testicular cancer(24%)[41], suggesting that these cancers may potentially have increased sensitivity to RK-33. In contrast to Sun *et al.* who found DDX3 to be pro-apoptotic in a p53-wildtype breast cancer cell line and anti-apoptotic in cell lines harboring a p53-mutation[42], we found DDX3 dependency not to differ in the presence or absence of p53.

Overall, we conclude that a subset of colorectal cancers is addicted to DDX3 expression. In these more often *APC*-wild-type cancers, inhibition of DDX3 causes a potent reduction of Wnt signaling and a G1 arrest. DDX3 inhibition with the small molecule inhibitor RK-33 is therefore a promising future treatment strategy in colorectal cancer.

Acknowledgements
We would like to acknowledge the following people: Bert Vogelstein and Fred Bunz for providing cell lines and advice, Min Xie and Saritha Tantravedi for synthesizing RK-33, Ashley Irving and Yehudit Bergman for general technical assistance, Hans Clevers for providing the TOP/FOP constructs, the molecular- and immunopathology laboratory at the UMC Utrecht for performing the β-catenin immunohistochemistry and the next-generation sequencing, Shona Kalkman for her help in the analysis of the immunohistochemistry and Folkert Morsink for provision of colorectal cancer TMAs.

REFERENCES

1 Society AC. *Cancer Facts & Figures*. American Cancer Society: Atlanta, 2015.
2 Comprehensive molecular characterization of human colon and rectal cancer. Nature 2012; **487**: 330-337.
3 Botlagunta M, Vesuna F, Mironchik Y, Raman A, Lisok A, Winnard P, Jr. *et al*. Oncogenic role of DDX3 in breast cancer biogenesis. Oncogene 2008; **27**: 3912-3922.
4 Bol GM, Vesuna F, Xie M, Zeng J, Aziz K, Gandhi N *et al*. Targeting DDX3 with a small molecule inhibitor for lung cancer therapy. EMBO molecular medicine 2015.
5 Cruciat CM, Dolde C, de Groot RE, Ohkawara B, Reinhard C, Korswagen HC *et al*. RNA helicase DDX3 is a regulatory subunit of casein kinase 1 in Wnt-beta-catenin signaling. Science 2013; **339**: 1436-1441.
6 Chen HH, Yu HI, Cho WC, Tarn WY. DDX3 modulates cell adhesion and motility and cancer cell metastasis via Rac1-mediated signaling pathway. Oncogene 2015; **34**: 2790-2800.
7 Pugh TJ, Weeraratne SD, Archer TC, Pomeranz Krummel DA, Auclair D, Bochicchio J *et al*. Medulloblastoma exome sequencing uncovers subtype-specific somatic mutations. Nature 2012; **488**: 106-110.
8 Jones DT, Jager N, Kool M, Zichner T, Hutter B, Sultan M *et al*. Dissecting the genomic complexity underlying medulloblastoma. Nature 2012; **488**: 100-105.
9 Robinson G, Parker M, Kranenburg TA, Lu C, Chen X, Ding L *et al*. Novel mutations target distinct subgroups of medulloblastoma. Nature 2012; **488**: 43-48.
10 Bunz F, Dutriaux A, Lengauer C, Waldman T, Zhou S, Brown JP *et al*. Requirement for p53 and p21 to sustain G2 arrest after DNA damage. Science 1998; **282**: 1497-1501.
11 Chan TA, Wang Z, Dang LH, Vogelstein B, Kinzler KW. Targeted inactivation of CTNNB1 reveals unexpected effects of beta-catenin mutation. Proceedings of the National Academy of Sciences of the United States of America 2002; **99**: 8265-8270.
12 Emmink BL, Van Houdt WJ, Vries RG, Hoogwater FJ, Govaert KM, Verheem A *et al*. Differentiated human colorectal cancer cells protect tumor-initiating cells from irinotecan. Gastroenterology 2011; **141**: 269-278.
13 Halling-Brown MD, Bulusu KC, Patel M, Tym JE, Al-Lazikani B. canSAR: an integrated cancer public translational research and drug discovery resource. Nucleic acids research 2012; **40**: D947-956.
14 Angus AG, Dalrymple D, Boulant S, McGivern DR, Clayton RF, Scott MJ *et al*. Requirement of cellular DDX3 for hepatitis C virus replication is unrelated to its interaction with the viral core protein. The Journal of general virology 2010; **91**: 122-132.
15 Trumpi K, Egan DA, Vellinga TT, Borel Rinkes IH, Kranenburg O. Paired image- and FACS-based toxicity assays for high content screening of spheroid-type tumor cell cultures. FEBS open bio 2015; **5**: 85-90.
16 Vesuna F, Lisok A, Kimble B, Domek J, Kato Y, van der Groep P *et al*. Twist contributes to hormone resistance in breast cancer by downregulating estrogen receptor-alpha. Oncogene 2012; **31**: 3223-3234.
17 van de Wetering M, Sancho E, Verweij C, de Lau W, Oving I, Hurlstone A *et al*. The beta-catenin/TCF-4 complex imposes a crypt progenitor phenotype on colorectal cancer cells. Cell 2002; **111**: 241-250.
18 Yuan JS, Reed A, Chen F, Stewart CN, Jr. Statistical analysis of real-time PCR data. BMC bioinformatics 2006; **7**: 85.
19 Kodach LL, Wiercinska E, de Miranda NF, Bleuming SA, Musler AR, Peppelenbosch MP *et al*. The bone morphogenetic protein pathway is inactivated in the majority of sporadic colorectal cancers. Gastroenterology 2008; **134**: 1332-1341.
20 The Medical Research Involving Human Subjects Act [In Dutch: Wet medisch-wetenschappelijk onderzoek met mensen, WMO]. *Burgerlijk Wetboek*, 1998.
21 van Diest PJ. No consent should be needed for using leftover body material for scientific purposes. For. BMJ 2002; **325**: 648-651.
22 Yang L, Lin C, Liu ZR. P68 RNA helicase mediates PDGF-induced epithelial mesenchymal transition by displacing Axin from beta-catenin. Cell 2006; **127**: 139-155.
23 Shin S, Rossow KL, Grande JP, Janknecht R. Involvement of RNA helicases p68 and p72 in colon cancer. Cancer research 2007; **67**: 7572-7578.
24 Choi YJ, Lee SG. The DEAD-box RNA helicase DDX3 interacts with DDX5, co-localizes with it in the cytoplasm during the G2/M phase of the cycle, and affects its shuttling during mRNP export. Journal of cellular biochemistry 2012; **113**: 985-996.
25 He B, Reguart N, You L, Mazieres J, Xu Z, Lee AY *et al*. Blockade of Wnt-1 signaling induces apoptosis in human colorectal cancer cells containing downstream mutations. Oncogene 2005; **24**: 3054-3058.
26 Voloshanenko O, Erdmann G, Dubash TD, Augustin I, Metzig M, Moffa G *et al*. Wnt secretion is required to maintain high levels of Wnt activity in colon cancer cells. Nature communications 2013; **4**: 2610.
27 de Sousa EM, Vermeulen L, Richel D, Medema JP. Targeting Wnt signaling in colon cancer stem cells. Clinical cancer research : an official journal of the American Association for Cancer Research 2011; **17**: 647-653.
28 Anastas JN, Moon RT. WNT signalling pathways as therapeutic targets in cancer. Nature reviews Cancer 2013; **13**: 11-26.
29 Oliver PG, LoBuglio AF, Zhou T, Forero A, Kim H, Zinn KR *et al*. Effect of anti-DR5 and chemotherapy on basal-like breast cancer. Breast cancer research and treatment 2012; **133**: 417-426.
30 Shih JW, Wang WT, Tsai TY, Kuo CY, Li HK, Wu Lee YH. Critical roles of RNA helicase DDX3 and its interactions with eIF4E/PABP1 in stress granule assembly and stress response. The Biochemical journal 2012; **441**: 119-129.
31 Lai MC, Chang WC, Shieh SY, Tarn WY. DDX3 regulates cell growth through translational control of cyclin E1. Molecular and cellular biology 2010; **30**: 5444-5453.
32 Hagerstrand D, Tong A, Schumacher SE, Ilic N, Shen RR, Cheung HW *et al*. Systematic interrogation of 3q26 identifies TLOC1 and SKIL as cancer drivers. Cancer discovery 2013; **3**: 1044-1057.

33 Huang JS, Chao CC, Su TL, Yeh SH, Chen DS, Chen CT *et al*. Diverse cellular transformation capability of overexpressed genes in human hepatocellular carcinoma. Biochemical and biophysical research communications 2004; **315**: 950-958.

34 Sun M, Song L, Li Y, Zhou T, Jope RS. Identification of an antiapoptotic protein complex at death receptors. Cell death and differentiation 2008; **15**: 1887-1900.

35 Chang PC, Chi CW, Chau GY, Li FY, Tsai YH, Wu JC *et al*. DDX3, a DEAD box RNA helicase, is deregulated in hepatitis virus-associated hepatocellular carcinoma and is involved in cell growth control. Oncogene 2006; **25**: 1991-2003.

36 Chao CH, Chen CM, Cheng PL, Shih JW, Tsou AP, Lee YH. DDX3, a DEAD box RNA helicase with tumor growth-suppressive property and transcriptional regulation activity of the p21waf1/cip1 promoter, is a candidate tumor suppressor. Cancer research 2006; **66**: 6579-6588.

37 Wu DW, Lee MC, Wang J, Chen CY, Cheng YW, Lee H. DDX3 loss by p53 inactivation promotes tumor malignancy via the MDM2/Slug/E-cadherin pathway and poor patient outcome in non-small-cell lung cancer. Oncogene 2014; **33**: 1515-1526.

38 Wu DW, Liu WS, Wang J, Chen CY, Cheng YW, Lee H. Reduced p21(WAF1/CIP1) via alteration of p53-DDX3 pathway is associated with poor relapse-free survival in early-stage human papillomavirus-associated lung cancer. Clinical cancer research : an official journal of the American Association for Cancer Research 2011; **17**: 1895-1905.

39 Heerma van Voss MR, van Kempen PMW, Noorlag R, van Diest PJ, Willems SM, Raman V. DDX3 has divergent roles in head and neck squamous cell carcinomas in smoking versus non-smoking patients. Oral diseases 2015; **21**: 270-271.

40 Lee CH, Lin SH, Yang SF, Yang SM, Chen MK, Lee H *et al*. Low/negative expression of DDX3 might predict poor prognosis in non-smoker patients with oral cancer. Oral diseases 2014; **20**: 76-83.

41 Sanger Institute. COSMIC: Catalogue of Somatic Mutations in Cancer, vol. 2015.

42 Sun M, Zhou T, Jonasch E, Jope RS. DDX3 regulates DNA damage-induced apoptosis and p53 stabilization. Biochimica et biophysica acta 2013; **1833**: 1489-1497.

43 Brattain MG, Fine WD, Khaled FM, Thompson J, Brattain DE. Heterogeneity of malignant cells from a human colonic carcinoma. Cancer research 1981; **41**: 1751-1756.

44 Eshleman JR, Lang EZ, Bowerfind GK, Parsons R, Vogelstein B, Willson JK *et al*. Increased mutation rate at the hprt locus accompanies microsatellite instability in colon cancer. Oncogene 1995; **10**: 33-37.

45 Fogh J. *Human Tumor Cells in Vitro*. Plenum Press: New York, USA, 1975.

46 Chen TR, Dorotinsky CS, McGuire LJ, Macy ML, Hay RJ. DLD-1 and HCT-15 cell lines derived separately from colorectal carcinomas have totally different chromosome changes but the same genetic origin. Cancer genetics and cytogenetics 1995; **81**: 103-108.

47 Gitelman I, Dexter DF, Roder JC. DNA amplification and metastasis of the human melanoma cell line MeWo. Cancer research 1987; **47**: 3851-3855.

48 Leibovitz A, Stinson JC, McCombs WB, 3rd, McCoy CE, Mazur KC, Mabry ND. Classification of human colorectal adenocarcinoma cell lines. Cancer research 1976; **36**: 4562-4569.

49 Semple TU, Quinn LA, Woods LK, Moore GE. Tumor and lymphoid cell lines from a patient with carcinoma of the colon for a cytotoxicity model. Cancer research 1978; **38**: 1345-1355.

SUPPLEMENTARY

Supplementary table 1. Clinical characteristics of the patients from which the cell lines in this study where derived

	Patient	Organ	Stage	Derived from	Reference
HCT116	48-year old male	Colon ascendens	Dukes' D	Primary tumor	Brattain, et al.,[43] Eshleman, et al.[44]
CRC29	81-year old female	Colon	T2N0Mx	Primary tumor	
HT29	44-year old female	Colon	Dukes' C	Primary tumor	Fogh, et al. [45]
CR9	73-year old male	Colon	T3N0M1	Primary tumor	
DLD-1	Male	Colon		Primary tumor	Chen, et al.[46], Dexter, et al.[47]
CRC47		Colon (Sigmoid)	T3N1Mx	Primary tumor	
SW480	50-year old male	Colon	Dukes' B	Primary tumor	Leibovitz, et al.[48]
Colo205	70-year old male	Colon cancer		Ascites	Semple, et al.[49]
L145	72-year old male	Colon cancer liver metastasis		Liver metastasis	

Supplementary table 2. mRNA expression of TCF4-target genes after DDX3 inhibition

		DDX3		***c-MYC***		***AXIN2***		***CCND1***		***BIRC5A***	
		fold change	**p-value**	**fold change**	**p-value**	**fold change**	**p-value**	**fold change**	**p-value**	**fold change**	**p-value**
HCT116	siDDX3	23.7	0.005	1.07	0.58	1.86	0.05	3.10	0.005	2.27	0.01
	RK-33			3.76	0.01	7.37	0.01	4.68	0.01	7.41	0.001
HT29	siDDX3	7.81	0.00003	1.40	0.09	1.08	0.30	1.79	0.007	1.47	0.07
	RK-33			1.11	0.17	1.73	0.09	1.38	0.03	2.31	0.04

Red = upregulated, green = downregulated. P-values calculated by a paired student's T-test.

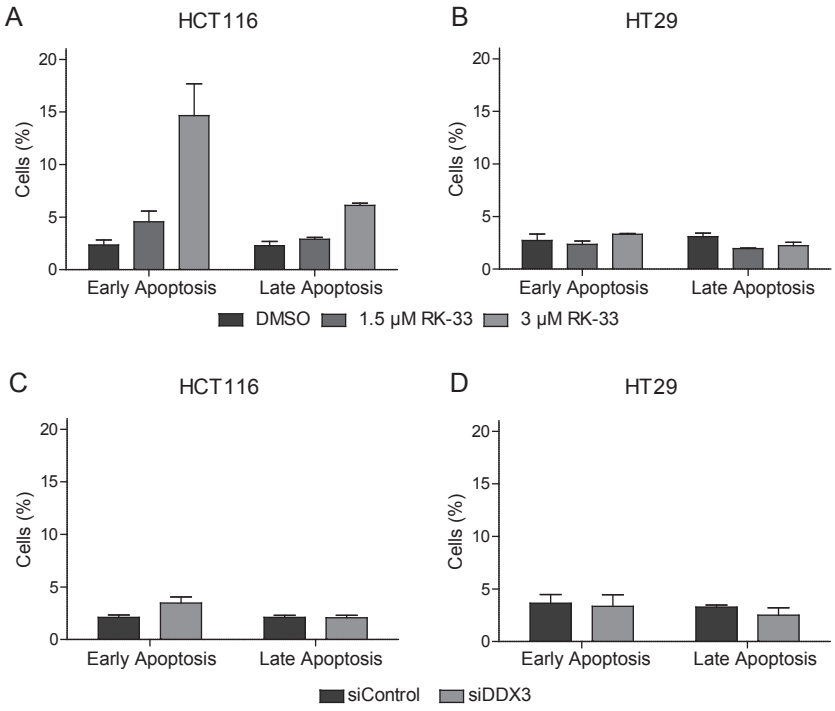

Supplementary Figure 1. Cells undergoing apoptosis after DDX3 inhibition
Histograms depicting the percentage of cells undergoing early apoptosis (Annexin V positive) or late apoptosis (Propidium Iodide labeled) as a result of DDX3 inhibition by RK-33 (A. & B.) or siDDX3 (C. & D.), analyzed by flow cytometry. Graph represents mean ± SD.

CHAPTER 5

Nuclear DDX3 Expression Predicts Poor Outcome in Colorectal and Breast Cancer

Marise R. Heerma van Voss, Farhad Vesuna, Guus M. Bol, Jan Meeldijk, Ana Raman, G. Johan Offerhaus, Horst Buerger, Arvind H. Patel, Elsken van der Wall, Paul J. van Diest, Venu Raman

ABSTRACT

DDX3 is an RNA helicase with oncogenic properties that shuttles between the cytoplasm and nucleus. The majority of DDX3 is found in the cytoplasm, but a subset of tumors has distinct nuclear DDX3 localization of yet unknown biological significance. This study aimed to evaluate the significance of and mechanisms behind nuclear DDX3 expression in colorectal and breast cancer.

Expression of nuclear DDX3 and the nuclear exporter CRM1 was evaluated by immunohistochemistry in 304 colorectal and 292 breast cancer patient samples. Correlations between the subcellular localization of DDX3 and CRM1 and the difference in overall survival between patients with and without nuclear DDX3 were studied. In addition, DDX3 mutants were created for *in vitro* evaluation of the mechanism behind nuclear retention of DDX3.

DDX3 was present in the nucleus of 35% of colorectal and 48% of breast cancer patient samples and was particularly strong in the nucleolus. Nuclear DDX3 correlated with worse overall survival in both colorectal (HR 2.34, $p < 0.001$) and breast cancer (HR 2.39, $p = 0.004$). Colorectal cancers with nuclear DDX3 expression more often had cytoplasmic expression of the nuclear exporter CRM1 (RR 1.67, p 0.04). *In vitro* analysis of DDX3 deletion mutants demonstrated that CRM1-mediated export was most dependent on the N-terminal nuclear export signal.

Overall, we conclude that nuclear DDX3 is partially CRM1-mediated and predicts worse survival in colorectal and breast cancers, putting it forward as a target for therapeutic intervention with DDX3 inhibitors under development in these cancer types.

INTRODUCTION

DDX3, also known as DDX3X, is a member of the DEAD box RNA helicase family of proteins. Like other family members it has ATPase dependent helicase activity, which allows for the unwinding of double-stranded RNA and restructuring of complex secondary RNA structures[1]. DDX3 has thus been associated with several steps of endogenous RNA metabolism, such as splicing[2, 3], nuclear mRNA export[4, 5], RNA interference[6, 7], ribosomal assembly and translation initiation[5, 8]. Recent studies have also indicated a role for DDX3 in neoplastic transformation. Functional studies have shown that DDX3 has anti-apoptotic properties[9-11] and is necessary for cell cycle progression[12, 13] and invasion[14, 15]. The tumor enhancing role of cytoplasmic DDX3 was corroborated by studies on DDX3 expression in patient cancer samples[6, 13].

DDX3 is known to shuttle between cytoplasm and nucleus[4], but in most human tissues and cell lines it is localized predominantly in the cytoplasm. We noticed that in a subgroup of colorectal and breast cancers, DDX3 can also be observed in the nucleus. It remains to be elucidated what exact role DDX3 plays in the nucleus of cancer cells and how the subcellular localization of DDX3 is regulated in these cells. It is known that DDX3 is exported out of the nucleus as part of mRNP complexes associated both with the tip-associated protein (TAP) dependent bulk mRNA export pathway[5, 16] and the alternative chromosome region maintenance 1 (CRM1) dependent pathway[4]. However, the exact nature of the relation between DDX3 expression and expression of the nuclear exporter CRM1 requires further mechanistic exploration and validation in patient samples.

Apart from the biological relevance of understanding the nuclear role of DDX3 in cancer cells, identification of nuclear DDX3 as a prognostic and therapeutic biomarker could facilitate selection of patients who would benefit from adjuvant treatment, specifically with DDX3 inhibitors that are under development[12, 17, 18]. In this study we therefore evaluated the correlation between nuclear DDX3 expression and survival in cohorts of breast and colorectal cancer patient samples. Because DDX3 is known to bind the nuclear exporter CRM1[4], we sought to determine whether nuclear retention of DDX3 can be explained by aberrant CRM1 expression. Finally, we carried out *in vitro* experiments to functionally validate mechanisms of nuclear DDX3 retention.

MATERIAL AND METHODS

Patient samples

Tissue microarrays (TMAs) with samples from 72 colorectal cancer patients from the Academic Medical Center, Amsterdam[19], 292 colorectal cancers from Paderborn Germany[13] and 315 breast cancers from the UMC Utrecht were used[20]. All TMAs included multiple cores per patient. Missing cases were due to damaged or detached cores during cutting or

staining, or due to cores not containing invasive carcinoma. Clinicopathological data were retrieved from the pathology report and patient files. The breast cancer cases in this cohort were classified into molecular subtypes as was described before[21, 22]. We used anonymous archival leftover pathology material. Therefore no ethical approval or informed consent is required according to Dutch legislation[23], as this use of redundant tissue for research purposes is part of the standard treatment agreement with patients in our hospitals[24].

Immunohistochemistry

Four μm thick sections were cut, mounted on SuperFrost slides (Menzel&Glaeser, Brunswick, Germany), deparaffinized in xylene and rehydrated in decreasing ethanol dilutions. Endogenous peroxidase activity was blocked with 1.5% hydrogen peroxide buffer for 15 minutes and was followed by antigen retrieval by boiling for 20 minutes in 10mM citrate buffer (pH 6.0) for DDX3 and EDTA buffer (pH 9.0) for CRM1. Slides were subsequently incubated in a humidified chamber for 1 hour with anti-DDX3 (1:1000, pAb r647)[25] or anti-CRM1 (1:500, ab84375, Abcam, Cambridge, UK). After washing with PBS, slides were incubated with poly-HRP-anti-mouse/rabbit/rat IgG (Brightvision, Immunologic, Duiven, The Netherlands) as a secondary antibody for 30 minutes at room temperature. Peroxidase activity was developed with diaminobenzidine and hydrogen peroxide substrate solution for 10 minutes. The slides were lightly counterstained with haematoxylin and mounted. Appropriate positive and negative controls were used throughout.

Scoring was performed by consensus of two observers (P.v.D. and M.H.v.V. or G.B.). Although the intensity of nuclear DDX3 in cells was similar, the fraction of positive cells varied. Therefore, the percentage of DDX3 positive nuclei was scored. The optimal cut-off point was selected using the online tool cut-off finder, which helps to select a cut-off that maximizes the difference in survival between groups[26]. Samples with ≥1% DDX3 staining were regarded positive. Almost all cells expressed cytoplasmic DDX3, but the intensity varied and was therefore scored semi-quantitatively as absent (0), low (1), moderate (2) or strong (3). Cases with score 0 to 2 were classified as having low DDX3 expression and evaluated against cases with strong expression as before[13]. Nuclear CRM1 was scored using a semiquantitative score that was previously described by Noske, *et al.*[27]. The percentage of positive cells was scored as 0 (0%), 1 (<10%), 2 (10-50%), 3 (51-80%) or 4 (>80%). The intensity of positive nuclei was scored on the same scale as cytoplasmic DDX3. An overall score was calculated by multiplying the two scores. Cases with a score of 9 and higher were considered to have high nuclear CRM1. Cytoplasmic CRM1 was scored as absent or present.

Statistics

Clinicopathological characteristics were compared between tumors with and without nuclear DDX3. Discrete variables were compared by $\chi 2$ or Fisher's exact test and relative risks (RR) were calculated with 95% confidence intervals (95% CI). The distribution of continuous variables was assessed graphically. Transformation was performed where

indicated. Student's t-test and Mann Whitney U-tests were calculated for normal and non-normal distributed variables respectively. Survival in patients with and without nuclear DDX3 was compared by plotting Kaplan-Meier curves and log-rank tests. Multivariate analysis was performed by including all factors that were found predictive ($p < 0.1$) in univariate analysis in a Cox-proportional hazard model. Stepwise backward selection based on AIC was used to select the final model. Effect modifiers were identified by including multiplicative interaction terms into the model. P-values smaller than 0.05 were considered statistically significant. All statistical analyses were performed with R version 3.2.0.

Cloning and transfections

A pEGFP-C1 vector containing a parental DDX3 construct (GenBank Accession: AF061337) N-terminally fused to a 6-HIS and EGFP sequence was used. An oligo containing three times the SV40 NLS sequence (5'-gatccaaaaaagaagagaaaggta-3', AA: DPKKKRKV) with flanking restriction sites was annealed and subcloned into the parental vector to create an NLS-EGFP-6HIS-DDX3 and an EGFP-NLS-6HIS-DDX3 construct. The DDX3 deletion constructs were created by selective amplification of the parental DDX3 construct lacking the deleted area with Phusion High-Fidelity Polymerase (New England Biosciences, Ipswich, MA, USA), followed by Dpn1 digestion of the bacterial backbone, gel-purification, phosphorylation and religation. All constructs were verified by sequencing before usage. HeLa cells were chosen for DDX3 localization as before[4]. The cell line was purchased from ATCC and last STR-profiled in November 2015. 2 x 10^4 HeLa cells were plated in a 24-well plate. After 24 hours the cells were transfected with 250 ng DDX3 construct, 50 ng H2B-mCherry construct and 1µl *Trans*IT-LT1 transfection reagent. After 12-16 hours the cells were treated with 10 nM Leptomycin B (Sigma, St louis, MO, USA) for four hours after which the number of DDX3 positive nuclei per high power field was counted and the cells were imaged with a confocal Zeiss 780FCS system.

RESULTS

Colorectal cancer patients with nuclear DDX3 have worse overall survival

DDX3 expression could be scored in 304 out of 364 colorectal cancers, of which 34.9% had >1% nuclear DDX3. As shown in Figure 1A, the percentage of cells with nuclear DDX3 varied. Some tumors expressed nuclear DDX3 in all cells, sometimes cells with nuclear DDX3 lay dispersed among negative cells. Heterogeneity between different areas of a tumor (different cores) was also observed. DDX3 was sometimes expressed in the nucleus of plasma cells and fibroblasts as well. Only DDX3 in the nuclei of cancer cells was considered for this analysis. As shown in Table 1, tumors with nuclear DDX3 more often had a larger tumor size ($p = 0.006$). Some tumors expressed DDX3 both in the cytoplasm and the

nucleus. The presence of nuclear DDX3 correlated negatively with cytoplasmic DDX3 (RR 0.62, p = 0.005), which was seen in 125/304 (41%) of cases (Figure 1B). Patients with nuclear DDX3 expression had a significantly decreased 5-year overall survival rate of 51.2%, as compared to 73.7% in those without nuclear DDX3 (HR 2.34, p = 0.0005; Figure 1E). Other usual predictors of survival were TNM-stage (p <0.001), differentiation grade (p = 0.040) and tumor size (p = 0.004). Nuclear DDX3 expression was retained in a Cox-proportional hazards model with TNM-stage ($HR_{adjusted}$ 1.69; p = 0.057; S1 Table). No significant association between high cytoplasmic DDX3 and survival was observed in colorectal cancer patients (HR 0.69, p = 0.160; S1 Figure).

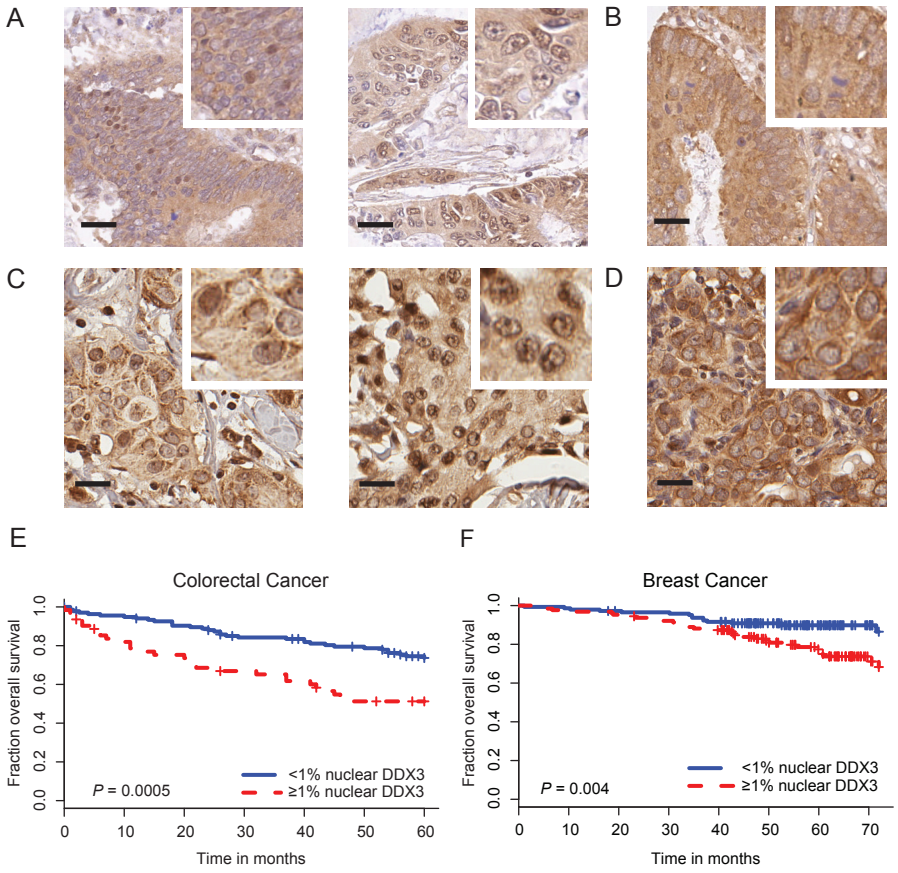

Figure 1 Nuclear DDX3 correlates with worse survival in colorectal and breast cancer patients
Example of (A) nuclear and (B) high cytoplasmic DDX3 expression in colorectal cancer samples. (C) Kaplan-Meier curve showing overall survival in colorectal cancer patients with and without DDX3 expression in ≥1% of the nuclei Example of (D) nuclear and (E) high cytoplasmic DDX3 expression in breast cancer samples. (F) Kaplan-Meier curve showing overall survival in breast cancer patients with and without DDX3 expression in ≥1% of the nuclei 40 x magnification, scale bar indicates 25 µm P-values calculated by log-rank test

Nuclear DDX3 is associated with worse overall survival in breast cancer patients

To assess whether our finding that nuclear DDX3 correlates with survival was also applicable to other tumors, we analyzed a cohort of 315 consecutive breast cancer cases. DDX3 expression could be evaluated in 292 breast cancer patients, of which 141 (48.3%) had nuclear DDX3 (Figure 1C). As shown in Table 2, these patients more often exhibited ductal histology ($p = 0.006$), higher grade ($p = 0.025$), larger tumor size ($p = 0.046$) and positive lymph nodes ($p = 0.003$). In addition, a trend was observed for higher MAI ($p = 0.058$). Nuclear localization of DDX3 did not correlate with cytoplasmic DDX3 expression in breast cancer patients (RR 0.91, $p = 0.493$; Figure 1D). Cytoplasmic DDX3 expression in this breast cancer cohort will be discussed more elaborately in a separate report. As seen in Figure 1F, similarly to colon cancer patients, breast cancer patients with nuclear DDX3 had a worse five year survival rate (75%) than those without (90%; HR 2.39, $p = 0.004$). Other variables that were significant predictors of poor survival were basal-like subtype ($p = 0.024$), positive lymph node status ($p = 0.027$), negative estrogen receptor status (ER; $p = 0.019$, negative progesterone receptor (PR) status ($p = 0.013$) and age over 50 ($p = 0.017$). Nuclear DDX3 remained a significant predictor ($HR_{adjusted}$ 2.63; $p = 0.010$) in a multivariate Cox-proportional hazards model with basal-like subtype, lymph node status and age (S2 Table).

The subcellular localization of the nuclear exporter CRM1 correlates with DDX3 localization

Because DDX3 is known to bind the nuclear exporter CRM1 we ascertained whether nuclear retention of DDX3 could be explained by aberrant CRM1 expression (Figure 2). CRM1 expression was mainly observed in the nucleus. High nuclear CRM1 expression was observed in 18% of colorectal cancer and 27% of breast cancer cases. Cytoplasmic expression was observed as well, more commonly in breast (36%) than colorectal cancer (8%). As shown in Figure 2A-B and Table 3, nuclear DDX3 was significantly associated with the presence of cytoplasmic CRM1 in colorectal cancers (RR 1.67, $p = 0.040$). In breast cancer, no significant correlation between nuclear DDX3 and CRM1 expression was observed, suggesting that aberrant CRM1 expression could only partly explain nuclear DDX3 retention. However, a strong correlation between the intensity of cytoplasmic DDX3 and CRM1 expression (Figure 2C-D) was observed: nuclear CRM1 was higher in tumors with high cytoplasmic DDX3 in both colorectal cancer (RR 1.77, $p < 0.001$) and breast cancer cases (RR 1.75, $p = 0.003$). Contrary to what was observed in colorectal cancer, a significant correlation between cytoplasmic CRM1 and high cytoplasmic DDX3 was observed in breast cancer (RR 2.45, $p < 0.001$).

Table 1. Correlation between nuclear DDX3 and other clinicopathological variables in colorectal cancer patients

		Nuclear DDX3			
	Total	**<1%**	**≥ 1%**	**RR (95% CI)**	**P-value**
Total, n (%)	304 (100)	198 (65)	106 (35)		
Sex, n (%)					0.478
Male	169 (56)	113 (57)	56 (53)	1	
Female	135 (44)	85 (43)	50 (47)	1.12 (0.82-1.52)	
Age, median (IQR)	71 (15.3)	71 (15.8)	72 (14)		0.476†
TNM-Stage, n (%)					0.100
1	22 (10)	18 (12)	4 (5)	1	
2	98 (43)	67 (44)	31 (40)	1.74 (0.68-4.42)	
3	80 (35)	51 (34)	29 (37)	1.99 (0.78-5.07)	
4	30 (13)	15 (10)	15 (19)	2.75 (1.06-7.15)	
Missing	74	47	27		
Differentiation grade, n (%)					0.913
Well	16 (5)	11 (6)	5 (5)	1	
Moderate	229 (76)	149 (76)	80 (76)	1.12 (0.53-2.36)	
Poor	57 (19)	36 (18)	21 (20)	1.18 (0.53-2.63)	
Missing	2	2	0		
Tumor size (mm)					
mean (SD)	52 (23)	50 (23)	56 (22)		0.006‡
Missing	17	12	5		
Site of origin, n (%)					0.064
Rectum	95 (31)	69 (35)	26 (25)	1	
Colon	209 (69)	129 (65)	80 (76)	1.4 (0.97-2.02)	
Histology					0.880§
Adenocarcinoma	276 (93)	179 (93)	97 (93)	1	
Mucinous	21 (7)	13 (7)	8 (8)	1.08 (0.61-1.91)	
Undifferentiated	1 (0)	1 (1)	0 (0)	NA	
Missing	6	5	1		
Cytoplasmic DDX3					0.005
Low	179 (59)	105 (53)	74 (70)	1	
High	125 (41)	93 (47)	32 (30)	0.62 (0.44-0.88)	

P-value calculated by chi-square test unless otherwise indicated. RR, relative risk; 95% CI, 95% confidence interval; IQR, interquartile range; SD, standard deviation; NA, not applicable. † Mann-Whitney U-test; ‡ students t-test; § Fisher exact test

Nuclear DDX3 localization is due to decreased CRM1-mediated export and increased import

To characterize the functional role of DDX3 in the nucleus, we made an attempt to mimick the nuclear DDX3 expression observed in patients in an *in vitro* setting. We generated a GFP-DDX3 fusion protein to study nucleocytoplasmic shuttling properties of DDX3 (Figure 3A). DDX3 is expressed primarily in the cytoplasm of HeLa cells (Figure 3B-C). Leptomycin B specifically inhibits CRM1 by covalent modification of Cys-529[28,29]. When export of DDX3 by CRM1 was inhibited with leptomycin B, an increase in nuclear DDX3 was observed in 46% of cells, but the majority of DDX3 remained in the cytoplasm (Figure 3B-C).

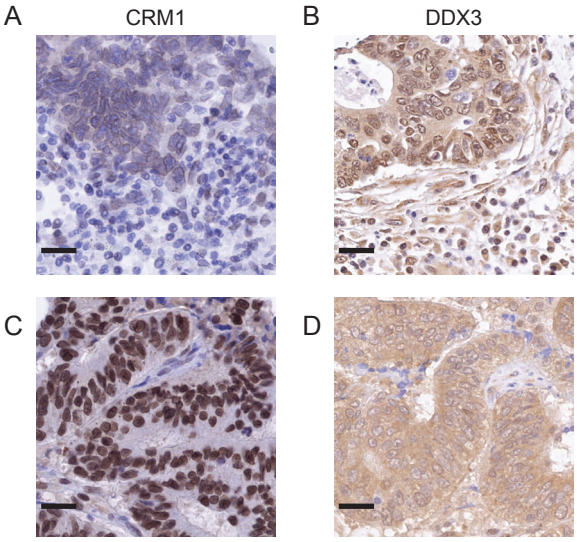

Figure 2. The subcellular localization of CRM1 correlates with the subcellular location of DDX3
Example of how (A) cytoplasmic CRM1 expression in a colorectal cancer correlates with (B) nuclear DDX3 expression in the same tumor. Example of how (C) high nuclear CRM1 expression correlates with (D) high cytoplasmic DDX3 expression 40 x magnification Scale bar indicates 25 µm

Next we determined whether high nuclear DDX3 levels could potentially be explained by increased nuclear import of DDX3. We fused three tandem repeats of the SV40 NLS to the GFP-DDX3 construct (Figure 3A). Only a minor increase of nuclear DDX3 was observed in 20% of cells with the SV40 NLS, indicating that nuclear export of DDX3 is very efficient and not saturated. However, when export of the GFP-NLS-DDX3 construct was inhibited by leptomycin B, DDX3 localized strongly to the nucleus in 100% of cells, whereas cytoplasmic DDX3 was reduced to 25% of cells (Figure 3B-C). These data show that an increase in DDX3 import in combination with reduced CRM1-mediated export can result in high nuclear DDX3 expression. Experiments with an NLS-GFP-DDX3 construct yielded similar results. Unfortunately, it was not possible to create a DDX3 construct that localized to the nucleus spontaneously without inhibition of CRM1. We were therefore unable to study functional effects of nuclear DDX3 in an isolated fashion. However, the created constructs can be used for proof of principle studies on regulation of the subcellular DDX3 localization.

DDX3 localizes to the nucleolus

High expression levels of DDX3 in the nucleus allowed for closer examination of the subnuclear expression pattern of DDX3. As can be observed in Figure 3C, DDX3 is expressed diffusely within the nucleus, but is often most intense in nucleoli. Nucleolar DDX3 was seen in 2-6% of cells after addition of either an NLS or leptomycin B. When import was increased and export was inhibited simultaneously, 30% of cells had clear localization to the nucleolus. This expression pattern resembled that observed in patient samples, although DDX3 expression also was strong at the nuclear membrane in those (Figure 1A&C).

Table 2. Correlations between nuclear DDX3 and other clinicopathological variables in breast cancer patients.

		Nuclear DDX3			
	Total	**<1%**	**≥1%**	**RR (95% CI)**	**P-value**
Total, n (%)	292 (100)	151 (52)	141 (48)		
Age, median (IQR)	58 (17)	60 (18)	56 (18)		0.252†
Histology, n (%)					0.006
Ductal	231 (81)	109 (74)	122 (88)	1	
Lobular	24 (8)	19 (13)	5 (4)	0.39 (0.18-0.87)	
Medullary	31 (11)	19 (13)	12 (9)	0.73 (0.46-1.16)	
Missing	6	4	2		
Grade, n (%)					
1	46 (17)	31 (22)	15 (11)	1	0.025
2	100 (36)	54 (38)	46 (34)	1.41 (0.88-2.25)	
3	132 (48)	59 (41)	73 (55)	1.7 (1.09-2.64)	
Missing	14	7	7		
MAI					
median (IQR)	13 (19)	11 (18)	15 (18)		0.058†
Missing	15	8	7		
Tumor size (mm)					
mean (SD)	24 (15)	23 (13)	26 (16)		0.046‡
Missing					
Molecular subtype					0.904§
Luminal A	224 (77)	117 (79)	107 (76)	1	
Luminal B	12 (4)	5 (3)	7 (5)	1.22 (0.74-2.00)	
HER2	10 (3)	5 (3)	5 (4)	1.05 (0.55-1.97)	
Basal-like	44 (15)	22 (15)	22 (16)	1.05 (0.76-1.45)	
Missing	2	2	0		
Lymph node status					0.003
Negative	124 (47)	73 (56)	50 (38)	1	
Positive	140 (53)	57 (44)	83 (62)	1.46 (1.13-1.88)	
Missing	29	21	8		
ER					0.927
Negative	59 (20)	30 (20)	29 (21)	1	
Positive	231 (80)	119 (80)	112 (79)	0.99 (0.74-1.32)	
Missing	2	2	0		
PR					0.840
Negative	98 (34)	51 (35)	47 (33)	1	
Positive	191 (66)	97 (66)	94 (67)	1.03 (0.80-1.32)	
Missing	3	3	0		
HER2					0.552
Negative	269 (92)	140 (93)	129 (92)	1	
Positive	22 (8)	10 (7)	12 (9)	1.14 (0.76-1.70)	
Missing	1	1	0		
Cytoplasmic DDX3					0.493
Low	194 (68)	98 (66)	96 (70)	1	
High	93 (32)	51 (34)	42 (30)	0.91 (0.70-1.19)	
Missing	5	2	3		

P-value calculated by chi-square test, unless otherwise indicated. RR, relative risk; 95% CI, 95% confidence interval; Grade, Bloom and Richardson grading; MAI, mitotic activity index; IQR, interquartile range; SD, standard deviation; † Mann-Whitney U-test, ‡ student's t-test on log-transformed data; § Fisher exact test

Table 3. Correlation between CRM1 and nuclear DDX3 in colorectal and breast cancers.

			Nuclear DDX3			Cytoplasmic DDX3		
			<1%	≥1%	P-value	low	high	P-value
Colorectal cancer	Cytoplasmic CRM1	absent	180 (95%)	87 (88%)	0.037	157 (2%)	110 (93%)	0.657
		present	10 (5%)	12 (12%)		14 (8%)	8 (7%)	
		missing	8	7		8	7	
	Nuclear CRM1	low	156 (82%)	81 (82%)	0.952	152 (89%)	85 (72%)	<0.001
		high	34 (18%)	18 (18%)		19 (11%)	33 (28%)	
		missing	8	7		8	7	
Breast cancer	Cytoplasmic CRM1	absent	80 (67%)	70 (61%)		116 (75%)	33 (42%)	<0.001
		present	40 (33%)	44 (39%)	0.402	38 (25%)	45 (58%)	
		missing	31	27		40	15	
	Nuclear CRM1	low	90 (75%)	82 (72%)		123 (80%)	48 (62%)	0.003
		high	30 (25%)	32 (28%)	0.595	31 (20%)	30 (38%)	
		missing	31	27		40	15	

P-value calculated by chi-square test.

Influence of CRM1 inhibition on subcellular localization of DDX3 mutants

CRM1 is known to export cargo from the nucleus by binding to a Leucine-rich nuclear export signal[30], which is conserved in the first 21 amino acids of the Ded1/DDX3 subfamily of DEAD box RNA helicases[31]. However, binding studies indicated that CRM1 binding occurs between amino acid 260 and 517 of DDX3[4]. We evaluated whether deletion of either the N-terminal NES domain or the 260-517 region of DDX3 results in increased retention of DDX3 in the nucleus, and whether these proteins were still responsive to CRM1 inhibition. As shown in Figure 3, deletion of the first 21 amino acids containing the NES resulted in 46% of cells having DDX3 in the nucleus. No further increase was observed after leptomycin B treatment and the expression pattern was comparable to that of wildtype DDX3 after CRM1 inhibition, indicating that deletion of the N-terminal NES largely abrogates nuclear export by CRM1.

Deletion of amino acids 260 to 517 resulted in a speckled DDX3 nuclear expression pattern in almost all cells, but the intensity of DDX3 remained strongest in the cytoplasm. When CRM1 was inhibited this pattern shifted to all cells having intense nuclear DDX3 expression, whereas only 7% of cells showed cytoplasmic DDX3 (Figure 3C). This indicates that although the 260-517 region has influence on the subcellular localization of DDX3, DDX3 localization is still responsive to CRM1 inhibition after deletion of this region.

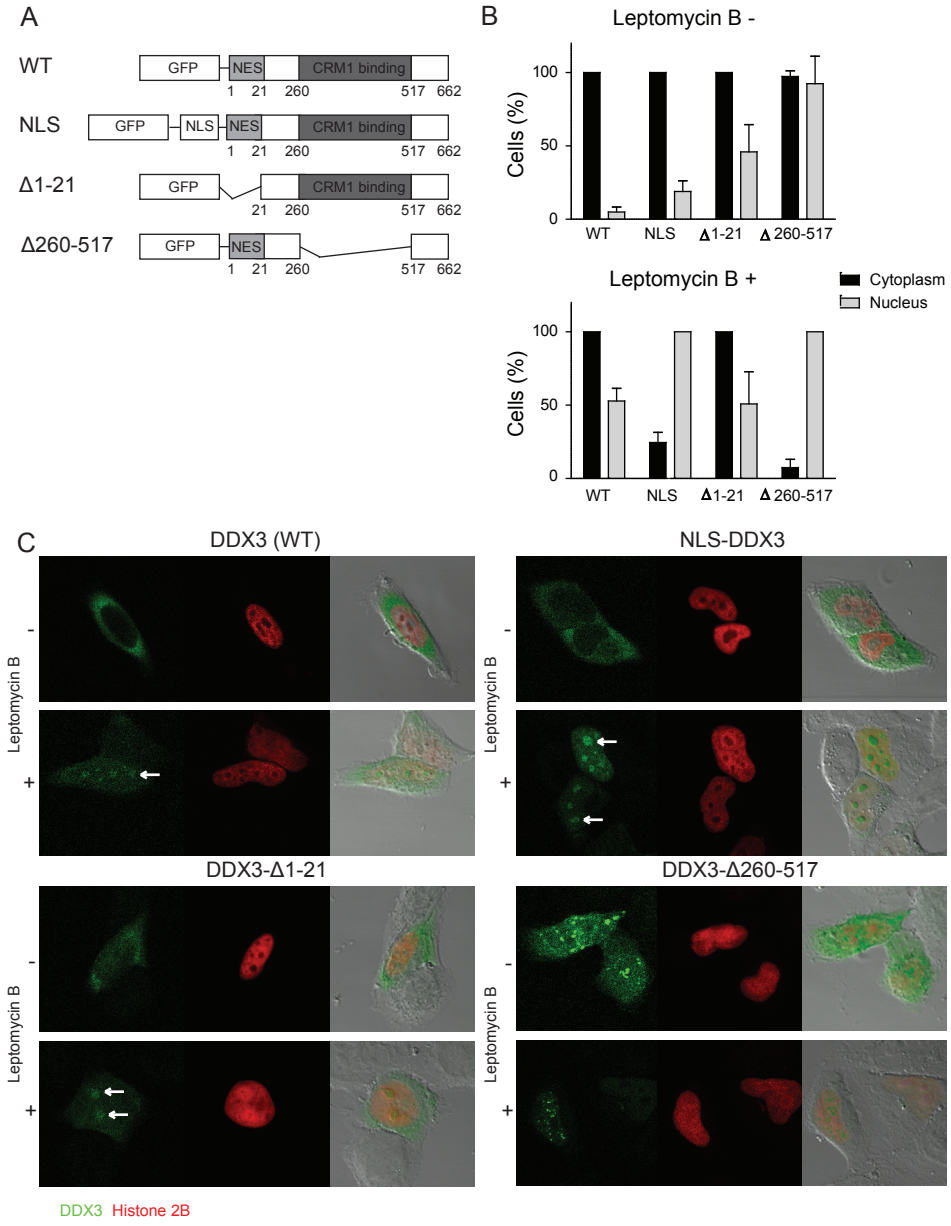

Figure 3. Influence of CRM1 inhibition on subcellular localization of DDX3 mutants
(A) Schematic overview of the DDX3 constructs. (B) Bar graphs showing the percentage of cells with DDX3 expression in the nucleus and cytoplasm in untreated and Leptomycin B treated HeLa cells (N.B. cells can have both nuclear and cytoplasmic DDX3). Error bars represent SD. Absence of error bars indicates that there was no variation, because 100% of transfected cells had DDX3 expression in that compartment. (C) Confocal fluorescent images showing the subcellular localization of GFP-DDX3, GFP-NLS-DDX3, GFP-DDX3Δ1-21 and GFP-DDX3Δ260-517 (green) before and after CRM1 inhibition with 10 nM Leptomycin B in HeLa cells. Nuclei are visualized by co-transfection of a Histone2B-mCherry construct (red) Nucleoli can be identified in the merged brightfield image 40 x magnification. Bars represent mean percentage of positive cells of multiple microscopic fields with SD. Arrows indicate nucleoli NLS = nuclear localization signal. NES = nuclear export signal. GFP = green fluorescent protein.

DISCUSSION

In this study we evaluated the relationship between nuclear DDX3 expression and survival in breast and colorectal cancer. We found the presence of nuclear DDX3 to be an independent predictor of worse survival in both colorectal and breast cancer. Mechanistically, in colorectal cancer nuclear DDX3 retention could in part be explained by dysregulation of the nuclear exporter CRM1, but no correlation between nuclear DDX3 and altered CRM1 expression could be observed in breast cancer. We functionally validated this finding *in vitro* by showing that inhibition of CRM1 with leptomycin B resulted in an increase in nuclear DDX3 levels. Analysis of the subcellular localization of DDX3 deletion mutants before and after CRM1 inhibition indicated that the N-terminal NES sequence of DDX3 is most important for this interaction. A much stronger increase in nuclear DDX3 retention was observed after addition of an NLS in combination with CRM1 inhibition, suggesting that nuclear DDX3 localization can also be regulated through nuclear import, by unknown mechanisms. Interestingly, we found DDX3 to strongly localize to the nucleolus *in vitro*, which resembled the expression pattern in patient samples.

DDX3 is an actively investigated molecule in cancer biology, but previous studies have focused on its cytoplasmic expression pattern in cancer cells[32]. Understanding the role of nuclear DDX3 expression in tumors is relevant given DDX3's function in RNA processing and its known nucleocytoplasmic shuttling capacities. DDX3 has been found to promote oncogenesis and DDX3 inhibitors are being developed for colorectal[13] and breast cancers[17] among other malignancies[12, 18, 33, 34]. In addition, DDX3 is essential for the nuclear export of the human immunodeficiency virus 1 (HIV-1) protein Rev and is therefore also a potential therapeutic target in the treatment of HIV infections[35, 36]. Understanding the cellular mechanisms behind increased nuclear retention of DDX3 may facilitate the development of therapies specifically targeting the export function of DDX3[37]. In addition, nuclear DDX3 could serve as a prognostic and potentially therapeutic biomarker for selecting cancer patients that may benefit from treatment with DDX3 inhibitors.

This is the first study to describe prognostic value of DDX3 expression specifically in the nucleus. Several other studies have reported a correlation between cytoplasmic DDX3 and survival in breast and colorectal cancers[32]. A study by Su *et al.* found no significant difference in breast cancer patients with high and low cytoplasmic DDX3 expression[38] and reported a correlation between low cytoplasmic DDX3 expression and worse survival in colorectal cancer patients. In our larger colorectal cancer cohort patients with high cytoplasmic DDX3 also did slightly better (HR 0.69), but this was not statistically significant. Potential explanations for the observed differences are the use of different cut-offs for positivity and different antibodies. We previously found cytoplasmic DDX3 to be associated with nuclear Beta-catenin expression in patient samples and to promote oncogenic Wnt-signaling. Although most colorectal cancers are driven by genetic alterations in the Wnt-

signaling pathway, only a subset of cancers shows strong nuclear Beta-catenin expression. Interestingly, this subgroup of colorectal cancer patients has a relatively favorable prognosis[39], explaining how cytoplasmic DDX3 can be driving Wnt-signaling, without being associated with worse overall survival. Since DDX3 spontaneously localizes to the nucleus only in a very small percentage of cells *in vitro* and we were unable to create a stable cell line overexpressing full length DDX3 in the nucleus, it is very hard to decipher the exact role of DDX3 in the nucleus on oncogenesis. However, the fact that the presence of DDX3 in the nucleus was associated with worse survival in two different cancer types, indicates that cancers may benefit from high nuclear DDX3 levels as well.

When trying to understand a protein's nuclear function, it is useful to know its location in the nucleus. High DDX3 expression was specifically seen in the nucleolus. This was previously observed after HIV-1 Tat and Rev overexpression[40, 41] and DDX3 was also identified in nucleolar extracts by proteomics[42]. The nucleolus is the structural-functional domain of the cell in which ribosomal biogenesis occurs. Prominent nucleoli have been recognized as a cytological hallmark of cancer as early as the 19th century[43], but recently received renewed attention as evidence accumulates that several onco- and tumor suppressor genes are directly involved in the regulation of ribosome production to meet the altered metabolic needs of cancer cells[44]. Interestingly, DDX3 is known to play a role in ribosomal assembly and translation initiation in the cytoplasm[45]. Our observation that DDX3 localizes specifically to the nucleolus, and that this feature corresponds with worse prognosis, indicates that DDX3 may also play a role in (pre-)ribosomal assembly in the nucleolus. The presence of high nuclear DDX3 could reflect increased protein synthesis demands in cancers. A recent study identified essential genes in hematological malignancies and found this group to be enriched in RNA processing genes including *DDX3X*. Many of these essential genes localized to the nucleolus[46]. Interestingly, the nucleolus is also increasingly recognized as a target for cancer therapy[47]. Further research is required to fully understand and characterize the function of DDX3 in this subcellular compartment.

With regard to the mechanism behind nuclear DDX3 retention, we observed a correlation between cytoplasmic expression of CRM1 and nuclear DDX3 expression in colorectal cancer. This suggests that dysregulation of CRM1 is one of the mechanisms of nuclear DDX3 expression. The binding site of DDX3 to CRM1 is a matter of debate. DDX3 has a classical N-terminal NES sequence that is conserved and required for CRM1-binding in the *Saccharomyces cerevisiae* homologue Ded1p[48, 49] and the *Xenopus laevis* homologue An3[31]. However, Yedavalli, *et al.* observed binding between CRM1 and amino acids 260-517 of DDX3[4]. Our analysis of DDX3 deletion mutants showed that deletion of both areas resulted in an increase in nuclear DDX3, but only the construct that lacked the NES lost its sensitivity to CRM1 inhibition, indicating that this is the essential domain for CRM1-mediated export. A similar conclusion was recently made by Fröhlich, *et al.*, who found the N-terminal to be essential for DDX3 transportation out of the nucleus into cytoplasmic

unspliced HIV-1 mRNA ribonucleoprotein complexes[50]. It is possible that the 260-517 region of DDX3 is necessary for binding other exporters of DDX3 like TAP[5]. Since cytoplasmic CRM1 expression was infrequent in colorectal cancer and did not correlate with nuclear DDX3 in breast cancer, dysregulation of CRM1 is not likely the sole mechanism behind nuclear DDX3. When, in addition to nuclear export inhibition, we stimulated nuclear import by addition of an NLS, we observed a complete shift of all DDX3 in the cell to the nucleus, showing that increased import can also contribute to increased nuclear DDX3 levels. However, the mechanism behind nuclear import of DDX3 remains unknown. DDX3 has a classical NLS sequence at amino acid 212[51], but it is also possible that DDX3 enters the nucleus as part of a complex. Future research on this topic is warranted.

CONCLUSION

Nuclear DDX3 expression predicts worse survival in breast and colorectal cancer and mechanistically can in part be explained by altered expression of the nuclear exporter CRM1.

Acknowledgements
This work was financially supported by the Utrecht University Alexandre Suerman Stipend, the Dutch Cancer Foundation (UU2013-5851), the Saal van Zwanenberg foundation and the JoKolk scholarship Foundation (Marise Heerma van Voss) and the Flight Attendant Medical Research Institute (Venu Raman). We would like to thank Ashley Irving and Yehudit Bergman for their help with cloning the DDX3 constructs, Natalie ter Hoeve and Petra van der Groep for their help with setting up immunohistochemistry protocols, Cathy Moelans, Liudmila Kodach and Folkert Morsink for generating tissue microarrays, Kai Kammers for his critical evaluation of statistical methods and Nikolas Stathonikos for his help with digital imaging.

REFERENCES

1 Leitao AL, Costa MC, Enguita FJ. Unzippers, resolvers and sensors: a structural and functional biochemistry tale of RNA helicases. International journal of molecular sciences 2015; **16**: 2269-2293.

2 Deckert J, Hartmuth K, Boehringer D, Behzadnia N, Will CL, Kastner B *et al*. Protein composition and electron microscopy structure of affinity-purified human spliceosomal B complexes isolated under physiological conditions. Molecular and cellular biology 2006; **26**: 5528-5543.

3 Merz C, Urlaub H, Will CL, Luhrmann R. Protein composition of human mRNPs spliced in vitro and differential requirements for mRNP protein recruitment. RNA 2007; **13**: 116-128.

4 Yedavalli VS, Neuveut C, Chi YH, Kleiman L, Jeang KT. Requirement of DDX3 DEAD box RNA helicase for HIV-1 Rev-RRE export function. Cell 2004; **119**: 381-392.

5 Lai MC, Lee YH, Tarn WY. The DEAD-box RNA helicase DDX3 associates with export messenger ribonucleoproteins as well as tip-associated protein and participates in translational control. Molecular biology of the cell 2008; **19**: 3847-3858.

6 Pek JW, Kai T. DEAD-box RNA helicase Belle/DDX3 and the RNA interference pathway promote mitotic chromosome segregation. Proceedings of the National Academy of Sciences of the United States of America 2011; **108**: 12007-12012.

7 Kasim V, Wu S, Taira K, Miyagishi M. Determination of the role of DDX3 a factor involved in mammalian RNAi pathway using an shRNA-expression library. PloS one 2013; **8**: e59445.

8 Lee CS, Dias AP, Jedrychowski M, Patel AH, Hsu JL, Reed R. Human DDX3 functions in translation and interacts with the translation initiation factor eIF3. Nucleic acids research 2008; **36**: 4708-4718.

9 Li Y, Wang H, Wang Z, Makhija S, Buchsbaum D, LoBuglio A *et al*. Inducible resistance of tumor cells to tumor necrosis factor-related apoptosis-inducing ligand receptor 2-mediated apoptosis by generation of a blockade at the death domain function. Cancer research 2006; **66**: 8520-8528.

10 Sun M, Song L, Li Y, Zhou T, Jope RS. Identification of an antiapoptotic protein complex at death receptors. Cell death and differentiation 2008; **15**: 1887-1900.

11 Shih JW, Wang WT, Tsai TY, Kuo CY, Li HK, Wu Lee YH. Critical roles of RNA helicase DDX3 and its interactions with eIF4E/PABP1 in stress granule assembly and stress response. The Biochemical journal 2012; **441**: 119-129.

12 Bol GM, Vesuna F, Xie M, Zeng J, Aziz K, Gandhi N *et al*. Targeting DDX3 with a small molecule inhibitor for lung cancer therapy. EMBO molecular medicine 2015; **7**: 648-669.

13 Heerma van Voss MR, Vesuna F, Trumpi K, Brilliant J, Berlinicke C, de Leng W *et al*. Identification of the DEAD box RNA helicase DDX3 as a therapeutic target in colorectal cancer. Oncotarget 2015; **6**: 28312-28326.

14 Botlagunta M, Vesuna F, Mironchik Y, Raman A, Lisok A, Winnard P, Jr. *et al*. Oncogenic role of DDX3 in breast cancer biogenesis. Oncogene 2008; **27**: 3912-3922.

15 Chen HH, Yu HI, Cho WC, Tarn WY. DDX3 modulates cell adhesion and motility and cancer cell metastasis via Rac1-mediated signaling pathway. Oncogene 2015; **34**: 2790-2800.

16 Topisirovic I, Siddiqui N, Lapointe VL, Trost M, Thibault P, Bangeranye C *et al*. Molecular dissection of the eukaryotic initiation factor 4E (eIF4E) export-competent RNP. The EMBO journal 2009; **28**: 1087-1098.

17 Xie M, Vesuna F, Botlagunta M, Bol GM, Irving A, Bergman Y *et al*. NZ51, a ring-expanded nucleoside analog, inhibits motility and viability of breast cancer cells by targeting the RNA helicase DDX3. Oncotarget 2015; **6**: 29901-29913.

18 Wilky BA, Kim C, McCarty G, Montgomery EA, Kammers K, DeVine LR *et al*. RNA helicase DDX3: a novel therapeutic target in Ewing sarcoma. Oncogene 2016; **35**: 2574-2583.

19 Kodach LL, Wiercinska E, de Miranda NF, Bleuming SA, Musler AR, Peppelenbosch MP *et al*. The bone morphogenetic protein pathway is inactivated in the majority of sporadic colorectal cancers. Gastroenterology 2008; **134**: 1332-1341.

20 Moelans CB, de Weger RA, van Blokland MT, Ezendam C, Elshof S, Tilanus MG *et al*. HER-2/neu amplification testing in breast cancer by multiplex ligation-dependent probe amplification in comparison with immunohistochemistry and in situ hybridization. Cellular oncology : the official journal of the International Society for Cellular Oncology 2009; **31**: 1-10.

21 Carey LA, Perou CM, Livasy CA, Dressler LG, Cowan D, Conway K *et al*. Race, breast cancer subtypes, and survival in the Carolina Breast Cancer Study. JAMA : the journal of the American Medical Association 2006; **295**: 2492-2502.

22 Vermeulen JF, van de Ven RA, Ercan C, van der Groep P, van der Wall E, Bult P *et al*. Nuclear Kaiso expression is associated with high grade and triple-negative invasive breast cancer. PloS one 2012; **7**: e37864.

23 The Medical Research Involving Human Subjects Act [In Dutch: Wet medisch-wetenschappelijk onderzoek met mensen, WMO]. *Burgerlijk Wetboek*, 1998.

24 van Diest PJ. No consent should be needed for using leftover body material for scientific purposes. For. BMJ 2002; **325**: 648-651.

25 Angus AG, Dalrymple D, Boulant S, McGivern DR, Clayton RF, Scott MJ *et al*. Requirement of cellular DDX3 for hepatitis C virus replication is unrelated to its interaction with the viral core protein. The Journal of general virology 2010; **91**: 122-132.

26 Budczies J, Klauschen F, Sinn BV, Gyorffy B, Schmitt WD, Darb-Esfahani S *et al*. Cutoff Finder: a comprehensive and straightforward Web application enabling rapid biomarker cutoff optimization. PloS one 2012; **7**: e51862.

27 Noske A, Weichert W, Niesporek S, Roske A, Buckendahl AC, Koch I *et al*. Expression of the nuclear export protein chromosomal region maintenance/exportin 1/Xpo1 is a prognostic factor in human ovarian cancer. Cancer 2008; **112**: 1733-1743.

28 Kudo N, Matsumori N, Taoka H, Fujiwara D, Schreiner EP, Wolff B *et al*. Leptomycin B inactivates CRM1/

exportin 1 by covalent modification at a cysteine residue in the central conserved region. Proceedings of the National Academy of Sciences of the United States of America 1999; **96**: 9112-9117.
29 Ishizawa J, Kojima K, Hail N, Jr., Tabe Y, Andreeff M. Expression, function, and targeting of the nuclear exporter chromosome region maintenance 1 (CRM1) protein. Pharmacology & therapeutics 2015; **153**: 25-35.
30 Fornerod M, Ohno M, Yoshida M, Mattaj IW. CRM1 is an export receptor for leucine-rich nuclear export signals. Cell 1997; **90**: 1051-1060.
31 Askjaer P, Rosendahl R, Kjems J. Nuclear export of the DEAD box An3 protein by CRM1 is coupled to An3 helicase activity. The Journal of biological chemistry 2000; **275**: 11561-11568.
32 Bol GM, Xie M, Raman V. DDX3, a potential target for cancer treatment. Molecular cancer 2015; **14**: 188.
33 Samal SK, Routray S, Veeramachaneni GK, Dash R, Botlagunta M. Ketorolac salt is a newly discovered DDX3 inhibitor to treat oral cancer. Scientific reports 2015; **5**: 9982.
34 Koshio J, Kagamu H, Nozaki K, Saida Y, Tanaka T, Shoji S *et al*. DEAD/H (Asp-Glu-Ala-Asp/His) box polypeptide 3, X-linked is an immunogenic target of cancer stem cells. Cancer immunology, immunotherapy : CII 2013; **62**: 1619-1628.
35 Yedavalli VS, Zhang N, Cai H, Zhang P, Starost MF, Hosmane RS *et al*. Ring expanded nucleoside analogues inhibit RNA helicase and intracellular human immunodeficiency virus type 1 replication. Journal of medicinal chemistry 2008; **51**: 5043-5051.
36 Radi M, Falchi F, Garbelli A, Samuele A, Bernardo V, Paolucci S *et al*. Discovery of the first small molecule inhibitor of human DDX3 specifically designed to target the RNA binding site: towards the next generation HIV-1 inhibitors. Bioorganic & medicinal chemistry letters 2012; **22**: 2094-2098.
37 Mahboobi SH, Javanpour AA, Mofrad MR. The interaction of RNA helicase DDX3 with HIV-1 Rev-CRM1-RanGTP complex during the HIV replication cycle. PloS one 2015; **10**: e0112969.
38 Su CY, Lin TC, Lin YF, Chen MH, Lee CH, Wang HY *et al*. DDX3 as a strongest prognosis marker and its downregulation promotes metastasis in colorectal cancer. Oncotarget 2015; **6**: 18602-18612.
39 Chung GG, Provost E, Kielhorn EP, Charette LA, Smith BL, Rimm DL. Tissue microarray analysis of beta-catenin in colorectal cancer shows nuclear phospho-beta-catenin is associated with a better prognosis. Clinical cancer research : an official journal of the American Association for Cancer Research 2001; **7**: 4013-4020.
40 Jarboui MA, Bidoia C, Woods E, Roe B, Wynne K, Elia G *et al*. Nucleolar protein trafficking in response to HIV-1 Tat: rewiring the nucleolus. PloS one 2012; **7**: e48702.
41 Yasuda-Inoue M, Kuroki M, Ariumi Y. Distinct DDX DEAD-box RNA helicases cooperate to modulate the HIV-1 Rev function. Biochemical and biophysical research communications 2013; **434**: 803-808.
42 Andersen JS, Lyon CE, Fox AH, Leung AK, Lam YW, Steen H *et al*. Directed proteomic analysis of the human nucleolus. Current biology : CB 2002; **12**: 1-11.
43 Derenzini M, Montanaro L, Trere D. What the nucleolus says to a tumour pathologist. Histopathology 2009; **54**: 753-762.
44 Ruggero D, Pandolfi PP. Does the ribosome translate cancer? Nature reviews Cancer 2003; **3**: 179-192.
45 Geissler R, Golbik RP, Behrens SE. The DEAD-box helicase DDX3 supports the assembly of functional 80S ribosomes. Nucleic acids research 2012; **40**: 4998-5011.
46 Wang T, Birsoy K, Hughes NW, Krupczak KM, Post Y, Wei JJ *et al*. Identification and characterization of essential genes in the human genome. Science 2015; **350**: 1096-1101.
47 Hein N, Hannan KM, George AJ, Sanij E, Hannan RD. The nucleolus: an emerging target for cancer therapy. Trends in molecular medicine 2013; **19**: 643-654.
48 Senissar M, Le Saux A, Belgareh-Touze N, Adam C, Banroques J, Tanner NK. The DEAD-box helicase Ded1 from yeast is an mRNP cap-associated protein that shuttles between the cytoplasm and nucleus. Nucleic acids research 2014; **42**: 10005-10022.
49 Hauk G, Bowman GD. Formation of a Trimeric Xpo1-Ran[GTP]-Ded1 Exportin Complex Modulates ATPase and Helicase Activities of Ded1. PloS one 2015; **10**: e0131690.
50 Fröhlich A, Rojas-Araya B, Pereira-Montecinos C, Dellarossa A, Toro-Ascuy D, Prades-Pérez Y *et al*. DEAD-box RNA helicase DDX3 connects CRM1-dependent nuclear export and translation of the HIV-1 unspliced mRNA through its N-terminal domain. Biochimica et Biophysica Acta (BBA) - Gene Regulatory Mechanisms 2016; **1859**: 719-730.
51 PSORT: Prediction of Protein Sorting Signals and Localization Sites in Amino Acid Sequences.

SUPPLEMENTARY

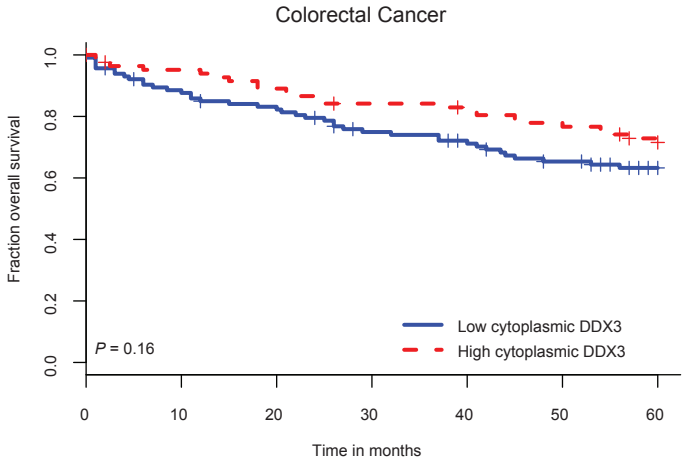

Supplementary Figure 1. Correlation between cytoplasmic DDX3 and survival in colorectal cancer
Kaplan-Meier curve showing the fraction overall survival in colorectal cancer patients with low and high cytoplasmic DDX3 expression. P-value calculated by log-rank test.

Supplementary Table 1. Univariate and multivariate cox proportional hazard model of survival in colorectal cancer patients

		Univariate		Multivariate	
		HR (95% CI)	**P-value†**	**HR (95% CI)**	**P-value‡**
Nuclear DDX3	<1%	1		1	
	≥1%	2.34 (1.43-3.85)	<0.001	1.69 (0.98-2.90)	0.057
TNM stage	1	1		1	
	2	2.9 (0.38-21.98)		2.56 (0.34-19.48)	0.364
	3	7.82 (1.06-57.70)		7.15 (0.97-52.86)	0.054
	4	44.34 (5.89-333.74)	<0.001	34.01 (4.45-260.15)	<0.001
Differentiation grade	Well	1			n.s.
	Moderate	1.24 (0.38-4.00)			
	Poor	2.38 (0.71-8.00)	0.041		
Tumor size	<40 mm	1			n.s.
	40-60 mm	2.68 (1.28-5.63)			
	>60 mm	3.57 (1.61-7.89)	0.004		

All variables significantly associated (p<0.1) in univariate analysis were entered into the multivariate cox-proportional hazards model. † P-value calculated by log-rank test. ‡ P-value of coefficient. HR = hazard ratio; 95% CI = 95% confidence interval; n.s. = no significant change in AIC observed by stepwise backward selection and therefore not included in the final multivariate model.

Supplementary Table 2. Univariate and multivariate cox proportional hazard model of survival in breast cancer patients.

		Univariate		Multivariate	
		HR (95% CI)	**p-value†**	**HR (95% CI)**	**p-value‡**
Nuclear DDX3	<1%	1	0.004	1	0.01
	≥1%	2.39 (1.29-4.43)		2.63 (1.26-5.51)	
MAI	<12	1	0.071		n.s.
	≥12	1.78 (0.94-3.34)			
Molecular subtype	non basal-like	1	0.024	1	0.045
	basal-like	2.27 (1.18-4.40)		2.17 (1.02-4.61)	
Lymphnode status	negative	1	0.027	1	0.048
	positive	2.17 (1.08-4.39)		2.06 (1.01-4.23)	
ER	negative	1	0.019		
	positive	0.48 (0.26-0.90)			
PR	negative	1	0.013		
	positive	0.49 (0.27-0.87)			
Age	<50	1	0.017	1	0.017
	≥50	2.94 (1.16-7.45)		3.55 (1.26-10.06)	

All variables significantly associated ($p<0.1$) in univariate analysis were entered into the cox-proportional hazards model, except for ER and PR receptor status, because these are included in the molecular subtype algorithm. † P-value calculated by log-rank test. ‡ P-value of coefficient. HR = hazard ratio; 95% CI = 95% confidence interval; B&R = Bloom and Richardson; MAI = mitotic activity index; n.s. = no significant change in AIC observed by stepwise backward selection and therefore not included in the final multivariate model.

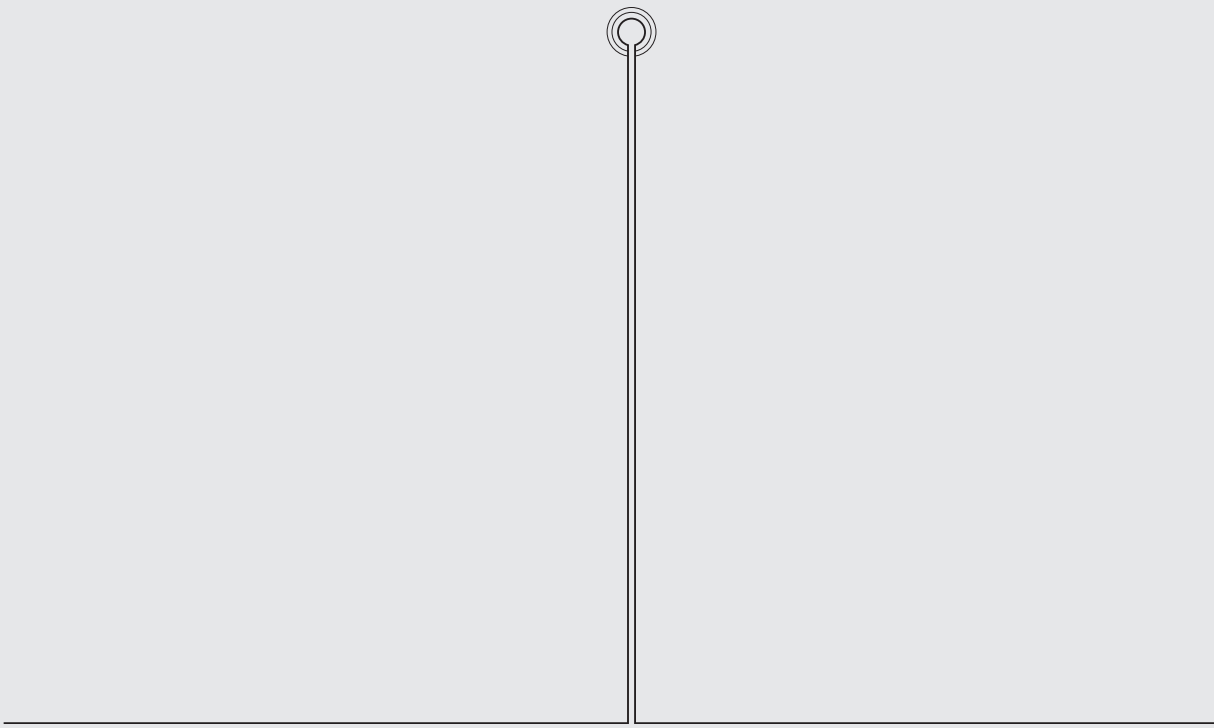

CHAPTER 6

The prognostic effect of DDX3 upregulation in distant breast cancer metastases

Clin Exp Metastasis. 2016 Dec 20

Marise R. Heerma van Voss, Willemijne A.M.E. Schrijver, Natalie D. ter Hoeve, Laurien D. Hoefnagel, Dutch Distant Breast Cancer Metastases Consortium, Quirine F. Manson, Elsken van der Wall, Venu Raman, Paul J. van Diest

ABSTRACT

Metastatic breast cancer remains one of the leading causes of death in women and identification of novel treatment targets is therefore warranted. Functional studies showed that the RNA helicase DDX3 promotes metastasis, but DDX3 expression was never studied in patient samples of metastatic cancer. In order to validate previous functional studies and to evaluate DDX3 as a potential therapeutic target, we investigated DDX3 expression in paired samples of primary and metastatic breast cancer.

Samples from 79 breast cancer patients with distant metastases at various anatomical sites were immunohistochemically stained for DDX3. Both cytoplasmic and nuclear DDX3 expression were compared between primary and metastatic tumors. In addition, the correlation between DDX3 expression and overall survival was assessed.

Upregulation of cytoplasmic (28%; OR 3.7; $p = 0.002$) was common in breast cancer metastases, especially in triple negative (TN) and high grade cases. High cytoplasmic DDX3 levels were most frequent in brain lesions (65%) and significantly correlated with high mitotic activity and triple negative subtype. In addition, worse overall survival was observed for patients with high DDX3 expression in the metastasis (HR 1.79, $p = 0.039$).

DDX3 expression is upregulated in distant breast cancer metastases, especially in the brain and in TN cases. In addition, high metastatic DDX3 expression correlates with worse survival, implying that DDX3 is a potential therapeutic target in metastatic breast cancer, in particular in the clinically important group of TN patients.

BACKGROUND

DDX3 (encoded by *DDX3X*) is a DEAD box RNA helicase with ATPase dependent helicase activity, which is involved in several steps of endogenous RNA metabolism and translation initiation[1-4]. DDX3 has been implicated in neoplastic transformation due to its role in cell cycle progression[5, 6] and its anti-apoptotic properties[7-9]. In addition, DDX3 has been shown to promote several steps of tumor metastasis. Overexpression of DDX3 resulted in increased motility and migration by induction of an epithelial-to-mesenchymal (EMT) phenotype with loss of E-cadherin[10, 11] and upregulation of Snail expression[12]. Furthermore, DDX3 was found to promote anchorage independent growth and invasive capacities of cancer cells through regulation of mRNA translation[13, 14]. DDX3 knockdown has also been shown to result in reduced breast cancer metastases in mice[15]. These findings have led to the development of DDX3 inhibitors for the treatment of breast cancer[15] among other malignancies[5, 6, 16, 17]. The tumor-enhancing role of DDX3 was corroborated by studies on DDX3 expression in patient samples of primary tumors[5, 6], but DDX3 expression was never studied in metastatic cancer samples.

Although therapeutic options for patients with metastatic breast cancer have increased, the vast majority of patients still develops resistance to treatment and eventually succumbs to the disease[18]. With 5-year survival rates of 25%[19] and approximately 40.000 deaths on a yearly basis in the United States, metastatic breast cancer still ranks second on the list of causes of cancer deaths in women, accounting for 15% of all cancer deaths[20]. Therefore the identification of novel therapeutic targets that inhibit the development and outgrowth of breast cancer metastases remains urgently wanted.

Upregulation of DDX3 in metastases would confirm the role of DDX3 in metastatic tumor progression that has been suggested in functional studies. In addition, high DDX3 expression levels in metastatic lesions could indicate that breast cancer metastases are reliant on high DDX3 expression, and that patients with advanced disease could benefit from treatment with DDX3 inhibitors under development. Therefore, this study aimed to evaluate DDX3 expression in distant breast cancer metastases as compared to their primary tumor.

METHODS

Patient samples

Tissue microarrays (TMAs) containing paired samples from 97 primary breast cancer and their distant metastases were previously assembled[21, 22]. All TMAs included multiple cores per patient. 18 pairs were incomplete due to damaged or detached cores during cutting or staining, or due to cores no longer containing invasive carcinoma. The TMA included metastases from various anatomical sites, including brain, skin, lung, liver, bone, ovaries,

uterus and the gastro-intestinal tract. Clinicopathological data and follow up data were retrieved from the pathology reports and patient files. Overall survival was calculated from the time of diagnosis of the metastatic lesion. For this study only anonymous archival leftover pathology material was used. Therefore no informed consent is required according to Dutch legislation[23], as this use of redundant tissue for research purposes is part of the standard treatment agreement with patients in the UMC Utrecht[24].

Immunohistochemistry

Four μm thick sections were cut, mounted on Surgipathe X-tra adhesive slides (Leica Biosystems, Milton Keynes, UK), deparaffinized in xylene and rehydrated in decreasing ethanol dilutions. Endogenous peroxidase activity was blocked with 1.5% hydrogen peroxide buffer for 15 minutes and was followed by antigen retrieval by boiling for 20 minutes in EDTA buffer (pH 9.0). Slides were blocked with protein block from Novolink Polymer Detection System (Leica Microsystems, Eindhoven, The Netherlands) and subsequently incubated in a humidified chamber for 1 hour with anti-DDX3 (1:50, mAb AO196)[25]. Post primary block, secondary antibodies and diaminobenzidine treatment were performed with the same Novolink Polymer Detection System according to the manufacturer's instructions. The slides were lightly counterstained with hematoxylin and mounted. Appropriate positive and negative controls were used throughout.

Scoring was performed by consensus of two observers (PvD. and MHvV.). DDX3 shuttles between the nucleus and cytoplasm[26]. Since we previously observed distinct cytoplasmic and nuclear expression patterns, we allocated separate scores to cytoplasmic and nuclear DDX3 expression, as before[5]. Almost all cells expressed cytoplasmic DDX3, but the intensity varied and was therefore scored semi-quantitatively as absent (0), weak (1), moderate (2) or strong (3). The optimal cut-off point was selected using the online tool cut-off finder, which helps to select a cut-off that maximizes the difference in survival between groups[27]. Cases with score 0 to 2 were classified as having low DDX3 expression and evaluated against cases with high (score 3) expression, as before[6]. Cytoplasmic DDX3 was considered upregulated when DDX3 expression was low in the primary tumor (0-2) and high in the metastasis (3). Although the intensity of nuclear DDX3 in cells was similar, the fraction of positive cells varied. Therefore, the percentage of DDX3 positive nuclei was scored, regarding samples with ≥ 1% DDX3 staining as positive. When nuclear DDX3 was absent from the primary tumor and present in the metastasis, nuclear DDX3 was considered upregulated.

Statistics

Dichotomized cytoplasmic and nuclear DDX3 scores in primaries and metastases of the same patient were compared. Paired odds ratios were calculated by taking the ratio of discrepant pairs. P-values were calculated by McNemar's test. Correlations between high

DDX3 in metastases and other clinicopathological variables were studied. Discrete variables were compared by $\chi 2$ or Fisher's exact test. The distribution of continuous variables was assessed graphically and Student's t-tests or Mann Whitney U-tests were used for normally and non-normally distributed variables, respectively. Overall survival data from the time of biopsy of metastatic lesions onward was available for 58 patients and compared between patients with low versus high metastatic DDX3 expression by plotting Kaplan-Meier curves and performing modified Wilcoxon tests. Potential confounders were analyzed by including variables associated with both DDX3 expression and survival in a multivariate cox-proportional hazards model. Effect measure modification was explored by including multiplicative interaction terms in a Cox proportional-hazards model. If sample size allowed stratified analysis was performed in the case of significant interaction. P-values smaller than 0.05 were considered statistically significant. All statistical analyses were performed with R version 3.2.0.

RESULTS

DDX3 is overexpressed in breast cancer metastases

DDX3 could be assessed in 79 paired primary breast cancers and corresponding metastases. High cytoplasmic DDX3 expression was observed in 19% of primary breast cancers and 39% of metastases. Pairwise analysis of primary tumors and metastasis in the same patient showed that 28% of metastases had upregulated DDX3 expression, whereas DDX3 was downregulated in only 8% of patients (table 1). This difference was highly statistically significant with an OR of 3.7 (95% CI 1.58-8.51; p = 0.002). Figure 1 shows examples of increased cytoplasmic DDX3 expression at different metastatic sites. DDX3 expression was especially prominent in breast cancer brain metastases, with 65% of metastases having high DDX3 expression and 48% of patients having an increase as compared to their primary tumor (OR 15.0, 95% CI 3.29-68.34, p < 0.001, Table 1).

Table 1. Changes in cytoplasmic DDX3 expression in breast cancers from primary to metastatic tumors at different sites.

		Cytoplasmic DDX3			
	N	High to Low	Low to High	OR (95% CI)	P-value
Total	79	6 (8%)	22 (28%)	3.7 (1.58-8.51)	0.002
Brain	31	1 (3%)	15 (48%)	15.0 (3.29-68.34)	<0.001
Lung	15	0 (0%)	3 (20%)	.	0.083
Skin	20	1 (5%)	4 (20%)	4.0 (0.53-30.31)	0.180
Other	13	4 (31%)	0 (0%)	.	0.046

Paired odds ratio (OR) is calculated by taking the ratio of discrepant pairs. Paired P-values are calculated by McNemar's test.

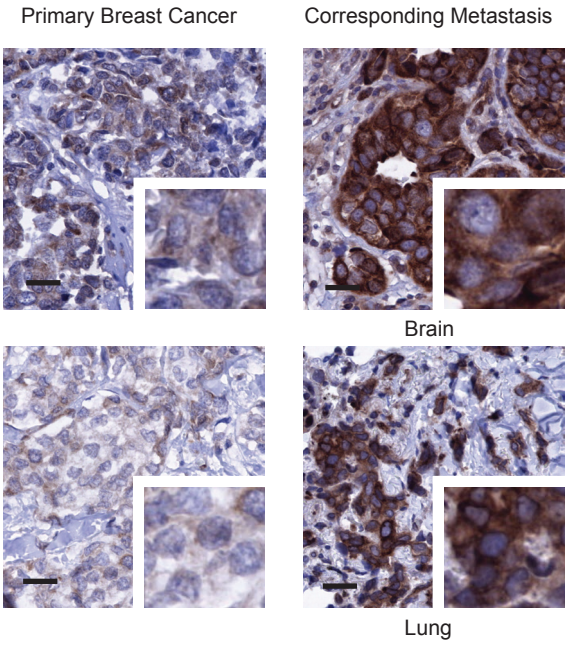

Figure 1. Cytoplasmic DDX3 expression is upregulated in breast cancer metastases
Examples of upregulation of cytoplasmic DDX3 expression in breast cancer metastases at different anatomical locations as compared to the originating primary breast cancer in the same patient. Analysis was performed in 79 pairs, 40 x magnification, scale bar indicates 25 µm.

Upregulation of cytoplasmic DDX3 expression was also common in lung (20%) and skin (20%) metastases. The low number of available liver (n=3) and bone (n=3) metastases did not allow subgroup analysis for these specific anatomical sites.
Nuclear DDX3 expression was observed in 22% of primary breast cancers and 13% of metastases. As shown in Table 2, conversion from nuclear DDX3 from absent in the primary tumor to present in the metastasis occurred in 9% of pairs, whereas the opposite occurred in 18% of patients (OR 0.5; 95% CI 0.21-1.22; p = 0.127).

Table 2. Changes in nuclear DDX3 expression in breast cancers from primary to metastatic tumors at different sites.

		Nuclear DDX3			
	N	**Present to Absent**	**Absent to Present**	**OR (95% CI)**	**P-value**
Total	79	14 (18%)	7 (9%)	0.5 (0.21-1.22)	0.127
Brain	31	5 (16%)	3 (10%)	0.6 (0.15-2.47)	0.480
Lung	15	3 (20%)	0 (0%)	.	0.083
Skin	20	5 (25%)	2 (10%)	0.4 (0.08-1.95)	0.257
Other	13	1 (8%)	2 (15%)	2.0 (0.19-21.04)	0.564

Paired odds ratio (OR) is calculated by taking the ratio of discrepant pairs. Paired P-values are calculated by McNemar's test.

Metastatic cytoplasmic DDX3 overexpression correlates with triple-negative receptor status and high mitotic activity

In order to catalogue what characterized patients with high metastatic DDX3, we explored correlations with other clinicopathological characteristics (table 3). High cytoplasmic DDX3 in metastasis was associated with a higher mitotic activity index (MAI) (30.3 vs. 21.3; p = 0.033) and triple-negative
molecular subtype (43% vs. 24%; p = 0.019) in the primary tumor and negative estrogen receptor (ER) status in the metastasis (72% vs. 45%; p = 0.043). Since DDX3 in metastases was associated with ER-negativity and possible negative selection pressure occurred on ER expression when patients were treated with hormonal treatment, we assessed whether adjuvant treatment of the primary tumor correlated with metastatic DDX3 expression. No correlation was found between high DDX3 in metastases and chemotherapy (47% vs. 54%; p = 0.795), hormonal therapy (21% vs 27%; p = 0.790) or treatment with trastuzamab (3% vs. 0%; p = 1). Nuclear DDX3 in metastases was associated with negative HER2 receptor status in the metastasis, but did not correlate with other clinicopathological variables (Supplementary Table 1).

Metastatic DDX3 expression correlates with worse survival

We performed survival analysis to see whether DDX3 expression correlated with clinical outcome in metastatic breast cancer patients (Figure 2). Median overall survival after the metastatic lesion was biopsied was shorter in patients with high cytoplasmic DDX3 (11.18 months) when compared to patients with low cytoplasmic DDX3 (20.14 months; HR 1.79; 95% CI 0.97-3.33; p = 0.039). Because the molecular subtype of the primary tumor and the location and ER-status of the metastasis were associated with both high cytoplasmic DDX3 and survival, potential confounding by these factors was explored in a multivariate model as much as sample size permitted. The association between cytoplasmic DDX3 and survival weakened after adjustment for individual covariates by Cox-regression analysis. This indicates that molecular subtype ($HR_{adjusted}$ 1.38; 95% CI 0.73-2.63; p = 0.324), ER status ($HR_{adjusted}$ 1.51; 95% CI 0.81-2.82; p = 0.200) and location of the metastasis ($HR_{adjusted}$ 1.52; 95% CI 0.9-2.94; p = 0.210) are confounding the relation between cytoplasmic DDX3 and survival.

In addition, a significant correlation between the presence of nuclear DDX3 in metastases and overall survival was observed. Patients with nuclear DDX3 had a shorter median survival of 8.8 versus 19.4 months (HR 3.28; 95% CI 1.23-8.75; p = 0.034). Unfortunately multivariate analysis was not possible due to the low number of patients with nuclear DDX3 in the metastasis. Overall we conclude that there is a relation between metastatic DDX3 expression and survival, which for cytoplasmic DDX3 can in part be attributed to the molecular subtype and location of these tumors.

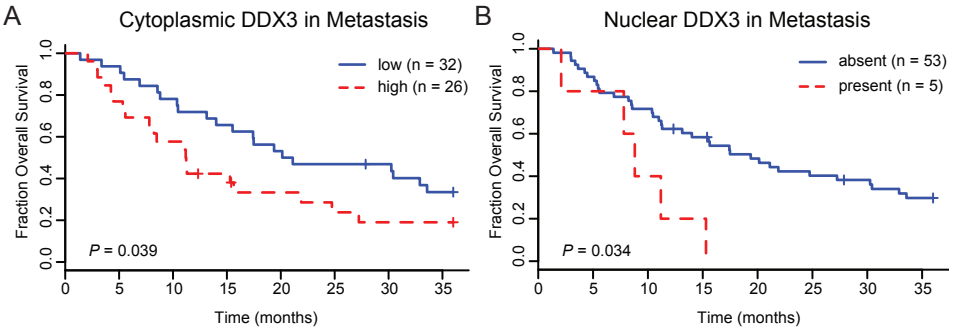

Figure 2. Metastatic DDX3 is associated with shorter survival in distant breast cancer metastases
(A) Kaplan-Meier curves showing overall survival after biopsy of the metastasis in breast cancer patients with high cytoplasmic (n = 26) as compared to those with low cytoplasmic (n = 32) DDX3 expression in the metastatic lesion (B) Kaplan-Meier curves showing overall survival after biopsy of the metastasis in breast cancer patients with nuclear DDX3 (n = 53) as compared to those without nuclear DDX3 (n = 5) in the metastatic lesion. P-values calculated by a modified Wilcoxon test

DISCUSSION

DDX3 is an RNA helicase with oncogenic properties, which has been found to promote metastasis in functional studies. However, DDX3 expression had never been specifically evaluated in metastatic cancer patient samples. In this study, we therefore compared DDX3 expression in primary breast cancers to that in corresponding distant metastatic lesions. Cytoplasmic DDX3 expression was significantly higher in metastatic cancer samples, especially in brain metastases and triple negative cases. In addition, there is a correlation between DDX3 expression in the metastasis and worse overall survival in patients with metastatic breast cancer. Previous studies have indicated that DDX3 overexpression facilitates dissemination of cancer cells through induction of an EMT phenotype[10-12]. Increased motility and anchorage independent growth have also been linked to the role DDX3 has in mRNA translation. Chen, *et al.* found DDX3 to increase invasive properties through a direct role in Rac1 translation, which in its turn stabilizes β-catenin expression resulting in activated Wnt-signaling[14]. Furthermore, Hagerstrand, *et al.* found that DDX3 mediates IRES-dependent translation, resulting in increased anchorage independent growth in cancers with 3q26 amplification. In addition to promoting the dissemination process, our finding that among patients with established metastases, those with DDX3 expression have worse overall survival is suggestive of DDX3 also providing a survival benefit to cancer cells after colonization of the metastatic niche. However, this difference can also be partly attributed to the frequent triple negative phenotype and brain localization of metastases with high cytoplasmic DDX3 expression. Notably, there are some contradictory reports in literature pointing towards DDX3 functioning as a tumor suppressor[28, 29]. It is possible that the role of DDX3 in oncogenesis differs between genetic backgrounds and cancer types[30].

Table 3. Correlation between cytoplasmic DDX3 expression and clinicopathological variables in breast cancer metastases.

		Cytoplasmic DDX3		
	Total	**Low**	**High**	**P-value**
Characteristics primary tumor				
Tumor size in cm, median (IQR)	7 (2)	7 (2.75)	7 (2)	0.657#
Histology, n (%)				
Ductal	67 (86)	39 (81)	28 (90)	0.857**
Lobular	8 (10)	6 (13)	2 (6)	
Metaplastic	3 (4)	2 (4)	1 (3)	
Apocrine	1 (1)	1 (2)	0	
Grade, n (%)				
I	1 (1)	1 (2)	0	0.670**
II	21 (27)	14 (30)	7 (23)	
III	55 (71)	31 (67)	24 (77)	
missing	2	2	0	
MAI, mean (SD)	24.8 (19.7)	21.3 (18.6)	30.3 (20.5)	0.033$
Lympnodes, n (%)				
negative	39 (49)	28 (58)	11 (35)	0.080*
positive	40 (51)	20 (42)	20 (65)	
Age, mean (SD)	52.2 (11.0)	54.0 (11.0)	49.5 (10.4)	0.074$
missing	1	1	0	
Molecular subtype, n (%)				
HER2-enriched	11 (15)	5 (12)	6 (20)	0.019**
luminal A	29 (41)	23 (56)	6 (20)	
luminal B	8 (11)	3 (7)	5 (17)	
triple negative	23 (32)	10 (24)	13 (43)	
missing	8	7	1	
Characteristics metastasis				
Location, n (%)				
brain	31 (39)	11 (23)	20 (65)	0.001*
skin	20 (25)	15 (31)	5 (16)	
lung	15 (19)	10 (20)	5 (16)	
other	13 (16)	12 (25)	1 (3)	
Estrogen receptor, n (%)				
negative	39 (57)	18 (45)	21 (72)	0.043*
positive	30 (43)	22 (55)	8 (28)	
missing	10	8	2	
Progesterone receptor, n (%)				
negative	39 (57)	26 (67)	22 (81)	0.295*
positive	30 (43)	13 (33)	5 (19)	
missing	13	9	4	
HER2 receptor, n (%)				
negative	48 (73)	31 (82)	20 (69)	0.363*
positive	18 (27)	7 (18)	9 (31)	
missing	12	10	2	
Nuclear DDX3, n (%)				
Absent	69 (87)	42 (79)	27 (26)	1**
Present	10 (13)	6 (21)	4 (74)	

P-value calculated by * chi-square test, ** Fisher exact test, # Mann-Whitney U test, $ student's t-test.

The mechanisms behind cytoplasmic overexpression and nuclear retention of DDX3 remain largely to be elucidated. Mutations in DDX3 have been detected in medulloblastomas[31], head and neck cancers[32] and hematological malignancies[33, 34], but were not identified in breast cancers[35]. In addition, there is no amplification of the DDX3 locus in DDX3 overexpressing breast cancer cell lines[10]. With regard to nuclear retention of DDX3, we know that DDX3 is exported out of the nucleus as part of messenger ribonucleoprotein complexes[2, 26, 36]. In the nucleus, DDX3 was previously found to localize to the nucleolus[37] where ribosomal assembly takes place, suggesting that nuclear DDX3 retention in metastases possibly reflects increased demands in protein synthesis. More research to further clarify the mechanisms of DDX3 overexpression and nuclear retention is needed.
We found a particularly large increase in cytoplasmic DDX3 expression rates in brain metastases. Brain metastases are more common in patients with triple negative or HER2 amplified primary breast cancers[38], which have relatively high DDX3 expression. However, discordance rates for DDX3 were much higher (48% upregulation) than for HER2 (2%) and estrogen receptor (13%)[21]. It is therefore hard to explain the DDX3 upregulation in brain metastases rates solely by an association with these molecular subtypes. Several other biological signatures have been found to characterize brain metastases. Wnt signaling mediates metastasis to the brain in both lung[39] and breast cancer[40]. DDX3 is a multilevel activator of the Wnt-signaling pathway[5, 6, 14, 41] and therefore potentially facilitates brain colonization in a Wnt-mediated fashion. Another feature of brain metastases is the expression of DNA repair genes[42, 43]. Inhibition of DDX3 reduced non-homologous end joining, a double strand break repair mechanism[5], implying that the high DDX3 levels in brain metastases could reflect a DNA damage response. Furthermore, overexpression of hypoxia-inducible factor 1α is common in brain metastases[44] and also associated with DDX3 expression in breast cancer[45]. However, metastatic DDX3 expression did not correlate with expression of the HIF-1α target genes carbonic anhydrase IX (CAIX) and Glucose transporter 1 (GLUT-1; data not shown), making it unlikely that high DDX3 expression in brain metastases is hypoxia-mediated. Last, metastatic niches differ also by the bioenergetic profile they impose on cells[46]. Brain metastases were demonstrated to upregulate glycolysis and oxidative phosphorylation capacity[47] and to have increased hexokinase 2 expression[48]. An additional reason for brain metastases to elevate DDX3 expression could be that DDX3 supports metabolic adaptation of cancer cells to the microenvironment of the brain. Although liver and bone metastases are also common in breast cancer patients, limited availability of tissue from these sites did not allow for subgroup analysis.
Besides biological relevance, high DDX3 expression in breast cancer metastases has potential clinical applications. Metastatic breast cancer, especially localized in the brain, is associated with short patient survival and severely impaired quality of life. Cerebral metastases occur early in triple negative cases[49], where the systemic therapeutic arsenal is particularly lacking. High DDX3 expression could serve as a therapeutic target in these

patients. There are several small molecule inhibitors of DDX3 currently under development[50]. Although diffusion of these compounds over an intact blood brain barrier is limited[5], the small size of the inhibitors and the compromised blood brain barrier in brain metastases[51] potentially do allow for therapeutic levels to be reached. The DDX3 inhibitor RK-33 has potent radiosensitizing abilities[10], which could enhance the effect of whole brain radiation to treat brain metastases. Furthermore, given the role of DDX3 early in the metastatic process, DDX3 inhibitors could potentially also be used to prevent the emergence of metastases. At last, evaluation of DDX3 expression in patient samples could serve both as a prognostic biomarker and facilitate selection of those patients benefiting most from DDX3 inhibitors.

CONCLUSIONS

Cytoplasmic DDX3 expression is increased in breast cancer metastases, especially those located in the brain and occurring in triple negative cases. In addition, patients with high DDX3 levels in the metastatic lesion have shorter overall survival, implying that DDX3 is a potential therapeutic target in metastatic breast cancer.

Acknowledgements
The Dutch Breast Cancer Consortium included Department of Pathology, University Medical Center Utrecht, Department of Pathology, Academic Medical Center, Amsterdam; Department of Pathology, Medical Center Alkmaar; Department of Pathology, Medical Center Zaandam; Department of Pathology, Radboud University Nijmegen Medical Center, Nijmegen; Department of Pathology, Canisius Wilhelmina Hospital, Nijmegen; Department of Pathology, VU University Medical Center, Amsterdam; Department of Pathology, The Netherlands Cancer Institute, Amsterdam; Laboratory for Pathology, Dordrecht; Department of Pathology, University Medical Center Groningen; Department of Pathology, St Antonius Hospital, Nieuwegein; Department of Pathology, Diakonessenhuis, Utrecht, Isala klinieken, Zwolle; Erasmus Medical Center Rotterdam; Gelre Hospital Apeldoorn, Laboratory Sazinon, Hoogeveen, and the Laboratory for Pathology Oost Nederland, Enschede, all in The Netherlands.

REFERENCES

1 Deckert J, Hartmuth K, Boehringer D, Behzadnia N, Will CL, Kastner B *et al*. Protein composition and electron microscopy structure of affinity-purified human spliceosomal B complexes isolated under physiological conditions. Molecular and cellular biology 2006; **26**: 5528-5543.

2 Lai MC, Lee YH, Tarn WY. The DEAD-box RNA helicase DDX3 associates with export messenger ribonucleoproteins as well as tip-associated protein and participates in translational control. Molecular biology of the cell 2008; **19**: 3847-3858.

3 Kasim V, Wu S, Taira K, Miyagishi M. Determination of the role of DDX3 a factor involved in mammalian RNAi pathway using an shRNA-expression library. PloS one 2013; **8**: e59445.

4 Lee CS, Dias AP, Jedrychowski M, Patel AH, Hsu JL, Reed R. Human DDX3 functions in translation and interacts with the translation initiation factor eIF3. Nucleic acids research 2008; **36**: 4708-4718.

5 Bol GM, Vesuna F, Xie M, Zeng J, Aziz K, Gandhi N *et al*. Targeting DDX3 with a small molecule inhibitor for lung cancer therapy. EMBO molecular medicine 2015; **7**: 648-669.

6 Heerma van Voss MR, Vesuna F, Trumpi K, Brilliant J, Berlinicke C, de Leng W *et al*. Identification of the DEAD box RNA helicase DDX3 as a therapeutic target in colorectal cancer. Oncotarget 2015; **6**: 28312-28326.

7 Li Y, Wang H, Wang Z, Makhija S, Buchsbaum D, LoBuglio A *et al*. Inducible resistance of tumor cells to tumor necrosis factor-related apoptosis-inducing ligand receptor 2-mediated apoptosis by generation of a blockade at the death domain function. Cancer research 2006; **66**: 8520-8528.

8 Sun M, Song L, Li Y, Zhou T, Jope RS. Identification of an antiapoptotic protein complex at death receptors. Cell death and differentiation 2008; **15**: 1887-1900.

9 Shih JW, Wang WT, Tsai TY, Kuo CY, Li HK, Wu Lee YH. Critical roles of RNA helicase DDX3 and its interactions with eIF4E/PABP1 in stress granule assembly and stress response. The Biochemical journal 2012; **441**: 119-129.

10 Botlagunta M, Vesuna F, Mironchik Y, Raman A, Lisok A, Winnard P, Jr. *et al*. Oncogenic role of DDX3 in breast cancer biogenesis. Oncogene 2008; **27**: 3912-3922.

11 Nozaki K, Kagamu H, Shoji S, Igarashi N, Ohtsubo A, Okajima M *et al*. DDX3X induces primary EGFR-TKI resistance based on intratumor heterogeneity in lung cancer cells harboring EGFR-activating mutations. PloS one 2014; **9**: e111019.

12 Sun M, Song L, Zhou T, Gillespie GY, Jope RS. The role of DDX3 in regulating Snail. Biochimica et biophysica acta 2011; **1813**: 438-447.

13 Hagerstrand D, Tong A, Schumacher SE, Ilic N, Shen RR, Cheung HW *et al*. Systematic interrogation of 3q26 identifies TLOC1 and SKIL as cancer drivers. Cancer discovery 2013; **3**: 1044-1057.

14 Chen HH, Yu HI, Cho WC, Tarn WY. DDX3 modulates cell adhesion and motility and cancer cell metastasis via Rac1-mediated signaling pathway. Oncogene 2015; **34**: 2790-2800.

15 Xie M, Vesuna F, Botlagunta M, Bol GM, Irving A, Bergman Y *et al*. NZ51, a ring-expanded nucleoside analog, inhibits motility and viability of breast cancer cells by targeting the RNA helicase DDX3. Oncotarget 2015; **6**: 29901-29913.

16 Xie M, Vesuna F, Tantravedi S, Bol GM, Heerma van Voss MR, Nugent K *et al*. RK-33 radiosensitizes prostate cancer cells by blocking the RNA helicase DDX3. Cancer research 2016: doi:10.1158/0008-5472.CAN-1116-0440.

17 Wilky BA, Kim C, McCarty G, Montgomery EA, Kammers K, DeVine LR *et al*. RNA helicase DDX3: a novel therapeutic target in Ewing sarcoma. Oncogene 2016; **35**: 2574-2583.

18 Zeichner SB, Herna S, Mani A, Ambros T, Montero AJ, Mahtani RL *et al*. Survival of patients with de-novo metastatic breast cancer: analysis of data from a large breast cancer-specific private practice, a university-based cancer center and review of the literature. Breast cancer research and treatment 2015; **153**: 617-624.

19 Steeg PS. Targeting metastasis. Nature reviews Cancer 2016; **16**: 201-218.

20 Society AC. *Cancer Facts & Figures*. American Cancer Society: Atlanta, 2015.

21 Hoefnagel LD, van de Vijver MJ, van Slooten HJ, Wesseling P, Wesseling J, Westenend PJ *et al*. Receptor conversion in distant breast cancer metastases. Breast cancer research : BCR 2010; **12**: R75.

22 Jiwa LS, van Diest PJ, Hoefnagel LD, Wesseling J, Wesseling P, Moelans CB. Upregulation of Claudin-4, CAIX and GLUT-1 in distant breast cancer metastases. BMC cancer 2014; **14**: 864.

23 The Medical Research Involving Human Subjects Act [In Dutch: Wet medisch-wetenschappelijk onderzoek met mensen, WMO]. *Burgerlijk Wetboek*, 1998.

24 van Diest PJ. No consent should be needed for using leftover body material for scientific purposes. For. BMJ 2002; **325**: 648-651.

25 Angus AG, Dalrymple D, Boulant S, McGivern DR, Clayton RF, Scott MJ *et al*. Requirement of cellular DDX3 for hepatitis C virus replication is unrelated to its interaction with the viral core protein. The Journal of general virology 2010; **91**: 122-132.

26 Yedavalli VS, Neuveut C, Chi YH, Kleiman L, Jeang KT. Requirement of DDX3 DEAD box RNA helicase for HIV-1 Rev-RRE export function. Cell 2004; **119**: 381-392.

27 Budczies J, Klauschen F, Sinn BV, Gyorffy B, Schmitt WD, Darb-Esfahani S *et al*. Cutoff Finder: a comprehensive and straightforward Web application enabling rapid biomarker cutoff optimization. PloS one 2012; **7**: e51862.

28 Wu DW, Lee MC, Wang J, Chen CY, Cheng YW, Lee H. DDX3 loss by p53 inactivation promotes tumor malignancy via the MDM2/Slug/E-cadherin pathway and poor patient outcome in non-small-cell lung cancer. Oncogene 2014; **33**: 1515-1526.

29 Chang PC, Chi CW, Chau GY, Li FY, Tsai YH, Wu JC *et al*. DDX3, a DEAD box RNA helicase, is deregulated in hepatitis virus-associated hepatocellular carcinoma and is involved in cell growth control. Oncogene 2006; **25**: 1991-2003.

30 Heerma van Voss MR, van Kempen PMW, Noorlag R, van Diest PJ, Willems SM, Raman V. DDX3 has divergent roles in head and neck squamous cell carcinomas in smoking versus non-smoking patients. Oral diseases 2015; **21**: 270-271.
31 Pugh TJ, Weeraratne SD, Archer TC, Pomeranz Krummel DA, Auclair D, Bochicchio J *et al*. Medulloblastoma exome sequencing uncovers subtype-specific somatic mutations. Nature 2012; **488**: 106-110.
32 Seiwert TY, Zuo Z, Keck MK, Khattri A, Pedamallu CS, Stricker T *et al*. Integrative and comparative genomic analysis of HPV-positive and HPV-negative head and neck squamous cell carcinomas. Clinical cancer research : an official journal of the American Association for Cancer Research 2015; **21**: 632-641.
33 Ojha J, Secreto CR, Rabe KG, Van Dyke DL, Kortum KM, Slager SL *et al*. Identification of recurrent truncated DDX3X mutations in chronic lymphocytic leukaemia. British journal of haematology 2015; **169**: 445-448.
34 Wang L, Lawrence MS, Wan Y, Stojanov P, Sougnez C, Stevenson K *et al*. SF3B1 and other novel cancer genes in chronic lymphocytic leukemia. The New England journal of medicine 2011; **365**: 2497-2506.
35 Nik-Zainal S, Davies H, Staaf J, Ramakrishna M, Glodzik D, Zou X *et al*. Landscape of somatic mutations in 560 breast cancer whole-genome sequences. Nature 2016; **534**: 47-54.
36 Topisirovic I, Siddiqui N, Lapointe VL, Trost M, Thibault P, Bangeranye C *et al*. Molecular dissection of the eukaryotic initiation factor 4E (eIF4E) export-competent RNP. The EMBO journal 2009; **28**: 1087-1098.
37 Andersen JS, Lyon CE, Fox AH, Leung AK, Lam YW, Steen H *et al*. Directed proteomic analysis of the human nucleolus. Current biology : CB 2002; **12**: 1-11.
38 Anders CK, Deal AM, Miller CR, Khorram C, Meng H, Burrows E *et al*. The prognostic contribution of clinical breast cancer subtype, age, and race among patients with breast cancer brain metastases. Cancer 2011; **117**: 1602-1611.
39 Nguyen DX, Chiang AC, Zhang XH, Kim JY, Kris MG, Ladanyi M *et al*. WNT/TCF signaling through LEF1 and HOXB9 mediates lung adenocarcinoma metastasis. Cell 2009; **138**: 51-62.
40 Pukrop T, Dehghani F, Chuang HN, Lohaus R, Bayanga K, Heermann S *et al*. Microglia promote colonization of brain tissue by breast cancer cells in a Wnt-dependent way. Glia 2010; **58**: 1477-1489.
41 Cruciat CM, Dolde C, de Groot RE, Ohkawara B, Reinhard C, Korswagen HC *et al*. RNA helicase DDX3 is a regulatory subunit of casein kinase 1 in Wnt-beta-catenin signaling. Science 2013; **339**: 1436-1441.
42 McMullin RP, Wittner BS, Yang C, Denton-Schneider BR, Hicks D, Singavarapu R *et al*. A BRCA1 deficient-like signature is enriched in breast cancer brain metastases and predicts DNA damage-induced poly (ADP-ribose) polymerase inhibitor sensitivity. Breast cancer research : BCR 2014; **16**: R25.
43 Woditschka S, Evans L, Duchnowska R, Reed LT, Palmieri D, Qian Y *et al*. DNA double-strand break repair genes and oxidative damage in brain metastasis of breast cancer. Journal of the National Cancer Institute 2014; **106**.
44 Berghoff AS, Ilhan-Mutlu A, Dinhof C, Magerle M, Hackl M, Widhalm G *et al*. Differential role of angiogenesis and tumour cell proliferation in brain metastases according to primary tumour type: analysis of 639 cases. Neuropathology and applied neurobiology 2015; **41**: e41-55.
45 Bol GM, Raman V, van der Groep P, Vermeulen JF, Patel AH, van der Wall E *et al*. Expression of the RNA helicase DDX3 and the hypoxia response in breast cancer. PloS one 2013; **8**: e63548.
46 Dupuy F, Tabaries S, Andrzejewski S, Dong Z, Blagih J, Annis MG *et al*. PDK1-Dependent Metabolic Reprogramming Dictates Metastatic Potential in Breast Cancer. Cell metabolism 2015; **22**: 577-589.
47 Chen EI, Hewel J, Krueger JS, Tiraby C, Weber MR, Kralli A *et al*. Adaptation of energy metabolism in breast cancer brain metastases. Cancer research 2007; **67**: 1472-1486.
48 Palmieri D, Fitzgerald D, Shreeve SM, Hua E, Bronder JL, Weil RJ *et al*. Analyses of resected human brain metastases of breast cancer reveal the association between up-regulation of hexokinase 2 and poor prognosis. Molecular cancer research : MCR 2009; **7**: 1438-1445.
49 Heitz F, Harter P, Lueck HJ, Fissler-Eckhoff A, Lorenz-Salehi F, Scheil-Bertram S *et al*. Triple-negative and HER2-overexpressing breast cancers exhibit an elevated risk and an earlier occurrence of cerebral metastases. Eur J Cancer 2009; **45**: 2792-2798.
50 Bol GM, Xie M, Raman V. DDX3, a potential target for cancer treatment. Molecular cancer 2015; **14**: 188.
51 Steeg PS, Camphausen KA, Smith QR. Brain metastases as preventive and therapeutic targets. Nature reviews Cancer 2011; **11**: 352-363.

SUPPLEMENTARY

Supplementary table 1. Correlation between nuclear DDX3 expression and clinicopathological variables in breast cancer metastases.

		Nuclear DDX3		
	Total	**Absent**	**Present**	**P-value**
Characteristics primary tumor				
Tumor size in cm, median (IQR)	7 (2)	7 (2)	7 (1.75)	0.868#
Histology, n (%)				
Ductal	67 (85)	57 (83)	10 (100)	0.763**
Lobular	8 (10)	8 (12)	0	
Metaplastic	3 (4)	3 (4)	0	
Apocrine	1 (1)	1 (1)	0	
Grade, n (%)				
I	1 (1)	1 (1)	0	0.754**
II	21 (27)	19 (28)	2 (20)	
III	55 (70)	47 (70)	8 (80)	
missing	2	2	0	
MAI, mean (SD)	24.8 (19.7)	24.7 (20.0)	25.5 (18.8)	0.973$
Lympnodes, n (%)				
negative	39 (49)	35 (51)	4 (40)	0.737**
positive	40 (51)	34 (49)	6 (60)	
Age, mean (SD)	52.2 (11.0)	52.3 (10.9)	52.0 (11.8)	0.951$
missing	1	1	0	
Molecular subtype, n (%)				
HER2-enriched	11 (15)	7 (11)	4 (44)	0.070**
luminal A	29 (41)	26 (42)	3 (33)	
luminal B	8 (11)	7 (11)	1 (11)	
triple negative	23 (32)	22 (35)	1 (11)	
missing	8	7	1	
Characteristics metastasis				
Location, n (%)				
brain	31 (39)	27 (39)	4 (40)	1**
skin	20 (25)	18 (26)	2 (20)	
lung	15 (19)	13 (19)	2 (20)	
other	13 (16)	11 (16)	2 (20)	
Estrogen receptor, n (%)				
negative	39 (57)	34 (56)	5 (63)	1**
positive	30 (43)	27 (44)	3 (38)	
missing	10	8	2	
Progesterone receptor, n (%)				
negative	39 (57)	43 (74)	5 (63)	0.673**
positive	30 (43)	15 (26)	3 (38)	
missing	13	11	2	
HER2 receptor, n (%)				
negative	48 (73)	47 (81)	4 (44)	0.030**
positive	18 (27)	11 (19)	5 (55)	
missing	12	11	1	

P-value calculated by * chi-square test, ** Fisher exact test, # Mann-Whitney U test, $ student's t-test.

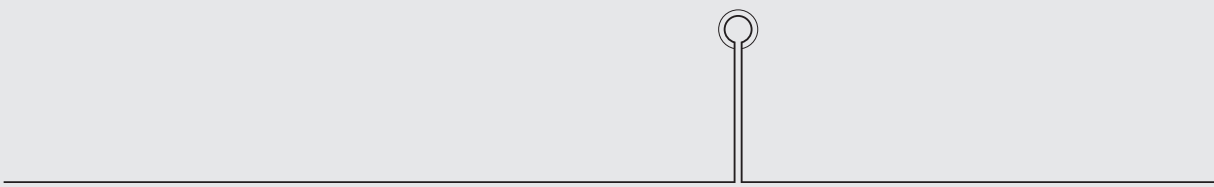

CHAPTER 7

DDX3 has divergent roles in head and neck squamous cell carcinomas in smoking vs non-smoking patients

Letter in Oral Dis. 2015 Mar;21(2):270-1

Marise R Heerma van Voss, Pauline MW van Kempen, Rob Noorlag, Paul J van Diest, Stefan Willems, Venu Raman

With great interest we have read the study of C-H Lee, *et al*[1], in which the authors find that low/negative DDX3 expression might predict poor prognosis in non-smoker patients with oral cancer. With respect to DDX3 functions in cellular biogenesis, there is conflicting data in the literature on whether DDX3 is a driver or suppressor of oncogenic transformation. For example, in medulloblastomas, non-synonymous substitution mutations in the helicase domain of *DDX3X* seem to have an activating role[2], but the nature of genomic alterations found in head and neck squamous cell carcinomas (HNSCC), for a large part homozygous deletions and frame shift and nonsense mutations, is more supportive of loss of function[3-5]. A recent study found *DDX3X* to be exclusively mutated in HPV-positive HNSCC. These results invoke the question of how to interpret DDX3 function in specific subgroups of HNSCC, like tumors occurring in smokers, which are more often HPV-negative and non-smokers which are more often HPV-positive.

To address this point, we recently evaluated DDX3 protein expression levels in 423 Dutch HNSCC. Tissue microarrays containing multiple cores per tumour of both oral (n=206) and oropharynx (n=217) squamous cell carcinomas were immunohistochemically stained with anti-DDX3 antibodies (r647, 1:1000, 60 min). Cytoplasmic expression was scored as being absent, weak, moderate or strong. Moderate to strong DDX3 expression was identified in 217 cases (51.3%). Overall, DDX3 expression did not correlate with survival in HNSCC. A stratified analysis in smokers and non-smokers, however, yielded an inversed relation between DDX3 expression and survival in both groups (Figure 1). As Lee *et al.* reported earlier, non-smokers with moderate to strong DDX3 expressing tumors had longer median overall survival[1], although this was not significant in our cohort (HR 0.88,

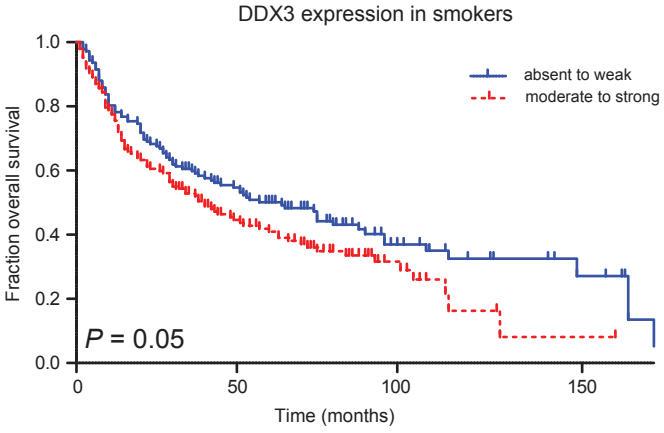

Figure 1. Moderate to strong DDX3 expression correlates with shorter overall survival in smoking HNSCC patients P-value is calculated by log-rank test.

95% CI 0.53-1.45, p = 0.61). However, in smokers we observed an inversed trend with a median survival of 40 months for cases with moderate to strong DDX3 expression as compared to 64 months for cases with absent or weak DDX3 expression (HR 1.34; 95% CI 1.00-1.81; p = 0.05). We therefore conclude that in smokers high DDX3 expression might be predictive of poor prognosis.

There are several other differences to be noted between our recent study and that of C-H Lee, *et al.* which can explain our divergent conclusions. Most strikingly, in the study of C-H lee, *et al.* only a small proportion of tumors have moderate to high DDX3 expression (10.5%). This might be due to the use of a different antibody isotype and scoring methods as well as differences between the study populations. The Dutch cohort we used has a higher percentage of smoking and female patients, whereas in the Taiwanese population betel quid chewing is far more common. These factors were also individually found to be associated with DDX3 expression. Another major difference is the inclusion of not just oral, but also oropharynx SCC in our study. However, since stratification based on anatomical site had no major influence on our findings, this probably does not explain the divergent findings between the two studies.

Our finding that high DDX3 expression is associated with poorer survival specifically in smokers, is in line with our earlier finding that exposure of breast cell lines to Benzo[a] pyrene diol epoxide, a carcinogen found in cigarette smoke, increased DDX3 expression resulting in malignant transformation[6]. Moreover, DDX3 has been shown to be an integral component of viral RNA propagation[7, 8] and to have a role in the modulation of the innate immune response[9]. It is therefore plausible that virally transformed cells benefit from lowering DDX3 levels, in order to increase their oncogenic potential. This hypothesis is also supported by the fact that E6 expression as a result of HPV infection in non-small cell lung cancer is associated with lower DDX3 expression[10]. Taken together, these findings project a model in which DDX3, when upregulated in response to cigarette smoke exposure, drives oncogenesis, whereas it might have alternative roles in virally induced transformation.

REFERENCES

1 Lee CH, Lin SH, Yang SF, Yang SM, Chen MK, Lee H *et al*. Low/negative expression of DDX3 might predict poor prognosis in non-smoker patients with oral cancer. Oral diseases 2014; **20**: 76-83.

2 Pugh TJ, Weeraratne SD, Archer TC, Pomeranz Krummel DA, Auclair D, Bochicchio J *et al*. Medulloblastoma exome sequencing uncovers subtype-specific somatic mutations. Nature 2012; **488**: 106-110.

3 Seiwert TY, Zuo Z, Keck MK, Khattri A, Pedamallu CS, Stricker T *et al*. Integrative and comparative genomic analysis of HPV-positive and HPV-negative head and neck squamous cell carcinomas. Clinical cancer research : an official journal of the American Association for Cancer Research 2015; **21**: 632-641.

4 Mutational landscape of gingivo-buccal oral squamous cell carcinoma reveals new recurrently-mutated genes and molecular subgroups. Nature communications 2013; **4**: 2873.

5 Stransky N, Egloff AM, Tward AD, Kostic AD, Cibulskis K, Sivachenko A *et al*. The mutational landscape of head and neck squamous cell carcinoma. Science 2011; **333**: 1157-1160.

6 Botlagunta M, Vesuna F, Mironchik Y, Raman A, Lisok A, Winnard P, Jr. *et al*. Oncogenic role of DDX3 in breast cancer biogenesis. Oncogene 2008; **27**: 3912-3922.

7 Yedavalli VS, Neuveut C, Chi YH, Kleiman L, Jeang KT. Requirement of DDX3 DEAD box RNA helicase for HIV-1 Rev-RRE export function. Cell 2004; **119**: 381-392.

8 Ko C, Lee S, Windisch MP, Ryu WS. DDX3 DEAD-Box RNA Helicase Is a Host Factor That Restricts Hepatitis B Virus Replication at the Transcriptional Level. Journal of virology 2014; **88**: 13689-13698.

9 Oshiumi H, Sakai K, Matsumoto M, Seya T. DEAD/H BOX 3 (DDX3) helicase binds the RIG-I adaptor IPS-1 to up-regulate IFN-beta-inducing potential. European journal of immunology 2010; **40**: 940-948.

10 Wu DW, Liu WS, Wang J, Chen CY, Cheng YW, Lee H. Reduced p21(WAF1/CIP1) via alteration of p53-DDX3 pathway is associated with poor relapse-free survival in early-stage human papillomavirus-associated lung cancer. Clinical cancer research : an official journal of the American Association for Cancer Research 2011; **17**: 1895-1905.

PARTNERS IN CRIME

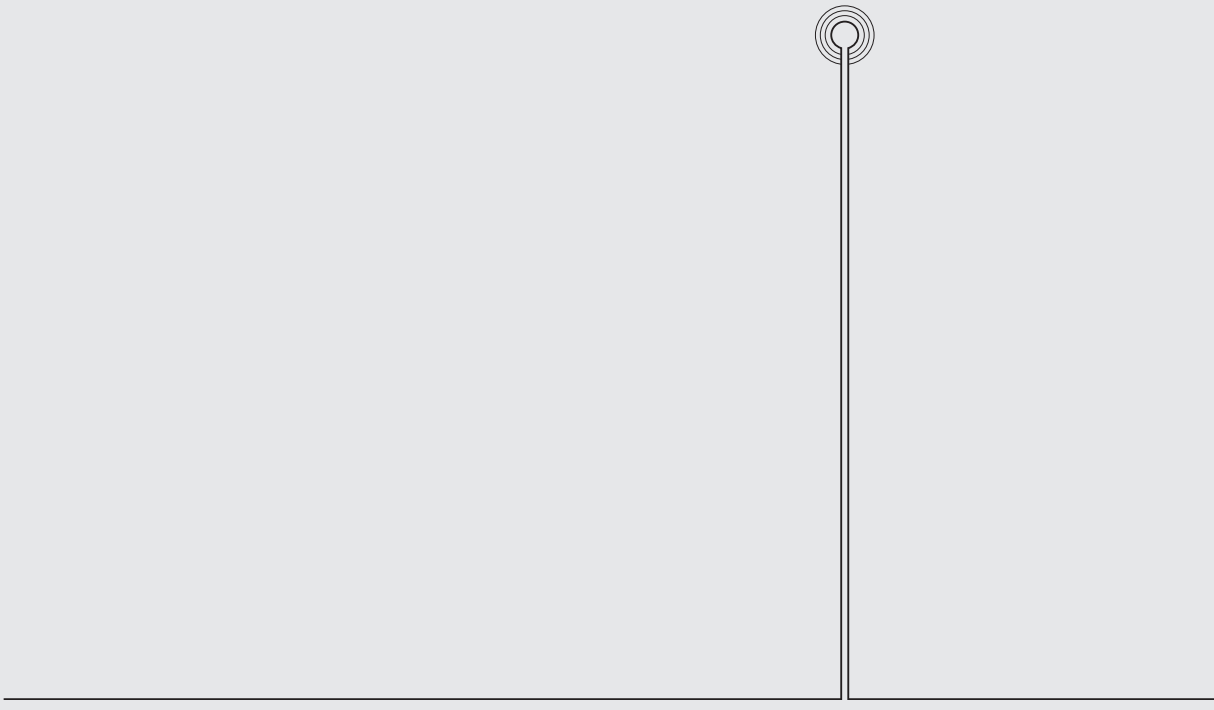

CHAPTER 8

Combination treatment using DDX3 and PARP inhibitors induces synthetic lethality in BRCA1-proficient breast cancer

Medical Oncology 2017, Mar;34(3):33

Marise R Heerma van Voss, Justin D Brilliant, Farhad Vesuna, Guus M Bol, Elsken van der Wall, Paul J van Diest, Venu Raman

ABSTRACT

Triple negative breast cancers have unfavorable outcomes due to their inherent aggressive behavior and lack of targeted therapies. Breast cancers occurring in *BRCA1* mutation carriers are mostly triple negative and harbor homologous recombination deficiency, sensitizing them to inhibition of a second DNA damage repair pathway by e.g., PARP inhibitors. Unfortunately, resistance against PARP inhibitors in BRCA1 deficient cancers is common and sensitivity is limited in BRCA1 proficient breast cancers. RK-33, an inhibitor of the RNA helicase DDX3, was previously demonstrated to impede non-homologous end-joining repair of DNA breaks. Consequently, we evaluated DDX3 as a therapeutic target in BRCA pro- and deficient breast cancers and assessed whether DDX3 inhibition could sensitize cells to PARP inhibition.

High DDX3 expression was identified by immunohistochemistry in breast cancer samples of 24% of *BRCA1* ($p = 0.337$) and 21% of *BRCA2* mutation carriers ($p = 0.624$), as compared to 30% of sporadic breast cancer samples. The sensitivity to the DDX3 inhibitor RK-33 was similar in BRCA1 pro- and deficient breast cancer cell lines, with IC50 values in the low micromolar range (2.8-6.6 μM). A synergistic interaction was observed for combination treatment with RK-33 and the PARP inhibitor olaparib in BRCA1 proficient breast cancer, with the mean combination index ranging from 0.59-0.62.

Overall, we conclude that BRCA pro- and deficient breast cancers have a similar dependency upon DDX3. Moreover, DDX3 inhibition by RK-33 synergizes with PARP inhibitor treatment, especially in breast cancers with a BRCA1- proficient background.

INTRODUCTION

Increased genomic instability is one of the underlying hallmarks of cancer[1]. Cancer cells often acquire a deficiency in one of the DNA damage repair (DDR) pathways, to allow continued proliferation in the presence of genetic aberrations. This leads to a greater dependency on the remaining pathways to deal with endogenous and exogenous DNA damage[2, 3], which is the principle behind synthetic lethality of pharmacologic PARP inhibition in cancers with a *BRCA1/BRCA2* mutation.

Women harboring a germline mutation in the *BRCA1* or *BRCA2* genes are at high risk of developing breast cancer, due to a deficiency in a DNA double strand break (DSB) repair mechanism, homologous recombination (HR)[4]. *BRCA1* related breast cancers are mostly estrogen receptor, progesterone receptor and HER2/*neu* negative (triple negative; TN)[5]. Patients with TN breast cancer (TNBC) have an unfavorable prognosis, due to the inherent aggressive behavior of this molecular subtype and the lack of targeted therapies[6]. PARP inhibitors, like olaparib, inhibit base excision repair (BER), a single strand break (SSB) repair mechanism, and have shown great promise in the treatment of tumors with a *BRCA1* or *BRCA2* mutation. However, a significant proportion of these patients show primary resistance[7]. Although only 5-10% of TNBC occurs in patients with a germline *BRCA1* mutation, BRCA proficient TNBCs are also characterized by impairments of DDR pathways. However, the effect of PARP inhibitors as a monotherapy in this group of patients is limited[8]. Therefore, development of new treatment strategies, specifically targeting *BRCA1* related - and TNBC is urgently required.

DDX3, also known as DDX3X, is DEAD box RNA helicase that has been associated with several cytosolic steps of mRNA processing[9] and plays an oncogenic role in the development of breast[10] and several other types of cancer[11-14]. DDX3 was found to have anti-apoptotic properties[15] and to stimulate cell cycle progression[11, 12], migration[10] and invasion[16]. In addition, DDX3 was shown to be upregulated in triple negative breast cancer[17]. RK-33 was developed as a small molecule inhibitor of DDX3 and showed promising preclinical activity as a radiosensitizer in models of lung[11] and prostate cancer[14]. Interestingly, the radiosensitizing capacities of RK-33 were attributed to inhibition of non-homologous end-joining (NHEJ), a second DNA DSB repair mechanism. Inhibition of NHEJ makes RK-33 an interesting candidate for the treatment of *BRCA1*-related breast cancer and TNBC. Given their pre-existing DDR deficiency, we hypothesized that BRCA deficient breast cancers might be dependent on DDX3 and therefore sensitive to DDX3 inhibition with RK-33. In addition, DDX3 inhibition could potentially sensitize cells to PARP inhibition. This study therefore focused on evaluating DDX3 as a therapeutic target in BRCA pro- and deficient breast cancer and assesses whether there is a potential synergistic interaction between DDX3 inhibition and PARP inhibition.

MATERIAL AND METHODS

Patient samples

Archived formalin fixed paraffin embedded breast cancer samples from 103 germline *BRCA1* mutation carriers and 29 germline *BRCA2* mutation carriers were previously processed into a tissue microarray (TMA) and compared against a TMA with 265 consecutive breast cancer cases not known to bear mutations in these genes (further denoted "sporadic")[18]. All patients in the hereditary group had been referred to the clinical genetics department of one of three academic hospitals in The Netherlands (VUMC, UMC Utrecht and UMC Groningen) and tissue was retrieved from the pathology departments of these hospitals or of local surrounding hospitals. All TMAs included multiple cores per patient. As we used anonymous archival leftover pathology material, no ethical approval or informed consent is required according to Dutch legislation[19], as this use of redundant tissue for research purposes is part of the standard treatment agreement with patients in our hospitals[20].

Immunohistochemistry

Four μm thick sections were deparaffinized in xylene and rehydrated in decreasing ethanol dilutions. Endogenous peroxidase activity was blocked with 1.5 % hydrogen peroxide buffer for 15 minutes and was followed by antigen retrieval by boiling for 20 minutes in 10 mM citrate buffer (pH 6.0). Slides were subsequently incubated for 1 hour with anti-DDX3 (1:1000, pAb r647 [21]), followed by poly-HRP-anti-mouse/rabbit/rat IgG (Brightvision, Immunologic, Duiven, The Netherlands) as a secondary antibody for 30 minutes. Peroxidase activity was developed with diaminobenzidine. The slides were lightly counterstained with hematoxylin and mounted. Appropriate positive and negative controls were used throughout.

Scoring was performed by consensus of two observers. Cytoplasmic DDX3 expression was fairly homogeneous, but the intensity varied and was therefore scored semi-quantitatively as absent (0), low (1), moderate (2) or strong (3). Cases with score 0 to 2 were classified as having low DDX3 expression and evaluated against cases with strong expression as before[17].

Statistics

DDX3 expression and other clinicopathological characteristics were compared between tumors in patients with a germline mutation in *BRCA1* or *BRCA2* versus sporadic breast cancers. Discrete variables were compared by $\chi 2$ or Fisher's exact test. Student's t-test and Mann Whitney U-tests were calculated for normally and non-normally distributed variables, respectively. Multivariate analysis was performed by including all factors significantly associated with both DDX3 expression and BRCA-mutation status in a logistic regression model. Effect modifiers were identified by including multiplicative interaction terms into the model. P-values smaller than 0.05 were considered statistically significant. All statistical analyses were performed with R version 3.2.0.

Immunoblotting

All cells were harvested at 50-70 % confluency. Cells were lysed in SDS-extraction buffer and sonicated on ice. 30 µg protein was loaded on SDS-PAGE gels for gel-electrophoresis. The blots were probed overnight with primary antibodies against DDX3 (1:1000, mAb AO196)[21], β-actin (1:10000, A5441, Sigma-Aldrich), followed by appropriate secondary antibodies, development with ECL (Bio-Rad, Hercules, CA, USA) and imaging with a G:BOX Chemi XR5 (Syngene, Frederick, MD, USA).

Cell viability assay

MCF7 and MDA-MB-231 were purchased from ATCC (ATCC, Manassas, VA, USA). MDA-MB-468, MDA-MB-435, SUM149-PT and HCC1937 were a kind gift of Shyam Sharan (NCI, Frederick, MD, USA). For cell viability assays 1 x 10^3 – 3 x 10^3 cells were plated per well in a 96-well plate. The following day RK-33 or DMSO (vehicle control) was added. The number of viable cells was estimated after 72 hours of drug exposure with an MTS assay. For this, the cells were incubated with MTS reagent (CellTiter 96 Aqueous One Solution, Promega, Madison, WI, USA) for 2 hours, after which absorbance was measured at 490 nm with a Victor^{3}V plate reader (PerkinElmer, Waltham, MA, USA).

Colony forming assay

Synergy between RK-33 and olaparib was evaluated by colony forming assays, as this is the most used assay to evaluate PARP inhibitor efficacy[22]. For HCC1937, 2500 cells were plated in 60 mm dishes. For all other cell lines 200-600 cells were plated in 6-well plates and allowed to attach overnight. Cells were treated with either RK-33, olaparib, or a combination of both, in the IC50 ratio for 24 hours, followed by either fresh media or fresh media containing olaparib addition every 4 days. When colonies reached a size of more than 50 cells, they were fixed in methanol with 0.5 % crystal violet. Colonies were counted and survival fractions were calculated.

Synergy analysis

Monotherapy and combination therapy curves of multiple independent experiments were modeled with nonlinear mixed-effects modeling, using the mixlow R package[23]. To evaluate dose-response interactions combination indices with 95% confidence intervals were calculated for every fraction affected (Fa) according to the Loewe additivity principle[24], as formulated in equation A.

(A) $$CI = \frac{C_{A,x}}{IC_{x,A}} + \frac{C_{B,x}}{IC_{x,B}}$$

$C_{A,x}$ and $C_{B,x}$ are the concentrations of olaparib and RK-33 in combination to achieve fraction affected x. $IC_{x,A}$ and $IC_{x,B}$ are the concentrations of the olaparib and RK-33 alone to achieve the same effect. Synergy was defined as a combination index significantly lower than one.

Table 1. DDX3 expression and other clinicopathological characteristics in breast cancer in *BRCA1* or *BRCA2* germline mutation carriers as compared to sporadic breast cancers.

	Sporadic	*BRCA1*	p-value	*BRCA2*	p-value
DDX3 expression, n (%)			0.337†		0.624†
absent	3 (1)	0		0	
weak	34 (13)	19 (18)		5 (17)	
moderate	148 (56)	59 (57)		18 (62)	
strong	80 (30)	25 (24)		6 (21)	
Age, median (IQR)	58 (18)	40 (11.5)	<0.001‡	50 (11)	<0.001‡
B&R Grade, n (%)			<0.001		0.014†
1	45 (17)	2 (2)		0	
2	99 (37)	15 (16)		8 (31)	
3	121 (46)	78 (82)		18 (69)	
missing	0	0		1	
MAI, median (IQR)	12 (18)	25 (25)	<0.001‡	17 (13)	0.110†
missing	0	13		3	
Histological type, n (%)			0.064		0.667†
invasive ductal carcinoma	225 (85)	80 (84)		25 (93)	
invasive lobular carcinoma	24 (9)	4 (4)		2 (7)	
other	15 (6)	11 (12)		0	
missing	1	8		2	
Tumor size (cm), median (IQR)	2 (2)	2 (2)	0.924‡	1 (1)	0.029‡
missing	22	26		6	
ER, n (%)			<0.001		1
negative	50 (19)	76 (77)		5 (19)	
positive	215 (81)	23 (23)		22 (81)	
missing	0	4		2	
PR, n (%)			<0.001		0.171
negative	87 (33)	81 (83)		13 (48)	
positive	177 (67)	17 (17)		14 (52)	
missing	1	5		2	
HER2, n (%)			0.828		1†
negative	243 (92)	94 (93)		26 (93)	
positive	22 (8)	7 (7)		2 (7)	
missing	0	2		1	
Molecular classification, n (%)			<0.001†		0.897†
luminal A	208 (78)	20 (21)		21 (81)	
luminal B	12 (5)	4 (4)		1 (4)	
HER2-overexpressing	10 (4)	4 (4)		0	
basal-like	35 (13)	67 (71)		4 (15)	
unclassified	0	0		0	

P-value calculated by chi-square test unless otherwise indicated.
n = number; B&R = Bloom and Richardson; MAI = mitotic activity index; IQR, interquartile range
† Fisher exact test
‡ Mann-Whitney U-test

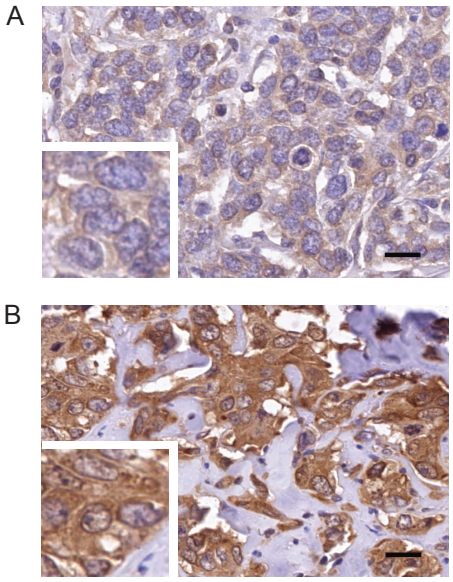

Figure 1. DDX3 expression in BRCA1 related breast cancer
Example of low (A.) and high (B.) immunohistochemical DDX3 expression in breast cancer occurring in patients with a germline BRCA1 mutation. Scale bar is 20 µm.

RESULTS

DDX3 expression in BRCA1 deficient breast cancer patient samples

To assess the dependence on DDX3 in cancer with a DDR deficiency, we evaluated DDX3 expression by immunohistochemistry in breast cancer samples of 103 germline *BRCA1* mutation carriers, 29 germline *BRCA2* mutation carriers and 265 women with sporadic breast cancer (Figure and Table 1). Strong cytoplasmic DDX3 expression was observed in 30% of sporadic cases, as compared to 24% of *BRCA1* ($p = 0.337$) and 21% of *BRCA2* related cases ($p = 0.624$), indicating that these mutations do not cause an increase in DDX3 expression levels. We did observe the usual known differences between our sporadic and *BRCA* deficient study populations, like lower age ($p < 0.001$) and higher grade ($p = 0.014$) in both *BRCA1* and *BRCA2* related cases and higher MAI ($p < 0.001$), negative ER status ($p < 0.001$), negative PR status ($p < 0.001$) and more frequent basal-like molecular classification ($p < 0.001$) in *BRCA1* mutation carriers.

To exclude that we were not observing a correlation between *BRCA1/2* mutation status and DDX3 expression levels due to incidental cancellation bias by another confounding factor, we performed logistic regression with all covariates that were associated both with mutation status and DDX3 expression. The presence of a germline *BRCA1* mutation became a borderline significant predictor of DDX3 expression ($OR_{adjusted}$ 0.53, $p = 0.053$) after correction for MAI, histological type and PR status, implying that DDX3 expression may

even be lower in *BRCA1* related breast cancers of equal MAI, histological type and PR status. No factors were significantly associated with both *BRCA2* mutation status and DDX3 expression. No effect modifiers were identified.

Equal sensitivity to the DDX3 inhibitor RK-33 in BRCA1 pro- and deficient breast cancer cell lines

In addition, DDX3 levels were evaluated in two cell lines with a *BRCA1* mutation (HCC1937 and SUM149-PT) and four *BRCA1* proficient cell lines (MCF7, MDA-MB-231, MDA-MB-435 and MDA-MB-468, Figure 2A). DDX3 expression was highest in the BRCA1 proficient cell line MDA-MB-468 and lowest in the BRCA1 deficient cell line HCC1937. All other cell lines had similar DDX3 expression levels. Sensitivity to DDX3 inhibition with the small molecule inhibitor RK-33 was evaluated with MTS assays (Figure 2B).

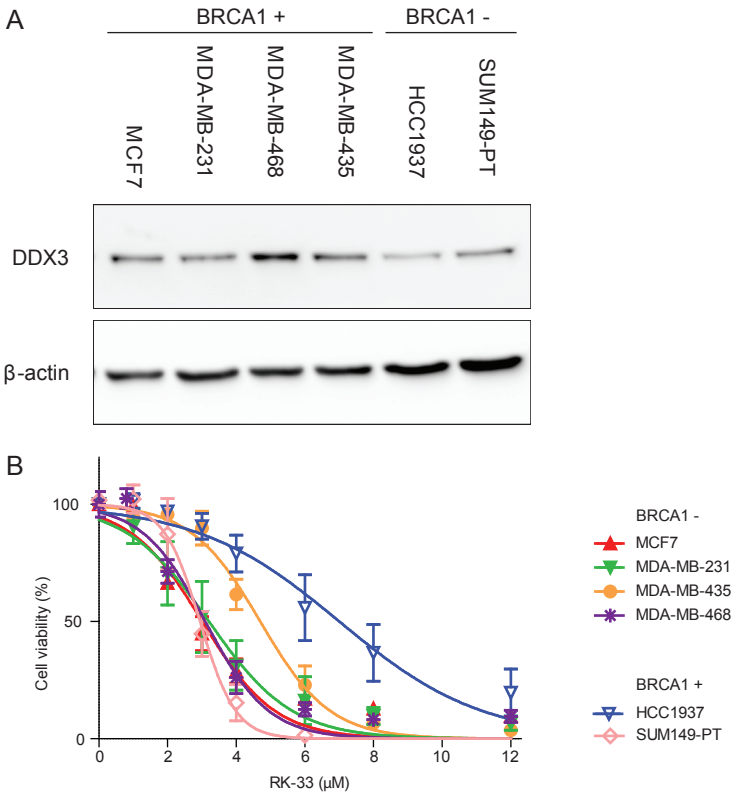

Figure 2. Sensitivity of BRCA1 pro- and deficient cell lines to the DDX3 inhibitor RK-33
A. Immunoblot showing DDX3 and β-actin expression in BRCA1 proficient cell lines (BRCA1+) and cell lines with mutated BRCA1 (BRCA1-). B. MTS assay showing RK-33 cytotoxicity in BRCA1 proficient cell lines and cell lines with mutated BRCA1. Graphs represent mean of independent experiments ± SD.

All IC50 values were in the low micromolar range (2.8-6.6 μM). Of the cell lines with a *BRCA1* mutation, an IC50 on the lower end of the spectrum (2.9 μM) was observed for SUM149-PT, whereas HCC1937 had the highest IC50 of all cell lines (6.6 μM). Overall, the DDX3 inhibitor RK-33 had a similar *in vitro* efficacy in *BRCA1* pro- and deficient cell lines.

Synergy between DDX3 inhibition with RK-33 and PARP inhibition with olaparib

Given the effect of RK-33 on DNA repair, we explored whether any synergy could be observed between the DDX3 inhibitor RK-33 and the PARP inhibitor olaparib. Figure 3 shows the effect of combined RK-33 and olaparib treatment as measured by colony forming assays. The fraction of cells surviving combination therapy was lower than the surviving fraction of monotherapy in all cell lines, except HCC1937 (Figure 3A). In order to evaluate whether the cytotoxicity of combined RK-33 and olaparib was more than additive, combination indices were calculated (Figure 3B). The mean combination index over the 20-95% fraction affected interval was lower than 1 for MCF7 (CI_{20-95} 0.59) and MDA-MB-468 (CI_{20-95} 0.62), indicating synergy in the BRCA1 proficient cell lines. In SUM149-PT synergy was observed only in case of a high Fa. Although the mean CI_{20-95} was 1.42, the CI of the actual measured data points (Fa 60-100%) was significantly lower than 1, indicative of synergy in this area. No synergy was observed for HCC1937 (CI_{20-95} 1.71).

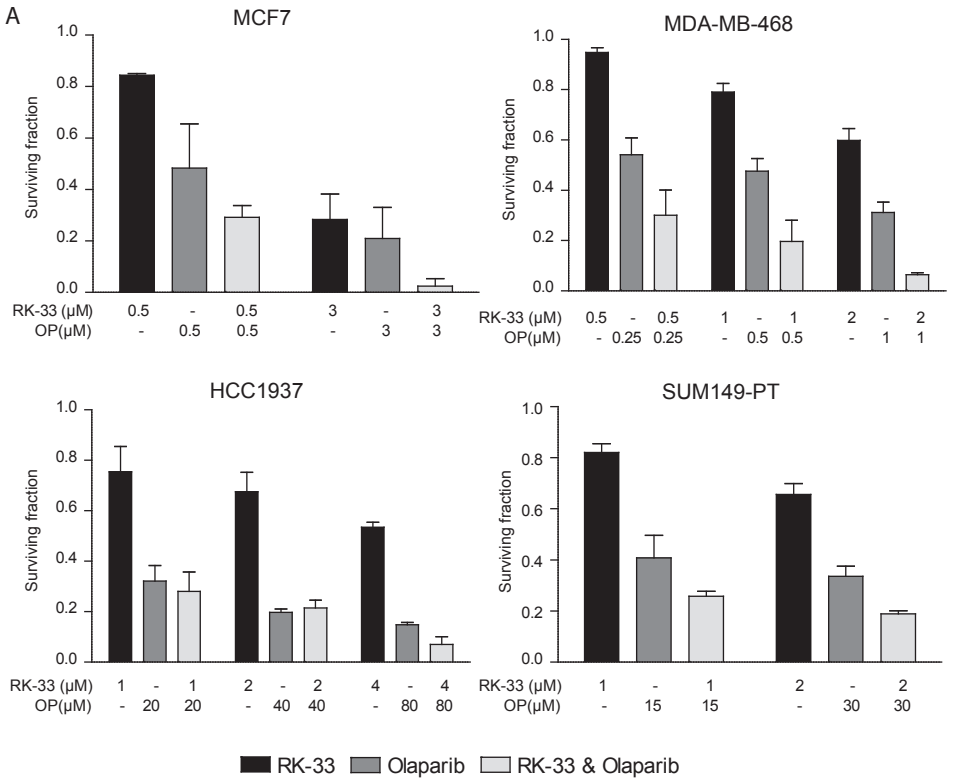

Figure 3. Synergy between RK-33 and the PARP inhibitor olaparib
A. Bar graphs representing the surviving fraction in a colony formation assay after RK-33, olaparib or combination treatment in BRCA1 proficient (MCF7 & MDA-MB-468) and BRCA1 deficient breast cancer cell lines (HCC1937 & SUM149-PT). (see next page for Figure 3B) ▶

DISCUSSION

This study evaluated the efficacy of DDX3 inhibition, by the small molecule inhibitor RK-33, in BRCA deficient breast cancer, with inherent impaired HR DNA repair pathway, in comparison with BRCA proficient breast cancer. RK-33 was previously found to inhibit NHEJ, an additional DSB repair mechanism [11]. Therefore, we hypothesized that BRCA deficient breast cancer might have an increased dependency on DDX3. However, DDX3 expression levels were similar in breast cancers in *BRCA1/BRCA2* germline mutation carriers and sporadic breast cancers and BRCA1 pro- and deficient breast cancer cell lines were equally sensitive to RK-33 treatment. We therefore concluded that high DDX3

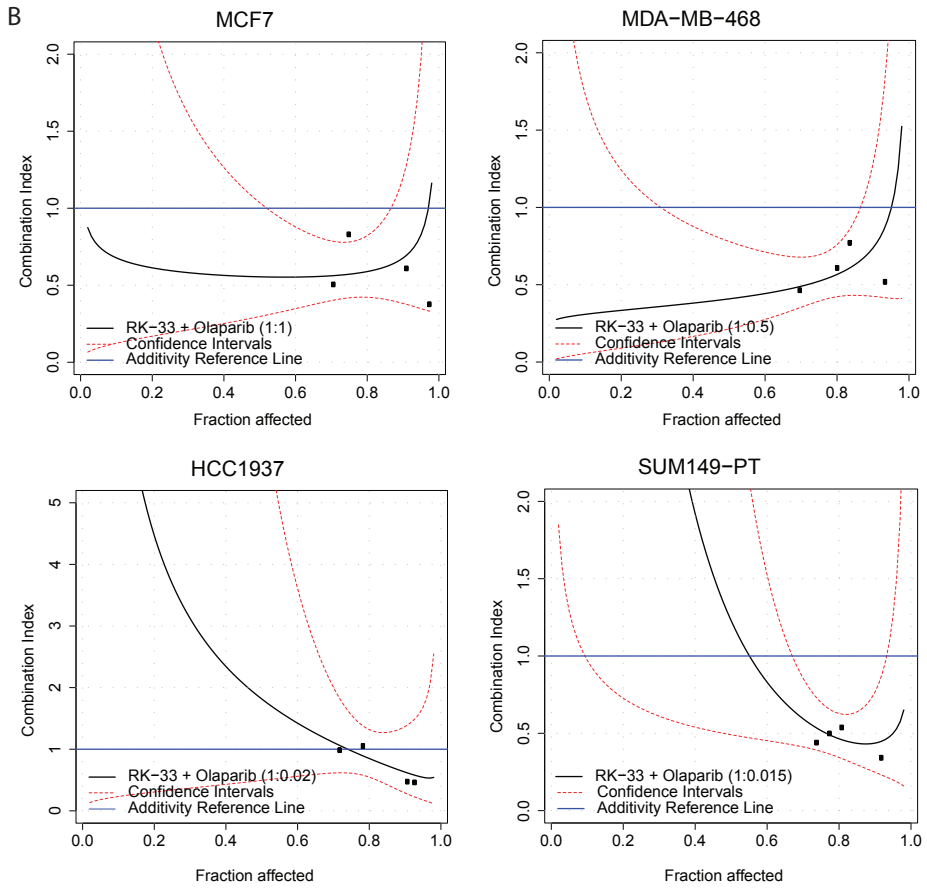

◀ **Figure 3.** Synergy between RK-33 and the PARP inhibitor olaparib
B. CI-Fa plots showing the combination index (CI) and 95% confidence intervals of RK-33 olaparib combination therapy for different fractions affected (Fa) in BRCA1 pro- and deficient cell lines. Lines represent modeled CI curves. Points represent CI values calculated from measured data points. Dashed red lines represent 95% confidence intervals. Blue lines represent additivity reference line. Graphs represent mean of independent experiments ± SD.

expression is present in BRCA-mutated breast cancers and they are sensitive to DDX3 inhibition. However, there was no clear indication of increased DDX3 dependency in BRCA deficient, when compared to BRCA proficient breast cancers. In addition, we evaluated whether DDX3 inhibition with RK-33 could sensitize BRCA pro- and deficient breast cancer cells to PARP inhibition with olaparib. We found a synergistic interaction mainly in BRCA1 proficient cell lines and to a certain extent in BRCA1 deficient cancers.

The mechanism behind the increased sensitivity of BRCA deficient cancers to PARP inhibition is an area of active investigation and several explanations have been proposed[25]. The most accepted mechanism is that PARP inhibitors impair BER, an SSB repair

mechanism. Persistent SSBs are converted to DSBs, which are normally repaired by HR, but remain unrepaired in HR deficient *BRCA1/BRCA2* mutant cells[25]. Our observation that PARP inhibitors synergize with NHEJ inhibition by RK-33 fits a variant of this model. Since HR is restricted to the S- and G2-phase of the cell cycle[26], accumulation of DSBs is likely to also require NHEJ for repair. This could explain the synthetic lethality observed after combination therapy with the PARP inhibitor olaparib and the DDX3 inhibitor RK-33 and previously reported radiosensitizing capacities of RK-33[11], since ionizing radiation causes DSB formation as well. Also, it may explain why the dependency on DDX3 is not increased in cells with a *BRCA1* mutation. In the absence of an agent that stimulates persistence of SSBs, the DSB production rate may not be high enough to increase the demand for NHEJ as an alternative repair strategy. In addition, the sensitivity of BRCA1 deficient cell lines to PARP inhibition is already very high, making it hard observe synergy with RK-33 in these cells. A second explanation for PARP inhibitor efficacy in BRCA deficient tumors is that PARP inhibitors have an activating effect on NHEJ, which is a more error-prone repair pathway than HR[27]. More research on the exact role of DDX3 in different DNA repair pathways is necessary to fully understand the mechanism behind the observed interactions between PARP inhibition and DDX3 inhibition in a BRCA1 pro- or deficient background. Sensitization of primary resistant BRCA proficient breast cancers to PARP inhibition by RK-33 could be of specific use in the treatment of TNBC, given their aggressive biology and the lack of specific therapeutic targets [6]. Secondary resistance in *BRCA1* mutant cancers is mainly due to restoration of HR defects, often by partially restoring *BRCA1* functionality[28]. Since RK-33 sensitizes BRCA1 proficient breast cancer cells to PARP inhibition, DDX3 inhibition could also have an application overcoming secondary resistance against PARP inhibitors. There is a risk of causing normal cell toxicity by enhancing the sensitivity of cancer cells to PARP inhibition[29]. Because cancer cells have higher endogenous DNA damage rates and greater DDR deficiency compared to normal cells, there is a potential therapeutic window for combination therapy with RK-33 and a PARP-inhibitor. In previous studies, no toxicity was observed after RK-33 used as a monotherapy or in combination with radiotherapy[11]. Future studies are needed to further evaluate the safety and efficacy of this combination regimen.

Overall, DDX3 expression levels are similar in breast cancers in *BRCA1/BRCA2* germline mutation carriers and sporadic breast cancers. BRCA1 pro- and deficient breast cancer cell lines were equally sensitive to RK-33 treatment and therefore show similar DDX3 dependency. Interestingly, DDX3 inhibition with RK-33 synergizes with PARP inhibitor treatment in breast cancer cells, especially in a BRCA1 proficient background.

Acknowledgements

We would like to thank Petra van der Groep, Yvonne Smolders and Joost Bart for selection of patients and assembling TMAs. This work was financially supported by the Utrecht

University Alexandre Suerman Stipend (MHVV), the Dutch Cancer Foundation (UU2013-5851; MHVV), the Saal van Zwanenberg foundation (MHVV), the JoKolk foundation (MHVV) and Safeway (VR).

REFERENCES

1 Hanahan D, Weinberg RA. Hallmarks of cancer: the next generation. Cell 2011; **144**: 646-674.
2 Jackson SP, Bartek J. The DNA-damage response in human biology and disease. Nature 2009; **461**: 1071-1078.
3 O'Connor MJ. Targeting the DNA Damage Response in Cancer. Molecular cell 2015; **60**: 547-560.
4 Moynahan ME, Chiu JW, Koller BH, Jasin M. Brca1 controls homology-directed DNA repair. Molecular cell 1999; **4**: 511-518.
5 Lakhani SR, Van De Vijver MJ, Jacquemier J, Anderson TJ, Osin PP, McGuffog L *et al*. The pathology of familial breast cancer: predictive value of immunohistochemical markers estrogen receptor, progesterone receptor, HER-2, and p53 in patients with mutations in BRCA1 and BRCA2. Journal of clinical oncology : official journal of the American Society of Clinical Oncology 2002; **20**: 2310-2318.
6 Bianchini G, Balko JM, Mayer IA, Sanders ME, Gianni L. Triple-negative breast cancer: challenges and opportunities of a heterogeneous disease. Nature reviews Clinical oncology 2016.
7 Tutt A, Robson M, Garber JE, Domchek SM, Audeh MW, Weitzel JN *et al*. Oral poly(ADP-ribose) polymerase inhibitor olaparib in patients with BRCA1 or BRCA2 mutations and advanced breast cancer: a proof-of-concept trial. Lancet 2010; **376**: 235-244.
8 Gelmon KA, Tischkowitz M, Mackay H, Swenerton K, Robidoux A, Tonkin K *et al*. Olaparib in patients with recurrent high-grade serous or poorly differentiated ovarian carcinoma or triple-negative breast cancer: a phase 2, multicentre, open-label, non-randomised study. The lancet oncology 2011; **12**: 852-861.
9 Linder P, Fuller-Pace FV. Looking back on the birth of DEAD-box RNA helicases. Biochimica et biophysica acta 2013; **1829**: 750-755.
10 Botlagunta M, Vesuna F, Mironchik Y, Raman A, Lisok A, Winnard P, Jr. *et al*. Oncogenic role of DDX3 in breast cancer biogenesis. Oncogene 2008; **27**: 3912-3922.
11 Bol GM, Vesuna F, Xie M, Zeng J, Aziz K, Gandhi N *et al*. Targeting DDX3 with a small molecule inhibitor for lung cancer therapy. EMBO molecular medicine 2015; **7**: 648-669.
12 Heerma van Voss MR, Vesuna F, Trumpi K, Brilliant J, Berlinicke C, de Leng W *et al*. Identification of the DEAD box RNA helicase DDX3 as a therapeutic target in colorectal cancer. Oncotarget 2015; **6**: 28312-28326.
13 Wilky BA, Kim C, McCarty G, Montgomery EA, Kammers K, DeVine LR *et al*. RNA helicase DDX3: a novel therapeutic target in Ewing sarcoma. Oncogene 2016; **35**: 2574-2583.
14 Xie M, Vesuna F, Tantravedi S, Bol GM, Heerma van Voss MR, Nugent K *et al*. RK-33 radiosensitizes prostate cancer cells by blocking the RNA helicase DDX3. Cancer research 2016: doi:10.1158/0008-5472.CAN-1116-0440.
15 Li Y, Wang H, Wang Z, Makhija S, Buchsbaum D, LoBuglio A *et al*. Inducible resistance of tumor cells to tumor necrosis factor-related apoptosis-inducing ligand receptor 2-mediated apoptosis by generation of a blockade at the death domain function. Cancer research 2006; **66**: 8520-8528.
16 Chen HH, Yu HI, Cho WC, Tarn WY. DDX3 modulates cell adhesion and motility and cancer cell metastasis via Rac1-mediated signaling pathway. Oncogene 2015; **34**: 2790-2800.
17 Bol GM, Raman V, van der Groep P, Vermeulen JF, Patel AH, van der Wall E *et al*. Expression of the RNA helicase DDX3 and the hypoxia response in breast cancer. PloS one 2013; **8**: e63548.
18 Moelans CB, de Weger RA, van Blokland MT, Ezendam C, Elshof S, Tilanus MG *et al*. HER-2/neu amplification testing in breast cancer by multiplex ligation-dependent probe amplification in comparison with immunohistochemistry and in situ hybridization. Cellular oncology : the official journal of the International Society for Cellular Oncology 2009; **31**: 1-10.
19 The Medical Research Involving Human Subjects Act [In Dutch: Wet medisch-wetenschappelijk onderzoek met mensen, WMO]. *Burgerlijk Wetboek*, 1998.
20 van Diest PJ. No consent should be needed for using leftover body material for scientific purposes. For. BMJ 2002; **325**: 648-651.
21 Angus AG, Dalrymple D, Boulant S, McGivern DR, Clayton RF, Scott MJ *et al*. Requirement of cellular DDX3 for hepatitis C virus replication is unrelated to its interaction with the viral core protein. The Journal of general virology 2010; **91**: 122-132.
22 Bryant HE, Schultz N, Thomas HD, Parker KM, Flower D, Lopez E *et al*. Specific killing of BRCA2-deficient tumours with inhibitors of poly(ADP-ribose) polymerase. Nature 2005; **434**: 913-917.
23 Boik JC, Newman RA, Boik RJ. Quantifying synergism/antagonism using nonlinear mixed-effects modeling: a simulation study. Statistics in medicine 2008; **27**: 1040-1061.
24 Chou TC, Talalay P. Quantitative analysis of dose-effect relationships: the combined effects of multiple drugs or enzyme inhibitors. Advances in enzyme regulation 1984; **22**: 27-55.
25 De Lorenzo SB, Patel AG, Hurley RM, Kaufmann SH. The Elephant and the Blind Men: Making Sense of PARP Inhibitors in Homologous Recombination Deficient Tumor Cells. Frontiers in oncology 2013; **3**: 228.
26 Huertas P. DNA resection in eukaryotes: deciding how to fix the break. Nature structural & molecular biology 2010; **17**: 11-16.
27 Patel AG, Sarkaria JN, Kaufmann SH. Nonhomologous end joining drives poly(ADP-ribose) polymerase (PARP) inhibitor lethality in homologous recombination-deficient cells. Proceedings of the National Academy of Sciences of the United States of America 2011; **108**: 3406-3411.
28 Bouwman P, Jonkers J. Molecular pathways: how can BRCA-mutated tumors become resistant to PARP inhibitors? Clinical cancer research : an official journal of the American Association for Cancer Research 2014; **20**: 540-547.
29 Ito S, Murphy CG, Doubrovina E, Jasin M, Moynahan ME. PARP Inhibitors in Clinical Use Induce Genomic Instability in Normal Human Cells. PloS one 2016; **11**: e0159341.

CHAPTER 9

Targeting RNA helicases in cancer: the translation trap

Marise R Heerma van Voss, Paul J van Diest, Venu Raman

ABSTRACT

Cancer cells are reliant on the cellular translational machinery for both global elevation of protein synthesis and the translation of specific mRNAs that promote tumor cell survival. Targeting translational control in cancer is therefore increasingly recognized as a promising therapeutic strategy. In this regard, DEAD/H box RNA helicases are a very interesting group of proteins, with several family members regulating mRNA translation in cancer cells. In this review, we delineate the mechanisms by which DEAD/H box proteins modulate oncogenic translation and how inhibition of these RNA helicases can be exploited for anti-cancer therapeutics.

INTRODUCTION

The crux of anti-cancer drug development is walking the fine line between efficacy in cancer cells and normal cell toxicity. In the current era of targeted therapy a common approach is to try to develop inhibitors for oncogenes that are driving a specific cancer, but are absent, (temporarily) redundant or compensated for in normal cells. Although this approach is logical and specific, it has the inherent problem that few driver mutations are actually targetable. In addition, in the last decade large-scale sequencing studies have shown that there are only a handful of oncogenes frequently mutated, whereas cancers are mostly driven by their own unique set of low-frequency genetic alterations[1], limiting the use of potential inhibitors to a small subset of patients. An alternative approach is not to target the genetic factors directly driving oncogenesis, but the vulnerabilities that arise as a result of stress phenotypes that allow cancers to thrive. Cancer cells are dependent on specific cellular pathways for execution of oncogenic functions and simultaneous maintenance of cellular homeostasis. Since these pathways are often shared among tumors with different genetic alterations, these so-called non-oncogene addiction factors could be the Achilles' heel of cancer and potentially provide more widely applicable targets for therapeutic development[2].

Specific stressors in cancer cells cause non-oncogene addiction to different potentially targetable cellular pathways. A well-known example is the dependence of certain cancer types on DNA damage repair pathways as a result of genomic instability[3]. Another example of non-oncogene addiction is the reliance on translation factors. Cancer cells are dependent on the translational machinery for both global elevation of protein synthesis, as well as the translation of specific mRNAs that promote tumor survival[4, 5]. The first observation indicating that regulators of mRNA translation are key facilitators of cancer cells is more than a decade old, when prominent nucleoli, reflecting increased ribosome production to meet enhanced protein synthesis demands[6], were recognized as a morphological hallmark of cancer[7]. Energetically translation is the most demanding and rate-limiting step of the gene expression process[8]. In addition, we now know that variation in protein abundance is only partially (~40%) determined by transcript abundance[9, 10], and instead was found to be predominantly controlled at the mRNA translation level[11]. It is therefore not surprising that translation is a prime target of several signaling pathways driving oncogenesis (e.g., mTORC1, MYC and MAPK signaling)[12-14]. In addition, both enhanced expression or activity of proteins involved in translation and uncoupling of translation inhibition from tumor cell stressors (e.g., hypoxia, nutrient deprivation) are commonly observed in cancer[4, 15, 16]. In the past years, we have gained a vast body of knowledge on what specific changes occur in the translational machinery in cancer cells[15, 17] and, although still in its infancy, the field of targeting translational control beholds great promise for anti-cancer drug development[5, 18-20].

DEAD/H box RNA helicases are an interesting group of proteins serving as potential translational targets in cancer. These proteins belong to superfamily 2, the largest group of eukaryotic RNA helicases, are named after a conserved amino sequence (Asp-Glu-Ala-Asp/His)[21] and have the ability to unwind and restructure RNA molecules with complex secondary structures in an ATPase dependent fashion. Unlike other helicases, DEAD/H box family members are not able to processively unwind long duplexes of more than two helical turns. However, by employing different mechanisms such as local strand separation[22], they nonetheless remodel complex RNA structures like hairpins and mRNP complexes[23-25]. They have been reported to play a pivotal role in virtually all steps of mRNA processing and translation[26]. Interestingly, cancer cells seem to rely heavily on RNA helicases to meet not only the increased general protein synthesis demand, but also for translation of specific pro-oncogenic mRNAs to enhance survival[5, 27, 28]. In this review, our main objective is to evaluate DEAD/H box RNA helicases as potential targets in cancer translation. We will focus specifically on the mechanisms by which DEAD/H box proteins modulate translation of oncogenes and how inhibition of these RNA helicases can be exploited for anti-cancer therapeutics.

ROLE OF DEAD/H BOX PROTEINS IN TRANSLATING THE CANCER GENOME

Human cells have multiple mechanisms to translate mRNAs into proteins. The most abundant translation mechanism in eukaryotes is cap-dependent translation. However, under stressed conditions, translation initiation can also occur in a cap-independent fashion, where the ribosomes are directly recruited to the start codon by binding a so-called internal ribosomal entry site (IRES). In addition, mitochondria have their own genome and independent translational machinery. In the following paragraphs we will explain how these three translational mechanisms are reliant on DEAD/H box RNA helicase activity, specifically for translating the cancer genome.

DEAD/H box RNA helicases mediate cap-dependent translation initiation of oncogenic mRNAs with a complex 5'UTR structure

In contrast to bacteria, where ribosomes are directly recruited to the initiation codon by binding the Shine-Dalgarno mRNA sequence, cap-dependent translation in eukaryotes is a more intricate process[29] (Figure 1A). The translation initation complex eIF4F recruits the 40S ribosomal unit to the 5' m^7G-cap structure of the mRNA. eIF4F consists of three subunits: (1) eIF4E binds the complex to the m^7G-cap, (2) eIF4A is a DEAD box RNA helicase that unwinds local RNA structures, and (3) eIF4G has scaffolding function and recruits the complex to mRNA through interaction with eIF3[30]. Oncogenic PI3K/Akt/mTOR signaling influences eIF4F formation in several ways. eIF4E is sequestered from the eIF4F complex by eIF4E binding proteins (4E-BPs). mTOR signaling results in 4E-BP

phosphorylation and inactivation, hereby liberating eIF4E[31]. In addition, it stimulates its downstream target S6K1, which phosphorylates and hereby causes degradation of PDCD4, an inhibitor of eIF4A[31]. A complex of translation initiation factors, among which eIF4F, eIF3, the initiator tRNA (Met- tRNA) and the 40S ribosomal unit together form the 43S ribosomal pre-initiation complex, which starts scanning the mRNA sequence in a 5' to 3' direction until it encounters the start codon. After base pairing of the Met-tRNA and the start codon, the 48S ribosomal complex is formed. Subsequently the 60S ribosomal unit gets recruited and after release of the initiation factors, the 48S and 60S complexes together form the mature 80S ribosomal complex that is competent for translation elongation[32]. Secondary structures, high GC content and bound proteins in the 5'UTR area impede ribosomal scanning for initiation sites and binding of the translation initiation machinery[33, 34]. Several DEAD/H box proteins facilitate translation initiation in the presence of a complex 5'UTR, which can be resolved by their helicase activity[29, 35]. Interestingly, among the proteins that have mRNAs with structured or long 5'UTRs, are many regulatory proteins involved in growth, proliferation and apoptosis[36-38]. Several oncogenes therefore require RNA helicase activity to be expressed to their fullest extent.

eIF4A and DHX29 are general unwinders of moderately complex 5'UTR

The most extensive evidence for requirement of RNA helicase activity for complex 5'UTR unwinding exists in the case of elongation initiation factor 4A (eIF4A). There are three human eIF4A isoforms that are encoded by separate genes. eIF4AI (DDX2A) and eIF4AII (DDX2B) have a 91% sequence identity[39] and although some differences with regard to their function in translation have been reported[40], most studies do not differentiate between the two. We will refer to both isoforms by eIF4A, unless one isoform is specifically indicated. eIF4III (DDX48) has distinct functions as a translational repressor[41]. eIF4A is the prototype DEAD box RNA helicase consisting only of a helicase core, while lacking the prominent N- and C-terminal domain present in most other family members. The activity of eIF4A is highest when it is incorporated into the eIF4F complex and is stimulated by its interacting partners eIF4B and eIF4H. For a more detailed description of the interactions between several RNA helicases and other translation initiation factors we refer to an excellent recent review[23]. Although general translation initiation is impaired after eIF4A inhibition[23, 42], the requirement for eIF4A for translation initiation was found to be directly proportion to the complexity of the mRNA 5'UTR region[43] (Figure 1B). Polysome profiling and ribosome footprinting experiments confirmed that the eIF4AI dependent translatome is enriched for mRNAs with a complex 5'UTR[44], in particular those characterized by long length, GGC repeats and the presence of G-quadruplexes[45, 46] (Figure 1B). Among the genes reliant on eIF4AI for efficient translation is a long list of oncogenes (e.g. MYC, NOTCH1, MYB, CDK6, MDM2, CCND3, BCL2, ETS1, ADAM10, LEF1, CARD11, BCL10, MALT1, ARF6, CCND1, ROCK1, MUC1-C)[45, 47-49].

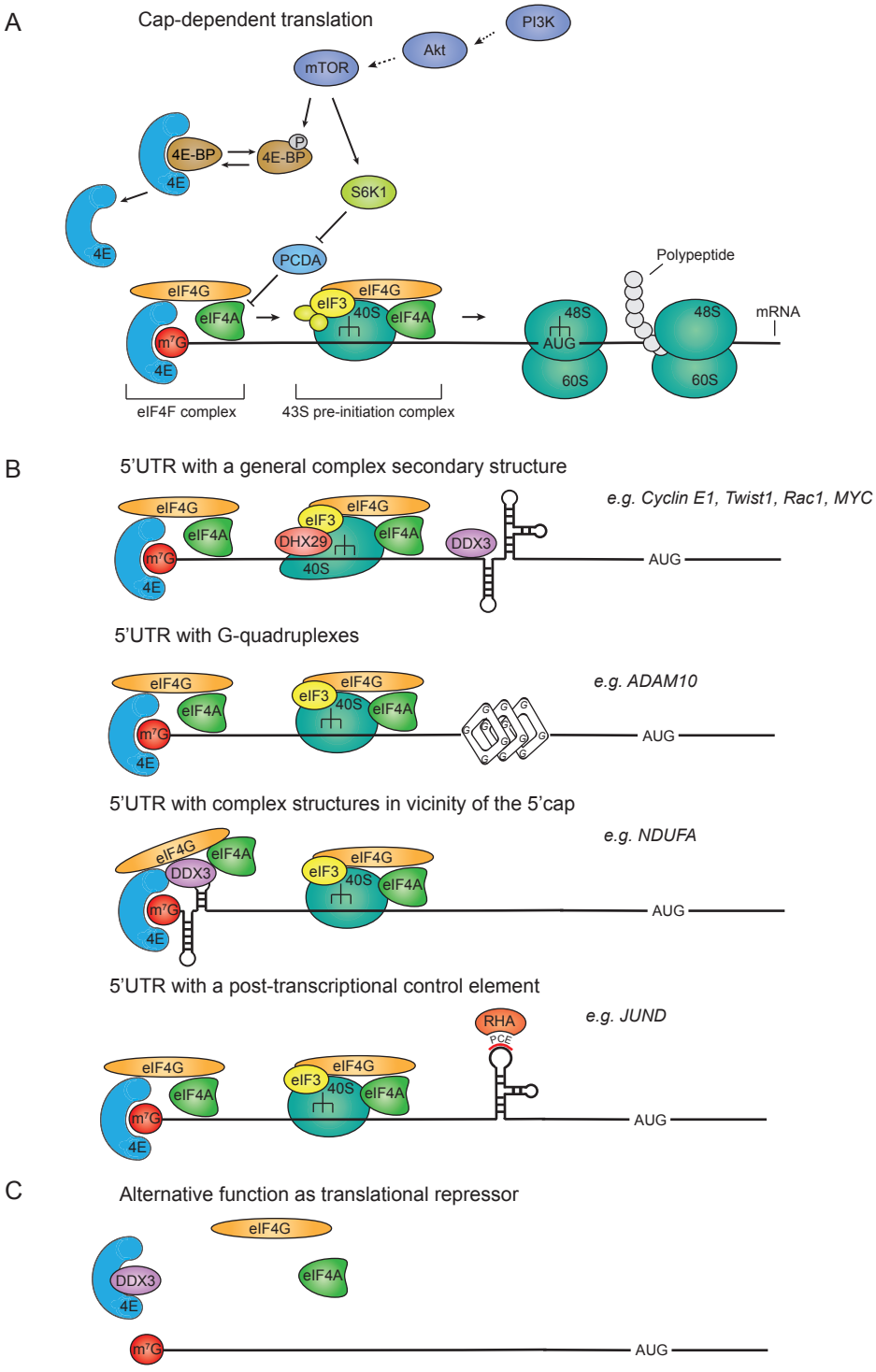
A
Cap-dependent translation
PI3K
Akt
mTOR
4E-BP
P
4E-BP
4E
S6K1
PCDA
Polypeptide
eIF4G
eIF4A
eIF3
40S
m7G
48S
AUG
60S
mRNA
eIF4F complex
43S pre-initiation complex
B
5'UTR with a general complex secondary structure
e.g. Cyclin E1, Twist1, Rac1, MYC
DHX29
DDX3
5'UTR with G-quadruplexes
e.g. ADAM10
5'UTR with complex structures in vicinity of the 5'cap
e.g. NDUFA
5'UTR with a post-transcriptional control element
e.g. JUND
RHA
PCE
C
Alternative function as translational repressor

Another DEAD/H box family member involved in translation initiation in general and especially of mRNAs with a complex 5'UTR is DHX29. Unlike DEAD box proteins, DEAH proteins lack the Q-motif that is responsible for binding specifically to adenosine and have the ability to hydrolyze several NTPs[26]. In addition, DEAH proteins seem to have more RNP remodeling than continuous RNA unwinding activity[50]. It is therefore not surprising that, unlike eIF4A, DHX29 does not seem to directly unwind secondary mRNA structures, but instead most likely modifies the 40S ribosomal unit to facilitate mRNA entry[51] and enhance its processing activity[52] (Figure 1B). Thus, DHX29 ensures correct mRNA position in the 43S ribosome and stimulates assembly of the 80S ribosomal complex[53], especially on mRNAs with a complex 5'UTR.

A specific role for DDX3 in unwinding very long and complex 5'UTRs in close vicinity to the 5' cap structure?

Although eIF4A has the ability to resolve most 5'UTR regions with secondary RNA structures, it has also been reported that very long 5'UTRs with multiple stem loops are resistant to eIF4A and that additional RNA helicases are needed to support cap-dependent translation[29]. Ded1, the yeast homologue of DDX3, was found to have more potent unwinding activity[54, 55]. Whether DDX3, like Ded1, is essential for general translation initiation in human cells is an ongoing investigation[56-58], with most studies inferring that DDX3 inhibition does not result in major changes in general protein synthesis[51, 59-61].

◀ **Figure 1.** DEAD/H box RNA helicases mediate cap-dependent translation initiation of oncogenic mRNAs with a complex 5'UTR structure.
A. Schematic representation of cap-dependent translation. The three subunits of the eIF4F translation initiation complex recruit the 40S ribosomal unit to the 5' m7G-cap mRNA structure and together with several initiation factors and the initiator tRNA form the 43S pre-initiation complex, which scans the 5'UTR until it encounters the AUG start codon. Subsequently, the 60S ribosomal unit is recruited and together with the now 48S small subunit forms the mature 80S ribosomal complex that is competent for translation elongation. Cap-dependent translation is stimulated by oncogenic PI3K/Akt/mTOR signaling through phosphorylation and hereby inactivation of eIF4E-binding protein (4E-BP), which sequesters eIF4E from eIF4F, and via activation of S6K1, which inactivates PCDA, an eIF4A inhibitor. B. Schematic representations of how RNA helicases facilitate cap-dependent translation of mRNAs with a complex 5'UTR region. eIF4A (DDX2) unwinds secondary structures in the 5'UTR and is essential for translation of mRNAs with G-quadruplexes[44, 45]. DHX29 modifies the 40S ribosomal subunit and hereby enhances its processing activity[52]. DDX3 was found to facilitate both translation of general complex secondary structures[61, 62], as well as mRNAs with secondary structure in immediate vicinity to their m7GTP cap[59]. RHA (DHX9) promotes translation of mRNAs with a specific RNA sequence containing two stemloop structures known as the post-transcriptional control element (PCE) in their 5' UTR[86, 87]. C. Alternative roles for DDX3 as a translational repressor through binding and sequestration of eIF4E have also been reported[56].

However, there is evidence that DDX3 plays a role in translation initiation of mRNAs with specific 5' UTR features. DDX3 facilitates local strand separation to allow loading of the pre-initiation complex and is required for translation initiation of mRNAs with a long 5' UTR[61, 62] or high GC content[62] and mRNAs with complex structures (e.g. stem loops) in immediate vicinity to their m^7GTP cap, which inhibit binding of the eIF4F complex[59] (Figure 1B). DDX3 was implied to allow RNA binding of the eIF4F complex by direct interaction with eIF4G[59] and eIF4A[61]. In addition, binding with the translation initiation promoting factor eIF3 was reported[57, 58]. Contradictory reports however found DDX3 to bind and sequester eIF4E, disabling proper formation of the eIF4F initiation complex[56] (Figure 1C). In addition, it was reported that human recombinant DDX3 has no effect on 48S formation in the presence of stem loops[51] and even that DDX3 inhibits translation of a reporter with a stem loop containing 5'UTR[63]. Potential explanations for these discrepancies are differences in cell lines or reporter types used, or the fact that an inhibitory role was mainly observed after overexpression of recombinant DDX3[56, 61]. Expression of RNA helicases has been suggested to maintain a 'Goldilocks zone' like equilibrium, where too little is harmful, but very high expression can have a disturbing effect on cellular functions as well[19]. In addition, production of full length human recombinant DDX3 for *in vitro* studies has been proven problematic[64] and studies on its enzymatic function are hampered by it being a constituent of several multiprotein complexes and having a dynamic nature with multiple conformations[23]. In support of a translation initiation promoting role for DDX3, it was found to be required for translation of several oncogenes with a complex or long 5'UTR, among which are cell cycle regulators like cyclin E1[62] and Rac1[65]. The combined evidence from literature is more supportive for a stimulatory role of DDX3 on translation initiation[29], but the exact role of DDX3 on cap-dependent translation initiation remains ambiguous and deserves further investigation.

DDX3 mutations were identified in several cancer types[66], among which medulloblastomas[67-70], head and neck squamous cell carcinomas (HNSCC)[71-73], and hematological malignancies[74-79] . In medulloblastomas, 50% of the Wnt subtype and 11% of the SHH subgroup tumors have a DDX3 mutation. All mutations in medulloblastomas are non-synonymous missense mutations in the helicase core domain. The mutations were primarily thought to be gain-of-function, since a stimulatory effect on oncogenic Wnt-signaling has been reported[67]. However, more recent reports have found that the mutations have inhibitory effects on mRNA translation. Specific mutations occurring in medulloblastoma were found to result in reduced RNA unwinding activity[80], defects in RNA-stimulated ATP hydrolysis[81] and hyper-assembly of RNA stress granules, which have a general inhibitory effect on translation[82]. It was proposed that inhibition of translation potentially provides a survival advantage to medulloblastoma cells during progression. Unlike medulloblastoma, where all mutations where single nucleotide variations, deleterious frameshift mutations were detected in HNSCC[71-73] and cancers of hematological origin[74-79].

Whether the functionality of these mutations is similar to those occurring in medulloblastoma remains to be evaluated. Genetic alterations in *DDX3X* are in stark contrast with the reports on overexpression of DDX3 in several cancers as compared to the normal tissue of origin[83]. High DDX3 expression correlated with high grade and worse overall survival in breast (chapter 2) and lung cancer[84]. DDX3 mutations were not frequently detected in genome wide mutation analyses in these cancer types. It is unclear why some cancers appear to benefit from low DDX3 activity, whereas others benefit from high DDX3 expression levels.

RNA helicase A and YTHDC2 facilitate translation by binding specific RNA sequences

Another example of a DEAD/H box family member that is not involved in general translation, but has a role in translation of specific mRNAs with a complex 5'UTR is the DEAH box protein, RNA Helicase A (RHA/DHX9). RHA was found to promote translation initiation of retroviral RNAs by interaction of its N-terminal double strand RNA binding motives (dsRBD)[85] with a specific RNA sequence containing two stemloop structures known as the post-transcriptional control element (PCE) in their 5' UTR[86, 87] (Figure 1B). Interestingly there are also mammalian mRNAs with 5'UTR containing a similar sequence, among which is the oncogene *JUND*[86].

YTHDC2 is another DEAH box RNA helicase with a conserved domain binding specific RNA sequences. The YTH domain binds to N6 methylated adenosines (m^6A)[88], a post-transcriptional RNA modification enriched in stop codons and the 3'UTR[89], which has been associated with modulation of translation efficiency through recruitment of translation initiation factors[90]. However, YTHDC2 has recently also been associated with translation initiation in the presence of a complex 5'UTR. Knockdown of YTHDC2 resulted in accumulation of several mRNAs in the 40S ribosomal fraction, indicating translation was stalled at the initiation phase. Overall this group of mRNAs was not characterized by long or complex mRNAs. However, reporter assays indicated YTHDC2 was required for translation of the proto-oncogenes *TWIST1* and *HIF1α* that both do have long a particularly long and structured 5'UTR[91]. Further studies are required to better characterize the YTHDC2 and RHA translatome.

It is interesting to note that some DEAD/H box family members are also involved in repression of mRNA translation through interaction with the 3'UTR. YBX1 and eIF4E recruit the general translation repressor DDX6 (RCK/p54) to the 3'UTR of mRNAs involved with self-renewal (e.g. CDK1, EZH2) and destabilizes them in a miRNA dependent manner[92]. DDX6 also interacts with A-rich elements (ARE) in the 3'UTR to negatively regulate translation[93]. Although interesting, negative regulation of translation by RNA helicases through miRNA involvement is beyond the scope of this review.

Specific DEAD/H box proteins are required for IRES-dependent translation due to oncogenic stress

Cellular stress conditions, like growth arrest, nutrient starvation, hypoxia, DNA damage, mitosis and apoptosis, occur frequently in cancer cells. In response to these stressors, cap-dependent translation is downregulated in order to preserve nutrients and energy[94, 95]. Many genes that are upregulated by cells to cope with stress conditions are translated in an IRES dependent fashion[96], which does not require a 5' cap structure, the cap-binding protein eIF4E or a free 5' end. Cellular IRES often have a strong secondary structure[97, 98] that recruits the 40S ribosomes to the translation initiation site, either by binding directly to the ribosome or indirectly by binding canonical translation initiation factors like eIF3 and eIF4G or specific IRES transacting factors (ITAFs)[52, 96](Figure 2). Because tumor cells are dependent on factors to maintain cellular homeostasis and survive under stressed conditions[99], IRES mediated translation has been put forward as a therapeutic target in cancer[100, 101].

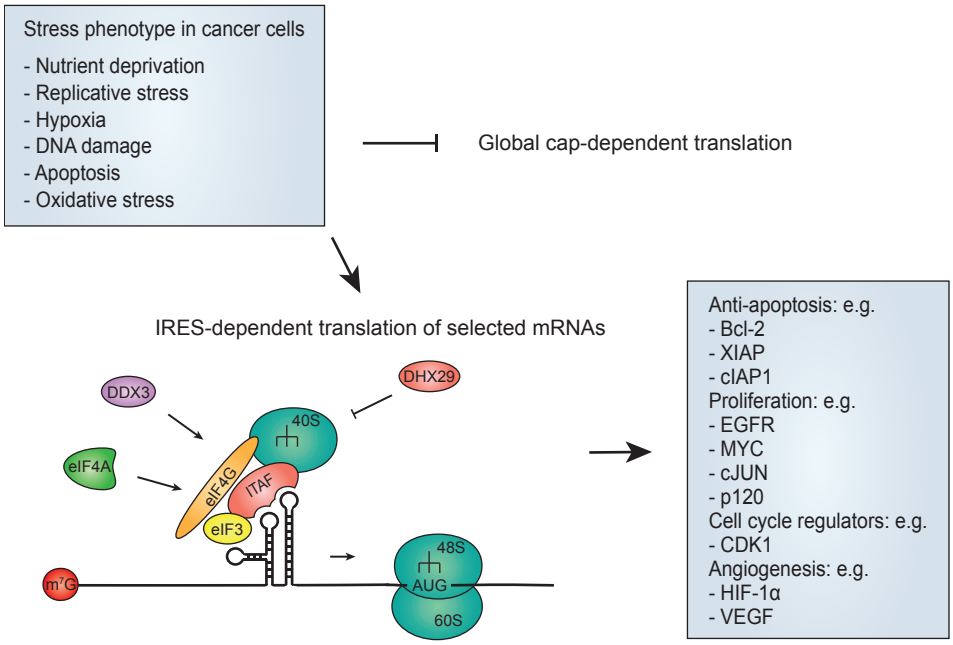

Figure 2. Specific DEAD/H box proteins are required for IRES-dependent translation due to oncogenic stress
Schematic representation of how cellular stress conditions that occur frequently in cancer cells inhibit global cap-dependent translation and activate IRES-dependent of selected mRNAs. 40S ribosomes are recruited to the secondary structure of the IRES, either directly or by binding canonical translation initiation factors like eIF3 and eIF4G or specific IRES transacting factors (ITAFs)[52, 96]. Both eIF4A and DDX3 facilitate IRES dependent translation of specific mRNAs[55, 57, 107, 108, 116], whereas the conformational changes imposed by DHX29 on the 40S ribosome, impede ribosomal binding to certain IRES[52].

Among the IRES mediated proteins are anti-apoptotic proteins like BCL-2[102], c-IAP1[103] and XIAP[95, 104], growth promoting proteins like MYC [105-107], EGFR[108], c-jun[109] and p120[110], cell cycle regulators CDK1[111] and regulators of angiogenesis like HIF-1A[112] and VEGF[113].
However, several IRES mediated transcripts have opposing functions and not all promote oncogenesis (e.g., p53[114]). In addition, not all cellular mRNA's that contain IRES elements function as such, and there is need for proper functional validation[5, 99].
Different IRES require different auxiliary translation initiation factors to facilitate ribosomal recruitment and translation onset[23, 42, 115]. DEAD/H box family members have been found to facilitate IRES dependent translation of certain oncogenic mRNAs. Inhibition of eIF4A was found to block IRES dependent translation of EGFR[108] and c-MYC[107, 116] under hypoxia and IRES dependent translation of the transcription factor LEF1[117] (Figure 2). DDX3 was found to have a stimulatory role on translation of the Hepatitis C Virus IRES[56, 58], potentially through its interaction with eIF4E, which is reported to function as a switch between cap-dependent and independent translation[118]. However, it remains to be seen whether DDX3 also mediates IRES dependent translation of cellular mRNAs.
Not all effects of DEAD/H box family members on IRES dependent translation are stimulatory or pro-oncogenic. The conformational changes imposed by DHX29 on the 40S ribosome, impede ribosomal binding to certain IRES[52]. In addition, DHX9 (RHA) mediates IRES dependent translation of p53 under genotoxic stress[119] and through this mechanism has more of a tumor suppressive role. Furthermore, DDX6 reduces IRES translation of VEGF in hypoxic cells[120].

Involvement of RNA helicases in mitochondrial translation

Mitochondria function as the ATP-generators of eukaryotic cells and most likely are derived from an incorporated bacterial ancestor. Although most of its genes have been transferred to the nuclear genome, mitochondria still have their own circular genome encoding 13 proteins, 2 rRNAs and 22 tRNAs[121]. These 13 genes all translate into subunits of four out of the five oxidative phosphorylation (OXPHOS) complexes (Figure 3). The remainder of the proteins in these complexes is encoded on the nuclear genome, translated in the cytoplasm and imported into the mitochondria. Together the OXPHOS complexes are responsible for generating an H^+-gradient over the mitochondrial inner membrane that fuels ATP-synthase (complex V). Mitochondria have maintained their own (nuclear encoded) transcriptional and translational machinery, which is uniquely different from general protein synthesis in both eukaryotes and bacteria. Excellent reviews that explain what is known about mitochondrial translation are already published[122, 123]. Briefly, the mitochondrial genome yields two poly-cistronic mtDNA transcripts that get cleaved into 9 mono-cistronic and 2 bi-cistronic mt-mRNAs. Mammalian mt-mRNAs lack a significant 5'UTR[124] (Figure 3). The mitoribosome consists out of a 28S small subunit and a 39S large subunit, which with the help of the mitochondrial initiation factors mtIF2 and mtIF3 bind

directly to the start codon of the mt-mRNA, hereby initiating translation[125]. The large subunit is anchored to the inner mitochondrial membrane and is believed to facilitate incorporation of the newly synthesized OXPHOS proteins[122].

Cancer metabolism is an area of renewed attention[126, 127]. One of the best known metabolic alterations in cancer cells is the upregulation of glycolysis in the presence of oxygen, the so-called Warburg effect. This aerobic glycolysis phenomenon is often erroneously interpreted as a sign of impaired OXPHOS in cancer. In fact, increasing evidence indicates that cancer cells are reliant on mitochondria for their bioenergetic machinery and macromolecule synthesis function[127-129], especially when encountering cellular stressors, like chemotherapy[127, 130], radiation therapy[131] or during metastasis[132].

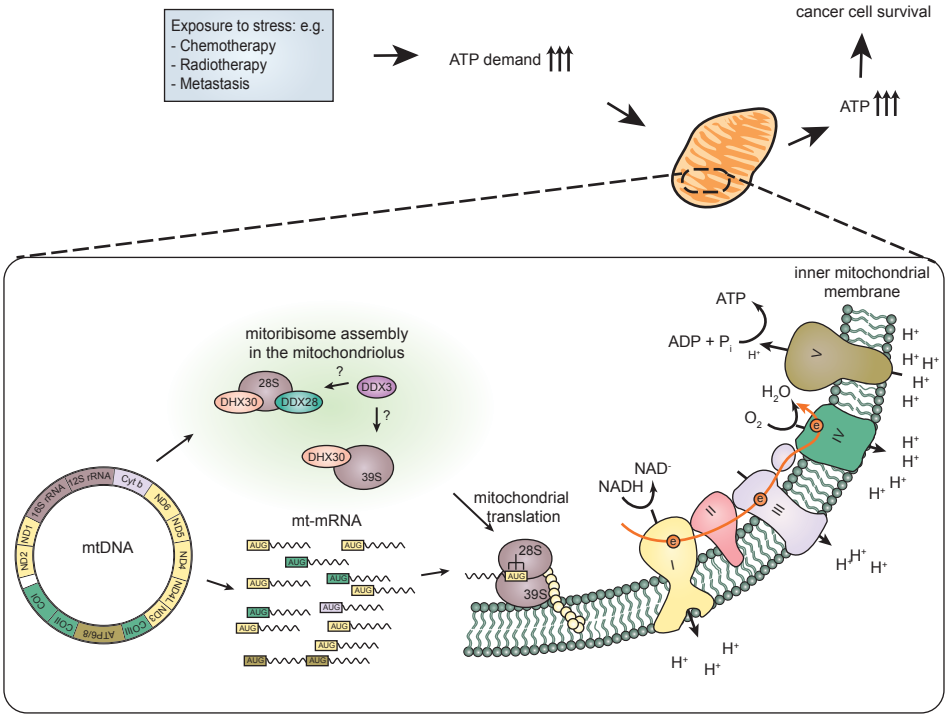

Figure 3. The involvement of RNA helicases in mitochondrial translation promotes cancer through synthesis of OXPHOS proteins

Schematic representation of how exposure to stressors in the cancer cell environment (e.g., radiotherapy) can cause a sudden increase in the need for ATP, which is met by mitochondrial upregulation of oxidative phosphorylation, hereby supporting cancer cell survival. Oxidative phosphorylation (OXPHOS) occurs on the inner mitochondrial membrane. Complexes I-IV of the electron transport chain create a H+-gradient that fuels ATP-synthase (complex V), which converts ADP into ATP. The mitochondrial genome (mtDNA) contains genes encoding 13 proteins that are all part of OXPHOS complexes. Mitochondrial mRNAs (mt-mRNA) are translated by the mitochondrial translation complex called the mitoribosome. Assembly of the 28S small and 39S large mitoribosome subunits occurs in a distinct mitochondrial area called the mitochondriolus[134], and is facilitated by DDX28[134], DHX30[135] and possibly DDX3 (chapter 2).

It is therefore not surprising that mitochondrial respiration is being recognized as viable target for cancer therapy[128]. Given the involvement of mitochondrial translation products in OXPHOS, targeting mitochondrial translation is an approach to selectively inhibit mitochondrial translation functions and has been identified as a therapeutic target in the treatment of acute myeloid leukemia[133].

Although mt-mRNA seems to lack a complex 5'UTR in need of unwinding, there is evidence for the (indirect) involvement of DEAD/H box RNA helicases in mitochondrial translation. The RNA helicases DDX28[134] and DHX30[135] facilitate mitoribosome assembly in the an area that serves as the mitochondrial equivalent of the nucleolus, called mitochondriolus[134] or processing body[136] (Figure 3). DDX28 interacts mainly with the 16S rRNA and large mitoribosomal unit, and DHX30 was identified in all mitoribosomal fractions[135]. The mitoribosome assembly process has only recently started being uncovered, and it is likely that other RNA helicases are involved in this process as well[137]. Interestingly, DDX3, DDX5 and RHA were detected by mass spectrometry in the immunoprecipitate of mitochondriolus' proteins GRSF1 and DDX28 after crosslinking[134, 135]. DDX3 does localize to the mitochondria[138] (chapter 2) and inhibition of DDX3 with the small molecule inhibitor RK-33 resulted in decreased mitochondrial translation, and hereby decreased synthesis of OXPHOS complexes. As a result, decreased OXPHOS capacity and increased ROS production were observed, culminating in bioenergetic catastrophe in cancer cells (chapter 2). Future studies are needed to further evaluate the specific role of DDX3 in mitochondrial translation facilitation.

DEAD/H box RNA helicases mediate oncogenesis through other cellular processes

DEAD/H box RNA helicase family members are involved in almost all steps of RNA metabolism and our knowledge of their involvement in oncogenesis remains growing. How RNA helicases mediate oncogenesis by other means than regulating translation lies beyond the scope of this review. However, it is worth mentioning that RNA helicases have additional roles in cancer biology through regulation of transcription and alternative splicing (e.g., DDX5, DDX17, RHA and DDX53), ribosomal biogenesis (e.g., DDX5, DDX21, DDX43 and DHX33), mRNA export (e.g., DDX5, DDX3), miRNA regulation (e.g., DDX3, DDX5, DDX6, DDX17, DDX23) and apoptosis (e.g., DDX3, RHA), among other processes. For a more elaborate and systematic overview of the additional roles of DEAD/H box RNA helicases in cancer, we refer to several more general recent reviews [27, 28, 139].

TARGETING ONCOGENIC TRANSLATION WITH DEAD/H BOX RNA HELICASE INHIBITORS

Development of eIF4A inhibitors

Knockdown experiments of eIF4A reduced proliferation and induced cell death in cancer cell lines[40, 140, 141]. In addition, in murine models overexpression of eIF4A accelerated leukemia development[45] and overexpression of PDCD4, an eIF4A inhibitor, reduced malignant epidermal progression[142]. Several eIF4A inhibitors are currently under development and are thought to exert their effect by translational inhibition of key oncogenes (e.g., *c-MYC*)[44, 45, 49, 141] (Table 1).

The polyoxugenated steroid Hippurastinol was isolated from the coral *Isis hippuris* and identified in a screen to inhibit protein synthesis[143]. Hippurastinol binds to the c-terminal domain of eIF4A[144] and was found to specifically inhibit its ATPase, helicase and mRNA binding activity[42], by keeping eIF4A in a closed confirmation[145] (Figure 4). Translation initiation could be rescued with recombinant eIF4A after Hippuristanol treatment, showing that Hippuristanol specifically mediates it effect through eIF4A inhibition[42]. mRNAs with a long or complex 5'UTR are most affected by Hippurastinol treatment[146].

The natural product Pateamine A (PatA) was derived from the marine sponge *Mycale sp.* and stimulates RNA binding activity of free eIF4A ($eIF4A_F$)[147]. Inhibition of $eIF4A_F$ was found to inhibit cap-dependent translation, most likely by a conformational change increasing the RNA affinity[148], hereby sequestering it and perturbing the interactions of $eIF4A_F$ with other translation initiation factors[149] (Figure 4). Surprisingly, PatA also increases the Helicase and ATPase activity of eIF4A[150, 151]. Both PatA and the PatA analogue des-methyl des-amino Pateamine A (DMDA-PatA) affect DNA and RNA synthesis, as well[150, 152] and PatA does not inhibit eIF4A incorporated in eIF4F ($eIF4A_c$), which has about 20-fold higher enzymatic activity[147]. Second generation DMDA-PatA derivatives are currently under development[153], however whether PatA analogues are directly exerting their working mechanism through eIF4A inhibition requires further evaluation.

Derivatives of the *Aglaia foveolata* plant (rocaglates/flavaglines), which are characterized by a common cyclopenta[b]benzofuran skeleton, were also found to inhibit protein synthesis through increasing the mRNA affinity of eIF4A[143], but unlike PatA affect both $eIF4A_f$ and $eIF4_C$[49, 154]. The specificity of Rocaglates for inhibition of eIF4AI was confirmed by genetic complementation and crispr/cas9 gene editing, using an eIF4A mutant with impaired rocaglate binding, while retaining its functionality[155]. Silvestrol, one of the most studied rocaglates, reduces translation initiation, especially of mRNAs with a complex 5'UTR[45 47] , and was originally thought to sequester eIF4A from the eIF4F complex by its increased RNA affinity[49, 154]. However, the sensitivity of translation of specific mRNAs to Silvestrol could only partially be explained by complex features in the 5'UTR[44], and a recent study by Iwasaki *et al.* indicated that in contrast to Hippurastinol, a complex 5'UTR was

Table 1. Inhibitors currently under development for RNA helicases involved in regulation of translation

Target	Compound	Mechanism	Developmental status	Results
eIF4A	Hippurastinol	Inhibits eIF4A RNA binding and helicase activity	Preclinical animal studies	Anticancer activity in several hematological cancer mouse models[161, 162, 171]
eIF4A	(DMDA)Pateamine A	Increase RNA binding affinity of $eIF4A_F$	Preclinical animal studies	Potent anticancer activity in multiple human cancer xenograft models[152] and activity against cachexia-induced muscle wasting in mice[168]
eIF4A	Rocaglates/ Flavaglines (Silvestrol, episilvestrol, FL-3, Rocaglamide, CR-1-31-B, (-)-SDS-/-021)	Increase RNA binding affinity of eIF4A	Preclinical animal studies	Potent anticancer activity in mouse models of both solid and hematoligical malignancies[45, 49, 154, 157, 163-166, 169, 170]
eIF4A	RNA aptamers against eIF4A	Inhibit ATP hydrolysis activity of eIF4A	Tissue Culture	anti-cancer activity not tested[160]
DDX3	REN analogs (NZ51)	Target ATP-binding domain of DDX3	Tissue Culture	reduces cancer cell viability and motility[176]
DDX3	RK-33 ($PLGA^{210}$-RK-33)	Targets ATP-binding domain of DDX3	Preclinical animal studies	Causes radiosensitization in several mouse models[84, 177] and has single agent activity in a Ewing Sarcoma mouse model[188]
DDX3	NSC305787	Inhibitor of the DDX3-Ezrin interaction	Tissue Culture	anti-cancer activity not tested[63]
DDX3	Ketorolac salt (ZINC00011012)	Targets ATP-binding domain of DDX3	Preclinical animal studies	anticancer activity in a mouse oral squamous cell carcinoma model[189]
DDX3	Rhodanine and Triazine derivatives	Target DDX3 ATP-binding domain	Tissue Culture	In vitro anti-viral activity, anti-cancer efficacy not tested[190, 191]
DDX3	16d	Inhibitor of RNA helicase activity	Tissue Culture	in vitro anti-viral activity, anti-cancer efficacy not tested[192]
RHA	YK-4-279	Inhibitor of the EWS-FLI interaction with RHA	Preclinical animal studies	Efficacy in several murine Ewing sarcoma models[194-196]

only a minor determinant of Rocaglamide A (RocA) efficacy. Instead they found RocA to clamp eIF4A on mRNAs that have short polypurine sequences in their 5'UTR, hereby putting up a roadblock for ribosomal scanning[146] (Figure 4). Unfortunately, RocA was not compared directly to Silvestrol in this study, and it remains to be determined whether the specificity for polypurine mRNA sequences is a feature of all rocaglates. Silvestrol was found to have suboptimal pharmacokinetic properties and to be sensitive to P-glycoprotein

multidrug resistance transporters[156]. Synthetic rocaglates with potent *in vivo* activity and reduced sensitivity to multidrug resistance were developed, of which FL-3[157, 158], CR-1-31-B[48] and (-)-SDS-/-021[159] are promising candidates. In addition to natural products, RNA aptamers selectively binding eIF4A and interfering with cap-dependent translation by inhibiting its ATPase activity have also been developed[160].

Efficacy of eIF4A inhibitors in preclinical studies

Single agent activity has been identified in human xenograft models of hematological and solid malignancies for Hippurastinol[161, 162], DMDA-PatA[152] and several rocaglates[163-165], such as Silvestrol[45, 49, 166, 167] and FL-3[157]. Interestingly DMDA-PatA was found to have a potential role in prevention of cachexia as well[168]. eIF4A inhibitors are also promising candidates for combination regimens. For instance, resistance to the BRAF-V600E inhibitor vemurafenib is mediated through upregulation of the MAPK and PI3K/AKT/mTOR signaling pathways, both of which induce translation initiation through eIF4F. Vemurafenib resistant melanoma cells had increased eIF4F formation. In line with these observations, the Silvestrol analogues CR-1-31-B and FL-3 synergize with vemurafenib in melanoma xenografts[157]. In addition, Silvestrol was found to synergize with Doxorubicin[154], Daunarubicin[169], rapamycin[170] and Dexamethason[141]. In a similar way, Hippurastinol overcomes resistance in PI3K/Akt/mTOR driven tumors and synergizes with the Bcl-2 family inhibitor ABT-373[171]. Overexpression of eIF4F was also found to mediate resistance against tyrosine kinase inhibitors of the human epidermal growth factor receptor (HER) family[172].

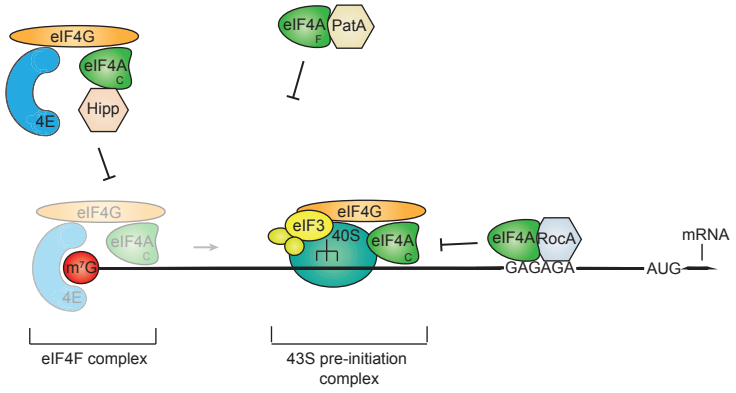

Figure 4. Working mechanism of eIF4A inhibitors
Schematic representation of how eIF4A inhibitors affect cap-dependent translation of mRNAs with specific 5'UTR features. Hippurastinol (Hipp) binds to the c-terminal domain of eIF4A144 and was found to specifically inhibit its ATPase, helicase and mRNA binding activity[42]. Pateamine A (PatA) stimulates RNA binding activity of free eIF4A (eIF4AF)[147], most likely hereby sequestering it and perturbing the interactions with other translation initiation factors[149]. Of the family of Rocaglates, Rocaglamide A (RocA) clamps eIF4A on mRNAs that have short polypurine sequences in their 5'UTR, hereby putting up a roadblock for ribosomal scanning[146]. Silvestrol, one of the most studied rocaglates is thought to sequester eIF4A from the eIF4F complex by its increased RNA affinity[49, 154], whether it also has a polypurine specificity remains to be determined.

The effect of DDX3 knockdown on oncogenic properties of cancer cells

DDX3 was found to have anti-apoptotic properties[173, 174] and knockdown reduces *in vitro* cancer cell proliferation[84, 175-177], cell cycle progression[84, 175], invasion[178], motility[65, 179] and survival under stressed conditions[180]. In addition, DDX3 knockdown resulted in reduced outgrowth and metastases in human xenograft models[173, 175]. However, similar to the controversy that exists on the role of DDX3 in translation initiation, there are also contradictory reports that argue that DDX3 has a tumor suppressing role. The group of YH Lee found that DDX3 reduces cell cycle progression via the p53-DDX3-p21 axis[181 182-184]. A potential explanation for the opposite roles of DDX3 described by this group is the fact that they mainly use DDX3 overexpression models, which can be problematic as explained earlier, and HPV, HBV or HCV driven cancer models. DDX3 is known to play a role in the anti-viral immune response[138]. It is plausible that virally transformed cells benefit from lowering DDX3 levels, whereas cancers with different carcinogenetic backgrounds (e.g. cigarette smoke[179, 185]) are dependent on high DDX3 expression.

Development and efficacy of DDX3 inhibitors

Several DDX3 inhibitors have been developed (Table 1). Ring expanded nucleoside (REN) analogues structurally mimic adenosine nucleosides and can be rationally designed to specifically target the ATP-binding cleft of DDX3, hereby inhibiting its helicase activity[186]. NZ-51 is a REN analogue that was found to inhibit *in vitro* viability and motility of breast cancer cells, but did not show any *in vivo* activity[176]. By using the X-ray crystallographic structure of the core domains of DDX3[64], REN analogues were structurally modified into a series of tricyclic 5:7:5-fused diimidazo[4,5-d:4',5'-f][1, 3]diazepine analogues[187]. Of these, RK-33 is the lead compound and the most studied DDX3 inhibitor in the cancer field. Biotin pull down experiments showed that RK-33 specifically binds DDX3 and not the closely related DEAD box RNA helicases DDX5 and DDX17 and reduces the helicase activity of the Ded1p, the yeast homologue of DDX3[84]. Interestingly, RK-33 has potent *in vitro* radiosensitizing activity[84, 177] (chapter 2), most likely by inhibiting double strand break repair[84] via blockage of the required increase in OXPHOS by inhibiting mitochondrial translation (chapter 2). RK-33 also acted like a radiosensitizer in mouse models of lung[84] and prostate cancer[177]. In addition, single agent activity was observed against Ewing sarcoma human xenografts with high DDX3 expression[188]. No normal tissue toxicity was observed after RK-33 treatment in mice[84].

Although less studied in the cancer field, there are several other DDX3 inhibitors under development. *In silico* screening of DDX3 inhibitors led to identification of Ketorolac salt as a potential DDX3 inhibitor. Ketorolac salt inhibited ATPase activity and tumor growth in a 4-NQO induced tongue oral squamous cell carcinoma mouse model[189]. In addition, due to the role of DDX3 in viral mRNA translation, an effort has been made to develop DDX3 inhibitors for anti-viral (e.g., HCV, HIV-1, West-Nile virus and dengue virus) therapy

as well[186, 190]. Rhodanine analogues and triazine derivatives were identified from databases of commercially available compounds to bind the ATP-binding site of DDX3[190, 191]. The small molecule inhibitor 16d was recently designed to bind the RNA-binding site of DDX3. 16D inhibited helicase activity of DDX3 and showed broad spectrum anti-viral activity *in vitro*[192]. It will be interesting to see further *in vivo* evaluation of these DDX3 inhibitors as potential anti-cancer drugs.

Other DDX/DHX family members as targets for cancer therapy

Besides eIF4A and DDX3, several other DEAD box RNA helicases have been designated as potential targets for anti-cancer therapy. EWS-FLI is a fusion oncogene occurring in Ewing sarcoma. RHA was found to augment the effect of EWS-FLI in modulating oncogenesis[193] and genetic knockdown of RHA reduced cell viability in Ewing sarcoma cell lines. YK-4-279 is a small molecule inhibitor of the EWS-FLI RHA interaction and was found to inhibit tumor growth in several murine Ewing sarcoma models[194-196]. The oncogenic effect of EWS-FLI and RHA in these models seemed to be mediated through regulation of alternative splicing[197] and so far no studies indicated an effect on translation of mRNAs with a complex 5'UTR containing PCEs. A recent study shows that RHA knockdown also reduces oncogenesis in the absence of the EWS-FLI translocation, without causing normal tissue toxicity[198]. Whether this effect is mediated through regulation of translation initiation of specific target mRNAs or through other functions of RHA remains to be determined. Knockdown of DHX29 was found to reduce *in vitro* proliferation, anchorage independent growth and colony forming ability of cancer cells and resulted in outgrowth of HeLa cells in nude mice through regulation of translation initiation[53]. Furthermore, knockdown of YTHDC2, another DEAD/H box family member that functions as a translation initiation regulator, reduced proliferation and motility in liver[199] and colorectal cancer cell lines[91] and reduced liver metastases after splenic injection of colorectal cancer cells[91]. Both DHX29 and YTHDC2 are potential candidates for targeting oncogenic translation as a therapeutic strategy.

Therapeutic window of DEAD/H box protein inhibitors

Since translation is a process occurring not only in fast proliferating cancer cells, but also in normal tissues, there are concerns about normal cell toxicity of translation inhibitors. The question is whether the dependence of cancer cells on translation initiation of oncogenic mRNAs is large enough to facilitate a therapeutic window. None of the DEAD/H box inhibitors currently under development have reached the stage of clinical assessment of toxicity in a human phase I trial. However, preclinical studies indicated that rocaglate inhibitors of eIF4A, like Silvestrol[49] and the DDX3 inhibitor RK-33[84] do not cause toxicity in mice at effective dose levels. Interestingly, inhibition of eIF4A with rocaglates has even been reported to have a chemoprotective role in normal cells, while simultaneously blocking

proliferation in cancer cells[200-202]. In addition, there are other inhibitors of translation initiation that have been clinically evaluated. Haploinsufficiency of eIF4E, and therefore the eIF4F complex, did not affect normal development, but did impair cellular transformation, indicating a differential requirement for eIF4E in normal and cancer cells[203]. Phase 1 trials with antisense oligo of eIF4E (4E-ASOs) found few adverse effects, but unfortunately also no significant anti-tumor response with single agent treatment[204]. Phase II trials with the combination of 4E-ASOs and chemotherapeutics are currently ongoing [NCT1234038; NCT0124025]. Furthermore, several drugs currently used in clinic were found to inhibit translation initiation. The anti-viral guanosine analogue ribavirin was found to inhibit eIF4E binding to the 7-methyl guanosine 5'UTR mRNA cap[205] and for this reason has been clinically evaluated as a potential treatment for acute myeloid leukemia[206]. In addition, PI3K/Akt/mTOR signaling is an upstream regulator of translation initiation[207] and mTOR inhibitors result in reduced translation of oncogenic mRNAs[208]. These examples show proof of principle that translation inhibitors can be used to selectively target cancer cells, without unacceptable normal cell toxicity. However, clinical trials in humans will need to determine whether there is a sufficient therapeutic window for the use of specific DEAD/H box inhibitors as anti-cancer drugs.

Biomarkers

Biomarkers can be of great aid to the development of new therapeutics. Markers associated with sensitivity can help selecting those patients that benefit most from a drug. Immunohistochemical assessment of DDX3 protein expression has been suggested to facilitate patient selection for DDX3 inhibitor treatment[84] (chapter 2). However, DDX3 expression did not correlate with DDX3 dependence in all cancer types[175] and further characterization of the factors predicting response to RK-33 and other DEAD/H box RNA helicase inhibitors is needed. Another type of biomarker is a marker that gives a measurement of *in vivo* target inhibition after drug administration. These so-called target engagement biomarkers[209] are particularly useful in the absence of a significant response in clinical trials, where they can differentiate between lack of inhibition of the target, due to potency or delivery issues, and lack of efficacy even though the drug target is sufficiently inhibited. Identification of target engagement markers is especially important for the inhibition of non-oncogene addiction genes, like DEAD/H box RNA helicases, since it remains to be determined in clinical trials whether there is a sufficiently large therapeutic window for them to be suitable targets for cancer therapy.

Concluding remarks

Overall there is strong evidence for the non-oncogene addiction of cancer cells to DEAD/H box RNA helicases due to their role in facilitation of translation initiation of mRNAs with specific 5'UTR features. DEAD/H box dependent translation facilitates both primary

oncogenic signaling and resistance to several therapies. However, more research is needed to further define the role in both translation initiation and oncogenesis of DDX3 and other RNA helicases. Efficacy has been shown for both eIF4A and DDX3 inhibitors in pre-clinical models, especially as an adjuvans to chemo- or radiotherapy, warranting the evaluation of this novel class of drugs in clinical trials.

REFERENCES

1 Kandoth C, McLellan MD, Vandin F, Ye K, Niu B, Lu C et al. Mutational landscape and significance across 12 major cancer types. Nature 2013; 502: 333-339.

2 Luo J, Solimini NL, Elledge SJ. Principles of cancer therapy: oncogene and non-oncogene addiction. Cell 2009; 136: 823-837.

3 Bryant HE, Schultz N, Thomas HD, Parker KM, Flower D, Lopez E et al. Specific killing of BRCA2-deficient tumours with inhibitors of poly(ADP-ribose) polymerase. Nature 2005; 434: 913-917.

4 Silvera D, Formenti SC, Schneider RJ. Translational control in cancer. Nature reviews Cancer 2010; 10: 254-266.

5 Truitt ML, Ruggero D. New frontiers in translational control of the cancer genome. Nature reviews Cancer 2016; 16: 288-304.

6 Ruggero D, Pandolfi PP. Does the ribosome translate cancer? Nature reviews Cancer 2003; 3: 179-192.

7 Derenzini M, Montanaro L, Trere D. What the nucleolus says to a tumour pathologist. Histopathology 2009; 54: 753-762.

8 Buttgereit F, Brand MD. A hierarchy of ATP-consuming processes in mammalian cells. The Biochemical journal 1995; 312 (Pt 1): 163-167.

9 Ghazalpour A, Bennett B, Petyuk VA, Orozco L, Hagopian R, Mungrue IN et al. Comparative analysis of proteome and transcriptome variation in mouse. PLoS genetics 2011; 7: e1001393.

10 Vogel C, Marcotte EM. Insights into the regulation of protein abundance from proteomic and transcriptomic analyses. Nature reviews Genetics 2012; 13: 227-232.

11 Schwanhausser B, Busse D, Li N, Dittmar G, Schuchhardt J, Wolf J et al. Global quantification of mammalian gene expression control. Nature 2011; 473: 337-342.

12 Roux PP, Topisirovic I. Regulation of mRNA translation by signaling pathways. Cold Spring Harbor perspectives in biology 2012; 4.

13 Rajasekhar VK, Viale A, Socci ND, Wiedmann M, Hu X, Holland EC. Oncogenic Ras and Akt signaling contribute to glioblastoma formation by differential recruitment of existing mRNAs to polysomes. Molecular cell 2003; 12: 889-901.

14 Barna M, Pusic A, Zollo O, Costa M, Kondrashov N, Rego E et al. Suppression of Myc oncogenic activity by ribosomal protein haploinsufficiency. Nature 2008; 456: 971-975.

15 Chu J, Cargnello M, Topisirovic I, Pelletier J. Translation Initiation Factors: Reprogramming Protein Synthesis in Cancer. Trends in cell biology 2016.

16 Leprivier G, Remke M, Rotblat B, Dubuc A, Mateo AR, Kool M et al. The eEF2 kinase confers resistance to nutrient deprivation by blocking translation elongation. Cell 2013; 153: 1064-1079.

17 Blagden SP, Willis AE. The biological and therapeutic relevance of mRNA translation in cancer. Nature reviews Clinical oncology 2011; 8: 280-291.

18 Grzmil M, Hemmings BA. Translation regulation as a therapeutic target in cancer. Cancer research 2012; 72: 3891-3900.

19 Pelletier J, Graff J, Ruggero D, Sonenberg N. Targeting the eIF4F translation initiation complex: a critical nexus for cancer development. Cancer research 2015; 75: 250-263.

20 Bhat M, Robichaud N, Hulea L, Sonenberg N, Pelletier J, Topisirovic I. Targeting the translation machinery in cancer. Nature reviews Drug discovery 2015; 14: 261-278.

21 Linder P, Lasko PF, Ashburner M, Leroy P, Nielsen PJ, Nishi K et al. Birth of the D-E-A-D box. Nature 1989; 337: 121-122.

22 Soto-Rifo R, Ohlmann T. The role of the DEAD-box RNA helicase DDX3 in mRNA metabolism. Wiley interdisciplinary reviews RNA 2013; 4: 369-385.

23 Marintchev A. Roles of helicases in translation initiation: a mechanistic view. Biochimica et biophysica acta 2013; 1829: 799-809.

24 Yang Q, Jankowsky E. The DEAD-box protein Ded1 unwinds RNA duplexes by a mode distinct from translocating helicases. Nature structural & molecular biology 2006; 13: 981-986.

25 Liu F, Putnam A, Jankowsky E. ATP hydrolysis is required for DEAD-box protein recycling but not for duplex unwinding. Proceedings of the National Academy of Sciences of the United States of America 2008; 105: 20209-20214.

26 Tanner NK, Linder P. DExD/H box RNA helicases: from generic motors to specific dissociation functions. Molecular cell 2001; 8: 251-262.

27 Robert F, Pelletier J. Perturbations of RNA helicases in cancer. Wiley interdisciplinary reviews RNA 2013; 4: 333-349.

28 Sarkar M, Ghosh MK. DEAD box RNA helicases: crucial regulators of gene expression and oncogenesis. Front Biosci (Landmark Ed) 2016; 21: 225-250.

29 Parsyan A, Svitkin Y, Shahbazian D, Gkogkas C, Lasko P, Merrick WC et al. mRNA helicases: the tacticians of translational control. Nature reviews Molecular cell biology 2011; 12: 235-245.

30 Pestova TV, Kolupaeva VG, Lomakin IB, Pilipenko EV, Shatsky IN, Agol VI et al. Molecular mechanisms of translation initiation in eukaryotes. Proceedings of the National Academy of Sciences of the United States of America 2001; 98: 7029-7036.

31 Mamane Y, Petroulakis E, LeBacquer O, Sonenberg N. mTOR, translation initiation and cancer. Oncogene 2006; 25: 6416-6422.

32 Jackson RJ, Hellen CU, Pestova TV. The mechanism of eukaryotic translation initiation and principles of its regulation. Nature reviews Molecular cell biology 2010; 11: 113-127.

33 Babendure JR, Babendure JL, Ding JH, Tsien RY. Control of mammalian translation by mRNA structure near caps. RNA 2006; 12: 851-861.

34 Pelletier J, Sonenberg N. Insertion mutagenesis to increase secondary structure within the 5' noncoding region of a eukaryotic mRNA reduces translational efficiency. Cell 1985; 40: 515-526.

35 Pestova TV, Kolupaeva VG. The roles of individual eukaryotic translation initiation factors in ribosomal scanning and initiation codon selection. Genes & development 2002; 16: 2906-2922.

36 Kozak M. An analysis of 5'-noncoding sequences from 699 vertebrate messenger RNAs. Nucleic acids research 1987; 15: 8125-8148.

37 Patel DJ, Phan AT, Kuryavyi V. Human telomere, oncogenic promoter and 5'-UTR G-quadruplexes: diverse higher order DNA and RNA targets for cancer therapeutics. Nucleic acids research 2007; 35: 7429-7455.

38 Pickering BM, Willis AE. The implications of structured 5' untranslated regions on translation and disease. Seminars in cell & developmental biology 2005; 16: 39-47.
39 Nielsen PJ, Trachsel H. The mouse protein synthesis initiation factor 4A gene family includes two related functional genes which are differentially expressed. The EMBO journal 1988; 7: 2097-2105.
40 Galicia-Vazquez G, Cencic R, Robert F, Agenor AQ, Pelletier J. A cellular response linking eIF4AI activity to eIF4AII transcription. RNA 2012; 18: 1373-1384.
41 Li Q, Imataka H, Morino S, Rogers GW, Jr., Richter-Cook NJ, Merrick WC et al. Eukaryotic translation initiation factor 4AIII (eIF4AIII) is functionally distinct from eIF4AI and eIF4AII. Molecular and cellular biology 1999; 19: 7336-7346.
42 Bordeleau ME, Mori A, Oberer M, Lindqvist L, Chard LS, Higa T et al. Functional characterization of IRESes by an inhibitor of the RNA helicase eIF4A. Nature chemical biology 2006; 2: 213-220.
43 Svitkin YV, Pause A, Haghighat A, Pyronnet S, Witherell G, Belsham GJ et al. The requirement for eukaryotic initiation factor 4A (eIF4A) in translation is in direct proportion to the degree of mRNA 5' secondary structure. RNA 2001; 7: 382-394.
44 Rubio CA, Weisburd B, Holderfield M, Arias C, Fang E, DeRisi JL et al. Transcriptome-wide characterization of the eIF4A signature highlights plasticity in translation regulation. Genome biology 2014; 15: 476.
45 Wolfe AL, Singh K, Zhong Y, Drewe P, Rajasekhar VK, Sanghvi VR et al. RNA G-quadruplexes cause eIF4A-dependent oncogene translation in cancer. Nature 2014; 513: 65-70.
46 Modelska A, Turro E, Russell R, Beaton J, Sbarrato T, Spriggs K et al. The malignant phenotype in breast cancer is driven by eIF4A1-mediated changes in the translational landscape. Cell death & disease 2015; 6: e1603.
47 Steinhardt JJ, Peroutka RJ, Mazan-Mamczarz K, Chen Q, Houng S, Robles C et al. Inhibiting CARD11 translation during BCR activation by targeting the eIF4A RNA helicase. Blood 2014; 124: 3758-3767.
48 Jin C, Rajabi H, Rodrigo CM, Porco JA, Jr., Kufe D. Targeting the eIF4A RNA helicase blocks translation of the MUC1-C oncoprotein. Oncogene 2013; 32: 2179-2188.
49 Cencic R, Carrier M, Galicia-Vazquez G, Bordeleau ME, Sukarieh R, Bourdeau A et al. Antitumor activity and mechanism of action of the cyclopenta[b]benzofuran, silvestrol. PloS one 2009; 4: e5223.
50 Pyle AM. Translocation and unwinding mechanisms of RNA and DNA helicases. Annual review of biophysics 2008; 37: 317-336.
51 Abaeva IS, Marintchev A, Pisareva VP, Hellen CU, Pestova TV. Bypassing of stems versus linear base-by-base inspection of mammalian mRNAs during ribosomal scanning. The EMBO journal 2011; 30: 115-129.
52 Pisareva VP, Pisarev AV, Komar AA, Hellen CU, Pestova TV. Translation initiation on mammalian mRNAs with structured 5'UTRs requires DExH-box protein DHX29. Cell 2008; 135: 1237-1250.
53 Parsyan A, Shahbazian D, Martineau Y, Petroulakis E, Alain T, Larsson O et al. The helicase protein DHX29 promotes translation initiation, cell proliferation, and tumorigenesis. Proceedings of the National Academy of Sciences of the United States of America 2009; 106: 22217-22222.
54 Marsden S, Nardelli M, Linder P, McCarthy JE. Unwinding single RNA molecules using helicases involved in eukaryotic translation initiation. Journal of molecular biology 2006; 361: 327-335.
55 Berthelot K, Muldoon M, Rajkowitsch L, Hughes J, McCarthy JE. Dynamics and processivity of 40S ribosome scanning on mRNA in yeast. Molecular microbiology 2004; 51: 987-1001.
56 Shih JW, Tsai TY, Chao CH, Wu Lee YH. Candidate tumor suppressor DDX3 RNA helicase specifically represses cap-dependent translation by acting as an eIF4E inhibitory protein. Oncogene 2008; 27: 700-714.
57 Lee CS, Dias AP, Jedrychowski M, Patel AH, Hsu JL, Reed R. Human DDX3 functions in translation and interacts with the translation initiation factor eIF3. Nucleic acids research 2008; 36: 4708-4718.
58 Geissler R, Golbik RP, Behrens SE. The DEAD-box helicase DDX3 supports the assembly of functional 80S ribosomes. Nucleic acids research 2012; 40: 4998-5011.
59 Soto-Rifo R, Rubilar PS, Limousin T, de Breyne S, Decimo D, Ohlmann T. DEAD-box protein DDX3 associates with eIF4F to promote translation of selected mRNAs. The EMBO journal 2012; 31: 3745-3756.
60 Fukumura J, Noguchi E, Sekiguchi T, Nishimoto T. A temperature-sensitive mutant of the mammalian RNA helicase, DEAD-BOX X isoform, DBX, defective in the transition from G1 to S phase. Journal of biochemistry 2003; 134: 71-82.
61 Lai MC, Lee YH, Tarn WY. The DEAD-box RNA helicase DDX3 associates with export messenger ribonucleoproteins as well as tip-associated protein and participates in translational control. Molecular biology of the cell 2008; 19: 3847-3858.
62 Lai MC, Chang WC, Shieh SY, Tarn WY. DDX3 regulates cell growth through translational control of cyclin E1. Molecular and cellular biology 2010; 30: 5444-5453.
63 Celik H, Sajwan KP, Selvanathan SP, Marsh BJ, Pai AV, Kont YS et al. Ezrin Binds to DEAD-Box RNA Helicase DDX3 and Regulates Its Function and Protein Level. Molecular and cellular biology 2015; 35: 3145-3162.
64 Hogbom M, Collins R, van den Berg S, Jenvert RM, Karlberg T, Kotenyova T et al. Crystal structure of conserved domains 1 and 2 of the human DEAD-box helicase DDX3X in complex with the mononucleotide AMP. Journal of molecular biology 2007; 372: 150-159.
65 Chen HH, Yu HI, Cho WC, Tarn WY. DDX3 modulates cell adhesion and motility and cancer cell metastasis via Rac1-mediated signaling pathway. Oncogene 2015; 34: 2790-2800.
66 Dunford A, Weinstock DM, Savova V, Schumacher SE, Cleary JP, Yoda A et al. Tumor-suppressor genes that escape from X-inactivation contribute to cancer sex bias. Nature genetics 2016.
67 Pugh TJ, Weeraratne SD, Archer TC, Pomeranz Krummel DA, Auclair D, Bochicchio J et al. Medulloblastoma exome sequencing uncovers subtype-specific somatic mutations. Nature 2012; 488: 106-110.
68 Jones DT, Jager N, Kool M, Zichner T, Hutter B, Sultan M et al. Dissecting the genomic complexity underlying medulloblastoma. Nature 2012; 488: 100-105.
69 Robinson G, Parker M, Kranenburg TA, Lu C, Chen X, Ding L et al. Novel mutations target distinct subgroups of medulloblastoma. Nature 2012; 488: 43-48.

70 Kool M, Jones DT, Jager N, Northcott PA, Pugh TJ, Hovestadt V et al. Genome sequencing of SHH medulloblastoma predicts genotype-related response to smoothened inhibition. Cancer cell 2014; 25: 393-405.
71 Stransky N, Egloff AM, Tward AD, Kostic AD, Cibulskis K, Sivachenko A et al. The mutational landscape of head and neck squamous cell carcinoma. Science 2011; 333: 1157-1160.
72 Mutational landscape of gingivo-buccal oral squamous cell carcinoma reveals new recurrently-mutated genes and molecular subgroups. Nature communications 2013; 4: 2873.
73 Seiwert TY, Zuo Z, Keck MK, Khattri A, Pedamallu CS, Stricker T et al. Integrative and comparative genomic analysis of HPV-positive and HPV-negative head and neck squamous cell carcinomas. Clinical cancer research : an official journal of the American Association for Cancer Research 2015; 21: 632-641.
74 Richter J, Schlesner M, Hoffmann S, Kreuz M, Leich E, Burkhardt B et al. Recurrent mutation of the ID3 gene in Burkitt lymphoma identified by integrated genome, exome and transcriptome sequencing. Nature genetics 2012; 44: 1316-1320.
75 Wang L, Lawrence MS, Wan Y, Stojanov P, Sougnez C, Stevenson K et al. SF3B1 and other novel cancer genes in chronic lymphocytic leukemia. The New England journal of medicine 2011; 365: 2497-2506.
76 Ojha J, Secreto CR, Rabe KG, Van Dyke DL, Kortum KM, Slager SL et al. Identification of recurrent truncated DDX3X mutations in chronic lymphocytic leukaemia. British journal of haematology 2015; 169: 445-448.
77 Vollbrecht C, Mairinger FD, Koitzsch U, Peifer M, Koenig K, Heukamp LC et al. Comprehensive Analysis of Disease-Related Genes in Chronic Lymphocytic Leukemia by Multiplex PCR-Based Next Generation Sequencing. PloS one 2015; 10: e0129544.
78 Jiang L, Gu ZH, Yan ZX, Zhao X, Xie YY, Zhang ZG et al. Exome sequencing identifies somatic mutations of DDX3X in natural killer/T-cell lymphoma. Nature genetics 2015; 47: 1061-1066.
79 Schmitz R, Young RM, Ceribelli M, Jhavar S, Xiao W, Zhang M et al. Burkitt lymphoma pathogenesis and therapeutic targets from structural and functional genomics. Nature 2012; 490: 116-120.
80 Floor SN, Condon KJ, Sharma D, Jankowsky E, Doudna JA. Autoinhibitory Interdomain Interactions and Subfamily-specific Extensions Redefine the Catalytic Core of the Human DEAD-box Protein DDX3. The Journal of biological chemistry 2016; 291: 2412-2421.
81 Epling LB, Grace CR, Lowe BR, Partridge JF, Enemark EJ. Cancer-associated mutants of RNA helicase DDX3X are defective in RNA-stimulated ATP hydrolysis. Journal of molecular biology 2015; 427: 1779-1796.
82 Valentin-Vega YA, Wang YD, Parker M, Patmore DM, Kanagaraj A, Moore J et al. Cancer-associated DDX3X mutations drive stress granule assembly and impair global translation. Scientific reports 2016; 6: 25996.
83 Bol GM, Xie M, Raman V. DDX3, a potential target for cancer treatment. Molecular cancer 2015; 14: 188.
84 Bol GM, Vesuna F, Xie M, Zeng J, Aziz K, Gandhi N et al. Targeting DDX3 with a small molecule inhibitor for lung cancer therapy. EMBO molecular medicine 2015; 7: 648-669.
85 Ranji A, Shkriabai N, Kvaratskhelia M, Musier-Forsyth K, Boris-Lawrie K. Features of double-stranded RNA-binding domains of RNA helicase A are necessary for selective recognition and translation of complex mRNAs. The Journal of biological chemistry 2011; 286: 5328-5337.
86 Hartman TR, Qian S, Bolinger C, Fernandez S, Schoenberg DR, Boris-Lawrie K. RNA helicase A is necessary for translation of selected messenger RNAs. Nature structural & molecular biology 2006; 13: 509-516.
87 Bolinger C, Sharma A, Singh D, Yu L, Boris-Lawrie K. RNA helicase A modulates translation of HIV-1 and infectivity of progeny virions. Nucleic acids research 2010; 38: 1686-1696.
88 Xu C, Liu K, Ahmed H, Loppnau P, Schapira M, Min J. Structural Basis for the Discriminative Recognition of N6-Methyladenosine RNA by the Human YT521-B Homology Domain Family of Proteins. The Journal of biological chemistry 2015; 290: 24902-24913.
89 Meyer KD, Saletore Y, Zumbo P, Elemento O, Mason CE, Jaffrey SR. Comprehensive analysis of mRNA methylation reveals enrichment in 3' UTRs and near stop codons. Cell 2012; 149: 1635-1646.
90 Wang X, Zhao BS, Roundtree IA, Lu Z, Han D, Ma H et al. N(6)-methyladenosine Modulates Messenger RNA Translation Efficiency. Cell 2015; 161: 1388-1399.
91 Tanabe A, Tanikawa K, Tsunetomi M, Takai K, Ikeda H, Konno J et al. RNA helicase YTHDC2 promotes cancer metastasis via the enhancement of the efficiency by which HIF-1alpha mRNA is translated. Cancer letters 2016; 376: 34-42.
92 Wang Y, Arribas-Layton M, Chen Y, Lykke-Andersen J, Sen GL. DDX6 Orchestrates Mammalian Progenitor Function through the mRNA Degradation and Translation Pathways. Molecular cell 2015; 60: 118-130.
93 Qi MY, Wang ZZ, Zhang Z, Shao Q, Zeng A, Li XQ et al. AU-rich-element-dependent translation repression requires the cooperation of tristetraprolin and RCK/P54. Molecular and cellular biology 2012; 32: 913-928.
94 Braunstein S, Karpisheva K, Pola C, Goldberg J, Hochman T, Yee H et al. A hypoxia-controlled cap-dependent to cap-independent translation switch in breast cancer. Molecular cell 2007; 28: 501-512.
95 Holcik M, Lefebvre C, Yeh C, Chow T, Korneluk RG. A new internal-ribosome-entry-site motif potentiates XIAP-mediated cytoprotection. Nature cell biology 1999; 1: 190-192.
96 Komar AA, Hatzoglou M. Cellular IRES-mediated translation: the war of ITAFs in pathophysiological states. Cell Cycle 2011; 10: 229-240.
97 Balvay L, Soto Rifo R, Ricci EP, Decimo D, Ohlmann T. Structural and functional diversity of viral IRESes. Biochimica et biophysica acta 2009; 1789: 542-557.
98 Baird SD, Lewis SM, Turcotte M, Holcik M. A search for structurally similar cellular internal ribosome entry sites. Nucleic acids research 2007; 35: 4664-4677.
99 Walters B, Thompson SR. Cap-Independent Translational Control of Carcinogenesis. Frontiers in oncology 2016; 6: 128.
100 Komar AA, Hatzoglou M. Exploring Internal Ribosome Entry Sites as Therapeutic Targets. Frontiers in oncology 2015; 5: 233.
101 Leprivier G, Rotblat B, Khan D, Jan E, Sorensen PH. Stress-mediated translational control in cancer cells. Biochimica et biophysica acta 2015; 1849: 845-860.
102 Sherrill KW, Byrd MP, Van Eden ME, Lloyd RE. BCL-2 translation is mediated via internal ribosome entry during

cell stress. The Journal of biological chemistry 2004; 279: 29066-29074.
103 Van Eden ME, Byrd MP, Sherrill KW, Lloyd RE. Translation of cellular inhibitor of apoptosis protein 1 (c-IAP1) mRNA is IRES mediated and regulated during cell stress. RNA 2004; 10: 469-481.
104 Holcik M, Yeh C, Korneluk RG, Chow T. Translational upregulation of X-linked inhibitor of apoptosis (XIAP) increases resistance to radiation induced cell death. Oncogene 2000; 19: 4174-4177.
105 Notari M, Neviani P, Santhanam R, Blaser BW, Chang JS, Galietta A et al. A MAPK/HNRPK pathway controls BCR/ABL oncogenic potential by regulating MYC mRNA translation. Blood 2006; 107: 2507-2516.
106 Jopling CL, Willis AE. N-myc translation is initiated via an internal ribosome entry segment that displays enhanced activity in neuronal cells. Oncogene 2001; 20: 2664-2670.
107 Spriggs KA, Cobbold LC, Jopling CL, Cooper RE, Wilson LA, Stoneley M et al. Canonical initiation factor requirements of the Myc family of internal ribosome entry segments. Molecular and cellular biology 2009; 29: 1565-1574.
108 Webb TE, Hughes A, Smalley DS, Spriggs KA. An internal ribosome entry site in the 5' untranslated region of epidermal growth factor receptor allows hypoxic expression. Oncogenesis 2015; 4: e134.
109 Blau L, Knirsh R, Ben-Dror I, Oren S, Kuphal S, Hau P et al. Aberrant expression of c-Jun in glioblastoma by internal ribosome entry site (IRES)-mediated translational activation. Proceedings of the National Academy of Sciences of the United States of America 2012; 109: E2875-2884.
110 Silvera D, Arju R, Darvishian F, Levine PH, Zolfaghari L, Goldberg J et al. Essential role for eIF4GI overexpression in the pathogenesis of inflammatory breast cancer. Nature cell biology 2009; 11: 903-908.
111 Marash L, Liberman N, Henis-Korenblit S, Sivan G, Reem E, Elroy-Stein O et al. DAP5 promotes cap-independent translation of Bcl-2 and CDK1 to facilitate cell survival during mitosis. Molecular cell 2008; 30: 447-459.
112 Lang KJ, Kappel A, Goodall GJ. Hypoxia-inducible factor-1alpha mRNA contains an internal ribosome entry site that allows efficient translation during normoxia and hypoxia. Molecular biology of the cell 2002; 13: 1792-1801.
113 Akiri G, Nahari D, Finkelstein Y, Le SY, Elroy-Stein O, Levi BZ. Regulation of vascular endothelial growth factor (VEGF) expression is mediated by internal initiation of translation and alternative initiation of transcription. Oncogene 1998; 17: 227-236.
114 Bellodi C, Kopmar N, Ruggero D. Deregulation of oncogene-induced senescence and p53 translational control in X-linked dyskeratosis congenita. The EMBO journal 2010; 29: 1865-1876.
115 Faye MD, Holcik M. The role of IRES trans-acting factors in carcinogenesis. Biochimica et biophysica acta 2015; 1849: 887-897.
116 Thoma C, Bergamini G, Galy B, Hundsdoerfer P, Hentze MW. Enhancement of IRES-mediated translation of the c-myc and BiP mRNAs by the poly(A) tail is independent of intact eIF4G and PABP. Molecular cell 2004; 15: 925-935.
117 Tsai BP, Jimenez J, Lim S, Fitzgerald KD, Zhang M, Chuah CT et al. A novel Bcr-Abl-mTOR-eIF4A axis regulates IRES-mediated translation of LEF-1. Open biology 2014; 4: 140180.
118 Svitkin YV, Herdy B, Costa-Mattioli M, Gingras AC, Raught B, Sonenberg N. Eukaryotic translation initiation factor 4E availability controls the switch between cap-dependent and internal ribosomal entry site-mediated translation. Molecular and cellular biology 2005; 25: 10556-10565.
119 Halaby MJ, Li Y, Harris BR, Jiang S, Miskimins WK, Cleary MP et al. Translational Control Protein 80 Stimulates IRES-Mediated Translation of p53 mRNA in Response to DNA Damage. BioMed research international 2015; 2015: 708158.
120 de Vries S, Naarmann-de Vries IS, Urlaub H, Lue H, Bernhagen J, Ostareck DH et al. Identification of DEAD-box RNA helicase 6 (DDX6) as a cellular modulator of vascular endothelial growth factor expression under hypoxia. The Journal of biological chemistry 2013; 288: 5815-5827.
121 Anderson S, Bankier AT, Barrell BG, de Bruijn MH, Coulson AR, Drouin J et al. Sequence and organization of the human mitochondrial genome. Nature 1981; 290: 457-465.
122 Hallberg BM, Larsson NG. Making proteins in the powerhouse. Cell metabolism 2014; 20: 226-240.
123 Mai N, Chrzanowska-Lightowlers ZM, Lightowlers RN. The process of mammalian mitochondrial protein synthesis. Cell and tissue research 2016.
124 Richter-Dennerlein R, Dennerlein S, Rehling P. Integrating mitochondrial translation into the cellular context. Nature reviews Molecular cell biology 2015; 16: 586-592.
125 Christian BE, Spremulli LL. Mechanism of protein biosynthesis in mammalian mitochondria. Biochimica et biophysica acta 2012; 1819: 1035-1054.
126 Koppenol WH, Bounds PL, Dang CV. Otto Warburg's contributions to current concepts of cancer metabolism. Nature reviews Cancer 2011; 11: 325-337.
127 Viale A, Corti D, Draetta GF. Tumors and mitochondrial respiration: a neglected connection. Cancer research 2015; 75: 3685-3686.
128 Weinberg SE, Chandel NS. Targeting mitochondria metabolism for cancer therapy. Nature chemical biology 2015; 11: 9-15.
129 Wang PY, Li J, Walcott FL, Kang JG, Starost MF, Talagala SL et al. Inhibiting mitochondrial respiration prevents cancer in a mouse model of Li-Fraumeni syndrome. The Journal of clinical investigation 2016.
130 Vellinga TT, Borovski T, de Boer VC, Fatrai S, van Schelven S, Trumpi K et al. SIRT1/PGC1alpha-Dependent Increase in Oxidative Phosphorylation Supports Chemotherapy Resistance of Colon Cancer. Clinical cancer research : an official journal of the American Association for Cancer Research 2015; 21: 2870-2879.
131 Qin B, Minter-Dykhouse K, Yu J, Zhang J, Liu T, Zhang H et al. DBC1 functions as a tumor suppressor by regulating p53 stability. Cell reports 2015; 10: 1324-1334.
132 LeBleu VS, O'Connell JT, Gonzalez Herrera KN, Wikman H, Pantel K, Haigis MC et al. PGC-1alpha mediates mitochondrial biogenesis and oxidative phosphorylation in cancer cells to promote metastasis. Nature cell biology 2014; 16: 992-1003, 1001-1015.

133 Skrtic M, Sriskanthadevan S, Jhas B, Gebbia M, Wang X, Wang Z et al. Inhibition of mitochondrial translation as a therapeutic strategy for human acute myeloid leukemia. Cancer cell 2011; 20: 674-688.
134 Tu YT, Barrientos A. The Human Mitochondrial DEAD-Box Protein DDX28 Resides in RNA Granules and Functions in Mitoribosome Assembly. Cell reports 2015.
135 Antonicka H, Shoubridge EA. Mitochondrial RNA Granules Are Centers for Posttranscriptional RNA Processing and Ribosome Biogenesis. Cell reports 2015.
136 Bogenhagen DF, Martin DW, Koller A. Initial steps in RNA processing and ribosome assembly occur at mitochondrial DNA nucleoids. Cell metabolism 2014; 19: 618-629.
137 De Silva D, Tu YT, Amunts A, Fontanesi F, Barrientos A. Mitochondrial ribosome assembly in health and disease. Cell Cycle 2015; 14: 2226-2250.
138 Oshiumi H, Sakai K, Matsumoto M, Seya T. DEAD/H BOX 3 (DDX3) helicase binds the RIG-I adaptor IPS-1 to up-regulate IFN-beta-inducing potential. European journal of immunology 2010; 40: 940-948.
139 Fuller-Pace FV. DEAD box RNA helicase functions in cancer. RNA biology 2013; 10: 121-132.
140 Eberle J, Fecker LF, Bittner JU, Orfanos CE, Geilen CC. Decreased proliferation of human melanoma cell lines caused by antisense RNA against translation factor eIF-4A1. British journal of cancer 2002; 86: 1957-1962.
141 Robert F, Roman W, Bramoulle A, Fellmann C, Roulston A, Shustik C et al. Translation initiation factor eIF4F modifies the dexamethasone response in multiple myeloma. Proceedings of the National Academy of Sciences of the United States of America 2014; 111: 13421-13426.
142 Jansen AP, Camalier CE, Colburn NH. Epidermal expression of the translation inhibitor programmed cell death 4 suppresses tumorigenesis. Cancer research 2005; 65: 6034-6041.
143 Novac O, Guenier AS, Pelletier J. Inhibitors of protein synthesis identified by a high throughput multiplexed translation screen. Nucleic acids research 2004; 32: 902-915.
144 Lindqvist L, Oberer M, Reibarkh M, Cencic R, Bordeleau ME, Vogt E et al. Selective pharmacological targeting of a DEAD box RNA helicase. PloS one 2008; 3: e1583.
145 Sun Y, Atas E, Lindqvist LM, Sonenberg N, Pelletier J, Meller A. Single-molecule kinetics of the eukaryotic initiation factor 4AI upon RNA unwinding. Structure 2014; 22: 941-948.
146 Iwasaki S, Floor SN, Ingolia NT. Rocaglates convert DEAD-box protein eIF4A into a sequence-selective translational repressor. Nature 2016; 534: 558-561.
147 Bordeleau ME, Matthews J, Wojnar JM, Lindqvist L, Novac O, Jankowsky E et al. Stimulation of mammalian translation initiation factor eIF4A activity by a small molecule inhibitor of eukaryotic translation. Proceedings of the National Academy of Sciences of the United States of America 2005; 102: 10460-10465.
148 Bordeleau ME, Cencic R, Lindqvist L, Oberer M, Northcote P, Wagner G et al. RNA-mediated sequestration of the RNA helicase eIF4A by Pateamine A inhibits translation initiation. Chemistry & biology 2006; 13: 1287-1295.
149 Low WK, Dang Y, Bhat S, Romo D, Liu JO. Substrate-dependent targeting of eukaryotic translation initiation factor 4A by pateamine A: negation of domain-linker regulation of activity. Chemistry & biology 2007; 14: 715-727.
150 Low WK, Dang Y, Schneider-Poetsch T, Shi Z, Choi NS, Merrick WC et al. Inhibition of eukaryotic translation initiation by the marine natural product pateamine A. Molecular cell 2005; 20: 709-722.
151 Low WK, Dang Y, Schneider-Poetsch T, Shi Z, Choi NS, Rzasa RM et al. Isolation and identification of eukaryotic initiation factor 4A as a molecular target for the marine natural product Pateamine A. Methods in enzymology 2007; 431: 303-324.
152 Kuznetsov G, Xu Q, Rudolph-Owen L, Tendyke K, Liu J, Towle M et al. Potent in vitro and in vivo anticancer activities of des-methyl, des-amino pateamine A, a synthetic analogue of marine natural product pateamine A. Molecular cancer therapeutics 2009; 8: 1250-1260.
153 Low WK, Li J, Zhu M, Kommaraju SS, Shah-Mittal J, Hull K et al. Second-generation derivatives of the eukaryotic translation initiation inhibitor pateamine A targeting eIF4A as potential anticancer agents. Bioorganic & medicinal chemistry 2014; 22: 116-125.
154 Bordeleau ME, Robert F, Gerard B, Lindqvist L, Chen SM, Wendel HG et al. Therapeutic suppression of translation initiation modulates chemosensitivity in a mouse lymphoma model. The Journal of clinical investigation 2008; 118: 2651-2660.
155 Chu J, Galicia-Vazquez G, Cencic R, Mills JR, Katigbak A, Porco JA, Jr. et al. CRISPR-Mediated Drug-Target Validation Reveals Selective Pharmacological Inhibition of the RNA Helicase, eIF4A. Cell reports 2016; 15: 2340-2347.
156 Gupta SV, Sass EJ, Davis ME, Edwards RB, Lozanski G, Heerema NA et al. Resistance to the translation initiation inhibitor silvestrol is mediated by ABCB1/P-glycoprotein overexpression in acute lymphoblastic leukemia cells. The AAPS journal 2011; 13: 357-364.
157 Boussemart L, Malka-Mahieu H, Girault I, Allard D, Hemmingsson O, Tomasic G et al. eIF4F is a nexus of resistance to anti-BRAF and anti-MEK cancer therapies. Nature 2014; 513: 105-109.
158 Thuaud F, Bernard Y, Turkeri G, Dirr R, Aubert G, Cresteil T et al. Synthetic analogue of rocaglaol displays a potent and selective cytotoxicity in cancer cells: involvement of apoptosis inducing factor and caspase-12. Journal of medicinal chemistry 2009; 52: 5176-5187.
159 Chu J, Cencic R, Wang W, Porco JA, Jr., Pelletier J. Translation Inhibition by Rocaglates Is Independent of eIF4E Phosphorylation Status. Molecular cancer therapeutics 2016; 15: 136-141.
160 Oguro A, Ohtsu T, Svitkin YV, Sonenberg N, Nakamura Y. RNA aptamers to initiation factor 4A helicase hinder cap-dependent translation by blocking ATP hydrolysis. RNA 2003; 9: 394-407.
161 Ishikawa C, Tanaka J, Katano H, Senba M, Mori N. Hippuristanol reduces the viability of primary effusion lymphoma cells both in vitro and in vivo. Marine drugs 2013; 11: 3410-3424.
162 Tsumuraya T, Ishikawa C, Machijima Y, Nakachi S, Senba M, Tanaka J et al. Effects of hippuristanol, an inhibitor of eIF4A, on adult T-cell leukemia. Biochemical pharmacology 2011; 81: 713-722.
163 Lee SK, Cui B, Mehta RR, Kinghorn AD, Pezzuto JM. Cytostatic mechanism and antitumor potential of novel 1H-cyclopenta[b]benzofuran lignans isolated from Aglaia elliptica. Chemico-biological interactions 1998; 115: 215-228.

164 Hwang BY, Su BN, Chai H, Mi Q, Kardono LB, Afriastini JJ et al. Silvestrol and episilvestrol, potential anticancer rocaglate derivatives from Aglaia silvestris. The Journal of organic chemistry 2004; 69: 3350-3358.

165 Callahan KP, Minhajuddin M, Corbett C, Lagadinou ED, Rossi RM, Grose V et al. Flavaglines target primitive leukemia cells and enhance anti-leukemia drug activity. Leukemia 2014; 28: 1960-1968.

166 Alachkar H, Santhanam R, Harb JG, Lucas DM, Oaks JJ, Hickey CJ et al. Silvestrol exhibits significant in vivo and in vitro antileukemic activities and inhibits FLT3 and miR-155 expressions in acute myeloid leukemia. Journal of hematology & oncology 2013; 6: 21.

167 Lucas DM, Edwards RB, Lozanski G, West DA, Shin JD, Vargo MA et al. The novel plant-derived agent silvestrol has B-cell selective activity in chronic lymphocytic leukemia and acute lymphoblastic leukemia in vitro and in vivo. Blood 2009; 113: 4656-4666.

168 Di Marco S, Cammas A, Lian XJ, Kovacs EN, Ma JF, Hall DT et al. The translation inhibitor pateamine A prevents cachexia-induced muscle wasting in mice. Nature communications 2012; 3: 896.

169 Cencic R, Carrier M, Trnkus A, Porco JA, Jr., Minden M, Pelletier J. Synergistic effect of inhibiting translation initiation in combination with cytotoxic agents in acute myelogenous leukemia cells. Leukemia research 2010; 34: 535-541.

170 Schatz JH, Oricchio E, Wolfe AL, Jiang M, Linkov I, Maragulia J et al. Targeting cap-dependent translation blocks converging survival signals by AKT and PIM kinases in lymphoma. The Journal of experimental medicine 2011; 208: 1799-1807.

171 Cencic R, Robert F, Galicia-Vazquez G, Malina A, Ravindar K, Somaiah R et al. Modifying chemotherapy response by targeted inhibition of eukaryotic initiation factor 4A. Blood cancer journal 2013; 3: e128.

172 Zindy P, Berge Y, Allal B, Filleron T, Pierredon S, Cammas A et al. Formation of the eIF4F translation-initiation complex determines sensitivity to anticancer drugs targeting the EGFR and HER2 receptors. Cancer research 2011; 71: 4068-4073.

173 Sun M, Song L, Li Y, Zhou T, Jope RS. Identification of an antiapoptotic protein complex at death receptors. Cell death and differentiation 2008; 15: 1887-1900.

174 Li Y, Wang H, Wang Z, Makhija S, Buchsbaum D, LoBuglio A et al. Inducible resistance of tumor cells to tumor necrosis factor-related apoptosis-inducing ligand receptor 2-mediated apoptosis by generation of a blockade at the death domain function. Cancer research 2006; 66: 8520-8528.

175 Heerma van Voss MR, Vesuna F, Trumpi K, Brilliant J, Berlinicke C, de Leng W et al. Identification of the DEAD box RNA helicase DDX3 as a therapeutic target in colorectal cancer. Oncotarget 2015; 6: 28312-28326.

176 Xie M, Vesuna F, Botlagunta M, Bol GM, Irving A, Bergman Y et al. NZ51, a ring-expanded nucleoside analog, inhibits motility and viability of breast cancer cells by targeting the RNA helicase DDX3. Oncotarget 2015; 6: 29901-29913.

177 Xie M, Vesuna F, Tantravedi S, Bol GM, Heerma van Voss MR, Nugent K et al. RK-33 Radiosensitizes Prostate Cancer Cells by Blocking the RNA Helicase DDX3. Cancer research 2016; 76: 6340-6350.

178 Su CY, Lin TC, Lin YF, Chen MH, Lee CH, Wang HY et al. DDX3 as a strongest prognosis marker and its downregulation promotes metastasis in colorectal cancer. Oncotarget 2015; 6: 18602-18612.

179 Botlagunta M, Vesuna F, Mironchik Y, Raman A, Lisok A, Winnard P, Jr. et al. Oncogenic role of DDX3 in breast cancer biogenesis. Oncogene 2008; 27: 3912-3922.

180 Shih JW, Wang WT, Tsai TY, Kuo CY, Li HK, Wu Lee YH. Critical roles of RNA helicase DDX3 and its interactions with eIF4E/PABP1 in stress granule assembly and stress response. The Biochemical journal 2012; 441: 119-129.

181 Chao CH, Chen CM, Cheng PL, Shih JW, Tsou AP, Lee YH. DDX3, a DEAD box RNA helicase with tumor growth-suppressive property and transcriptional regulation activity of the p21waf1/cip1 promoter, is a candidate tumor suppressor. Cancer research 2006; 66: 6579-6588.

182 Chang PC, Chi CW, Chau GY, Li FY, Tsai YH, Wu JC et al. DDX3, a DEAD box RNA helicase, is deregulated in hepatitis virus-associated hepatocellular carcinoma and is involved in cell growth control. Oncogene 2006; 25: 1991-2003.

183 Wu DW, Liu WS, Wang J, Chen CY, Cheng YW, Lee H. Reduced p21(WAF1/CIP1) via alteration of p53-DDX3 pathway is associated with poor relapse-free survival in early-stage human papillomavirus-associated lung cancer. Clinical cancer research : an official journal of the American Association for Cancer Research 2011; 17: 1895-1905.

184 Wu DW, Lee MC, Wang J, Chen CY, Cheng YW, Lee H. DDX3 loss by p53 inactivation promotes tumor malignancy via the MDM2/Slug/E-cadherin pathway and poor patient outcome in non-small-cell lung cancer. Oncogene 2014; 33: 1515-1526.

185 Heerma van Voss MR, van Kempen PM, Noorlag R, van Diest PJ, Willems SM, Raman V. DDX3 has divergent roles in head and neck squamous cell carcinomas in smoking versus non-smoking patients. Oral diseases 2015; 21: 270-271.

186 Yedavalli VS, Zhang N, Cai H, Zhang P, Starost MF, Hosmane RS et al. Ring expanded nucleoside analogues inhibit RNA helicase and intracellular human immunodeficiency virus type 1 replication. Journal of medicinal chemistry 2008; 51: 5043-5051.

187 Kondaskar A, Kondaskar S, Kumar R, Fishbein JC, Muvarak N, Lapidus RG et al. Novel, Broad Spectrum Anti-Cancer Agents Containing the Tricyclic 5:7:5-Fused Diimidazodiazepine Ring System. ACS medicinal chemistry letters 2010; 2: 252-256.

188 Wilky BA, Kim C, McCarty G, Montgomery EA, Kammers K, DeVine LR et al. RNA helicase DDX3: a novel therapeutic target in Ewing sarcoma. Oncogene 2016; 35: 2574-2583.

189 Samal SK, Routray S, Veeramachaneni GK, Dash R, Botlagunta M. Ketorolac salt is a newly discovered DDX3 inhibitor to treat oral cancer. Scientific reports 2015; 5: 9982.

190 Maga G, Falchi F, Garbelli A, Belfiore A, Witvrouw M, Manetti F et al. Pharmacophore modeling and molecular docking led to the discovery of inhibitors of human immunodeficiency virus-1 replication targeting the human cellular aspartic acid-glutamic acid-alanine-aspartic acid box polypeptide 3. Journal of medicinal chemistry 2008; 51: 6635-6638.

191 Maga G, Falchi F, Radi M, Botta L, Casaluce G, Bernardini M et al. Toward the discovery of novel anti-HIV drugs. Second-generation inhibitors of the cellular ATPase DDX3 with improved anti-HIV activity: synthesis, structure-activity relationship analysis, cytotoxicity studies, and target validation. ChemMedChem 2011; 6: 1371-1389.
192 Brai A, Fazi R, Tintori C, Zamperini C, Bugli F, Sanguinetti M et al. Human DDX3 protein is a valuable target to develop broad spectrum antiviral agents. Proceedings of the National Academy of Sciences of the United States of America 2016; 113: 5388-5393.
193 Toretsky JA, Erkizan V, Levenson A, Abaan OD, Parvin JD, Cripe TP et al. Oncoprotein EWS-FLI1 activity is enhanced by RNA helicase A. Cancer research 2006; 66: 5574-5581.
194 Erkizan HV, Kong Y, Merchant M, Schlottmann S, Barber-Rotenberg JS, Yuan L et al. A small molecule blocking oncogenic protein EWS-FLI1 interaction with RNA helicase A inhibits growth of Ewing's sarcoma. Nature medicine 2009; 15: 750-756.
195 Hong SH, Youbi SE, Hong SP, Kallakury B, Monroe P, Erkizan HV et al. Pharmacokinetic modeling optimizes inhibition of the 'undruggable' EWS-FLI1 transcription factor in Ewing Sarcoma. Oncotarget 2014; 5: 338-350.
196 Lamhamedi-Cherradi SE, Menegaz BA, Ramamoorthy V, Aiyer RA, Maywald RL, Buford AS et al. An Oral Formulation of YK-4-279: Preclinical Efficacy and Acquired Resistance Patterns in Ewing Sarcoma. Molecular cancer therapeutics 2015; 14: 1591-1604.
197 Selvanathan SP, Graham GT, Erkizan HV, Dirksen U, Natarajan TG, Dakic A et al. Oncogenic fusion protein EWS-FLI1 is a network hub that regulates alternative splicing. Proceedings of the National Academy of Sciences of the United States of America 2015; 112: E1307-1316.
198 Lee T, Paquet M, Larsson O, Pelletier J. Tumor cell survival dependence on the DHX9 DExH-box helicase. Oncogene 2016; 35: 5093-5105.
199 Tanabe A, Konno J, Tanikawa K, Sahara H. Transcriptional machinery of TNF-alpha-inducible YTH domain containing 2 (YTHDC2) gene. Gene 2014; 535: 24-32.
200 Li-Weber M. Molecular mechanisms and anti-cancer aspects of the medicinal phytochemicals rocaglamides (=flavaglines). International journal of cancer Journal international du cancer 2015; 137: 1791-1799.
201 Becker MS, Schmezer P, Breuer R, Haas SF, Essers MA, Krammer PH et al. The traditional Chinese medical compound Rocaglamide protects nonmalignant primary cells from DNA damage-induced toxicity by inhibition of p53 expression. Cell death & disease 2014; 5: e1000.
202 Fahrig T, Gerlach I, Horvath E. A synthetic derivative of the natural product rocaglaol is a potent inhibitor of cytokine-mediated signaling and shows neuroprotective activity in vitro and in animal models of Parkinson's disease and traumatic brain injury. Molecular pharmacology 2005; 67: 1544-1555.
203 Truitt ML, Conn CS, Shi Z, Pang X, Tokuyasu T, Coady AM et al. Differential Requirements for eIF4E Dose in Normal Development and Cancer. Cell 2015; 162: 59-71.
204 Hong DS, Kurzrock R, Oh Y, Wheler J, Naing A, Brail L et al. A phase 1 dose escalation, pharmacokinetic, and pharmacodynamic evaluation of eIF-4E antisense oligonucleotide LY2275796 in patients with advanced cancer. Clinical cancer research : an official journal of the American Association for Cancer Research 2011; 17: 6582-6591.
205 Kentsis A, Topisirovic I, Culjkovic B, Shao L, Borden KL. Ribavirin suppresses eIF4E-mediated oncogenic transformation by physical mimicry of the 7-methyl guanosine mRNA cap. Proceedings of the National Academy of Sciences of the United States of America 2004; 101: 18105-18110.
206 Assouline S, Culjkovic B, Cocolakis E, Rousseau C, Beslu N, Amri A et al. Molecular targeting of the oncogene eIF4E in acute myeloid leukemia (AML): a proof-of-principle clinical trial with ribavirin. Blood 2009; 114: 257-260.
207 Dorrello NV, Peschiaroli A, Guardavaccaro D, Colburn NH, Sherman NE, Pagano M. S6K1- and betaTRCP-mediated degradation of PDCD4 promotes protein translation and cell growth. Science 2006; 314: 467-471.
208 Hsieh AC, Liu Y, Edlind MP, Ingolia NT, Janes MR, Sher A et al. The translational landscape of mTOR signalling steers cancer initiation and metastasis. Nature 2012; 485: 55-61.
209 Simon GM, Niphakis MJ, Cravatt BF. Determining target engagement in living systems. Nature chemical biology 2013; 9: 200-205.
210 Bol GM, Khan R, Heerma van Voss MR, Tantravedi S, Korz D, Kato Y et al. PLGA nanoparticle formulation of RK-33: an RNA helicase inhibitor against DDX3. Cancer chemotherapy and pharmacology 2015; 76: 821-827.

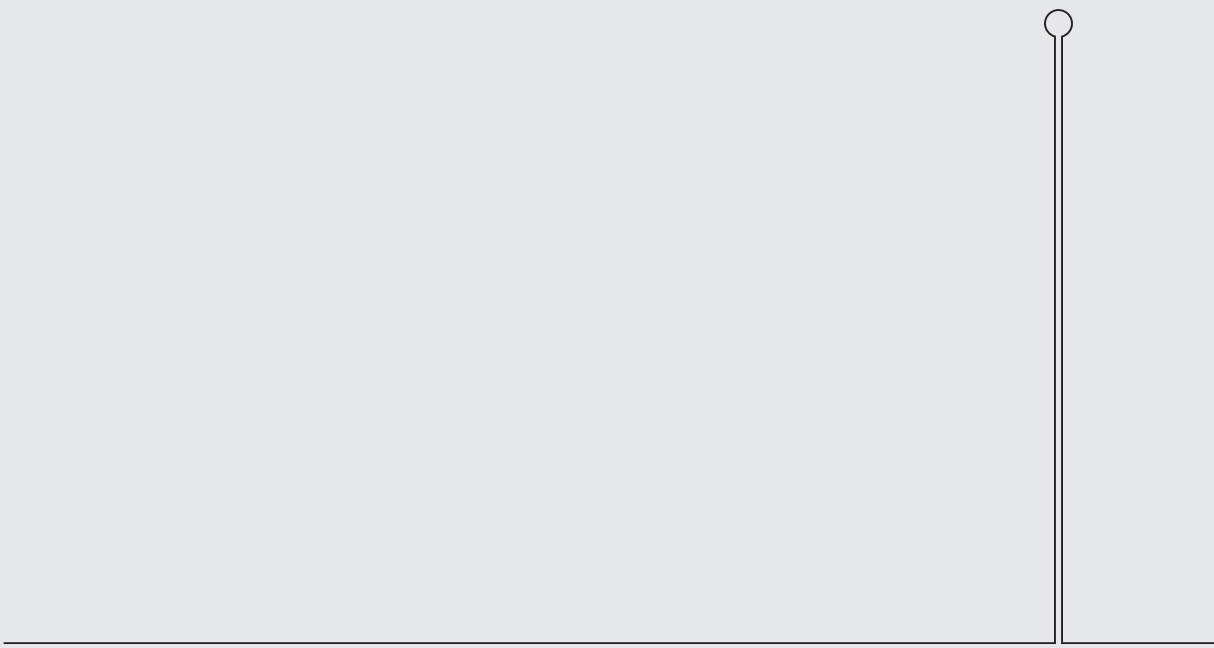

CHAPTER 10

Summarizing discussion

A good therapeutic target in cancer is a factor that cancer cells are heavily dependent on for their survival, but is not essential, or needed to a lesser extent in normal cells. In addition, it needs to be targetable and ideally we would also like to be able to predict which cancers are most dependent on this specific target. Lastly, it is important to know how different therapeutic targetable pathways relate to each other, in order to make smart combination therapy choices. In this thesis, we evaluated several aspects of DDX3 as a therapeutic target in cancer.

MOTIVES: WHY INHIBITING DDX3 HURTS CANCER

The DDX3 inhibitor RK-33 has shown potent activity in preclinical cancer models. However, the mechanism behind the antineoplastic activity of RK-33 remains largely unknown. In chapters 2 and 3 we describe how we used (phospho)proteomics to further elucidate the RK-33 working mechanism.

In **chapter 2** we evaluated the effect of DDX3 inhibition by RK-33 on the metabolic profile of breast cancer cells. Using a quantitative proteomics approach, we identified mitochondrial translation as a potential target of RK-33 therapy. We showed that DDX3 localizes to the mitochondria and that mitochondrial translation is reduced after DDX3 inhibition with RK-33, resulting in decreased oxygen consumption rates and intracellular ATP concentrations and increased reactive oxygen species (ROS). Mitochondrial respiration is increasingly recognized as a viable target for anti-cancer therapy[1-4]. Interestingly, a recent study showed that irradiated cells increase oxidative phosphorylation (OXPHOS) to facilitate DNA repair and hereby induce resistance to radiation therapy[5]. We found RK-33 to antagonize the increase in oxygen consumption and ATP production observed after exposure to ionizing radiation, and to reduce DNA repair. In addition, both ionizing radiation and RK-33 increase the intracellular ROS levels. Together, these treatments result in a bioenergetic catastrophe. Our results explain the selective anti-cancer activity observed after RK-33 treatment, especially in combination with radiation therapy, and put inhibition of mitochondrial translation forward as a novel radiosensitization strategy.

Although RK-33 is designed to inhibit DDX3 and we found RK-33 to reduce mitochondrial translation, we have yet to completely decode the role for DDX3 in mitochondrial translation. However, that RK-33 exerts its effects through DDX3 is highly likely, because it binds RK-33 specifically over other DEAD box RNA helicase members and it inhibits the helicase activity of the yeast DDX3 homologue, ded1[6]. In addition, the fact that we and others[7] found DDX3 to localize to the mitochondria further supports a role for DDX3 in mitochondrial translation. In addition, the RNA helicases DDX28 and DHX30 were recently found to be responsible for the assembly of mitochondrial ribosomes, and DDX3 was identified by mass spectrometry analysis of the mitochondrial DDX28 and DHX30

interactome[8, 9], implying that DDX3 might also be involved in mitochondrial ribosome assembly. The role of DDX3 in general mRNA translation initiation is still under investigation[10], but it is possible that RK-33 treatment also has an effect on cytoplasmic translation. In line with this, nuclear DDX3 expression (chapters 5 and 6) could reflect a need for increased nuclear-encoded protein synthesis in cancers. However, the timeline of events with decreased mitochondrial translation as early as two hours after treatment onset, does suggest that the effect of RK-33 on mitochondrial translation is direct.
Since not only cancer, but also normal cells are dependent on mitochondrial translation, toxicity of RK-33 treatment can be a concern. However, no toxicity was observed after RK-33 treatment in extensive toxicology studies performed in mice[6]. The limited effect of DDX3 inhibition on normal cells is in line with the fact that normal cells have a relatively low baseline ATP demand, encounter less stressors (e.g., DNA damage) that cause sudden increases in energy demand, have low ROS levels, and express low amounts of DDX3.
In **chapter 3**, we used a dual strategy to further elucidate the working mechanism of DDX3 inhibition with RK-33. DEAD box RNA helicases are multifunctional proteins and regulate cellular processes beyond their role in mRNA processing. DDX3 has for instance been shown to directly modulate the kinase activity of CK1ε[11]. To monitor the changes after RK-33 treatment on protein abundance, as well as phosphorylation status, we performed a quantitative phosphoproteomics experiment. At the proteome level, we mainly observed changes in proteins involved in mitochondrial translation (see chapter 2), cell division pathways and cell cycle progression. Analysis of the phosphoproteome indicated decreased CDK1 activity after RK-33 treatment. In addition, since previous studies also found a role for DDX3 in cell cycle progression [12, 13], and cell cycle status strongly influences the phosphoproteomic landscape of the cell, we used a single cell tracking approach to monitor cell cycle progression of cells. DDX3 inhibition resulted in a global delay in cell cycle progression in all interphases and mitosis and increased endoreduplication. Both single cell tracking and (phospho)proteomic data indicated a central role for CDK1, which deserves further validation in the future. It is likely that the dependence of cancer cells on DDX3 is related to not one but several processes. Additional roles for DDX3 in oncogenesis have been described in literature and involve the regulation of Wnt-signaling (as discussed in chapter 4)[6, 14], migration [15, 16], invasion [14, 17, 18] and apoptosis [19-21].

TARGETS: DDX3 DEPENDENCE IN DIFFERENT CANCER TYPES

Targeting DDX3 has previously been recognized as a suitable therapeutic strategy for breast[15, 18], lung[6] and prostate cancer[22]. In **chapter 4**, we evaluated whether DDX3 plays a role in the constitutively active Wnt-signaling pathway that drives colorectal cancer. We found that 39% of tumors overexpress DDX3 and that high cytoplasmic DDX3 expression

correlates with nuclear β-catenin expression, a marker of activated Wnt signaling. We proceeded to functionally validate these findings *in vitro* and showed that inhibition of DDX3 with siRNA or RK-33 resulted in reduced TCF4-reporter activity and downstream gene expression and hereby reduced proliferation and cell cycle progression, supporting a potential oncogenic role of DDX3 in colorectal cancer. Treatment of colorectal cancer cell lines and patient-derived 3D cultures with RK-33 inhibited growth and promoted cell death. The clinical relevance of the development of Wnt signaling inhibitors which work in a constitutively activated setting is tremendous, since mutations in the Wnt-signaling pathway are not only the first and most frequent genetic alterations in the adenoma-carcinoma sequence, but advanced colorectal cancers with mutations in *APC* or *CTNNB1* remain dependent on upstream Wnt signaling activity[23, 24].

Within our experimental setting, DDX3 expression levels in colorectal cancer cells did not correlate with the sensitivity to RK-33. This could be due to the fact that the levels of DDX3 essential to maintain cellular homeostasis are variable in different colorectal cancer cells. Another possibility is that DDX3 dependence is related to other genetic alterations. The highest RK-33 sensitivity was observed in the absence of an *APC* mutation and the presence of a mutation in *CTNNB1*. However, a larger sample size with bigger differences in RK-33 sensitivity is needed to make any definite claims on this regard.

Although the majority of DDX3 protein in human cancers is found in the cytoplasm, a subset of tumors also has distinct nuclear DDX3 localization. In **chapter 5**, we aimed to evaluate the significance of and mechanisms behind nuclear DDX3 expression in colorectal and breast cancer. Nuclear DDX3 was present in 35% of colorectal and 48% of breast cancer patient samples and expression was particularly strong in the nucleolus. The nucleolus is the cellular compartment where ribosomal biogenesis takes place and high nucleolar DDX3 levels in cancers therefore potentially reflect the high protein synthesis demands in cancers. The presence of nuclear DDX3 was identified as an independent predictor of worse survival in both colorectal and breast cancer. This correlation with worse survival indicates that nuclear DDX3 might have an oncogenic role in these cancer types. Unfortunately, we were not able to overexpress functional DDX3 specifically in the nucleus, and therefore could not evaluate the functionality of nuclear DDX3 directly. With regard to the mechanism behind nuclear DDX3 retention, we found a correlation with dysregulated expression of the nuclear exporter CRM1 in colorectal cancer, but not in breast cancer. In addition, inhibition of CRM1 with leptomycin B resulted in an increase in nuclear DDX3 levels. Experiments with (deletion) mutants indicated the N-terminal nuclear export signal (NES) sequence of DDX3 is most important for this interaction. In addition, our data show that DDX3 is possibly also regulated at the import level by unknown mechanisms. Knowledge on the cellular mechanisms behind nuclear DDX3 retention may facilitate the development of therapies specifically targeting the mRNA export function of DDX3[25]. In addition, nuclear DDX3 could serve as a prognostic and potentially therapeutic biomarker for selecting cancer

patients that may benefit from treatment with DDX3 inhibitors. Whether it is most relevant to look at cytoplasmic DDX3 expression, which could represent both the free cytosolic and mitochondrial DDX3 fraction, or nuclear DDX3 for this purpose remains to be determined in clinical studies of DDX3 inhibitors.

In order to validate functional studies that showed that DDX3 facilitates invasion and migration of cancer cells [14, 15, 17, 18], we investigated DDX3 expression in paired samples of primary and metastatic breast cancer in **chapter 6**. We found cytoplasmic DDX3 expression to be increased in metastases, especially in triple negative cases and brain lesions. DDX3 upregulation in 48% of brain metastases was particularly striking and cannot be solely explained by the association with triple negative (TN) and HER2-enriched subtypes, which were less frequently upregulated (13% and 2% of paired cases respectively). High expression of both cytoplasmic and nuclear DDX3 in the metastases correlated with worse overall survival, implying that DDX3 is a potential therapeutic target in metastatic breast cancer, in particular in the clinically important group of TN patients and patients with brain metastases. Several functional studies support a pro-metastatic role of DDX3[15, 16, 26 14, 17]. However, the survival difference between metastases with low and high cytoplasmic DDX3 expression is partly attributable to their frequent triple negative phenotype and brain localization. Although diffusion of the DDX3 inhibitor RK-33 over an intact blood brain barrier is limited[6], its small size and the compromised blood brain barrier in brain metastases[27] potentially do allow for therapeutic levels to be reached. RK-33 has potent radiosensitizing abilities[15], which could enhance the effect of whole brain radiation to treat brain metastases. Further evaluation of effective drug concentrations *in vivo* and diffusion of RK-33 over leaky blood-brain barriers in metastases is warranted.

Besides the role of DDX3 as an non-oncogene addiction gene, there are some contradictory studies reporting that DDX3 functions as a tumor suppressor[28, 29]. The role of DDX3 in oncogenesis potentially differs between genetic backgrounds and cancer types. Inactivating *DDX3X* mutations were for instance an exclusive feature of HPV-positive head and neck squamous cell carcinomas (HNSCCs), whereas we described **in chapter 7** that the relation between DDX3 expression and survival differs for smoking and non-smoking patients with HNSCC. Overall, DDX3 expression did not correlate with survival in this cancer type. However, a trend was observed for worse survival in smoking HNSCC patients, whereas Lee *et al* reported an opposite correlation in non-smoking, mainly HPV positive, patients[30]. These findings indicate a model in which DDX3, when upregulated in response to cigarette smoke exposure, drives oncogenesis, whereas it might have alternative roles in virally induced transformation. However, expression levels of a protein and associations with survival do not always directly reflect dependence of cancer cells on that particular protein. Future functional studies should address the potential different roles of DDX3 expression levels and *DDX3X* mutations in different genetic backgrounds and how this relates to RK-33 sensitivity.

PARTNERS IN CRIME: DDX3 INHIBITORS IN COMBINATION WITH PARP INHIBITORS

In order to exploit DDX3 inhibition in cancer to the furthest extent, it is essential to know how DDX3 inhibitors interact with other anti-cancer therapeutics. Breast cancers with a *BRCA1* mutation are homologous recombination deficient, sensitizing them to inhibition of another DNA damage repair pathway by PARP inhibitors. Since RK-33 was previously demonstrated to impede non-homologous end-joining repair of DNA breaks, we evaluated DDX3 as a therapeutic target in BRCA pro- and deficient breast cancers in **chapter 8** and assessed whether DDX3 inhibition could sensitize cells to PARP inhibition. We found sporadic breast cancers and breast cancers occurring in *BRCA1* and *BRCA2* germline mutation carriers to have similar DDX3 expression levels and RK-33 sensitivity. However, a synergetic interaction was observed for combination treatment with RK-33 and the PARP inhibitor olaparib in BRCA1 proficient breast cancer.

PARTNERS IN CRIME: TARGETING OTHER RNA HELICASES IN CANCER

DDX3 is part of a large family of DEAD and DEAH box RNA helicases that play a role in virtually all steps of mRNA metabolism. Recent studies have indicated that targeting the mRNA translation machinery holds great promise for anti-cancer drug development[31-33] and several DDX/DHX family members have therefore been put forward as viable therapeutic targets. In **chapter 9** we review DEAD/H box RNA helicases as potential targets in oncogenic mRNA translation, to put DDX3 inhibition with RK-33 in a broader context. Several RNA helicases (eIF4A, DDX3, DHX9, DHX29, YTHDC2) facilitate translation of the cancer genome by unwinding different types of complex 5'UTR regions, which are common in mRNAs that promote oncogenesis. The DEAD box proteins eIF4A and DDX3 play an additional role in internal ribosome entry site (IRES) dependent translation that supports tumor cell survival in response to oncogenic stress. Mitochondria have their own translational machinery, which recent studies also recognize as a therapeutic target[34]. DHX30 and DDX28 facilitate mitochondrial ribosome assembly, and as previously mentioned in chapter 3, DDX3 inhibition with RK-33 reduces mitochondrial translation. Studies evaluating the effect of several RNA helicase inhibitors targeting eIF4A and DDX3 are showing promising pre-clinical anti-cancer activity, making RNA helicase inhibitors a highly anticipated novel class of drugs for clinical development.

FUTURE PERSPECTIVES

In this thesis, we further elucidated the working mechanism behind the DDX3 inhibitor RK-33. We also identified several subgroups of cancer patients that could benefit from DDX3 inhibitors and evaluated potential combination treatment strategies. However, the road from potential target identification to clinical use of an inhibitor is long and several steps need to be taken in order to proceed to investigational new drug approval and clinical evaluation of DDX3 inhibitors. Formulation and drug delivery are specific issues requiring attention, given the relative hydrophobicity of RK-33. Ultimately, efficacy and toxicity of DDX3 inhibitors can only be evaluated in clinical trials. However, large scale *in vitro* efficacy studies on patient-derived 3D cultures of human cancers can be used to further evaluate biomarkers of RK-33 sensitivity in tumors. Good biomarkers of DDX3 dependence can facilitate optimal patient selection in clinical trials. In addition, biomarkers that give a measurement of *in vivo* DDX3 inhibition after drug administration, so-called target engagement biomarkers, could make the drug development process more efficient. In the absence of an effect they can differentiate between lack of inhibition of DDX3, due to potency or delivery issues, and lack of efficacy even though DDX3 is sufficiently inhibited. Currently, there are no target engagement biomarkers of DDX3 that could be used in a clinical setting. Novel ribosome profiling techniques could help us to further elucidate our understanding of the specific changes in the cancer translatome after DDX3 inhibition[35]. In addition, since RNA helicase assays on clinical samples are technically challenging, identification of the DDX3 translational signature could serve as an alternative biomarker for evaluation of target engagement in clinical trials.

CONCLUDING REMARKS

The last decade has witnessed huge advances in our knowledge on DEAD box RNA helicases. Several DDX family members, among which DDX3, have been added to the list of potential therapeutic targets in cancer. In this thesis, we have evaluated several aspects of DDX3 expression and inhibition with the small molecule inhibitor RK-33 in cancer cells. Future studies on formulation, delivery and target engagement markers should further pave the way for clinical development of DDX3 inhibitors.

REFERENCES

1 Weinberg SE, Chandel NS. Targeting mitochondria metabolism for cancer therapy. Nature chemical biology 2015; **11**: 9-15.

2 Jones RA, Robinson TJ, Liu JC, Shrestha M, Voisin V, Ju Y *et al*. RB1 deficiency in triple-negative breast cancer induces mitochondrial protein translation. The Journal of clinical investigation 2016.

3 Wang PY, Li J, Walcott FL, Kang JG, Starost MF, Talagala SL *et al*. Inhibiting mitochondrial respiration prevents cancer in a mouse model of Li-Fraumeni syndrome. The Journal of clinical investigation 2016.

4 Sansone P, Ceccarelli C, Berishaj M, Chang Q, Rajasekhar VK, Perna F *et al*. Self-renewal of CD133(hi) cells by IL6/Notch3 signalling regulates endocrine resistance in metastatic breast cancer. Nature communications 2016; **7**: 10442.

5 Qin B, Minter-Dykhouse K, Yu J, Zhang J, Liu T, Zhang H *et al*. DBC1 functions as a tumor suppressor by regulating p53 stability. Cell reports 2015; **10**: 1324-1334.

6 Bol GM, Vesuna F, Xie M, Zeng J, Aziz K, Gandhi N *et al*. Targeting DDX3 with a small molecule inhibitor for lung cancer therapy. EMBO molecular medicine 2015; **7**: 648-669.

7 Oshiumi H, Sakai K, Matsumoto M, Seya T. DEAD/H BOX 3 (DDX3) helicase binds the RIG-I adaptor IPS-1 to up-regulate IFN-beta-inducing potential. European journal of immunology 2010; **40**: 940-948.

8 Tu YT, Barrientos A. The Human Mitochondrial DEAD-Box Protein DDX28 Resides in RNA Granules and Functions in Mitoribosome Assembly. Cell reports 2015.

9 Antonicka H, Shoubridge EA. Mitochondrial RNA Granules Are Centers for Posttranscriptional RNA Processing and Ribosome Biogenesis. Cell reports 2015.

10 Tarn WY, Chang TH. The current understanding of Ded1p/DDX3 homologs from yeast to human. RNA biology 2009; **6**: 17-20.

11 Cruciat CM, Dolde C, de Groot RE, Ohkawara B, Reinhard C, Korswagen HC *et al*. RNA helicase DDX3 is a regulatory subunit of casein kinase 1 in Wnt-beta-catenin signaling. Science 2013; **339**: 1436-1441.

12 Lai MC, Chang WC, Shieh SY, Tarn WY. DDX3 regulates cell growth through translational control of cyclin E1. Molecular and cellular biology 2010; **30**: 5444-5453.

13 Rosner A, Rinkevich B. The DDX3 subfamily of the DEAD box helicases: divergent roles as unveiled by studying different organisms and in vitro assays. Current medicinal chemistry 2007; **14**: 2517-2525.

14 Chen HH, Yu HI, Cho WC, Tarn WY. DDX3 modulates cell adhesion and motility and cancer cell metastasis via Rac1-mediated signaling pathway. Oncogene 2015; **34**: 2790-2800.

15 Botlagunta M, Vesuna F, Mironchik Y, Raman A, Lisok A, Winnard P, Jr. *et al*. Oncogenic role of DDX3 in breast cancer biogenesis. Oncogene 2008; **27**: 3912-3922.

16 Sun M, Song L, Zhou T, Gillespie GY, Jope RS. The role of DDX3 in regulating Snail. Biochimica et biophysica acta 2011; **1813**: 438-447.

17 Hagerstrand D, Tong A, Schumacher SE, Ilic N, Shen RR, Cheung HW *et al*. Systematic interrogation of 3q26 identifies TLOC1 and SKIL as cancer drivers. Cancer discovery 2013; **3**: 1044-1057.

18 Xie M, Vesuna F, Botlagunta M, Bol GM, Irving A, Bergman Y *et al*. NZ51, a ring-expanded nucleoside analog, inhibits motility and viability of breast cancer cells by targeting the RNA helicase DDX3. Oncotarget 2015; **6**: 29901-29913.

19 Li Y, Wang H, Wang Z, Makhija S, Buchsbaum D, LoBuglio A *et al*. Inducible resistance of tumor cells to tumor necrosis factor-related apoptosis-inducing ligand receptor 2-mediated apoptosis by generation of a blockade at the death domain function. Cancer research 2006; **66**: 8520-8528.

20 Sun M, Song L, Li Y, Zhou T, Jope RS. Identification of an antiapoptotic protein complex at death receptors. Cell death and differentiation 2008; **15**: 1887-1900.

21 Shih JW, Wang WT, Tsai TY, Kuo CY, Li HK, Wu Lee YH. Critical roles of RNA helicase DDX3 and its interactions with eIF4E/PABP1 in stress granule assembly and stress response. The Biochemical journal 2012; **441**: 119-129.

22 Xie M, Vesuna F, Tantravedi S, Bol GM, Heerma van Voss MR, Nugent K *et al*. RK-33 Radiosensitizes Prostate Cancer Cells by Blocking the RNA Helicase DDX3. Cancer research 2016; **76**: 6340-6350.

23 He B, Reguart N, You L, Mazieres J, Xu Z, Lee AY *et al*. Blockade of Wnt-1 signaling induces apoptosis in human colorectal cancer cells containing downstream mutations. Oncogene 2005; **24**: 3054-3058.

24 Voloshanenko O, Erdmann G, Dubash TD, Augustin I, Metzig M, Moffa G *et al*. Wnt secretion is required to maintain high levels of Wnt activity in colon cancer cells. Nature communications 2013; **4**: 2610.

25 Mahboobi SH, Javanpour AA, Mofrad MR. The interaction of RNA helicase DDX3 with HIV-1 Rev-CRM1-RanGTP complex during the HIV replication cycle. PloS one 2015; **10**: e0112969.

26 Nozaki K, Kagamu H, Shoji S, Igarashi N, Ohtsubo A, Okajima M *et al*. DDX3X induces primary EGFR-TKI resistance based on intratumor heterogeneity in lung cancer cells harboring EGFR-activating mutations. PloS one 2014; **9**: e111019.

27 Steeg PS, Camphausen KA, Smith QR. Brain metastases as preventive and therapeutic targets. Nature reviews Cancer 2011; **11**: 352-363.

28 Wu DW, Lee MC, Wang J, Chen CY, Cheng YW, Lee H. DDX3 loss by p53 inactivation promotes tumor malignancy via the MDM2/Slug/E-cadherin pathway and poor patient outcome in non-small-cell lung cancer. Oncogene 2014; **33**: 1515-1526.

29 Chang PC, Chi CW, Chau GY, Li FY, Tsai YH, Wu JC *et al*. DDX3, a DEAD box RNA helicase, is deregulated in hepatitis virus-associated hepatocellular carcinoma and is involved in cell growth control. Oncogene 2006; **25**: 1991-2003.

30 Lee CH, Lin SH, Yang SF, Yang SM, Chen MK, Lee H *et al*. Low/negative expression of DDX3 might predict poor prognosis in non-smoker patients with oral cancer. Oral diseases 2014; **20**: 76-83.

31 Grzmil M, Hemmings BA. Translation regulation as a therapeutic target in cancer. Cancer research 2012; **72**: 3891-3900.
32 Pelletier J, Graff J, Ruggero D, Sonenberg N. Targeting the eIF4F translation initiation complex: a critical nexus for cancer development. Cancer research 2015; **75**: 250-263.
33 Bhat M, Robichaud N, Hulea L, Sonenberg N, Pelletier J, Topisirovic I. Targeting the translation machinery in cancer. Nature reviews Drug discovery 2015; **14**: 261-278.
34 Skrtic M, Sriskanthadevan S, Jhas B, Gebbia M, Wang X, Wang Z *et al*. Inhibition of mitochondrial translation as a therapeutic strategy for human acute myeloid leukemia. Cancer cell 2011; **20**: 674-688.
35 Truitt ML, Ruggero D. New frontiers in translational control of the cancer genome. Nature reviews Cancer 2016; **16**: 288-304.

APPENDIX

Nederlandse samenvatting
Acknowledgements
List of publications
Contributing authors
Curriculum Vitae

NEDERLANDSE SAMENVATTING

Hoe ontwikkel je medicijnen tegen kanker? Door factoren te identificeren die essentieel zijn voor kankercellen om te overleven, maar normale, gezonde weefsels kunnen missen. Een veel gebruikte strategie voor medicijnontwikkeling is proberen de factoren te herkennen die de verandering van een normale cel in een kankercel veroorzaken. We kijken dan bijvoorbeeld naar zogenaamde mutaties, veranderingen die hebben plaatsgevonden in de genen van de kankercellen. Vervolgens proberen we medicijnen te ontwikkelen tegen deze mutaties, ook wel oncogenen genoemd. Hoewel deze gerichte strategie logisch is beredeneerd, kent ze ook een aantal problemen. Zo zijn er maar heel weinig kanker veroorzakende mutaties waartegen remmers te ontwikkelen zijn. Daarnaast blijkt uit grootschalige studies naar het genetische profiel van kankercellen dat verschillende vormen van kanker meestal maar een paar gemeenschappelijke mutaties hebben: de meeste kankers worden aangedreven door hun eigen, unieke set van zeldzame genetische veranderingen[1]. Als het al mogelijk is een remmer voor zo'n oncogen te ontwikkelen, kan deze daardoor vaak maar bij een kleine groep patiënten worden ingezet.
Een alternatieve aanpak bij het ontwikkelen van medicijnen is kijken naar de zwakke plekken van kankercellen die ontstaan doordat maligne veranderingen hoge eisen stellen aan de cel. Kankercellen raken verslaafd aan bepaalde cellulaire processen waarmee ze maligne taken uitvoeren en tegelijkertijd de cel voldoende in balans houden om te kunnen overleven[2]. Interessant genoeg lijken deze cascades, die de cel in evenwicht houden, wel vaak te worden gedeeld door verschillende vormen van kanker, ook al worden die aangedreven door een heel verschillende genetische achtergrond. Remmers die op de secundaire verslavingen van kankercellen zijn gericht, zouden daardoor geschikt kunnen zijn voor grotere groepen patiënten[3]. Het eiwit DDX3 is speelt mogelijk een rol in dergelijke processen waaraan kankercellen verslaafd zijn. In dit proefschrift wordt DDX3 onder de loep genomen als mogelijk therapeutisch doelwit.

De DEAD box familie van RNA-helicasen
Eiwitten zijn de bouwstenen van de cel. Of een cel zich als een kankercel kan gedragen, hangt af van de hoeveelheden van bepaalde eiwitten waarover ze beschikt. De genetische informatie van een cel ligt opgeslagen in het DNA. Het DNA codeert voor het RNA in de cel, en RNA-moleculen coderen op hun beurt voor de eiwitten in de cel. De RNA-moleculen worden via een proces, dat RNA-translatie wordt genoemd, afgelezen, met eiwit synthese als gevolg. Recente studies hebben laten zien dat de hoeveelheid van eiwitten die aanwezig zijn in de cel (eiwit expressie), hoofdzakelijk gecontroleerd wordt op het niveau van RNA-translatie[4-6]. DEAD box RNA-helicasen, ook wel DDX-eiwitten genoemd, kunnen de structuur van het RNA bewerken. Ze hebben een gemeenschappelijke aminozuursequentie (D-E-A-D) en karakteristieke domeinen die RNA-structuren kunnen veranderen en

ontwinden (helicase activiteit) en ATP kunnen binden (ATPase activiteit)[7]. Door het vermogen om structuren in het RNA te veranderen, spelen zogenoemde DEAD box RNA-helicasen een rol in vrijwel alle processen waarbij RNA betrokken is [8, 9] en hebben ze grote invloed op het totale eiwit expressie profiel van cellen.

DDX3 is een factor die kankercellen stimuleert

DDX3, ook wel bekend als DDX3X, is een van de meest bestudeerde DEAD box RNA-helicasen. DDX3 kwam voor het eerst op de radar als een eiwit dat mogelijk een rol speelt in kankercellen, toen het geïdentificeerd werd als een factor, waarvan cellen meer gingen maken na blootstelling aan BPDE, een carcinogeen bestanddeel van sigarettenrook[10]. Sindsdien zijn er een aantal studies verschenen die lieten zien dat DDX3 een rol speelt in de ontwikkeling van verschillende vormen van kanker[11-13], waaronder borstkanker[10]. Zo is aangetoond dat DDX3 een remmende werking heeft op apoptosis, een een proces dat het afsterven van cellen in gang zet en beschermt tegen de ontwikkeling van kanker [14-16]. Daarnaast stimuleert DDX3 het vermogen van cellen om zich te delen[36, 37], te verplaatsen[26, 33] en andere weefsels binnen te dringen[34, 35].

Ontwikkeling van de DDX3-remmer RK-33

Om DDX3 te kunnen remmen in kankercellen hebben wij een moleculaire remmer, RK-33, ontwikkeld. In een voorafgaande studie hebben we laten zien dat RK-33 specifiek aan DDX3 bindt en niet aan andere DEAD box RNA-helicasen[11]. Daarnaast lieten we zien dat RK-33 de RNA-helicase activiteit remt[11]. De effectiviteit van RK-33 is aangetoond in verschillende preklinische modellen van kanker. RK-33 maakt onder andere longkanker-[11] en prostaatkankercellen[13] gevoeliger voor radiotherapie. Daarnaast werd RK-33 als monotherapie effectief bevonden in Ewing-sarcoommodellen met een hoge DDX3-expressie[12]. Studies in muizen naar de toxiciteit van RK-33 lieten geen grote bijwerkingen zien[11]. Hoewel het duidelijk is dat RK-33 het herstelmechanisme van DNA na bestraling kan beïnvloeden, is het nog onbekend via welk mechanisme dit gebeurd.Om het werkingsmechanisme achter DDX3-remmers beter te kunnen begrijpen, onderzoekt dit proefschrift verschillende aspecten van DDX3 als therapeutisch doelwit bij kanker.

MOTIEVEN: WAARDOOR ZIJN KANKERCELLEN AFHANKELIJK VAN DDX3?

Het mechanisme achter de anti-kankerwerking van de DDX3-remmer RK-33 blijft grotendeels onbekend. Om dit te verhelderen hebben we gebruikgemaakt van een techniek die proteomics heet. Hiermee kunnende breedschalige veranderingen die op eiwitniveau in de cel plaatsvinden in kaart gebracht worden.

In **hoofdstuk 2** hebben we het effect van DDX3-remming door RK-33 op de stofwisseling van kankercellen in kaart gebracht. Een groep eiwitten die minder tot expressie kwam na DDX3-remming speelt een rol in de zogenoemde mitochondriale translatie, een proces dat mogelijk een rol speelt in de anti-kanker werking van RK-33. De mitochondriën zijn de celorganellen die verantwoordelijk zijn voor de energieproductie van de cel. Als enige van alle celorganellen bezitten de mitochondriën hun eigen DNA en ook de machinerie om dit eigen DNA, via RNA, in eiwitten te vertalen, met behulp van mitochondriale translatie. We hebben laten zien dat DDX3 in de mitochondriën aanwezig is en dat na RK-33-behandeling mitochondriale translatie geremd is. Dit leidt ertoe dat de mitochondriën minder actief zijn en minder energie in de vorm van ATPmoleculen produceren. Daarnaast neemt het aantal zuurstofradicalen in de cel toe, doordat de mitochondriën niet goed kunnen functioneren. Mitochondriale energieproductie wordt steeds meer herkend als een therapeutisch doelwit in kankercellen[17-20]. In een recente studie is aangetoond dat in bestraalde cellen de mitochondriale activiteit toeneemt, om energie te produceren voor de reparatie van DNA-schade, en dat hierdoor de gevoeligheid van kankercellen voor radiotherapie afneemt[21]. We laten zien dat RK-33 de mitochondriale energieproductie na bestraling remt en hierdoor ook de reparatie van DNA in bestraalde kankercellen remt. Daarnaast doen zowel RK-33-behandeling als bestraling het aantal zuurstofradicalen in de cel toenemen. Deze effecten samen leiden tot een bio-energetische catastrofe in de kankercel, waardoor zij uiteindelijk doodgaat. Onze bevindingen verklaren een deel van de anti-kankeractiviteit van RK-33, met name in combinatie met bestraling, en suggeren dat het remmen van mitochondriale translatie een nieuwe manier is om kankercellen gevoeliger te maken voor radiotherapie.

Naast kankercellen zijn ook de normale cellen afhankelijk van mitochondriale translatie. Zijn er dus bijwerkingen van RK-33? In eerdere muisstudies werden geen bijwerkingen in normale cellen geobserveerd[11]. Dit kan mogelijk worden verklaard door hun relatief lage energiebehoefte, het feit dat ze minder worden blootgesteld aan stressoren die de energiebehoefte plotseling doen stijgen (zoals DNA-schade), hun relatieve lage zuurstafradicaalspiegels en de lage expressie van DDX3 in deze cellen.
In **hoofdstuk 3** gebruiken we twee strategieën om het effect van DDX3-remming met RK-33 op de celcyclus verder in kaart te brengen. Eiwitten kunnen van een inactieve naar een actieve vorm switchen, doordat zogenaamde kinases en fosfatases een fosfaatgroep kunnen aan- of afkoppelen. Dit proces wordt (de)fosforylering genoemd en wordt veelvuldig gebruikt in onder andere de celcyclus. Door middel van een tweede proteomicsexperiment hebben we gekeken naar de verandering in fosforylering die optreedt na RK-33-behandeling. Onze data suggereren vooral een afname in activiteit van de kinase CDK1, die een belangrijke rol speelt in regulatie van de celcyclus. Om het effect van DDX3-remming op de celcyclus verder in kaart te brengen, hebben we gebruikgemaakt van time-

lapsemicroscopie, waarbij individuele cellen over een periode van 24 uur kunnen worden gevolgd. Door deze cellen bepaalde markers mee te geven, konden we de progressie van een enkele cel door de verschillende fasen van de celcyclus na DDX3-remming bestuderen. Remming van DDX3 leidde tot een globale afremming in alle fasen van de celcyclus, en niet tot een blokkade in een bepaalde fase, zoals eerder vaak werd gedacht.

DOELWITTEN: DDX3-AFHANKELIJKHEID IN VERSCHILLENDE VORMEN VAN KANKER

Eerdere studies hebben al laten zien dat DDX3 een potentieel therapeutisch doelwit is in borst-[15, 18], long-[11] en prostaatkanker[22]. In **hoofdstuk 4** hebben we onderzocht of DDX3 ook in de ontwikkeling van darmkanker een rol speelt. Recente studies hebben laten zien dat DDX3 de Wnt-signaleringscascade activeert[11, 23]. In de meeste darmkankers zijn mutaties in deze signaleringscascade aanwezig, waardoor zij continu is geactiveerd. Omdat darmkankers zo afhankelijk lijken te zijn van Wnt-signalering, is het interessant om te zien of ze ook afhankelijk zijn van DDX3. We vonden dan 39% van de darmkankers DDX3 tot overexpressie brengt. Daarnaast bleek DDX3-expressie samen te hangen met expressie van β-catenine in de celkern, een marker van geactiveerde Wnt-signalering. We vonden dat remming van DDX3 in darmkankercellen een verminderde Wnt-signaleringsactiviteit tot gevolg had. Daarnaast leidde RK-33-behandeling in 3D-kweken van darmkanker tot verminderde groei en toename van celdood. Concluderend lijkt DDX3-remming met RK-33 Wnt-signalering in darmkankercellen te verminderen en lijkt DDX3 dus een nieuw therapeutisch doelwit voor darmkanker te zijn.

Hoewel het grootste deel van de DDX3-expressie in de cel zich in het cytoplasma lijkt te bevinden, viel het ons op dat er in sommige tumoren ook veel DDX3 in de celkern te vinden was. In **hoofdstuk 5** zijn we op zoek gegaan naar de betekenis van deze zogenoemde nucleaire DDX3-expressie. Nucleaire DDX3 werd gevonden in 35% van de darmkankers en in 48% van de borstkankers. De aanwezigheid van DDX3 in de celkern werd geassocieerd met een slechtere prognose in zowel darm- als borstkankerpatiënten. Deze correlatie met overleving suggereert dat nucleaire DDX3-expressie mogelijk de ontwikkeling en progressie van kanker bevordert. We laten verder zien dat DDX3-expressie in de celkern samenhangt met de expressie van het nucleaire exporteiwit CRM1 in darmkanker, en welk deel van het DDX3-eiwit het belangrijkste is voor lokalisatie in de celkern. Toekomstige studies moeten laten zien of DDX3 in de kern of in het cytoplasma het meest belangrijk is voor de rol van DDX3 in kanker, en welke van de twee lokalisaties het best gebruikt kan worden om te voorspellen of een kanker gevoelig is voor DDX3-remmers.

Eerdere functionele studies hebben laten zien dat DDX3 invasie en motiliteit van kankercellen faciliteert[10, 23-25]. Om deze bevindingen te valideren hebben we in **hoofdstuk 6** DDX3-expressie onderzocht in het weefsel van primaire borsttumoren en uitzaaiingen

in dezelfde patiënt. We vonden dat cytoplasmatische DDX3-expressie toeneemt in uitzaaiingen. Dit effect was het grootst in tumoren met een zogenaamd triple-negatief receptorprofiel en in hersenmetastasen. Zowel hoge cytoplasmatische als nucleaire DDX3-expressie in uitzaaiingen correleerde met een slechtere overleving, wat suggereert dat DDX3-remmers mogelijk ook in uitgezaaide borstkanker een therapeutische toepassing kunnen hebben.

Naast de studies die laten zien dat DDX3 een eiwit is waarvan kankercellen in hoge mate afhankelijk zijn, zijn er ook tegenstrijdige studies, die suggereren dat DDX3 de maligne ontwikkeling van kankercellen kan onderdrukken[28, 29]. Het is mogelijk dat de rol van DDX3 in kankercellen afhankelijk is van het type kanker en de bijbehorende genetische achtergrond. In **hoofdstuk 7** beschrijven we dat de relatie tussen DDX3-expressie en overleving verschilt tussen rokers en niet-rokers met hoofd-halskanker. Als we alle hoofd-halskankers samennemen, vinden we geen correlatie tussen overleving en DDX3-expressie. Als we echter alleen naar rokers met hoofd-halskanker kijken, zien we wel een relatie tussen DDX3-expressie en lagere overleving. Een recente studie van Lee et al. bij niet-rokende hoofd-halskankerpatiënten uit Taiwan liet het omgekeerde verband zien, namelijk dat DDX3-expressie juist correleerde met een hogere overleving[26]. Deze bevindingen suggereren een model waarin DDX3-opregulatie als reactie op blootstelling aan sigarettenrook de ontwikkeling van kanker stimuleert, terwijl de rol van DDX3 in de ontwikkeling van hoofd-halskanker bij niet-rokers mogelijk anders is. In de toekomst zullen functionele studies zich moeten ontfermen over de rol van DDX3-expressielevels en mutaties in kankers met een verschillende genetische achtergrond, en over de vraag wat dit betekent voor de gevoeligheid voor DDX3-remmers.

HANDLANGERS: COMBINATIETHERAPIE MET PARP EN DDX3-REMMERS

Voor de optimale ontwikkeling van DDX3-remmers als kankertherapie is het essentieel te weten welke interacties er zijn tussen DDX3-remmers en andere anti-kankermedicijnen. Borstkanker cellen met een afwijking in het BRCA1 gen hebben een verminderde DNA herstelcapaciteit. Hierdoor zijn ze zeer gevoelig voor remming van een ander DNA herstelmechanisme door PARP remmers. Omdat het in eerdere studies is aangetoond dat RK-33 een derde DNA herstelmechanisme remt[11], hebben we in **hoofdstuk 8** DDX3 als doelwit in borstkanker met en zonder BRCA1 mutatie bestudeerd. Daarnaast hebben we gekeken of RK-33 borstkanker cellen gevoeliger kon maken voor PARP remmers. We vonden dat er vergelijkbare hoeveelheden DDX3 tot expressie komen in borstkankers in BRCA1/2 mutatiedraagsters en sporadische borstkankers en dat de gevoeligheid voor RK-33 niet afhankelijk was van BRCA1 expressie. RK-33 vergroot echter wel de gevoeligheid van borstkanker waarin BRCA1 niet gemuteerd is voor PARP remmers.

HANDLANGERS: VERSCHILLENDE RNA HELICASES ALS DOELWIT IN DE BEHANDELING VAN KANKER

DDX3 maakt onderdeel uit van een grote familie van DEAD/H box RNA-helicasen, die een rol spelen in vrijwel alle cellulaire processen waar RNA bij betrokken is. In **hoofdstuk 9** geven we een overzicht van de literatuur op het gebied van RNA-helicasen als mogelijke therapeutische doelwitten, voor de bestrijding van kanker bevorderende RNA-translatie. Zo plaatsen we de DDX3-remmer RK-33 in een bredere context. Verschillende RNA-helicasen (eIF4A, DDX3, DHX9, DHX29 en YTHDC2) faciliteren de vertaling van het kankergenoom in eiwitten, door complexe structuren in mRNA te ontwinden. Deze complexe structuren komen vaker voor bij genen die kankercellen stimuleren. RNA-helicasen stimuleren kankercellen stimuleren van zogenoemde IRES-afhankelijke translatie, die een rol speelt in de stressrespons, en de mitochondriale translatie te bevorderen. Remmers van zowel DDX3 als eIF4A bleken zeer effectief in preklinische modellen van kanker.
In het afgelopen decennium is onze kennis over DEAD box RNA-helicasen sterk gegroeid. Verscheidene DEAD box RNA-helicasen, waaronder DDX3, zijn toegevoegd aan de lijst van mogelijke doelwitten voor kankertherapie. Toekomstige studies moeten zich richten op formulering van DDX3-remmers, de optimale toedieningsvorm en biomarkers voor de optimale selectie van patiënten, om zo DDX3-remmers klaar te stomen voor verdere klinische ontwikkeling.

REFERENCES

1 Kandoth C, McLellan MD, Vandin F, Ye K, Niu B, Lu C et al. Mutational landscape and significance across 12 major cancer types. Nature 2013; 502: 333-339.

2 Dobbelstein M, Moll U. Targeting tumour-supportive cellular machineries in anticancer drug development. Nature reviews Drug discovery 2014; 13: 179-196.

3 Luo J, Solimini NL, Elledge SJ. Principles of cancer therapy: oncogene and non-oncogene addiction. Cell 2009; 136: 823-837.

4 Ghazalpour A, Bennett B, Petyuk VA, Orozco L, Hagopian R, Mungrue IN et al. Comparative analysis of proteome and transcriptome variation in mouse. PLoS genetics 2011; 7: e1001393.

5 Vogel C, Marcotte EM. Insights into the regulation of protein abundance from proteomic and transcriptomic analyses. Nature reviews Genetics 2012; 13: 227-232.

6 Schwanhausser B, Busse D, Li N, Dittmar G, Schuchhardt J, Wolf J et al. Global quantification of mammalian gene expression control. Nature 2011; 473: 337-342.

7 Soto-Rifo R, Ohlmann T. The role of the DEAD-box RNA helicase DDX3 in mRNA metabolism. Wiley interdisciplinary reviews RNA 2013; 4: 369-385.

8 Tanner NK, Linder P. DExD/H box RNA helicases: from generic motors to specific dissociation functions. Molecular cell 2001; 8: 251-262.

9 Linder P, Fuller-Pace FV. Looking back on the birth of DEAD-box RNA helicases. Biochimica et biophysica acta 2013; 1829: 750-755.

10 Botlagunta M, Vesuna F, Mironchik Y, Raman A, Lisok A, Winnard P, Jr. et al. Oncogenic role of DDX3 in breast cancer biogenesis. Oncogene 2008; 27: 3912-3922.

11 Bol GM, Vesuna F, Xie M, Zeng J, Aziz K, Gandhi N et al. Targeting DDX3 with a small molecule inhibitor for lung cancer therapy. EMBO molecular medicine 2015; 7: 648-669.

12 Wilky BA, Kim C, McCarty G, Montgomery EA, Kammers K, DeVine LR et al. RNA helicase DDX3: a novel therapeutic target in Ewing sarcoma. Oncogene 2016; 35: 2574-2583.

13 Xie M, Vesuna F, Tantravedi S, Bol GM, Heerma van Voss MR, Nugent K et al. RK-33 radiosensitizes prostate cancer cells by blocking the RNA helicase DDX3. Cancer research 2016: doi:10.1158/0008-5472.CAN-1116-0440.

14 Li Y, Wang H, Wang Z, Makhija S, Buchsbaum D, LoBuglio A et al. Inducible resistance of tumor cells to tumor necrosis factor-related apoptosis-inducing ligand receptor 2-mediated apoptosis by generation of a blockade at the death domain function. Cancer research 2006; 66: 8520-8528.

15 Sun M, Song L, Li Y, Zhou T, Jope RS. Identification of an antiapoptotic protein complex at death receptors. Cell death and differentiation 2008; 15: 1887-1900.

16 Shih JW, Wang WT, Tsai TY, Kuo CY, Li HK, Wu Lee YH. Critical roles of RNA helicase DDX3 and its interactions with eIF4E/PABP1 in stress granule assembly and stress response. The Biochemical journal 2012; 441: 119-129.

17 Weinberg SE, Chandel NS. Targeting mitochondria metabolism for cancer therapy. Nature chemical biology 2015; 11: 9-15.

18 Jones RA, Robinson TJ, Liu JC, Shrestha M, Voisin V, Ju Y et al. RB1 deficiency in triple-negative breast cancer induces mitochondrial protein translation. The Journal of clinical investigation 2016.

19 Wang PY, Li J, Walcott FL, Kang JG, Starost MF, Talagala SL et al. Inhibiting mitochondrial respiration prevents cancer in a mouse model of Li-Fraumeni syndrome. The Journal of clinical investigation 2016.

20 Sansone P, Ceccarelli C, Berishaj M, Chang Q, Rajasekhar VK, Perna F et al. Self-renewal of CD133(hi) cells by IL6/Notch3 signalling regulates endocrine resistance in metastatic breast cancer. Nature communications 2016; 7: 10442.

21 Qin B, Minter-Dykhouse K, Yu J, Zhang J, Liu T, Zhang H et al. DBC1 functions as a tumor suppressor by regulating p53 stability. Cell reports 2015; 10: 1324-1334.

22 Xie M, Vesuna F, Tantravedi S, Bol GM, Heerma van Voss MR, Nugent K et al. RK-33 Radiosensitizes Prostate Cancer Cells by Blocking the RNA Helicase DDX3. Cancer research 2016; 76: 6340-6350.

23 Chen HH, Yu HI, Cho WC, Tarn WY. DDX3 modulates cell adhesion and motility and cancer cell metastasis via Rac1-mediated signaling pathway. Oncogene 2015; 34: 2790-2800.

24 Hagerstrand D, Tong A, Schumacher SE, Ilic N, Shen RR, Cheung HW et al. Systematic interrogation of 3q26 identifies TLOC1 and SKIL as cancer drivers. Cancer discovery 2013; 3: 1044-1057.

25 Xie M, Vesuna F, Botlagunta M, Bol GM, Irving A, Bergman Y et al. NZ51, a ring-expanded nucleoside analog, inhibits motility and viability of breast cancer cells by targeting the RNA helicase DDX3. Oncotarget 2015; 6: 29901-29913.

26 Lee CH, Lin SH, Yang SF, Yang SM, Chen MK, Lee H et al. Low/negative expression of DDX3 might predict poor prognosis in non-smoker patients with oral cancer. Oral diseases 2014; 20: 76-83.

ACKNOWLEDGEMENTS

De meeste clichés over promoveren zijn waar. Iemand vertelde mij ooit dat om klaar te zijn met promoveren, je er vooral ook echt klaar mee moet zijn. Degenen die mij de afgelopen tijd met regelmaat gesproken hebben, zullen bevestigen dat ik aan deze voorwaarde voldaan heb. Maar een ding is zeker, in mijn eentje zou ik nooit op dit punt gekomen zijn en waren de afgelopen jaren ook niet half zo leuk geweest. Er zijn velen die mij geholpen hebben met het bereiken van deze mijlpaal. Een aantal van hen wil ik in het bijzonder bedanken.

Professor van Diest, Paul!* Het is inmiddels bijna 10 jaar geleden dat ik als eigenwijze snotneus bij je aanklopte met de boodschap dat ik onderzoek wilde doen. Ik had toen totaal niet voor ogen dat dit boekje het resultaat zou kunnen zijn. Maar jij nam mij vanaf het begin serieus, daagde me uit, wees me de weg en opende deuren voor me, tot ik uiteindelijk met een beurs naar het Hopkins vertrok. Ook daar heb je me gedurende vele skypegesprekken door het wel en wee van mijn PhD geloodst. Ik kan je niet genoeg bedanken voor je vertrouwen, steun en betrokkenheid. Je optimisime en de manier waarop jij dag en nacht voor je promovendi klaarstaat is inspirerend.

Dr Raman, dear Venu, thanks for giving me the opportunity to explore the wild world of molecular biology under your auspices. When I came to Baltimore I was a complete rookie, and I cannot thank you enough for the time and patience you took to guide me. Thanks to Dutch (or just my) stubborness our monday morning meetings often ended in fierce discussions over a wide variety of topics. You taught me to always think outside the box, and I am very greatful for that.

Professor van der Wall, beste Elsken. Als allround dokter weet jij nieuwe wetenschappelijke bevindingen in de dagelijkse praktijk te implementeren en stel je bij wetenschappelijk onderzoek, ook al is het fundamenteel van aard, altijd de vraag wat een uitkomst betekent voor de patient. Voor mij ben je een groot rolmodel. Dank voor je input, steun en vertrouwen.

Geachte leden van de leescomissie: prof. dr. Kranenburg, prof. dr. Linn, prof. dr. Beijnen, prof. dr. Verheij en prof. dr. Offerhaus. Heel hartelijk dank voor het zitting nemen in mijn commissie en het beoordelen van mijn proefschrift.

Dr Vesuna, dear Farhad, thank you for your patience and guidance. The lab (and my thesis) would be nowhere without you. You managed to safe my blots, my phone, my laptop and probably also my sanity. I miss the cynical jokes coming from the desk behind me. Thank you for everything!

Ashley and Yehudit thanks for all your help and the endless chats while waiting for our alarm to go off. Min and Saritha, where would our lab be without your chemistry. Thanks for the pile of RK-33 you synthesized for me and all the other things as well! Sahini and Justin, thanks for being great students. I wish you all the best!

Many thanks to all the excellent scientists at Hopkins for sharing their knowledge and expertise. Junaid, Seahorse guru and Dr Anne Le, cancer metabolism expert. Thanks to both of your independent crash courses on cellular metabolism, chapter 2 is the one I am most proud of. Dr. Andrew Holland thank you for all your help with the timelapse microscopy. Dr Phouc Tran thank you for your guidance with regard to radiation therapy. Reem thank you for helping me out with my crazy nightly radiation schemes. You made my trips to CRBII a lot more fun. Dr Kammers, dear Kai, thank you for your help with all the proteomics stats and R-magic, but even more for all the beers and barbeques. We will beat you on the soccer field one day.

Beste medewerkers van het PRL van vroeger en van nu. Dankzij jullie voelde het lab in Utrecht bijna als een tweede thuis. Dankjulliewel voor het warme welkom als ik tussen de coschappen in proefjes kwam doen, of over was uit Baltimore. Petra, je leerde me pipetteren, buffers maken en nog veel meer. Ik herinner het me nog als de dag van gister. Dank voor al je steun door de jaren heen! Karijn, Geert, Laura, Danielle, Jolien, Cigdem, Stefanie en Robert onderzoekers van het eerste uur, ik herinner me een fantastische trip naar Dresden, mijn eerste congres. Laurien, samen bij de kerstman op schoot in San Antonio. Het was een eer om naast je te mogen staan op jouw grote dag! Marijn, labvriendinnetje, ik ben zo trots op hoe jij de dingen aanpakt. Succes in het Oosten! Jan, zonder jou had ik nu nog steeds geen kloppende kloon gehad, waanzinnig bedankt voor je hulp. Rob en Pauline top om met mijn oude studiegenoten (en vrienden) samen te mogen werken. Lucas! Wanneer worden we weer collega's? Folkert, Wendy, Niels, Roel en Cathy dank voor jullie hulp in het lab. Yvonne, super om tegelijk met jou in de VS te zijn! Natalie, immunoheldin. Waanzinnig veel dank voor je hulp en gezelligheid. Dit boekje zou een aantal figuren lichter zijn zonder jou. Nikolas, dankjewel voor het mogelijk maken van transatlantische digitale pathologie! Ze zaten er met grote ogen naar te kijken in de States. Ellen, partner in crime, super fijn dat we alletwee straks klaar zijn! Aernoud, mede-paranimf, het orka pak stond je prachtig! Joost, Emma, Selena, Liling, Quirine en Lilian aan jullie de taak om de PRL-eer hoog te houden. Qua gezelligheid zit het in ieder geval wel snor. Alle leden van de mammagroep, heel veel dank voor jullie input!

Willy, zonder jou was ik nergens. Dankjewel voor het inplannen van last-minute meetings, adhoc coupe-score-sessies en skypemeetings in verschillende tijdzones. Niets bleek onmogelijk dankzij jouw hogere agenda- en hoogleraar-manage-kunde.

Beste assistenten, internisten, geriaters, long- en MDL-artsen uit het Meander MC. Ik prijs me zeer gelukkig de komende jaren te mogen werken met zulke leuke en bekwame collega's. Dankjulliewel voor het warme welkom.

Guus! Grote schoenen om in te gaan staan. Dank voor al je tips en tricks en bovenal voor je (over)levenslessen in B'more. Ik hoop nog eens een mooi onderzoeksproject met je te ondernemen, maar laten we eerst weer een keer gaan klimmen en bier drinken!

Steve, thank you for providing me with an American home, the moment I landed in Baltimore. You guided me through my culture shock with netflix, turkey for thanksgiving, beers on st Patricks day, and much more. You and Ricky are welcome in Amsterdam any time!

Beste Dutchies in Baltimore, medebewoners van de greatest city in America. Dankzij jullie werd het een toptijd! Maite en Egbert, onze Baltimore besties, jammer dat we niet meer om de hoek wonen. Ik mis jullie! Lodewijk en Anne, dankjulliewel voor het familiegevoel. Ik kom graag nog een keer oppassen in Arnhem. Niek, Michael, Wendy, Thomas en Emma, heerlijk om met jullie op de Guilford Avenue te wonen, te bankhangen achter de enorme TV, burgers te eten bij Pete's grill, BBQ op de porch... Emma zo fijn dat jij mijn liefde voor yoga deelde. Heel veel succes met alles daar en tot snel! Wenzel, Joost, Shoko, Patrick en Marleen, jullie ook heel erg bedankt voor de gezellige tijd! Kari, ik vond het waanzinnig leuk dat jij de moeite nam om persoonlijk je 3D-kweken in Baltimore te komen inspecteren!

Dr Too Real, lieve Annie, wat hebben we veel meegemaakt in Beverly B'more samen. We zijn getuige geweest van al elkaars PhD ups en downs (ok, laten we eerlijk zijn, in jouw geval vooral onwaarschijnlijk veel ups!) en praatte elkaar bij over een koffietje in de DG, sushi van Minato, aan het zwembad, of gewoon achter onze keukentafel. Super om te zien hoe je als rising star de cardiologie in binnen- en buitenland verovert! Maar bovenal, fijn dat het altijd zo gezellig is. Ik prijs me zeer gelukkig om je bij mijn verdediging aan mijn zijde te hebben.

Dr Schrijvers, lieve Wil! Als mede-mamma-meisje hadden wij elkaar al snel gevonden in Utrecht. Jouw arbeidsethos is op het PRL ongeëvenaard. Maar meer nog dan dat ben je vooral een superleuke en betrokken collega. Waar jij de energie vandaan haalt is me een raadsel. Ik ken niemand anders die op zoek moest naar hobby's naast een fulltime baan als assistent chirurgie, maar ik kom binnenkort graag genieten van je nieuw-opgedane vinologische kennis. Ik was apetrots jouw paranimf te mogen zijn en weet zeker dat het met mij ook goed gaat komen met zo'n sterk team naast me.

Veel dank ook voor de vrienden die me door dik en dun gesteund hebben tijdens dit hele traject. Lieke, Claire, Annelies, Shona, Lisa, Roos, Laura, Layla, Francine en Kyra, ik prijs me gelukkig met zulke diverse, creatieve en bijzondere vrouwen om me heen. Teun, super dat we een gelijktijdig Amerikaans avontuur hadden. Pieter en Diederik, dank voor al die keren dat ik op de Rooseveltlaan mocht crashen. Sjors en Ankie, fijn dat jullie er voor Ynte waren, als ik er niet was. Ankie in het bijzonder dank voor je last minute redigeer werk. Rodrigo, thanks for showing me the best library spots in Porto.

Lieve familie, het warme nest waar ik altijd op terug kan vallen, al is het vanaf de andere kant van de oceaan. Dank voor al jullie betrokkenheid, enthousiasme en steun. Vanaf nu beloof ik weer steevast van de partij te zijn.

Lieve Bas, mama zei het vroeger al: "als kind kun je nog zoveel ruzie maken als broer en zus, maar wacht maar tot je groot bent, dan zul je de halve wereld afreizen om elkaar te zien". Ik geloof niet dat ze het als zo'n letterlijke aanmoediging bedoelde, maar het is wel een feit dat we elkaar al op een aantal continenten opgezocht hebben. Ik ben blij met jou als mijn 'broertje', trots op wat je allemaal wel al niet bereikt hebt en ik vind het ook niet erg dat je nu op 5 minuten fietsen woont. Dat er nog maar veel mooie reisjes mogen volgen.

Lieve papa en mama. Dit boekje is opgedragen aan jullie. Een kritische, empirische geest was bij ons aan de keukentafel altijd al een vereiste en dat ik dit proefschrift heb kunnen schrijven is dan ook in hoge mate dankzij jullie. Ik ben heel dankbaar voor jullie steun en betrokkenheid. Ik waardeer de solide basis die jullie bieden en realiseer me dat dit niet vanzelfsprekend is. Bedankt voor alles.

Lieve lieve Ynte, wat ben ik blij dat je van mijn avontuur in Baltimore, ons avontuur hebt gemaakt. Ik ben je oneindig dankbaar voor je vertrouwen en steun, maar vooral ook voor het geduld dat jij met me gehad hebt, zodat ik aan de andere kant van de oceaan aan mijn proefschrift kon werken. Ik ben gelukkiger dan ooit nu we samen in Amsterdam wonen en kijk uit naar al onze toekomstige avonturen samen.

*Ik sluit me bij Guus aan wat betreft de passende interpunctie.

LIST OF PUBLICATIONS

Heerma van Voss, M.R., van der Groep, P., Bart, J., van der Wall, E. & van Diest, P. J. Lymphovascular invasion in BRCA related breast cancer compared to sporadic controls. *BMC. Cancer.* 10:145., 145 (2010).

Heerma van Voss, M.R., van der Groep, P., Bart, J., van der Wall, E. & van Diest, P. J. Expression of the stem cell marker ALDH1 in the normal breast of BRCA1 mutation carriers. *Breast Cancer Res. Treat.* 123, 611-612 (2010).

Heerma van Voss, M.R., van der Groep, P., Bart, J., van der Wall, E. & van Diest, P. Expression of the stem cell marker ALDH1 in BRCA1 related breast cancer. *Cellular Oncology* 34, 3-10 (2011).

Teunis, T., **Heerma van Voss, M.R.**, Kon, M. & van Maurik, J.F. CT-angiography prior to diep flap breast reconstruction: a systematic review and meta-analysis. *Microsurgery* 33, 496-502 (2013).

Heerma van Voss, M.R., van Diest P.J., Smolders, Y.H.C., Bart J., van der Wall E., van der Groep, P. Distinct claudin expression characterizes BRCA1 related breast cancer. *Histopathology* 65, 814-27 (2014)

Heerma van Voss, M.R., van Kempen, P.M., Noorlag, R., van Diest, P.J., Willems, S.M., Raman, V., DDX3 has divergent roles in head and neck squamous cell carcinomas in smoking versus non-smoking patients. *Oral Diseases* 21, 270-1 (2015)

Bol, G.M., Vesuna, F., Xie, M., Zheng, J., Aziz, K., Gandhi, N., Levine A., Irving, A., Korz, D., Tantravedi,S., **Heerma van Voss, M.R.,** Gabrielson, K., Bordt, E., Polster, B., Cope, L., van der Groep, P., Kondaskar, A., Rudek, M., Hosmane, R., van der Wall, E., van Diest, P.J., Tran, P., Raman, V. Targeting DDX3 with a small molecule inhibitor for lung cancer therapy. *EMBO Mol Med* 7, 648-69 (2015)

Bol, G.M., Khan, R., **Heerma van Voss, M.R.**, Tantravedi, S., Korz, D., Kato, Y., Raman, V. PLGA nanoparticle formulation of RK-33: an RNA helicase inhibitor against DDX3. *Cancer Chemother Pharmacol* 4, 821-7 (2015)

Heerma van Voss, M.R., Vesuna, F., Trumpi, K., Brilliant, J., Berlinicke, C., de Leng, W., Kranenburg, O., Offerhaus, G.J., Bürger, H., van der Wall, E., van Diest, P.J., Raman, V. Identification of the DEAD box RNA helicase DDX3 as a therapeutic target in colorectal cancer. *Oncotarget* 6, 28312-26 (2015)

Xie M., Vesuna F., Tantravedi S., Bol G.M., **Heerma van Voss M.R.**, Nugent K., Malek R., Gabrielson K., van Diest P.J., Tran P.T., Raman V. RK-33 Radiosensitizes Prostate Cancer Cells by Blocking the RNA Helicase DDX3. *Cancer Research* 76, 6340-6350 (2016)

Thorek D.L., Watson P.A., Lee S.G., Ku A.T., Bournazos S., Braun K., Kim K., Sjöström K., Doran M.G., Lamminmäki U., Santos E., Veach D., Turkekul M., Casey E., Lewis J.S., Abou D.S., **Heerma van Voss M.R.**, Scardino P.T., Strand S.E., Alpaugh M.L., Scher H.I., Lilja H., Larson S.M., Ulmert D. Internalization of secreted antigen-targeted antibodies by the neonatal Fc receptor for precision imaging of the androgen receptor axis. *Science Translational Medicine* 8, 367ra167 (2016)

Heerma van Voss M.R., Schrijver W.A., Ter Hoeve N.D., Hoefnagel L.D., Manson Q.F., van der Wall E., Raman V., van Diest P.J.; Dutch Distant Breast Cancer Metastases Consortium. The prognostic effect of DDX3 upregulation in distant breast cancer metastases. *Clin Exp Metastasis* 34, 85-92 (2017)

Heerma van Voss M.R., Brilliant J.D., Vesuna F., Bol G.M., van der Wall E., van Diest P.J., Raman V. Combination treatment using DDX3 and PARP inhibitors induces synthetic lethality in BRCA1-proficient breast cancer. *Med Oncol* 34, 33 (2017)

Heerma van Voss M.R., Vesuna F., Bol G.M., Afzal J., Bergman Y., Kammers K., Lehar M., Malek R., Ballew M., ter Hoeve N., Abou D., Thorek D., Berlinicke C., Yazdankhah M., Sinha D., Le A., Abrahams A., Tran P.T., van Diest P.J., Raman V. Targeting mitochondrial translation by inhibiting DDX3: a novel radiosensitization strategy for cancer treatment, *submitted*

Heerma van Voss M.R., Kammers K., Vesuna F., Brilliant J.D., Bergman Y., Tantravedi S., Wu X., Cole R.N., Holland A., van Diest P.J., Raman V. Global effects of DDX3 inhibition on cell cycle regulation identified by a combined phosphoproteomics and single cell tracking approach, *manuscript in preparation*

Heerma van Voss M.R., Vesuna F., Bol G.M., Meeldijk J., Raman A., Offerhaus G.J., Buerger H., Patel A.H., van der Wall E., van Diest P.J., Raman V. Nuclear DDX3 Expression Predicts Poor Outcome in Colorectal and Breast Cancer, *submitted*

Heerma van Voss M.R., van Diest P.J., Raman V. Targeting RNA helicases in cancer: the translation trap, *manuscript in preparation*

CONTRIBUTING AUTHORS

Diane Abou
Department of Radiology and Radiological Sciences, Johns Hopkins University, School of Medicine, Baltimore, MD, USA

Roselle Abrahams
Department of Cardiology, Johns Hopkins University, School of Medicine, Baltimore, MD, USA

Junaid Afzal
Department of Cardiology, Johns Hopkins University, School of Medicine, Baltimore, MD, USA

Matthew Ballew
Department of Radiation Oncology, Johns Hopkins University, School of Medicine, MD, USA

Yehudit Bergman
Department of Radiology and Radiological Sciences, Johns Hopkins University, School of Medicine, Baltimore, MD, USA

Cynthia Berlinicke
Wilmer Eye Institute, Johns Hopkins University, School of Medicine, MD, USA

Guus M. Bol
Department of Pathology, University Medical Center Utrecht, Utrecht, The Netherlands
Department of Radiology and Radiological Sciences, Johns Hopkins University, School of Medicine, Baltimore, MD, USA

Justin D. Brilliant
Department of Radiology and Radiological Sciences, Johns Hopkins University, School of Medicine, Baltimore, MD, USA

Horst Bürger
Institute of Pathology, Paderborn, Germany

Robert N. Cole
Mass spectrometry and Proteomics Core, Johns Hopkins University, School of Medicine, Baltimore, MD, USA

Paul J. van Diest
Department of Pathology, University Medical Center Utrecht, Utrecht, The Netherlands
Department of Oncology, Johns Hopkins University, School of Medicine, MD, USA

Laurien D. Hoefnagel
Department of Pathology, University Medical Center Utrecht, Utrecht, The Netherlands

Natalie ter Hoeve
Department of Pathology, University Medical Center Utrecht, Utrecht, The Netherlands

Andrew Holland
Department of Molecular Biology and Genetics, Johns Hopkins University, School of Medicine, Baltimore, MD, USA

Kai Kammers
Department of Biostatistics, Johns Hopkins University, Bloomberg School of Public Health, Baltimore, MD, USA

Onno Kranenburg
Department of Surgery, University Medical Center Utrecht, Utrecht, The Netherlands

Anne Le
Department of Pathology, Johns Hopkins University, School of Medicine, MD, USA

Mohamed Lehar
Department of Otolaryngology, Johns Hopkins University, School of Medicine, MD, USA

Wendy de Leng
Department of Pathology, University Medical Center Utrecht, Utrecht, The Netherlands

Reem Malek
Department of Radiation Oncology, Johns Hopkins University, School of Medicine, MD, USA

Quirine F. Manson
Department of Pathology, University Medical Center Utrecht, Utrecht, The Netherlands

Jan Meeldijk
Laboratory of Translational Immunology, University Medical Center Utrecht, Utrecht, The Netherlands

G. Johan Offerhaus
Department of Pathology, University Medical Center Utrecht, Utrecht, The Netherlands

Arvind H. Patel
MRC, University of Glasgow Centre for Virus Research, Glasgow, United Kingdom

Ana Raman
Department of Pharmacology, Johns Hopkins University, School of Medicine, Baltimore, MD, USA

Venu Raman
Department of Radiology and Radiological Sciences and Department of Oncology, Johns Hopkins University, School of Medicine, Baltimore, MD, USA
Department of Pathology, University Medical Center Utrecht, Utrecht, The Netherlands

Willemijne A.M.E. Schrijver
Department of Pathology, University Medical Center Utrecht, Utrecht, The Netherlands

Debasish Sinha
Wilmer Eye Institute, Johns Hopkins University, School of Medicine, MD, USA

Saritha Tantravedi
Department of Radiology and Radiological Sciences, Johns Hopkins University, School of Medicine, Baltimore, MD, USA

Daniel Thorek
Department of Radiology and Radiological Sciences, Johns Hopkins University, School of Medicine, Baltimore, MD, USA

Phuoc T. Tran
Department of Radiation Oncology and Urology, Johns Hopkins University, School of Medicine, MD, USA

Kari Trumpi
Department of Surgery, University Medical Center Utrecht, Utrecht, The Netherlands

Farhad Vesuna
Department of Radiology and Radiological Sciences, Johns Hopkins University, School of Medicine, Baltimore, MD, USA

Elsken van der Wall
Department of Internal Medicine, University Medical Center Utrecht, Utrecht, The Netherlands

Xinyan Wu
McKusick-Nathans Institute of Genetic Medicine, Johns Hopkins University, School of Medicine, Baltimore, MD, USA

Meysam Yazdankhah
Wilmer Eye Institute, Johns Hopkins University, School of Medicine, MD, USA

CURRICULUM VITAE

Marise Rosa Heerma van Voss was born on June 12th, 1988 in Amsterdam, the Netherlands, to Lex Heerma van Voss and Anke Brand. She grew up in Diemen with her younger brother Bas. After obtaining her high school degree at the Vossius Gymnasium in Amsterdam, she started medical school at the University of Utrecht in 2006. During her bachelor degree she participated in the honors program of medicine and started doing research on BRCA1 related breast cancer at the department of Pathology under supervision of Paul van Diest, MD, PhD and Elsken van der Wall, MD, PhD. Marise completed her final year in medical school with senior rotations at the department of medical oncology (Antoni van Leeuwenhoek ziekenhuis) and intensive care (Ziekenhuis Gelderse Vallei) and a research internship at the Johns Hopkins University (Baltimore, USA), under supervision of Venu Raman, PhD. She obtained her medical degree in March 2013 with honors. She was able to obtain personal funding from the Alexandre Suerman MD/PhD stipend and the Dutch Cancer Foundation to continue her research in the form of a collaborative PhD project at both the Johns Hopkins University and University Medical Center Utrecht, under supervision of Venu Raman, Paul van Diest and Elsken van der Wall. She investigated the use of DDX3 inhibitors in cancer, as described in this thesis. Her work won her a scholar award at the 2014 AACR annual meeting. In addition, she obtained a certificate degree in pharmacoepidemiology and drug safety at the Johns Hopkins Bloomberg School of Public Health. In December 2016 Marise started her internal medicine residency at the Meander Medical Center, Amersfoort, supervised by R.J. Bosma, MD, PhD and R. Fijnfeer MD, PhD. Marise lives in Amsterdam with Ynte de Boer.